STUDIES TO ALLOW THE CONSISTENT FABRICATION OF MANY UNITS OF ENGINEERED TISSUE

A thesis submitted to the University of London as part of the requirements for the degree of Doctor of Philosophy

Christopher Mason FRCS

2005

Department of Biochemical Engineering
University College London
Roberts Building
Torrington Place
London WC1E 7JE

ProQuest LLC
789 East Eisenhower Parkway
P.O. Box 1346
Ann Arbor, MI 48106-1346

ABSTRACT

Tissue engineering is the regeneration of tissues through the use of cells with the aid of scaffolds. Such *in vitro* fabrication of tissues is beginning to become an option for the management of patients who have irreversible failure of an organ. There are many technical challenges to overcome before 'off-the-shelf' tissues that represent the translation of scientific discoveries into routine treatments for millions of patients becomes a reality. To meet this demand, the products must be manufactured reproducibly and in large numbers employing current good tissue practice (cGTP). This thesis takes a whole bioprocess approach and includes:

Bioreactor design

A new and novel methodology is described which potentially allows any tubular organ to be fabricated using an easily scalable liquid based technique suited to automated mass-production. It is novel in that it employs a single multitasking chamber which functions as both a "dynamic former" to create a precise tubular cell/polymer construct and then acts as the core of the bioreactor in which to grow the tissue.

Optical coherence tomography (OCT)

OCT is an advanced non-invasive high-resolution clinical imaging technique. This thesis describes both its initial application to the engineering of tissue as a means of imaging a construct within its individual bioreactor and also the use of Doppler enhanced OCT to qualitatively and quantitatively image the flow of culture medium through the construct.

Polymer scaffold

Typically, tissue engineers construct a scaffold and then seed it with cells. This has inherent difficulties including the achievement of homogeneous seeding densities. An alternative is described whereby cells and liquid polymer are mixed prior to scaffold formation.

Stem cells

Because of the novel approach to construct fabrication, rat smooth muscle cells were used for "range-finding" experiments. Later experiments deployed human adult mesenchymal stem cells (MSCs) which were shown to network within the tubular constructs.

ACKNOWLEDGEMENTS

I am greatly indebted to my supervisor **Professor Peter Dunnill** (Department of Biochemical Engineering, UCL) for his continual advice, encouragement, amazing patience and friendship throughout the course of this thesis and beyond.

I must also thank another key individual, **Martin Town** (Department of Biochemical Engineering, UCL), without whose mechanical engineering genius and persistence to fabricate the perfect tube-forming system, the project would never have succeeded.

Other important collaborators and facilitators included; **Dr. David Becker** (Department of Anatomy and Developmental Biology, UCL), **Professor Chris Boshoff** (Wolfson Institute for Biomedical Research), **Professor Ian Charles** (Wolfson Institute for Biomedical Research), **Neil Cruttenden** (ISP Alginates (UK) Ltd), **Garr Chau** (Department of Biochemical Engineering, UCL), **Dr. Mark Clements** (Wolfson Institute for Biomedical Research), Professor Fred Fitzke (Insitute of Ophthalmology), **Dr. Vanya Gant** (Centre for Infectious Diseases, UCLH), **Andy Godfrey** (Wolfson Institute for Biomedical Research), **Dr. Yonhong He** (Cranfield Biomedical Centre, Cranfield University), **Dave Higgs** (School of Life Sciences, Kingston University), **Professor Mike Hoare** (Department of Biochemical Engineering, UCL), **Dr. Dearbhla Hull** (Department of Histopathology, Bart's and the London Hospitals), **Mr. Jo Lau** (Cardiothoracic Department, Guy's Hospital), **Julia Markusen** (Merck and Co.), **Dr. Julian Mason** (School of Life Sciences, Kingston University), **Professor Jo Martin** (Department of Histopathology, Bart's and the London Hospitals), **Dr. Sergey Proskurin** (Cranfield Biomedical Centre, Cranfield University), **Ros Selfe** (Department of Chemistry, UCL), **Dr. Alethea Tabor** (Department of Chemistry, UCL), **Professor Ricky Wang** (Cranfield Biomedical Centre, Cranfield University), **Dr. Mike Watts** (Department of Haematology, UCLH), **Mike Wren** (Centre for Infectious Diseases, UCLH), **Dr. Kwee Yong** (Department of Haematology, UCLH) and **Dr. Patricia Zunszain** (Department of Chemistry, UCL).

A big thank you must also go to all the technicians in the Department including **Clive Orsborn**, **Ian Buchanan** and **Billy Doyle** plus **Julian Perfect** (Department of Chemical Engineering, UCL).

Thanks are also due to the **Medical Research Council** for the major funding via the granting of a Clinical Research Fellowship (1999 - 2002) plus additional funds from the **National Endowment for Science, Technology and the Arts (NESTA)** for being awarded Overall Winner of the Medical Futures Innovaion Awards (2002) and **Accenture** for winning the Best Biotech Start-Up Innovation Award (2002).

Finally, the largest possible thank you goes to my fabulous wife, **Dr. Louise Mason**.

TABLE OF CONTENTS

LIST OF FIGURES

1.0 Overview

Regenerative medicine is an emerging multi-disciplinary field demanding the integration of life sciences, engineering and clinical medicine, which is likely to have a major impact on a number of fields including patient therapies, drug discovery and development, diagnostics and biosensors.

Currently multiple approaches exist for the treatment of tissue or organ failure or loss, e.g. diabetic patients can be treated by dietary advice, tablets, injections or pancreas transplantation. None of these options however cures the patient, they just manage the disease i.e. attempt to reduce its symptoms or progression. However to achieve a true cure, the patient would need to regenerate the lost tissue or organ - revivification of the particular body part. The capacity to regenerate whilst common in "simpler" animals and human fetuses, is very much reduced in the adult human and is largely replaced with only the capacity to repair. Repair is generally a faster process but results in permanently scarred tissues and organs with decreased or absent function.

Regenerative medicine proposes three main approaches to restore human tissues and organs. Whilst small molecule pharmaceutical compounds may still have a role to play e.g. controlling stem cell differentiation (Ding *et al*, 2003 and Wu *et al*, 2004), the initial and simplest approach to regenerative medicine is to employ genes or proteins as therapies e.g. gene therapy for the cure of severe combined immunodeficiency disease (SCID) (Gasper *et al*, 2003) and recombinant granulocyte colony stimulating factor (G-CSF - Neupogen, Amgen, Thousand Oaks, CA, USA) to accelerate the production, maturation and activation of neutrophils following chemotherapy (Hubel and Engert, 2003). If this initial approach fails or is inappropriate then two further options need to be considered; cell therapies and tissue engineering. Cell therapies involve the direct introduction of cells into the appropriate structure in the patient e.g. stem cells injected into the myocardium to restore cardiac function (Perin *et al*, 2003 and Menasche, 2004) and fetal dopaminergic tissue implantation into the substantia nigra area of the brain for Parkinson's disease (Helmuth, 1999). However the direct addition of cells alone is not always possible e.g. where an organ's architecture is irretrievably lost such as occurs when atherosclerosis blocks an artery or the tissue or organ is lost in entirety e.g. bone resection for the surgical treatment of sarcoma. In such situations, the regenerative medicine option is to grow a replacement organ or tissue - tissue engineering. This can be done either outside the body, inside the body or by a combination of the two approaches (Vacanti and Langer, 1999). Regenerative medicine thus has a continuum of overlapping treatment options for a broad range of complex pathologies.

Virtually all surgical procedures that restore failing or damaged organs require some form of

replacement components. Conventionally, these components include totally artificial prosthesis (e.g. metal hip joints), non-living processed tissue (e.g. porcine derived heart valves), autologous transplant (e.g. saphenous vein for cardiac artery bypass grafting), live donor transplant (e.g. kidney transplant between siblings) or cadaveric donor transplant (e.g. heart transplant). Unfortunately all these components have inherent limitations. Tissue engineering is emerging as a significant potential alternative, whereby organ failure or damage is corrected by implanting living tissue or organs that are either fully functional prior to implantation or that grow or direct growth *in vivo* in order to gain the required functionality.

Regenerative medicine including tissue engineering are no longer just the dream of the research scientist. At of the start of 2003, there were over 2600 scientists and support staff spread over 89 companies with an annual spend of just under $500M - see Figure 1.1. This figure is based on a number of surveys by Michael Lysaght at CytoTherapeutics/Brown University over almost a decade. Lysaght has chosen to sub-divide his "tissue engineering" market into three categories:

1. Cellular (stem cell and therapeutic cloning)
2. Metabolic (bioartificial liver, pancreas and kidney)
3. Structural and three-dimensional tissue-surrogates (cells plus scaffold)

In this thesis, for simplicity and uniformity, Lysaght's all encompassing category of "tissue engineering" will be reclassified as regenerative medicine (excluding gene and protein therapies) and "structural tissue engineering" will be referred to as tissue engineering. This approach is in keeping with the definition, "Tissue engineering is the regeneration of biological tissues through the use of cells, with the aid of supporting structures and/or biomolecules" which was provided by the European Commission in 2001 and adopted again by the Commission in 2003 (European Commission 2001 and 2003). Thus it is only the tissue engineering subdivision of regenerative medicine and in particular the potential automation of this subdivision which this thesis addresses. Figure 1.1 shows the underlying trend in progressive growth of both the regenerative medicine industry and the tissue engineering subdivision until 1997 which is then followed by a period of extremely rapid expansion and then decline which by 2002 left the industry at approximately its 1997 level. During this turbulent time, the market leaders, Organogenesis (Canton, MA, USA) and Advanced Tissue Sciences (La Jolla, CA, USA) filed voluntary petitions for reorganisation under Chapter 11 of the US Bankruptcy Code. Many of the other companies in the subsector either went out of business (n = 13) or downsized (n = 8) during the period 2000-2002 (Lysaght and Hazelhurst, 2004). In 2002, despite substantial investment over a decade, there were only three FDA approved tissue engineered products; Apligraf (Organogenesis), Dermagraft (Advanced Tissue Sciences) and OrCel (Ortec, New York, NY, USA) with sales of $23M (25,000 units),

Year ending	1994	1997	2000	2002
Regenerative medicine - Excluding gene and protein therapies				
Annual spend	$256	$453M	$610M	$487M
Companies	>40	39	73	89
Scientists and support staff	>1,500	2,380	3,300	2,611
Cumulative investment since 1990	$1.3B*	$2.0B*	$3.5B	$4.5B
Tissue engineering subsector				
Annual spend	$41M*	$161M	$363M	$185M
Companies	6*	13*	34*	25
% Total industry's annual spend	16%	36%	60%	40%
Scientists and support staff	240*	955	1,980	975
% Total industry's scientists and support staff	16%*	40%	60%	37%
Annual spend per employee*	$171,000	$169,000	$183,000	$188,000

*Estimated/extrapolated from other data

Figure 1.1

Comparison of the trends in the economic parameters underlying both the entire regenerative medicine industry and its subsector industry, tissue engineering (Lysaght, 1995, Lysaght *et al*, 1998, Lysaght and Reyes, 2001, Lysaght 2003 and Lysaght and Hazelhurst, 2004).

$4.5M (4,500 units) and less than $100,000 respectively. Total sales for the period were less than $50M - (Carticel by Genzyme was the only other regenerative medicine product with FDA approval and sales of 2,500 units ($25M), is not included since it is an autologous cell therapy) (Lysaght and Hazelhurst, 2004). These market trends are in agreement with other independent market research reports for the period e.g. Clinica (Bromley, 2001 and 2003). Ironically during 2002, sales of Dermagraft more than tripled from $1M in the first six months to $3.5M in the last six months. The economic data for the period 1994 - 2000 indicates that the tissue engineering industry out-paced the general regenerative medicine industry, but then declined faster losing out to cell based therapies mainly stem cells. This divergence in part reflects the difference in complexities and perceived closeness to market between cell only versus cell and scaffold products. However many complex medical products had a history of early poor results followed by major success as they underwent the essential transition from research and development to product based enterprises e.g. modern pharmaceuticals (1945 - 1955), controlled release/drug delivery (1970 - 1980) and monoclonal antibodies (1985 -2000) (Lysaght, 2003).

The long term aim of tissue engineering is to facilitate the routine surgical replacement of failing organs. The established general principles of tissue engineering involve starting with a cell friendly polymer, shaping it into the desired geometry to form a scaffold, seeding the scaffold with living cells and then growing it in tissue culture medium. As the cells multiply they populate the scaffold and synthesise extracellular matrix to create a three-dimensional tissue. To date only a handful of structural tissue engineered products have been FDA approved; Apligraf (Organogenesis, Canton, MA, USA), Dermagraft (Smith and Nephew (formerly Advanced Tissue Sciences), La Jolla, CA, USA) and OrCel (Ortec, New York, NY, USA). All are skin substitutes and all are made using low volume "cottage industry" techniques e.g. Organogenesis, which at its peak as the undisputed market leader, only produced Apligraf at the rate of 500 seven centimetre diameter discs of skin per week, this was despite being Medicare approved in all fifty US states and with a potential FDA approved market (venous and diabetic ulcers) in the order of 1 - 2 million patients in the USA alone. These first generation products came directly from academia and thus did not have the necessary and important commercial considerations incorporated into to their initial research stage e.g. overall design of the construct, preclinical/clinical trials and FDA approval planning, quality control and scalable economic manufacture, marketing, distribution and reimbursement strategies (Kemp, 2003a).

Tissue engineered products could benefit a vast number of patients. In pivotal clinical trials of the first tissue engineered product, Apligraf (skin) has admirably demonstrated its benefit over traditional treatment both in terms of number of ulcers healed, speed of healing and reduced

recurrence (Falanga *et al*, 1998) but has so far failed to show the substantial cost benefits a new product requires if it is to universally displace current therapy and best practice (Schonfeld *et al*, 2000, Sibbald *et al*, 2001, Redekop *et al*, 2003). The European Commission noted that, "the comparison of treatment costs alone is not sufficient, as different treatments can result in different outcomes. The effectiveness of treatments needs to be included in the comparison" however even taking these wider cost implications into account, the current data on tissue-engineered products did not provide clear economic evidence of their superiority (European Commission 2003). This shortfall is mainly due to the high cost of manufacture associated with low volume production e.g. Organogenesis reported "...Cost of product sales continues to exceed product sales due to the high costs associated with low volume production..." (Organogenesis, United States Securities and Exchange Commission, Form 10K, 20/5/02).

Today's increasing emphasis placed on cost containment by healthcare providers is an important issue. Without efficient scale translation techniques, the resulting high cost of tissue engineering products will effectively limit their market despite the potentially overwhelming benefits to both the patient and society (Mason, 2003). In addition, aside from the issue of tissue-engineered products being expensive to produce, it is also no use being only able to make a few organs at a time when the potential demand is orders of magnitude larger e.g. today two million US patients with chronic leg ulcers could potentially benefit from current tissue engineered products. Presently tissue engineers are almost exclusively focused on proof of principle techniques rather than economic "mass production". This issue was amongst those highlighted by Lysaght and Hazlehurst when discussing the industries poor performance to date, "although scientifically strong, the companies lacked the skill sets required to develop low-cost manufacturing procedures" (Lysaght and Hazlehurst, 2004). Griffith and Naughton have also suggested that, "there are still many technical challenges to overcome before we create 'off-the-shelf' tissues that represent the translation of scientific discoveries into treatments for millions of patients. The successful large-scale production of engineered tissues requires an adequate source of healthy expandable cells, the optimization of scaffolds, and the creation of bioreactors, which mimic the environment of the body and that are amenable to scale-up" (Griffith and Naughton, 2002). These same issues, were highlighted by the National Institutes of Health Bioengineering Consortium, "For tissue engineering to meet the true clinical demands, the products must be manufactured reproducibly, in large numbers, and be available on demand. The use of an allogeneic cell source permits an 'off-the-shelf' product to be made. Scaleable manufacturing processes permit many units to be made in a unified manner, and allow diseases that effect large patient populations to be addressed in an efficient and cost effective way" (National Institutes of Health Bioengineering Consortium, 2001).

This thesis describes a novel platform technology, which potentially allows any flat sheet or tubular organ to be fabricated using an easily scalable technique ideally suited to automated mass production. It is novel in that it employs low cost disposables technology to produce a single multitasking chamber that functions as:

- The initial "mould" to give the cell-scaffold construct a specific geometry
- The bioreactor in which to grow the construct
- The delivery package for transport to the surgeon
- Potential to act as a cartridge for loading into a robotic surgical system

By keeping the tissue engineered organ in the same chamber from initial "creation" to just prior to implantation has both bioengineering (e.g. no human handling is required and therefore reduced chance of contamination) as well as major cost benefits e.g. ease of automation. Automation in turn potentially could allow cost effective operation including minimising the requirement for specialist technical support whilst reducing human error whilst satisfying the general desire by clinicians to provide a high level of quality assurance to their patients (Armstrong *et al*, 1995).

To date, in order to protect the intellectual property generated by the project a number of patents have been filed which after clustering together into discrete families/areas has resulted in 4 international and 2 national patent applications (Mason, 2000, Mason and Town, 2002a, 2002b, 2003a and 2003b, Mason *et al* 2003). Whilst the methodology is potentially suited to a range of organs and tissues, the focus of this thesis is on laying the foundations for automated production of arterial blood vessels suitable for coronary artery bypass surgery where globally over a million metres of vessel are transplanted each year.

In addition to the direct clinical applications, engineered tissue is beginning to be considered for an important role in drug discovery and development (Barnes, 2004 and Kelm and Fussenegger, 2004) including vascular applications (L'Heureux *et al*, 2001). Coupled to the established concept of high-throughput technologies such as tissue microarrays (Sauter *et al*, 2003), the automated engineering of human tissue could provide a far better alternative to current pharmaceutical research for new drug compounds (Kelm and Fussenegger, 2004). For example, if multiple "mini" human blood vessels could be produced in an automated manner and using current high throughput microwell or microfluidic based technology, then potentially, new blood pressure control compounds could be discovered more easily and far more reliably than using current "single cell thick" microwell and animal models. Likewise the testing of potential drug candidate compounds e.g. uptake, toxicity and pathogeneicity, is also a potential option.

1.1 Historical perspective

Transplant surgery to replace damaged or failing organs has had a long history of development. Physicians in India were performing skin grafts for reconstructive surgery from about 800 B.C. (Patrick *et al*, 1998a). The best known operation practiced in India at that time was rhinoplasty. This was performed by rotating a skin flap in order to reconstruct a nose, that had been amputated either in battle or as a punishment (Burnand *et al*, 1998). The basic concept of allografting is an ancient idea, Saint Cosmas and Saint Damian were third century AD twins who trained to be doctors in Syria, who having been martyred for their Christian beliefs triggered a number of "myths". The most well known example is of a Caucasian man with an ulcerated leg who collapses, the deceased twin doctors instruct the surgeons to amputate the affected leg and to replace it with the leg of a Moor who had just died in the next bed. This myth is graphically depicted, in the fresco by Fra Angelico, where a black skinned leg is attached orthotopically to a white male body. The concept of replacing one tissue with another by the 16th century was well recognised and practiced. In 1597 Gasper Tagliacozzi of Bologna published De Curtorum Chirurgia per Institionem (On the Surgery of the Mutilated by Grafting). This work was the first "manual" of plastic surgery. It gave step by step instructions on how to reconstruct noses, ears and ear lobes e.g. a description of how to use a forearm flap to make a nose replacement. It is interesting to note that The Roman Catholic Church condemned this "manual" for attempting to improve God's own handiwork! In reality it was probably because early nose reconstructions were attempts to restore the devastating stigmata of syphilis.

Complex organ transplants were not possible until "modern surgical techniques" were developed e.g. general anaesthesia by William Morton in October 1846 (In December 1846, Robert Liston performed an above knee amputation under ether anaesthetic at University College London), antisepsis by Joseph Lister in 1867 and the ability to precisely anastomose blood vessels by Alexis Carrel in 1902 (Burnand *et al*, 1998). Baronio of Milan in 1804 using free skin grafts on sheep was the first to demonstrate that autografts generally took very successfully whilst allografts were "rejected". Rejection remained the major obstacle to allografts until Peter Medawar in 1943 conducted a series of experiments showing that rejection of allografts was due to immunological attack. In 1951 Medawar demonstrated that immunosuppression significantly prolonged the survival of skin allografts in rabbits (Burnand *et al*, 1998). David Hume and Joseph Murray in Boston used immunosuppression in the first successful human kidney allografts in the 1950's. The first successful liver transplant was performed in 1967 by Thomas Starzl at the University of Colorado. Christiaan Barnard (who trained under David Hume) transplanted the first human heart on 3rd December 1967 in Cape Town. Barnard's patient Louis Washkansky was a 54 year old dentist who lived for 18 days

after the procedure (Stark, 1996a).

As of December 2003, nearly 80,000 US citizens were on transplant waiting lists compared to just over 50,000 in 1996 (1996 and 2003 Annual Reports of the US Organ Procurement and Transplantation Network and the Scientific Registry for Transplant Recipients, Richmond VA, USA). Transplant lists whilst ever growing also grossly underestimate the massive size of the problem, for example many patients who would benefit from a transplant organ are excluded from being placed on the waiting lists due to defined exclusion criteria e.g. only patients under 65 years of age with end stage renal failure are eligible under Medicare for renal transplantation. Increasing numbers of patients die whilst waiting e.g. there were over 6,000 reported US waiting list deaths in 2003 as compared to 3,000 in 1996 (1996 and 2003 Annual Reports of the US Organ Procurement and Transplantation Network and the Scientific Registry for Transplant Recipients). Some organs due to their high demand do not have "formal" waiting lists e.g. there are nearly 20 million insulin dependent diabetics in the USA who would greatly benefit from pancreas transplantation, thus this huge group is not accounted for in waiting list figures.

Demand will continue to out pace supply as the average life expectancies of the populations in the Western World continue to rise, mainly due to the reduction in infectious diseases among infants and children. Furthermore, over the next three decades most of the "baby-boomer" generation will reach retirement age e.g. today, 10% of the population is now over the age of 60, and by 2050 this figure is expected to rise to 20% (US Census Bureau 2004). Other factors compound this overall increase in demand including the "obesity epidemic" which is sweeping the Western World. Obesity is associated with many diseases including type 2 diabetes, hypertension, cardiovascular disease and osteoarthritis (House of Commons Health Committee. Obesity Report. May 2004).

Many attempts have been made to increase the supply of organs including government funded publicity campaigns, donor card systems and organisations set up in order to coordinate the exchange of organs between countries e.g. Eurotransplant (Benelux countries, Austria and Germany) (Stark, 1996b). Unfortunately none of these attempts has worked.

Another possible alternative is the use of xenografts i.e. the transplant of an organ from one species into the body of an animal of a different species. The earliest attempts were made in France and Germany. In 1906, Mathieu Jaboulay in Lyon transplanted a pig kidney into a 48 year old woman. The pig's kidney survived two days during which time it performed a physiological role including the production of urine. On the third day the kidney was rejected. Jaboulay tried again, this time using a goat's kidney but with no more success. In 1909, Ernest Unger in Berlin transplanted the kidneys from a Borneo macaque monkey into a 21 year old

seamstress who promptly rejected the kidneys and died the following day. After these failures, few surgeons were prepared to try again. Chimpanzee kidneys were transplanted secretly in the 1960's with reasonable results by Keith Reemtsma at Tulane USA e.g. Reemtsma's first patient, a 43 year old dock worker survived nine weeks after the operation. Once this work and other primate transplant work became public knowledge, emotive public outcry put an end to virtually all future primate donors. Primates being our closest "relative" in the animal kingdom are the most logical choice for organ donation. However, on ethical grounds, primates as sources of organs continued to be regarded as being too close to humans for comfort by society. As a direct result, xenograft research moved onto the pig. Pigs were selected on the basis that pig organs are of similar size to human plus pigs are slaughtered in vast numbers everyday to provide food, therefore it was thought that there would be little in the way of ethical objection. John Wallwork a transplant surgeon and David White an immunologist formed Imutran in Cambridge UK to investigate the use of pigs as xenograft material. Funded by the merchant bank, Warburg Pincus (New York, USA), work commenced in 1984. By the early 1990's genetically modified pigs were bred by Imutran which contained certain human genes which reduced early hyperacute rejection due to the species difference between pig and man. Once again emotive public opinion curtailed the research programme. Leaving aside ethical considerations, there are still a number of major scientific questions to be fully answered including whether potential "exotic" infectious elements e.g. porcine retroviruses and prions can be transmitted from the pig into the human recipient and then on to the public at large (Fox, 2001). Reportedly, the FDA is however willing to permit xenotransplant trials but only on a case-by-case basis, whilst the rest of the Western World is far less enthusiastic e.g. Japan has an outright ban on xenografts (Couzin, 2002).

Today it is surgically possible to transplant well over 20 different allograft organs including bone, cartilage, bone marrow, cornea, hearts, lungs, kidney, liver and pancreas. Due to supply and economic pressures i.e. a massive imbalance between limited supply and overwhelming demand, a new industry has been born.

The alternative source of organs and tissue is to engineer them. In the spring of 1987, the Engineering Directorate of the National Science Foundation (USA) held a major discussion meeting focused on the future of bioengineering. Whole organ replacement systems and cell culture based methods were discussed and grouped together under the working title, "tissue engineering". At this meeting the term "tissue engineering" was coined by Professor Y.C. Fung. Further meetings on tissue engineering later in 1987 involved the National Science Foundation, National Institutes of Health, National Aeronautics and Space Administration, other US government departments and US academia working in the fields of cell, molecular biology, medicine and bioengineering. In October 1987, the National Science Foundation

recognised that tissue engineering was an emerging technology with potential for rapid industrial expansion and recommended that a workshop be held to identify appropriate areas of tissue engineering research. This workshop was held in February 1988 at Lake Tahoe California. At this meeting the term "tissue engineering" was formally accepted for the fledgling industry. Following this meeting the National Science Foundation started an initiative to fund tissue engineering projects (Patrick *et al*, 1998a).

In principle tissue engineered organs could overcome the majority of problems associated with a vast shortage of available organs. Tissue engineered products need to be easily available as well as more cost effective overall than conventional donor organs e.g. allowing successful surgical intervention at a far earlier stage in a disease thus cutting hospitalisation costs whilst waiting for transplantation, reducing working days lost due to illness, improving the quality of patient's lives earlier whilst avoiding critical illness and death due to worsening organ failure.

The early pioneers of tissue engineering include Levi, Chick, Bell and Yannis. For example, Levi in the late 1970s experimented with calf skin derived collagen as an artificial mucosa for the repair of experimentally prepared wounds in the oral cavity of rabbits and dogs. No adverse effects were observed and a possible slight improvement in the rate of healing may have been observed (Levin *et al*, 1979).

In the 1980s there was a great increase in R&D in tissue engineering and biomaterials (Persidis, 1999). In 1981, a bilayer artificial skin consisting of a temporary Silastic (Dow Corning, New York, USA) epidermis covering a porous collagen dermis cross-linked with chondroitin sulphate was used to treat patients with severe burns with promising functional and cosmetic results (Burke *et al*, 1981).

In the 1990's, several tissue engineered products reached the U.S. market. For example, in 1993 Interpore International's (Irvine, USA) Pro-osteon coral-derived bone graft material was introduced, in 1996 Integra Lifescience's (Plainsboro, USA) Artificial Skin was approved as an *in vivo*, nonbiological tissue regeneration product (Persidis, 1999). In May 1998, the General and Plastic Surgery Devices Advisory Panel to the US Food and Drug Administration recommended unconditional approval of Apligraf (Graftskin) Human Skin Equivalent for the treatment of venous leg ulcers. Apligraf, produced by Organogenesis, was the first manufactured living human organ to obtain FDA approval.

1.2 Current status

To date the majority of funding for tissue engineering in the US has come from the private sector whilst in the rest of the world government funding has been more dominant (albeit at a much

lower level) (World Technology Evaluation Centre (WTEC) Panel Report on Tissue Engineering Research, January 2002). However, some of the interest and support for tissue engineering comes from diverse areas including the armed forces and very recently the prevention of bioterrorism campaign, for example, numerous battlefield related medical applications exist for tissue engineered products and biomaterials. Advanced Tissue Sciences had part of its clinical trial for Dermagraft for the treatment of chemical burns funded by the US Army Institute of Chemical Defence (Persidis, 1999). Dermagraft is an engineered living human dermis produced by seeding dermal fibroblasts onto a three dimensional bioabsorbable scaffold. Likewise other groups have received funding to create hybrid bio-electronic sensors using tissue-engineering techniques. These sensors are aimed at being part of the "front-line defences against biological attack" (Griffith, 2003).

A major nonclinical application of tissue engineered products is in the field of toxicology and the "*in vitro*" testing markets, as alternatives to certain types of animal testing e.g. cosmetics. Currently there are only a few companies in this field but their numbers are growing. For example in March 1995 Stratum Laboratories (La Jolla, CA, USA) acquired part of the *In vitro* Laboratory Testing business of Advanced Tissue Sciences for US$5 million. Stratum received licence rights to manufacture and sell Skin2 *in vitro* laboratory testing kits. Skin2 is living human skin tissue equivalent used to test skin care, household, chemical and pharmaceutical products for a variety of indications. Skin2 is already approved by the US Department of Transportation and Transport for use in corrosivity testing (Persidis, 1999). In Europe, a similar product Episkin (Imedex-Saduc, Chaponost, France) is approved by the European Commission (European Centre for the Validation of Alternative Methods – Ispra, Italy) for corrosive and pharmaceutical *in vitro* skin studies as a valid alternative to many animal studies. Other companies also employing tissue engineering technologies for toxicology testing include MatTek (Ashland, MA, USA) and SkinEthic (Nice, France).

1.3 Current good tissue practice

Good manufacturing practices for tissue engineering is a major challenge for the industry, as a result, there is continuous effort by both the regulatory authorities and the tissue engineering industry to create appropriate quality control standards and evaluate them (Mayhew *et al*, 1998). For example, the Food and Drug Administration (FDA) requires that human cell, tissue and tissue-based products (HCT/P) establishments must follow current good tissue practice (CGTP). Following two FDA discussion documents in the late 1990's ("Reinventing the regulation of human tissue" and "A proposed approach to the regulation of cellular and tissue-based products"), the FDA has now published three rules for CGTP with respect to HCT/Ps. The first rule to come into force (January 2004) , required tissue facilities to register with the FDA and to list their products ("Establishment, registration and listing for

manufacturers of human cellular and tissue based products"). The two other rules, "Suitability determination for donors of human cellular and tissue-based products" which concentrates on donor screening and testing in order to prevent contaminated tissue entering the production process, and "Current good tissue practise for human cell, tissue, and cellular and tissue-based establishments; Inspection and enforcement" which requires manufacturers to recover, process, store, label, package and distribute HCT/Ps in a way that prevents the introduction, transmission or spread of communicable diseases, will both come into effect in May 2005. (Interestingly, in light of the financial failure of the major pioneers in the field inpart due to regulatory issues, the FDA's goals with these rules is to improve protection of the public health whilst keeping regulatory burden to a minimum, and thus encourage significant innovation in the field.) (Federal Register, 2005 and FDA News, 2004)

Industry is likewise developing standards, for example, Genzyme BioSurgery (Cambridge, USA), has an ongoing quality control program (Genzyme Cartilage Repair Registry) for its Carticel (autologous cultured chondrocytes) used to repair damaged knee cartilage (as of spring 2000 there was over 4000 patients being monitored). The control program is based on the analysis of several quantifiable parameters, including viability and freedom from pathogens as well as more subjective clinical function tests e.g. Cincinnati Knee Rating System. Results to date (48 months of data) are highly favourable both in terms of patient satisfaction and in the standard of the quality of the follow up programme (Genzyme Cartilage Repair Registry).

1.4 The rôle of the engineer

The specific rôle of the engineer in the construction of a neoorgan can best be appreciated by examining the separate phases of tissue engineering an organ. For example, a much simplified view of tissue engineering can break the process down into eight discrete steps, each of which can then be studied separately (Modified from Hutmacher *et al*, 2000):

1. Fabrication of a bioresorbable three-dimensional scaffold
2. Harvest cells from animal or human patient
3. Cell seeding onto the scaffold in a suitable bioreactor
4. Cell proliferation and differentiation
5. Growth of mature tissue
6. Storage and transportation
7. Surgical implantation
8. *In vivo* assimilation and adaptation

Each phase must be fully understood in order to create a fully functional, reliable and reproducible tissue engineering construct.

1.5 Components

Yannas at MIT (Cambridge, MA, USA) has attempted to crystalise the interaction of the various components required to synthesis *de novo* tissues and organs into some universal "rules" (Yannas 2004). Interestingly, Yannas's conclusions include:

1. Following severe trauma of an adult organ in which the stroma has been severely injured, the wound closes by contraction and scar synthesis. When the stroma has been spared, the wound closes by spontaneous regeneration; contraction is not observed
2. The synthetic barrier to overcome during induced regeneration of most organs is the synthesis of the non-regenerative tissue, the stroma
3. The central problem in the synthesis of most organs is stroma synthesis, a process that requires the presence of an active scaffold

What therefore are the components for the successful engineering of tissue? The European Commission defined tissue engineering as the regeneration of biological tissues through the use of cells, with the aid of supporting structures (scaffolds) and biomolecules (European Commission, 2001). Thus the important basic components that the tissue engineer can choose from in order to make a product include; cells, scaffolds, and bioactive molecules. A bioreactor, not a component of the tissue is needed to combine them together. One or more of the components may be required depending upon the final desired product.

1.5.1 Cells

The source of cells to use is an interesting topic. The "ideal" cells must function physiologically and biochemically, integrate fully and be non-immunogenic which at the present day means from the patient themselves e.g. Carticel (a sample of healthy cartilage is arthroscopically removed from the patient. The chondrocytes are grown *in vitro* (Genzyme Biosurgery (Cambridge USA)) for several weeks to obtain a sufficient quantity of cells prior to surgical implantation back into the same patient). Since these cells are autologous, immune rejection is not an issue. The drawbacks to autologous cells is time and cost. Culturing takes weeks and may not always be successful, thus these cells would not be an ideal choice in anything other than elective procedures. Furthermore there is significant interpatient variability e.g. biopsy size, sterility, endotoxin levels, cell viability and population doubling times (Mayhew *et al*, 1998). Cost is another factor, growing up individual batches of cells is much more expensive than batch processing of a single cell line (Lowel, 2003).

Cells from nonself i.e. allograft have advantages e.g. easily available but also have drawbacks e.g. potentially immunogenic and potentially can carry pathogenic agents. Cells producing immunogenic effects would require long term immunosuppressive drugs (far from ideal) in

order to avoid tissue rejection, fortunately not all cells produce such a reaction. For example Organogenesis uses human dermal fibroblasts and epidermal keratinocytes derived from neonatal foreskins to produce Apligraf. These cells are non immunogenic because they do not express Major Histocompatability (MHC) Class II surface proteins. In order to reduce the chance of pathogen transfer Organogenesis treats the harvested cells with antibiotics and antifungals. Also prior to production of a master cell bank, the maternal blood and neonatal foreskins are screened for viruses e.g. HIV, Hepatitis A, B and C. Once the master bank was produced the cells are repeatedly tested for viruses, bacteria, yeasts and mycoplasma. Furthermore, each bank is also tested for carcinogenic potential, biochemical defects and chromosomal abnormalities.

Since allogenic cells are much more suitable for the production of off the shelf tissue engineered organs, it may well be an option to genetically engineer the cells in order to reduce immune rejection, but to do this and ensure safely is likely to be a protracted process.

Recently pluripotent embryonic stem cells (ES cells) have become a serious option for tissue engineering. Stem cells are self replicating and can also generate a number of more specialised cell types as they multiply. Stem cells are highly plentiful in the early embryo but very difficult to find in the adult. At conception, the egg and sperm fuse to produce a zygote (one single cell), this then divides countless times to generate the 216 different cell types to produce a human. The zygote and the 8 cells created by the first 3 divisions are each capable of developing into an entire human, these stem cells are termed totipotent stem cells. As the cells continue to divide the number of different cell types each stem cell can produce becomes reduced. After 5 days a hollow ball of cells (blastocyst) is formed. The outer layer of cells goes on to form the placenta whilst the inner group (approximately 50 cells) is ready to produce the embryo. This inner group of cells can make most embryonic cell types, but cannot make all the cell types needed to develop an entire functional human, these stem cells are termed pluripotent embryonic stem cells. As the cells divide further so the cells become more specialised (differentiated) and lose their ability to produce different cell types (multipotent) (Medical Research Council, 2000).

Human ES cells were gown for the first time *in vitro* in February 1998, by James A. Thompson at the University of Wisconsin USA, (John D. Gearhart of John Hopkins University and researchers at Geron Corporation (Menlo Park, CA) were also carrying out related studies). Thompson's blastocyst derived ES cells after a 4 month period of undifferentiated proliferation were capable of deriving all three embryonic germ cell layers i.e. ectoderm, endoderm and mesoderm. This revolutionary work was published in Science on the 6th November 1998 (Thompson *et al*, 1998). Previously only mouse stem cells had been successfully cultured *in vitro*. The basic technique for producing human ES cells involves; culturing a human blastocyst,

removing the outer layer of cells to leave only the inner cell mass, this inner cell mass is then chemically disaggregated in order to separate the individual cells. Individual cells can then be grown up into colonies on a feeder layer of non-dividing mouse fibroblasts. Finally, by adding specific differentiation factors, different differentiated cell types can be produced e.g. "gut epithelium (endoderm); cartilage, bone, smooth muscle, and striated muscle (mesoderm); and neural epithelium, embryonic ganglia, and stratified squamous epithelium (ectoderm)" (Thompson *et al.* 1998). However to date, mouse embryonic stem cell work continues to be more advanced than its human equivalent e.g. Klug in 1996 at Indiana University, produced a greater than 99% pure culture of highly differentiated cardiomyocytes from murine ES cells which *in vitro* rhythmically beat and *in vivo* survived for a minimum of 7 weeks when implanted into the hearts of adult dystrophic mice (Klug *et al*, 1996), it was not until recently that similar *in vitro* observations have been reported using human embryonic stem cells (He at al, 2003).

One potential problem of using ES cells for tissue engineering is that all the cells must become sufficiently differentiated so as to be incapable of producing unwanted cell types within the finished product. Rigorous purification of ES cells will therefore be required. Another challenge is in the area of immunogenicity. One potential option is to take cells from the specific patient, remove the DNA and then inject this into donated human eggs (the fundamental step in therapeutic cloning) which have previously had their own DNA removed (usually termed: somatic cell nuclear transfer), this "egg" is then matured to form a blastocyst and the above procedure performed. This method should produce cell types genetically identical (apart from the mitochondrial DNA) as the patient, thus in theory no rejection problems. The drawbacks include time and cost. A potential alternative could be to produce a "universal donor" ES cell i.e. an ES cell which is compatible with any recipient. In order to create such a cell type all the molecules recognised as foreign by the host's immune system would have to be altered/ removed probably by disrupting or altering a significant number of genes (Denning and Priddle, 2003). However, in theory if such an ES cell were constructed it could potentially be used to make universal tissue engineered products which could then be an off the shelf item.

An alternative source of stem cells is from bone marrow and includes adult mesenchymal stem cells (MSCs). These could either be autologous or like ES cells be potentially modified to avoid detection by the host's immune system thus allowing a universal cell line to be created. Osiris Therapeutics (Baltimore, USA) was one of the first tissue engineering companies to develop MSC technology. Under the direction of Mark Pittenger, Osiris is working with MSCs in the areas of orthopaedic and cardiovascular regeneration (Cahill *et al*, 2003).

A final potential source of cells is from animals i.e. xenogeneic. Animals cells are easy to produce, however, since they are from a different species these cells will require extensive

genetic manipulation in order to make the cells "invisible" to the human immune system. Furthermore, as in the case of whole organ xenotransplantation concerns over pathogen transmission e.g. prions and retroviruses, has not yet been conclusively settled.

In conclusion, whilst autologous cells are very unlikely to be the long term future for tissue engineering, initially these cells are likely to be the best route forward for the majority of applications. This strategy provides the highest level of patient safety as it avoids the potential disease transmission and immunological complications inherent in the alternative options, but does incur more challenging processing issues posed e.g. initial biopsy collection, 100% reliable tracking from the biopsy leaving the patient to the tissue being implanted back and interpatient cell variability.

1.5.2 Scaffolds

In order to produce an *in vitro* biological tissue or to repair tissues *in vivo* there is very often a need for an initial structure, which is generally referred to as a scaffold. This scaffold is itself assembled on a solid object either a mould or a former, which will be referred to as a mould/former. Thus the mould/former sets the overall structure and dimensions of the scaffold. In principle to create organs, donor material is obtained, the tissue is dissociated into individual cells, the cells are attached to a scaffold, and this device is implanted into the patient in a favourable location where the immobilised cells grow and function.

Scaffolds must ideally possess the following characteristics; be an adhesive substrates for cells, promote cell growth, and allow retention of differentiated cell function. Materials used as scaffolds for cell transplantation must be biocompatible and biodegradable, processable into desirable shapes, highly porous with large surface:volume ratios, and finally possess adequate mechanical strength. The scaffold can take the form of a simple sheet, tube or a more complex three-dimensional structure. The scaffold allows the transplanted cells a means to organise into a newly forming organ.

If cells are to be seeded onto preformed scaffolds, these need to be highly porous structures in order to allow large numbers of cells to both penetrate the three-dimension shape and to be accommodated. Furthermore, to allow initial access, the pore diameter must be much larger than the specific cells that are intended to populate it plus as most cells are anchorage-dependent, total pore surface area must be large enough to accommodate high cell growth rates. Thus a homogeneous interconnecting pore network is essential for uniform cell seeding, growth and diffusion of nutrients and metabolites (Vacanti *et al*, 1991).

1.5.3 Bioactive molecules

The biochemical environment of a tissue plays a major role in its development, maturation

and physiology e.g. co-ordination, both *in vitro* and *in vivo*.

The co-ordination of cell activity allows physically associated cells to act in a coordinated manor. In multicellular organisms, information is transmitted from a single cell back to itself (autocrine), one cell to another by direct intercellular communication (paracrine), systemic fluid transport of soluble signalling molecules (endocrine), and local cellular deposition of insoluble signalling molecules i.e. the extra cellular matrix (ECM). It has been proposed that "dynamic reciprocity" exists between cells and their extracellular matrix, which partially determines cell shape, biosynthesis, migration and attachment (Bornstein *et al*, 1982). Two way communication between the cells and their surrounding ECM is essential for embryonic development, wound repair, and tumour metastasis.

In tissue engineering a range of bioactive molecules have already been experimented with ranging from simple ions e.g. copper ions (Ahmed *et al*, 1999) to more complex molecules e.g. growth factors. Several cell receptors are known to be sensitive to copper and zinc ion concentration. Ahmed *et al* (1999) have shown that individual cell types behave differently when exposed to different copper ion concentrations e.g. Schwann cells grew in a fibronectin mat incorporating 1 μM copper ions but their growth was inhibited above 10 μM, this is a stark contrast to fibroblasts whose growth was unaffected at up to 200 μM incorporated into the mat (Ahmed *et al*, 1999). These ions can regulate the adhesion and mobility of cells to a surface or to each other. Growth factors can either stimulate or inhibit cell division, differentiation, and migration. They can up regulate or down regulate cellular processes such as gene expression, DNA and protein synthesis, and autocrine and paracrine agent release. Growth factors can interact with one another in additive, cooperative, synergistic or antagonistic manners (Patrick *et al*, 1998b). These factors have long been added to cell culture media *in vitro* to enhance cell proliferation. Alternatively, growth factors can be added to the scaffold either during its manufacture or coated onto the scaffold after manufacture in order to influence subsequent cell behaviour. Controlled delivery of growth factors is possible by using a scaffold made from an appropriate biodegradable materials loaded with the desired factor. The growth factor can be strategically located within the scaffold, thereby creating a gradient to preferentially enhance cell attachment and/or direct cell migration. Possible growth factors for successful tissue engineering include; basic fibroblast growth factor (bFGF) for endothelial and smooth muscle cells and vascular endothelial cell growth factor (VEGF) for endothelial cells (Moses *et al*, 1995). Scaffolds can be made more "cell friendly" by the incorporation of specific bioactive sequences. Short peptide sequences derived from cell binding regions of extracellular matrix proteins can be utilised to achieve biospecific adhesion of cells to biomaterials e.g. arginine-glycine-aspartic acid (RGD) (fibronectin, collagen, vitronectin, laminin A and B and thrombospondin active repeat cell binding sequence), valine-glycine-

valine-alanine-proline-glycine (VGVAPG) (elastin active repeat cell binding sequence). Hydrogels containing RGD peptide sequences significantly improve the healing of diabetic ulcers, a notoriously difficult lesion to treat (Steed *et al*, 1995). Similar constructs again using the RGD fragment have been demonstrated to be of benefit in treating partial thickness burns (Hansbrough *et al*, 1995). Specific short peptide fragments e.g. RGD have an advantage over the complete "parent" protein in that they may be more stable during processing i.e. able to better resist denaturation and degradation that can occur with "natural proteins" thus be more amenable to processing without losing their vital biological function.

A complicated area of research is the effect of growth factors on one another e.g. they may up-regulate or down-regulate the production of other growth factors. Another important factor is whether the cells are quiescent or active in the construct. Whether they are in a two or three-dimensional arrangement will influence endogenous growth factor production and thus also the response to exogenously applied bioactive molecules. For example, when growing a tissue engineered blood vessel it will be necessary to co-culture smooth muscle cells and endothelial cells at the same time, these two cell types cultured together may well respond differently to exogenous growth factors than will cultures of each cell type alone due to their own interactions.

Johnson of Alkermes Inc (Cambridge, MA, USA) has successfully incorporated a bioactive protein (recombinant human growth hormone (rhGF)) into PLGA microspheres using an encapsulation technique which is "cryogenic, non aqueous and did not utilise surfactants or emulsification", i.e. near ideal for preserving protein bioactivity. Since no water is present during the encapsulation process this greatly reduces unwanted chemical modifications, denaturing and aggregation. The rhGF retained its bioactivity, which was demonstrated both *in vitro* and *in vivo*. *In vivo* experiments included injecting subcutaneously the microspheres into rhesus monkeys resulting in elevated serum levels of recombinant human growth hormone for more than one month. This period of time was twenty times the length of the control i.e. unencapsulated rhGF (Johnson *et al*, 1997). This result suggests that possibly any protein could be stabilised in a similar manner i.e. forming a complex with zinc, atomising this protein-zinc complex followed by lyophilising into a powder and finally encapsulation within a polymer which can release the protein in an unaltered and controlled manner.

1.5.4 Bioreactors

Freed and Vunjak-Novakovic have defined tissue-engineering bioreactors as, "*in vitro* culture systems designed to perform at least 1 of the 4 following functions:

1. Establish spatially uniform cell distributions on three-dimensional scaffolds

2. Maintain desired concentrations of gases and nutrients in the culture medium
3. Provide efficient mass transfer to the growing tissue
4. Expose developing tissues to physical stimuli" (Freed *et al*, 2000)

To this list needs to be added the ability to be produced in an economically viable and scalable manner which is compliant with CGTP, quality control and other regulatory issues plus allowing close monitoring of its environment including dissolved oxygen tension, pH, temperature, nutrient uptake and allowing the living construct to be directly visualised e.g. cell and overall construct morphology (Griffith and Naughton, 2002, National Institutes of Health Bioengineering Consortium, 2001).

The simplest bioreactor is a static culture, where mass transfer from the culture medium is via molecular diffusion since there is no fluid movement within the bioreactor and gas exchange is via culture medium/gas surface aeration. More complex bioreactors involve the movement of the culture medium relative to the construct e.g. rotating vessels ideally have a laminar flow of culture medium over the developing construct (Martin *et al*, 2004).

A great variety of different bioreactors aimed at tissue engineering have been tried. These include spinner flasks, rotating vessels, rotating wall perfused vessels, perfused columns and perfused chambers (Temenoff *et al*, 2000 and Freed *et al*, 2000). These different bioreactors employ a host of different properties including; the constructs are either fixed in place, or allowed to freely move and medium exchange is either batchwise or continuously recirculated and exchanged. Gaseous exchange is usually continuous either by an internal or an external membrane. Laminar culture medium flow is aimed at in the reactors. To date no one method has been proven to be any better than any other, nor has any one approach proven to be entirely satisfactory. Niklason, however, has demonstrated that a pulsatile bioreactor which mimics embryonic blood vessel development does produce tissue engineered blood vessels with much greater wall strength and superior histology to previous attempts at blood vessel engineering using non-pulsatile reactors (Niklason *et al*, 1999).

1.5.4.1 Mechanical and physiological stimuli

Mechanical forces on cells and tissue engineered constructs like the biochemical environment play a significant role in their development and maturation (Guilak, 2002). The mechanical environment provides physical stimuli to the cells. These stimuli are "translated" by the cells into biochemical stimuli resulting in a change in the cells behaviour e.g. up or down regulating gene expression, release of autocrine or paracrine factors. Mechanical forces on cells are a natural event occurring all the time *in vivo* e.g. when a skeletal muscle contracts its tendon exert a force on its bone attachment likewise cartilage responds to mechanical forces by

remodelling itself to match the local requirement i.e. load bearing surfaces are thicker and stronger than non load bearing surfaces within the same joint. A good example of the role of mechanical stimuli is the artery. Arteries are subjected to repeated pressure changes (cyclical strain) due to the rhythmical nature of the pumping action of the heart. Furthermore, the blood flowing through the arteries exerts a shear force on the lining endothelium. These forces produce significant biochemical changes in both the endothelium (Patrick *et al*, 1995) and the smooth muscle cells in the wall of the vessel (Owens, 1995). Blood flow induced wall shear stress and cyclical strain modulate gene expression of certain bioactive molecules synthesised and secreted by endothelial cells (Patrick *et al*, 1995). Excessive i.e. pathological intraluminal pressure via the cells in the vessel wall as in hypertension, leads to an overall increase in the absolute amounts of both collagen and elastin in the wall (Wolinsky, 1970).

Niklason of Duke University USA and others have demonstrated that the mechanical environment in which a tissue engineered construct such as an artery is grown and matured has a significant effect upon its biological and functional properties (Niklason *et al*, 1999). Niklason tissue engineered small calibre arteries using a PGA tubular scaffold and a pulsatile perfusion system. Experimental constructs were cultured under conditions of pulsatile radial stress for eight weeks with control constructs cultured without this stress. After 8 weeks, the histological appearance of the pulsed constructs was much more similar to natural artery than the control vessels. The mechanical properties of tissue engineered blood vessels is due to the smooth muscle cells and the extracellular matrix which they produce since the PGA scaffold fragments and degrades with time. Pulsed constructs had thicker walls and far higher burst strengths than non-pulsed constructs. This is in part explained by the fact that collagen level in pulsed vessels was statistically similar to native artery whereas non pulsed vessels contained significantly less. In *in vivo* studies the pulsed constructs performed significantly better than their non-pulsed controls.

1.5.5 Storage

Having been manufactured using CGTP, it will be necessary to make the finished product easily available to the surgeon to implant. Presently this issue revolves around the question; deliver fresh with a short shelf life or deliver in a cryopreserved form with a much longer shelf life but with more overall product complexity. Cryopreservation of cell lines is relatively well understood, however, successfully cryopreserving three-dimensional tissue constructs is still in its infancy. Organogenesis opted to deliver their skin product Apligraf fresh with its own temperature controlled packaging with a life span of five days (Parenteau, 1999). Advanced Tissue Sciences instead opted to cryopreserve their skin product, Dermograft at -70°C (Naughton, 1999). Long shelf life is highly desirable if tissue engineered products are to be widely used and especially if these products are to be employed in non-elective

procedures.

1.6 Project aims

Overall the challenges for tissue engineering are not discrete entities isolated from one another. Therefore this thesis study investigated the topic in a holistic manner by addressing a number of overlapping and interacting factors centred on the brief to provide a foundation for the design of a commercially viable, automatable and scalable bioreactor platform technology. The areas covered include bioreactor design, construct fabrication, polymer selection and derivatisation with bioactive molecules, cell selection and monitoring/imaging solutions.

2.0 Alginate

After thorough discussions and review of the scientific literature, and for certain characteristics required by the tube fabricating devices described in later chapters, it was decided to focus on alginate as the scaffold polymer. This chapter contains the background relating directly to the choice of alginate, while in Appendix I, there is a review of some of the other potential polymers that were considered.

2.1 Background

In 1883, the Scottish manufacturing chemist Stanford was the first to describe algic acid and algins now termed alginic acid and its salts, alginates respectively (Stanford, 1883a; Stanford 1883b). Two years earlier Stanford had patented a process to extract algin from seaweed and subsequently set up a company to exploit the technology (Stanford, 1881; Draget *et al*, 2004). The patent outlined how alginate could be extracted under pressure from a solution of pulped seaweed using sodium carbonate and then precipitating the alginate from the resulting solution by the addition of acid. From his research, Stanford demonstrated that alginic acid contained only carbon, hydrogen, oxygen and nitrogen (the entire nitrogen component is now attributed to impurities) (Stanford, 1883c; Draget *et al*, 2004). However, in the 1920's various groups concluded that alginate was in fact composed of polyuronic acid residues. Later these residues were shown to be β-D-mannuronic acid (abbreviated to M) and α-L-guluronic acid (abbreviated to G). These residues are either in continuous runs to create blocks of one type of uronic acid residue or in mixed runs. There are four main types of seaweed which produce commercial alginate, see Figure 2.1.

Younger seaweeds are richer in polyM but as seaweed matures the proportion of G residues increase. This increase is due to the action of epimerases. The alginate content of seaweed is in the range 10 - 50% depending upon species, season of the year and part of the plant. There is also variability within the plant with respect to the M:G ratio, this is to allow different parts of the plant to have different and thus structurally appropriate roles i.e. the M:G ratio decreases from the fronds to the stem (stipe) to the anchor/holdfast. This change in ratio provides good strength at the anchor and good flexibility at the fronds (Tombs *et al*, 1998).

In the 1990's the total annual production of alginate was in the region of 30,000 tonnes (Rehm and Valla, 1997). Currently commercial alginates are extracted from seaweed by initially milling and washing, this is followed by dissolution by heating with alkali and then precipitation with calcium chloride. The precipitate is decolourised, acid treated and soaked in sodium carbonate solution (3%). Finally the product is dried and milled to produce an off-white powder (Draget *et al*, 2004). Alginates are either single source or often blends of alginates with different M:G ratios to give an alginate of a desired property e.g. Manucol DM

Seaweed source	Harvesting location	Seaweed component	Average alginate content %	Average M:G monomer ratio
Laminaria hyperborea	Scotland + Ireland	Fronds	25 - 38	1.1
		Stipes		0.5
Laminaria digitata	Norway + France	N/A	18 - 26	1.5
Macrocystis pyrifera	North America	Fronds	20 - 31	1.6
Ascophyllum nodosum	Scotland + Ireland	N/A	19 - 30	1.5

Figure 2.1

Table demonstrating the variability in both quantity and composition of alginate from the most common seaweed sources.
(Based on Chaoyuan, 1990)

(Kelco, San Diego, USA).

In 1964, Linker and Jones were the first to describe alginate to be a natural product of bacteria (interestingly isolated from the sputum of a cystic fibrosis patient with a Pseudomonas chest infection) (Linker and Jones, 1964). This discovery has helped pave the way for alginate to be potentially produced by industrial fermentation, a far more controlled process than harvesting seaweed (Sabra *et al*, 2001). However, exploitation has not been rapid due to the current pricing of seaweed alginate at an average of \$5 - 20 Kg^{-1} (Rehm and Valla, 1997). At this price range, bacterial alginate cannot currently compete. However, this may change due to environmental concerns associated with the harvesting and processing of seaweed. Another important driver is there is a rising demand for high purity alginates by the pharmaceutical industry where the average price is nearer \$40,000 Kg^{-1} (Sabra *et al*, 2001; Rehm and Valla, 1997)

2.2 Alginate chemistry

Alginate is a family of unbranched binary copolymers composed of G and M subunits (Thu *et al*, 1996a). The copolymers are highly variable with respect to the order of the G and M monomers with both inter and intra organism variation (Figure 2.1). Furthermore, variability is also effected by external influences e.g. seasonal changes and different growing conditions (Saraswathi *et al*, 2003, Chaoyuan, 1990). In general, the monomers are in continuous runs (blocks) of either M or G interrupted by regions of alternating structure i.e. -MG-. No regular repeat sequences have been observed (Thu *et al*, 1996a). Characterisation of the coploymers e.g. quantifying the frequency of short runs of -GGGG-, can be performed using nuclear magnetic resonance (NMR) technology (Grasdalen, 1983).

For alginate, X-ray diffraction studies have revealed that polyM acid regions bind divalent ions to form an extended "three fold ribbon like" conformation, whereas polyG acid regions bind with divalent ions to form a "buckled two fold " structure (Atkins *et al*, 1973). Both types of structure can bind calcium ions, however, homopolymeric polyG continuous sequences of approximately 20 residues or greater bind far more strongly than polyM segments and mixed polyG/polyM segments, thus polyM segments and mixed polyG/polyM segments only play a very minor role in alginate gel binding. The homopolymeric polyG 20+ continuous sequences leads to the formation of "junction zones". Junction zones are terminated when polyguluronic residues are no longer continuous i.e. a mannuronic residue disrupts the sequence (Morris *et al*, 1978). The "three fold ribbon like" structure has been likened to an "egg box" (Grant *et al*, 1973). Positively charged calcium ions (eggs) occupying negatively charged cavities within the overall structure (egg box). This egg box structure is relatively unchanged when the water is removed from the hydrogel. To further clarify: the egg box process involves intrachain

polyG regions interacting with divalent ions e.g. calcium, strontium and barium. Calcium ions are commonly used for gelation processes in the food industry. There is an optimal calcium ion concentration depending upon the amount of polyG residues in the specific alginate, usually to a maximum of 0.5 M (Tombs *et al*, 1998). In general, higher polyG alginates at an appropriate calcium ion concentration give stronger gels, however, higher polyM alginates are less sensitive to calcium ion concentration.

The calcium ion concentration and the speed with which the calcium ions are added is crucial to the overall properties of the resulting gel. Too few calcium ions gives rise to weaker gels, however, if too many calcium ions are added too quickly this results in the formation of a precipitate and not a pure hydrogel. Cross-linking to form alginate hydrogels can be accomplished either by allowing divalent ions to diffuse in (diffusion setting) e.g. exposing sodium alginate to $CaCl_2$ solution or by internal setting where a slower acting cross-linking agent is premixed with the alginate e.g. $CaSO_4$. The two methods have totally different gelling kinetics, diffusion setting is very rapid whilst internal setting is far slower and is therefore generally considered to be more controllable (Draget *et al*, 2004). For the diffusion setting method, upon addition of the cross-linking solution e.g. $CaCl_2$ solution, interfacial polymerisation is instantaneous with precipitation of calcium alginate followed by a more gradual gelation of the interior as calcium ions diffuse through the alginate (Zhang *et al*, 2000). One of the main characteristics of the diffusion setting method is that the final gel distribution is not homogeneous i.e. a high concentration at the interface but gradually decreasing towards the centre of the gel (Skjåk-Braek *et al*, 1988). Maximum inhomogeneity is achieved with a low molecular weight alginate cross-linked with a dilute cross-linking solution; conversely maximum homogeneity is achieved with high molecular weight alginates cross-linked with high concentration cross-linking agents. One other factor of importance is the presence or not of non-gelling ions These ions result in increasing homogeneity with their increasing concentration (Draget *et al*, 1997).

As alginate gels set, there is an initial overall volume reduction (shrinkage) of the initial volume of unset alginate (Martinsen *et al*, 1989). The degree of initial shrinkage is dependant on a number of factors including the concentration of the cross-linking agent (increased concentration leads to increased shrinkage), alginate composition (overall higher G contents leads to lower shrinkage) and average length of the monomer runs/blocks (higher fractions of G blocks results in less shrinkage) (Martinsen *et al*, 1989). After this initial shrinkage, which is complete in minutes depending upon environment (e.g. pH), both further shrinkage or swelling (volume expansion) can occur. The time frame for these secondary volume changes is hours to months (Zhang *et al*, 2000).

Alginate gels are thermostable and only melt when heated to in excess of 120°C (Sutherland,

1990). The physical properties of alginate gels depend upon the ratio of homopolymeric polyguluronic 20+ continuous sequences to other sequences. Gels high in homopolymeric polyguluronic 20+ continuous sequences are much more brittle than gels low in homopolymeric polyguluronic 20+ continuous sequences which are weaker but more flexible (Sutherland, 1990). The stiffness of gels increases in the order poly MG, poly M, poly G, i.e. gels composed predominantly of poly MG gels are the weakest, whereas gels composed mainly of homopolymeric polyG 20+ continuous sequences are strongest. The average degree of polymerisation of an alginate gel varies between different seaweed species (80 - 700) giving a wide range of molecular weights (150,000 - greater than one million Daltons). By comparison alginates produced from bacteria tend to be far smaller (Tombs *et al*, 1998).

2.3 Regulatory issues

In order for alginate hydrogels to be used as a tissue engineering scaffold, the polymer must meet certain key pharmacological and toxicological requirements including high biocompatability, predictable degradation and excretion. Oral administration of alginate (a long-standing indigestion medication) has an impeccable track record e.g. routinely prescribed in pregnancy with no known significant safety concerns (Lindow *et al*, 2003). Animal studies deploying radio-labelled alginate have demonstrated that oral administered alginate is not absorbed systemically (Hagen *et al*, 1996). Data e.g. elimination rate, bioavailability and tissue distribution for non-oral administration (intravenous, intramuscular, intraperitoneal and subcutaneous routes) is starting to become available in the scientific literature. For example, the fate of alginate following intravenous and intraperitoneal (intraabdominal cavity) injection has been found in a rodent model to be dependent upon its molecular weight. Fractions less than 48,000 KDa were excreted in the urine, whilst the larger polymer fraction remained in the circulation but with little deposition in organs at 24 hours (Al-Shamknani *et al*, 1995). Similar data were recorded by Hagen *et al*, who also found some alginate accumulation in the tissues (spleen, liver and kidneys). This data suggests that since alginates are not readily degraded under physiological conditions, the molecular weight of any alginate implanted in the body needs to be below the renal filtration threshold (in man, the renal filtration threshold is approximately 69,000 KDa which equates almost exactly to the size of the smallest plasma protein albumin (Guyton, 1986). With the increasing biomedical and pharmaceutical applications of alginate during the late 1990's, more data was deemed necessary (Skaugrud *et al*, 1999). In response, the American Society for the Testing of Materials (ASTM) (West Conshohocken, PA, USA) in May 2001 produced a guide (F 2064 - 00) titled "Standard guide for characterisation and testing of alginates as starting materials intended for use in biomedical and tissue-engineered medical product applications" in response to the growing interest of alginate for tissue engineering. The regulatory issues covered include;

documentation, impurity levels, safety and toxicology, good manufacturing practice (GMP)/ ISO 9000 guidelines and regulatory standards. Included in the guidelines is information on the selection of appropriate testing methodologies and safety criteria. Critical parameters are also described including; G and M monomer content, molecular weight, viscosity, dry matter content, heavy metal content, bioburden and endotoxin content. This guide represents some of the drive ASTM is making to ensure quality and standardisation of tissue-engineered medical products (TEMPS) whilst being an aid for success clinical applications plus helping expedite the necessary regulatory approvals (Dornish *et al*, 2001).

Today, the majority of commercially available alginates are not fully characterised with respect to the endotoxin levels, impurities, M:G ratio, their source or viscosity. Implanted impure alginates are known to trigger the host's immune system e.g. foreign body response (Zhang *et al*, 2001). Because there is much confusion in the scientific literature, the source of this immune reaction in well characterised alginates and whether human monocytes/macrophages produce a fibrotic response to alginates is under investigation by the FDA, Centre for Devices and Radiological Health, Office of Science and Technology (Annual Report, May 2000). Commercial alginates have been demonstrated to contain at least 10 - 20 immunoreactive contaminants which if removed by electrophoresis results in a highly significant reduction in fibrotic reaction when implanted for three weeks into a rodent model (Zimmermann *et al*, 1992). Pronova ultrapure (UP) sterile sodium alginates manufactured by Nova Matrix (FMC Biopolymer, Oslo, Norway) are produced in compliance with current Good Manufacturing Practice (cGMP - 21 CFR 210,211) using validated analytical methods and documented in a Drug Master File (DMF) submitted to the FDA. The process operations are compliant with ISO 9001:2000 and ISO 13485:2003 (medical device directive). Furthermore Pronova UP alginate satisfies ASTM F 2064 - 00 for use in tissue engineering.

On an historical note, many researchers have reported that alginates with M and MG runs/ blocks both *in vivo* and *in vitro* resulted in an inflammatory response and fibrotic over-growth (foreign body reaction) (Zimmermann *et al*, 2000; Otterlei *et al*, 1991; Draget *et al*, 1997). For example, Otterlei *et al*, showed that human immune cells (monocytes) secreted various inflammatory cytokines (tumour necrosis factor alpha (TNF-alpha), interleukin 1 (IL-1) and interleukin 6 (IL-6) in response to alginates. Low G alginates were an order of magnitude more potent in inducing inflammatory cytokine production compared to high G alginates. Similar results were obtained by others and the conclusion drawn was that the M component was suspected as being the causative agent (Otterlei *et al*, 1991; Sabra *et al*, 2001). Today, with the availability of purified alginates, this conclusion is generally agreed to no longer hold, and that the adverse events observed were the result of contamination and not the M or G components of the polymer (Klock *et al*, 1994; Klock *et al*, 1997).

2.4 Life science research and clinical applications

Whilst alginates have many commercial human applications including extensive utilisation in the food and drink industry, see Figure 2.2, it is its existing roles in life science research and clinical applications which potentially justify its deployment for tissue engineering. The major applications are in pharmaceuticals, surgery and wound care and cell encapsulation.

2.4.1 Pharmaceutical applications

Alginate is currently deployed by the pharmaceutical industry as both a treatment and as an excipient (a harmless substance added to a drug to assist its administration).

Oral alginate-based treatments for the symptomatic relief of gastritis and oesophagitis ("heart burn") e.g. Gaviscon (GlaxoSmithKline, Brentford, Middlesex, UK) have been a part of routine clinical medicine since the 1940's (Mandel *et al*, 2000). The mechanism of action being that in the presence of stomach acid, alginates precipitate to form gels. If bicarbonate is included in the preparation, the bicarbonate in the presence of stomach acid reacts to form carbon dioxide which is trapped in the gel, thus creating a foam which floats on the gastric contents. These so called, "raft-forming" formulations have full FDA approval, minimal if any side effects, non toxic and are therefore sold freely as over-the-counter medicines. (The FDA does not specify an acceptable daily intake (ADI) for alginate - this is the highest possible classification for a food additive.)

The use of alginate as an excipient in oral drug formulations is because of their unique thickening, gel forming and stabilising properties (Tonnesen *et al*, 2002). Traditionally and in the main, alginates have been used as tablet binding agents (with a high margin of safety given their lack of toxicity), however their other roles include controlled release systems and as masking agents for unpleasant tasting medications (Tonnesen *et al*, 2002, Office of Science and Technology Annual Report 2000 and Skjåk-Braek *et al*, 1996). (Microencapsulation and controlled release systems using alginate are used for the immobilisation and controlled release of pesticides, biocatalysts products (Skjåk-Braek *et al*, 1996))

The use of alginate as an excipient in parenteral (non-oral) preparations is also being evaluated in animal models e.g. subcutaneous injections for chemotherapy agents (Yoshikawa *et al*, 1999).

2.4.2 Surgical applications

Anecdotal evidence suggests that the use of seaweed for dressing wounds has a long history, going back possibly thousands of years (Thomas, 2000). However the modern use of alginates in surgery and wound management can trace its origins back to Major George Blaine of

Industry	Sub-sector	% Total alginate used	Examples of use/products
Textile printing	All	50%	Thickening agents
Food	All	30%	Gelling, thickening agents + stabilisers
Paper coating	All	6%	Paper coating - surface sizing
Health	Medical	5%	Wound dressings and stomach ulcer medication
	Pharmaceutical		Microencapsulation and controlled release additives
	Dental		Dental impressions
Welding	Welding rods	5%	Flux for welding rods
Other	All	5%	Pigment suspension in paint

Figure 2.2

Table giving examples of alginates extensive use in a range of diverse industries. (Adapted from Chaoyuan, 1990)

the Directorate of Biological Research, War Office and Royal Army Medical Corps. During World War II, Blaine was actively looking for new materials for dressing wounds. The current bandages were inadequate for a number of important reasons including toxicity, wound adhesion (making removal painful and difficult without disrupting the healing surface), slow wound healing and lack of ability to decrease/control capillary haemorrhage (Gensheimer, 1993).

Initially Blaine conducted two types of experiment using calcium alginate and animal models; either direct injection into damaged tissues or by topical application (Blaine, 1946 and Blaine, 1947). Blaine's conclusions from his pioneering work in both the laboratory and aboard troopship hospitals in the Far East, concluded that, alginate accelerated wound healing by keeping wounds moist but not sticking to the healing wound, was sterilisable by autoclaving, absorbable by tissue, non-toxic (even when directly injected into the wound) and importantly for the time, compatible with penicillin (Blaine, 1946; Blaine, 1947; Blaine, 1951 and Oliver *et al*, 1950).

Because of a lack of facilities and "exigences of the Services", full follow-up of the clinical cases was not possible. However, encouraged by the preliminary findings, a three month clinical trial at Croydon Hospital (Surrey, UK) was conducted. Burns, lacerations, ulcers and amputations were all treated with alginate. The results confirmed the beneficial advantages of alginates in wound care (Bray *et al*, 1948).

Additional successful clinical pilot studies have also been undertaken in aural wound healing, neurosurgery and in the management of pulmonary tuberculosis (sealing of bronchi) (Passe *et al* 1948, Oliver and Blaine, 1950 and Blaine 1946).

Because of the early successes with alginate dressings, commercial products soon followed, thus bringing alginate dressings into routine clinical practice. Unfortunately in the 1970's due to market forces (large-scale production of alginate fibre ceased due to an overall drop in demand - alginate medical products were less than 10% of the total market) and expensive production technologies, these products were withdrawn (Thomas, 2000). However by the 1980's, technology advances and improved production techniques led to a major comeback for alginate dressings. Today, there are numerous types of alginate dressings including Kaltostat (ConvaTec, Princeton, NJ, USA), Tegagen (3M, St Paul, MN, USA), Sorbsan (Maersk, Lynge, Denmark) and Algisite (Smith and Nephew, London, UK). A major additional benefit of these dressings is the calcium ions involved with the gelling process further assist wound healing by promoting the blood coagulation process thus these dressings also have a degree of haemostatic activity. This property also allowed alginate to be used to produce absorbable surgical haemostats to control internal blood loss during surgery (Blaine, 1951). Absorbable

haemostats have the big advantage of being able to be left *in situ* prior to being harmlessly absorbed post operatively by the local tissue.

Since Blaine's initial work in the 1940's, there have been numerous clinical trials of alginate based dressings mainly in Europe plus a few in the U.S.A. The general conclusions are that alginate dressings are preferable to conventional bandages in the two key areas; improved quality of patient life (faster wound healing, little/no pain during dressing changes, reduced wound odour, non-sensitizing, non-toxic and shorter hospital stays) and lower healthcare provider costs (faster healing rates, shorter hospital stays, less nursing time required per bandage change due to ease of application and removal) (Gensheimer, 1993).

Other surgical applications of alginate include "bone wax substitute" to control intra operative bleeding from the cut ends of bones and biodegradable stents (Oliver and Blaine, 1950, Office of Science and Technology Annual Report 2000 and Ronan and Thompson, 2001).

2.4.3 Cell encapsulation

Whilst the encapsulation of microbial cells, subcellular organelles and enzymes has a long history dating back to the 1970's, mammalian cell encapsulation is still at an earlier stage in its development (Kierstan *et al*, 1997 and Hackel *et al*, 1975). Alginate has a combination of unique properties which enable it to be deployed as an artificial matrix for encapsulation of biological materials and cells:

- Relatively inert aqueous environment
- Mild room temperature encapsulation process not requiring harsh solvents
- Rapid (almost instantaneous) initial gelling property
- High gel porosity which allows high diffusion rates of macromolecules
- Potential to control porosity with simple coating process e.g. poly-L-lysine
- Dissolution and biodegradation occurs under normal physiological conditions

(Adapted from Gombotz *et al*, 1998)

Stable alginate hydrogel beads are formed by dropping a mixture of sodium alginate and cells into calcium chloride solution i.e. diffusion setting. Alginate has the ability to encapsulate mammalian cells in order to both physically protect as well as immunoprotect if used *in vivo*. Alginate gels are biocompatible. Examples of the use of alginate encapsulated cells include: hybridoma cells in the production of monoclonal antibodies, hepatocyctes in the extracorporal detoxification of blood in patients with acute liver failure and the isolation of islets of Langerhans insulin producing cells for the potential *in vivo* treatment of diabetics (clinical trial data only) (Soon Shiong *et al*, 1994). High polyG alginates tend to be the alginates of choice for these applications i.e. where cells are encapsulated in alginate beads. Beads can be produced ranging from a few μm to several mm in diameter. Encapsulation

devices are available commercial e.g. Inotech Encapsulator which is based on a harmonically vibrating nozzle (Inotech Biosystems International, Rockville, Maryland, USA). Commercial devices allow the production of defined bead diameters and high throughput for drugs, animal cells, plant cells, microorganisms and enzymes. High polyG alginates give stronger beads with high resistance to gel degrading agents e.g. monovalent ions which compete with calcium ions and calcium ion sequesters. In comparison, polyM alginates produce weaker but much more flexible beads (Thu *et al*, 1996b). Porosity also correlates with G content, alginate beads with high G content having the largest pore sizes, ranging from 5 - 200 nm (Martinsen *et al*, 1989 and Miura *et al*, 1986). Pores of this size allow the free diffusion of macromolecules in and out of the bead. Furthermore, the host immune response can be reduced substantially by using alginate with a low M:G ratio (Otterlei *et al*, 1991). Smaller pores reduce the size of the macromolecules, which can get in and out of the bead whilst still allowing the nutrients, metabolites and gas to freely permeate the bead. Coating the surface of alginate beads with a cross-linked alginate-polycationic polymer e.g. poly-L-lysine helps to stabilise the bead and also helps improve the quality of the pore controlled release system.

Microencapsulation of mammalian cells involves suspending the cells in an ultra pure sodium alginate solution (typically 1 - 2% weight/volume) to a density in the region of a million cells per ml of alginate. The suspension is sprayed through a 22 G needle located inside an air jet head droplet forming apparatus into a solution containing calcium ions (typically a 1 - 2% weight/volume calcium chloride solution), alginate microspheres containing cells are formed which gel on contact with the calcium ions. Beads can now either be used directly or coated with poly-L-lysine prior to use. An example of this technique is that of Joki (Joki *et al*, 2001), who genetically engineered baby hamster kidney epithelial cells to express endostatin (an antitumour agent) and then encapsulated them in sodium alginate to form beads. The beads were then coated in poly-L-lysine. The beads contained immobilised cells in an "artificial extracellular matrix" which allows free exchange of proteins, nutrients and oxygen between the encapsulated cells and the animal host. These beads where injected into mice, which had been previously treated to produce primary glioma tumours. Biologically active endostatin was released from the beads resulting in a significant reduction of the tumour mass. Similar results were observed by Read (Read *et al*, 2001), on performing a similar experiment, except the beads did not receive a poly-L-lysine coat.

There have been many successful animal studies involving surgically implanted encapsulated cells with some of these studies starting to progress into the clinic including; Chondrogel (Reprogenesis now Curis, Cambridge, MA, USA) implantation for urinary dysfunction, islets of Langerhans transplantation for diabetes and parathyroid gland transplantation for hypoparathyroidism (Caldamone *et al*, 2001, Elliott *et al*, 2000 and Hasse *et al*, 1997). Whilst

all three applications deploy cells mixed with alginate, the functional role of the alginate differs greatly. Chondrogel uses autologous cells (chondrocytes) and therefore the alginate functions more as a scaffold or bulking agent. The islets of Langerhans and parathyroid glands were either allogeneic or xenografic in origin, thus the alginate is required to function as a barrier to protect immune attack whilst allowing hormones to be released from the encapsulated cells. In general, for alginates suitable to act as a protective barrier high M content alginate is preferable since high G gels exhibit very high permeability towards antibodies compared to the much lower permeability of the gels rich in mannuronic acids (Klock *et al*, 1997). A brief description of each of the above applications follows.

2.4.3.1 Chondrogel

Chondrogel was developed as an autologous chondrocyte in alginate gel suspension for the treatment of vesicoureteric reflux following the successful animal experiments of Vacanti and Atala (Vacanti *et al* 1991, Atala *et al*, 1993 and Atala *et al*, 1994). Vesicoureteric reflux is a congenital condition (affects 3% of children) which presents early in life with urine flowing backwards up the ureters i.e. from the bladder towards the kidney. If uncorrected, this results in frequent urinary tract infections and eventually renal damage. Chondrogel is a structural tissue product composed of autologous chondrocytes and alginate. Atala has demonstrated that the alginate acts as a substrate for delivery purposes and then harmlessly degrades, the remaining cells secrete extracellular matrix which maintains the volume of the initial cells/ alginate solution. This results in autologous cartilage being produced *de novo* (Atala *et al*, 1993 and Atala *et al*, 1994). For Chondrogel, cells are harvested from the patient's ear, expanded in culture (six weeks), mixed with alginate and cross-linked immediately prior to injection via a cystoscope into the tissue adjacent to the vesicoureteric (bladder/ureter) junction. Injection volumes varied from 0.16 - 3 ml in total. The results of the phase II clinical trial was reported at both three months and at greater than one year (some up to 3 years) (Diamond *et al*, 1998 and Caldamone *et al*, 2001). A total of 29 children (age range: 1 - 15 years) were enrolled into this study, each requiring a minimum of one injection of Chrondrogel at initial operation (the majority requiring two i.e. one for each ureter). If there was no improvement by three months, the therapy was repeated using chondrocytes which were stored for this purpose. The conclusion drawn from this study were that Chondrogel was a safe and reasonably effective treatment for vesicoureteric reflux. There was no significant complications, however the relapse rate (35% of patients at 1 year) was deemed unacceptable and as a result the alginate underwent reformulation prior to the phase III clinical trial (Relapses were mainly due to loss of bulk at the site of injection). Commencing February 1999, a total of 61 patients (age range: 6 months to 18 years) were enrolled into the phase III clinical trial by September 2000 (FDA Office of Orphan Products Development Study ID Number 199/14267 REPRO-

FDR001514;REPRO-99-07). The results of this phase III study are as yet unpublished due to Curis in February 2002 deciding to halt several of its programmes including Chondrogel in order to focus on stem cell therapies (Curis company press release, February 2002). Curis plans only to revive the programmes if a pharmaceutical company is prepared to act as a strategic partner.

Chondrogel has also been trialed as a therapy for intrinsic sphincter deficiency. Intrinsic sphincter deficiency is a severe form of urinary stress incontinence caused by either an inherited or acquired deficiency in the urethral sphincter mechanism (Bent *et al*, 2001). A preliminary study of 32 patients (age range 36 - 81) each received an injection of Chondrogel in to the tissue surrounding the neck of the bladder in order to cause an occlusion. At one year follow-up, once again Chondrogel was demonstrated to be safe and clinically effective (Bent *et al*, 1999 and Bent *et al*, 2001).

2.4.3.2 Islets of Langerhans encapsulation

Type I diabetes results from the destruction of the insulin secreting cells (islets of Langerhans) in the pancreas. Whilst insulin therapy can be beneficial, it remains far from ideal. Another option is to transplant either autologous or xenogeneic islets. Following successful animal studies, a number of groups have moved into pilot studies in the clinic using alginate to encapsulate the cells (Sambanis, 2003 and Soon-Shiong, 1993). The alginate is deployed to prevent both allogeneic immune response as well as the autoimmune component which caused the patient's type I diabetes whilst allowing insulin to freely leave. Soon-Shiong in 1993 first demonstrated the principle on a 38 year old man, Steven Craig (Soon-Shiong *et al*, 1994). Craig had long standing type I diabetes with multiple complications including renal failure which necessitated a living related donor transplant. This transplant required him to be on low dose immunosuppression therapy (cyclosporin and azathiopine). Human islet cells were isolated from eight cadaveric donor pancreases, expanded in culture for 22 days and encapsulated in alginate prior to being implanted into the abdominal cavity (peritoneal space). The initial dose was 10,000 islet cells per kilogram of body weight (approximately half the number required to achieve full insulin production). After six months a further 5,000 islet cells per kilogram were encapsulated and implanted. At five years, there have been no side effects from the therapy and whilst not fully producing adequate insulin (total replacement was not the aim of the study) to be a total replacement for insulin therapy, had resulted in a much reduced requirement (King, 1998). In 1994, the FDA granted Soon-Shiong permission to perform the same technique in a further 19 patients, all immunosuppressed kidney transplants (King, 1998).

Scharp also implanted encapsulated allogeneic islet cells but into non-immunosuppressed

patients (Scharp *et al*, 1994). To avoid the necessity to use immunosuppression, islet cells were mixed with alginate. This suspension was then injected into acrylic-copolymer hollow fibres which had a permselective membrane on both its outer and inner surfaces (molecular weight cut off 65,000). The alginate was gelled by briefly immersing the fibres in a dilute calcium chloride solution after which the ends of the fibres were sealed with adhesive. Fibres were implanted in nine patients and explanted after 2 weeks. The results demonstrated that the biocompatability of the devices was excellent, there were no adverse patient complications and islet cell survival was also observed.

Elliott in his clinical study involving two type I diabetic patients, deployed porcine islet cells (Elliott *et al*, 2000). Porcine islet cells were encapsulated in alginate by VivoRx (now AmCyte) (Los Angeles, LA, USA) and implanted into the abdominal cavity. Follow up was reported to 19 months post implantation. Both patients benefited from the procedure by requiring less insulin therapy with no side effects.

Following the successes of these early studies, in May 2004, a larger clinical study (ten patients) was commenced by Calafiore at the University of Perugia (Perugia, Italy). The study uses allogeneic islet cells encapsulated only in alginate implanted into the abdominal cavity of nonimmunosuppressed patients with type I diabetes. Early results from the first patient treated at 40 days post implantation are highly encouraging including requiring 30 - 40% less insulin and "absolutely no side effects from the graft" (Calafiore, 2004).

As the clinical successes continue, biotech companies have started to take up the challenge to commercialise these alginate based therapies including Cerco Medical (formerly, Islet Sheet Medical, San Francisco, CA, USA) and AmCyte (formerly VivoRx). For example, Cerco Medical plans to cure type I diabetes by means of bio-artificial pancreases built as thin sheets for implantation.

2.4.3.3 Parathyroid gland encapsulation

The clinical value of alginate microencapsulated cells has also been demonstrated in the field of parathyroid allotransplantation without immunosuppression (Hasse *et al*, 1997). Hasse reported on 2 female patients in their 50's who underwent subtotal bilateral thyroidectomy for multinodular goitre. Both subsequently became profoundly hypoparathyroid (tetany, bone pain, depression and impaired vision) despite intravenous calcium and high dose vitamin D (The parathyroid glands (usually 4) are intimately related to the thyroid gland and being only 2 - 3 mm in diameter and variable in both location and total number, accidental removal is a recognised surgical complication of a thyroidectomy (Greatorex, 1991). Subsequent blood tests failed to detect the presence of parathyroid hormone. Allogeneic parathyroid cells were provided by an ABO matched HLA mismatched donor. Microcapsules were made

by adding these cells to an alginate solution and then cross-linking with 10 $mmolL^{-1}$ barium chloride for 7 minutes. The microcapsules were cultured for 2 days prior to 20 of them being implanted into the patients' forearm muscles. The alginate allowed nutrients and parathyroid hormone to freely pass whilst preventing antibodies and immune mediators from coming into contact with the allogeneic cells. Both patients' symptoms dramatically improved and no immunosuppressive therapy was required. No side effects of complications have been reported in either patient.

2.4.4 Alginate and tissue engineering

Alginate can be processed to form microcapsules, fibres and three-dimensional hydrogels, this coupled with a good record of *in vivo* biocompatibility (Klock *et al*, 1997), low cost (Jork *et al*, 2000) and availability make it a potential choice for tissue engineering applications. An example of its potential is that it can be gelled using reagents and conditions which are not harmful to cells e.g. low concentration $CaCl_2$ solutions at between 4 - 37°C. Likewise, alginate can be turned from its hydrogel state to a liquid merely by increasing the monovalent cation concentration i.e.

$$Ca^{2+} + \text{Na-Alginate (solution)} \rightarrow 2Na^{+} + \text{Ca-Alginate (hydrogel)}$$

This property potentially gives control over the rate the alginate leaves the newly forming tissue. A balance between scaffold strength due to the hydrogel and tissue due to extracellular matrix produced by the cells is critical. However, currently alginate does have some challenges including:

1. Alginate dissolves in culture medium or *in vivo* due to the substitution of divalent ions from the alginate construct with monovalent ions e.g. sodium. This may or may not be a problem depending upon the desired outcome, however, predictable degradation will be essential.
2. Alginate is unable to specifically interact with mammalian cells in terms of cell attachment and proliferation. However, cell "friendliness" can be achieved e.g. covalently coupling RGD cell adhesion peptide sequences to alginate prior to cell seeding (Rowley *et al*, 1999).
3. Sterility is also an important issue with commercial alginates. There are currently only two routes for obtaining sterile alginate. Firstly a few groups including Zimmermann's from IBMT (St. Ingbert, Germany) carefully manufacture their own alginate from carefully selected seaweeds and then assay the finish product (Leinfelder *et al*, 2003). The only other alternative source of sterile alginate is from NovaMatrix (FMC BioPolymer. Oslo, Norway) who manufacture in accordance with FDA guidelines for current good manufacturing practice

(cGMP).

Voluntary guidelines for the development of tissue-engineered products have been suggested which could be used with respect to alginate and tissue engineering (Omstead *et al*, 1998). However, more significantly, the American Society for the Testing of Materials (ASTM) in May 2001 produced their guide "Standard guide for characterisation and testing of alginates as starting materials intended for use in biomedical and tissue-engineered medical product applications" (F 2064 - 00) in response to the growing interest of alginate for tissue engineering. This interest would appear to be fairly substantial. It is generally recognised that the field of tissue engineering in general is rapidly expanding especially since the late 1990's. This can be from both the expansion of the intellectual property in the field (Figure 2.3) and by the increasing number of scientific publications (Figure 2.4). Alginate is likewise undergoing an increasing popularity (Figure 2.3 and Figure 2.5). Interestingly however is the extremely rapid period of growth that the combination of alginate - tissue engineering has undergone since the year 2000 Figure (2.3 and Figure 2.6). Whilst patenting and scientific publications can only suggest a trend, the trend does appear to be gaining momentum.

2.5 The focus of the thesis

The sharp rise in publications and patents in the field of regenerative medicine in the last five years is an indication of the perceived promise. However, the recent commercial set backs are also a pointer to the difficulty in achieving a consistent outcome which can yield affordable materials. The thesis topics focus on this aspect whilst taking a whole bioprocess approach. An initial scoping study on powders helped to sharpen the view of what was needed (not included in this thesis for the sake of brevity) and the selection of engineered tubular constructs as a test target. There followed detailed design and testing of a potentially disposable bioreactor which would ultimately allow automated construction and maturation of the tissue. The rapid scientific developments in stem cell science encouraged a switch from a rodent immortalised smooth muscle cell line to human stem cells and a preliminary examination of the differentiation to smooth muscle cells to populate the construct made with derivatised alginate. To allow the properties of the tubes to be evaluated without sacrifice of precious tubes, beads of the same material were prepared using a novel device. Finally, the issues raised by the study were summarised as a basis for future work.

Area	U.S. patents issued since 1976	U.S. patent applications published since 15th March 2001
Tissue engineering and related to tissue engineering	780	1,277
Alginate - All areas	22,146	10,718
Alginate tissue engineering and related to alginate tissue engineering	187	396

Figure 2.3

Table of U.S. patents and patent applications published for tissue engineering, alginate and the combination of alginate and tissue engineering.
Source: United States Patent and Trademark Office - 9th December 2004.

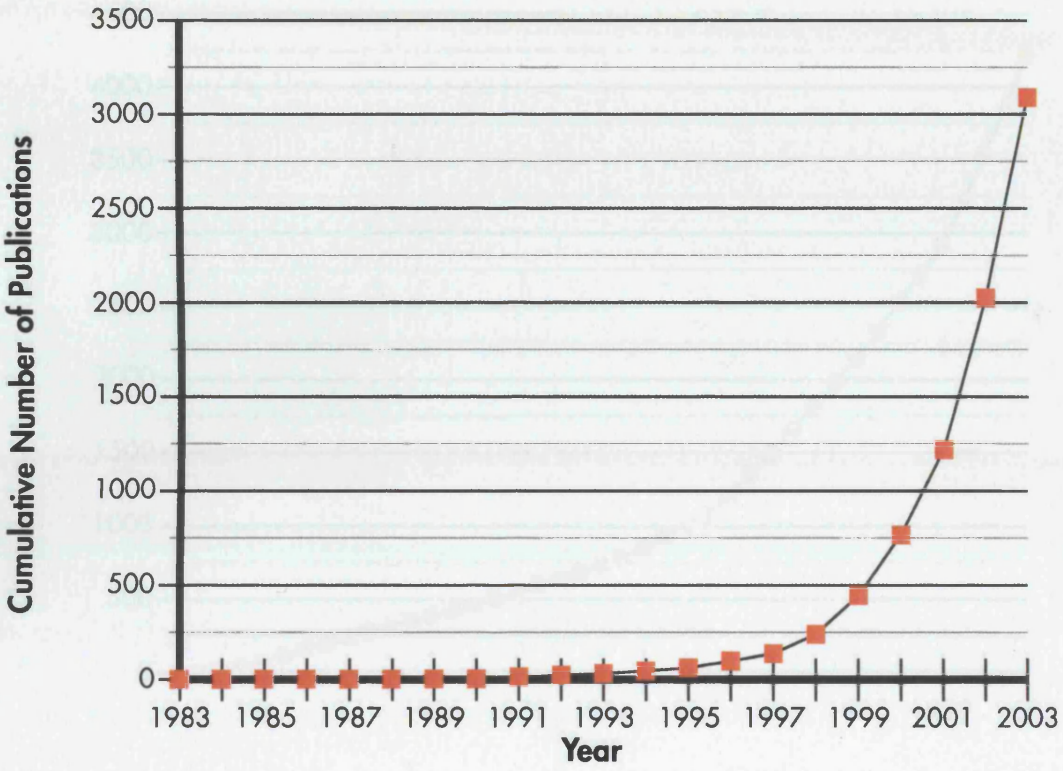

Figure 2.4

Graph of cumulative number of scientific publications for all of tissue engineering 1983 - 2003.

Source: MEDLINE Plus - Ovid Technologies Inc.

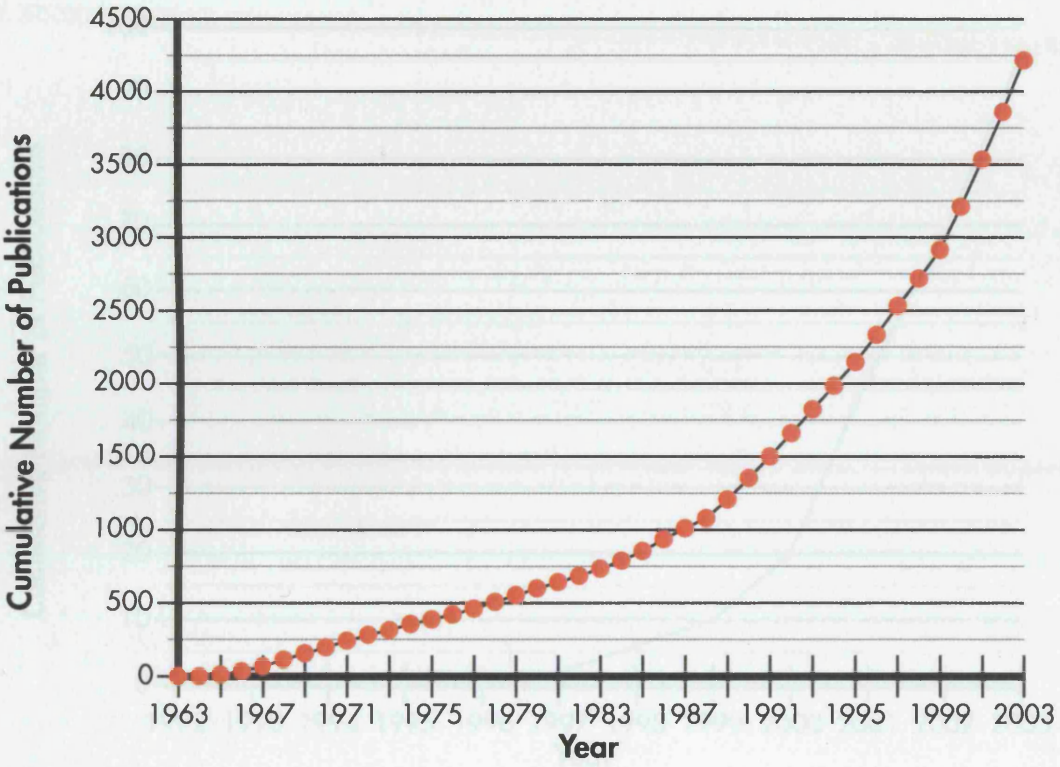

Figure 2.5

Graph of cumulative number of scientific publications for alginate in life science journals 1963 - 2003.

Source: MEDLINE Plus - Ovid Technologies Inc.

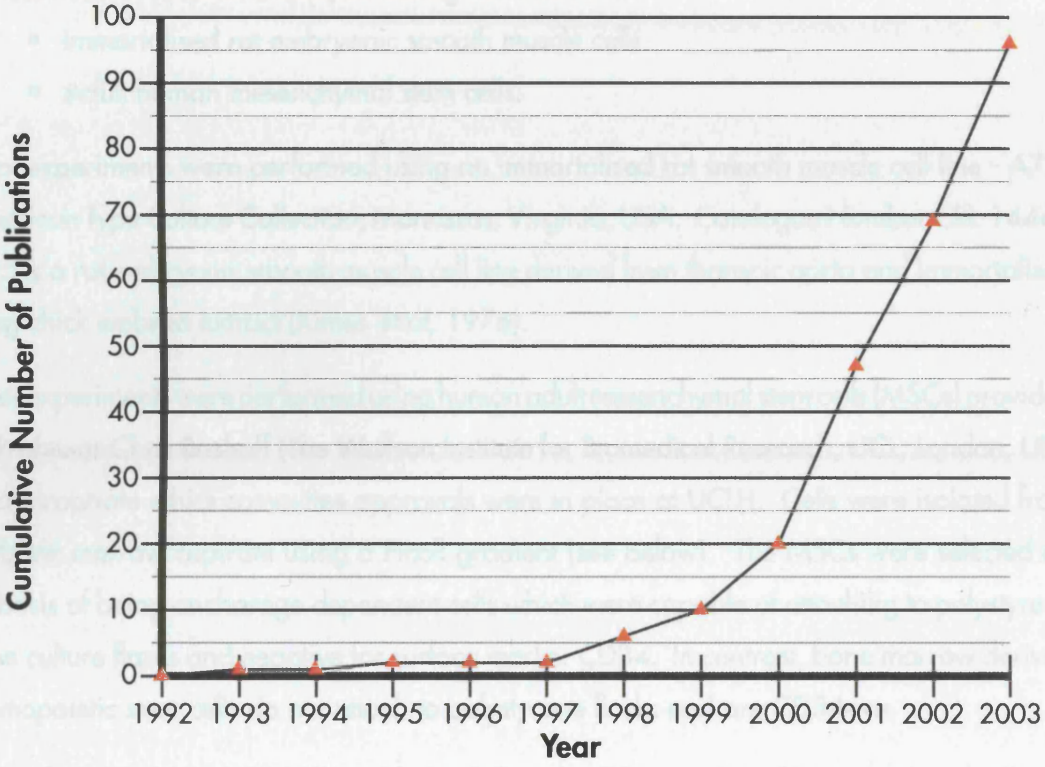

Figure 2.6

Graph of cummulative number of scientific publications for alginate in all of tissue engineering 1992 - 2003.

Source: MEDLINE Plus - Ovid Technologies Inc.

3.0 Materials and methods

This chapter contains the materials and methods relating to Chapter 7 (the study of cell in alginate scaffolds) and Chapter 8 (the study of cells in derivatise alginate scaffolds).

3.1 Cell lines

Two cell lines have been employed during this research:

- Immortalised rat embryonic smooth muscle cells.
- Adult human mesenchymal stem cells.

Initial experiments were performed using an immortalised rat smooth muscle cell line - A7r5 (American Type Culture Collection, Manassas, Virginia, USA. Catalogue Number CRL-1444). A7r5 is a rat embryonic smooth muscle cell line derived from thoracic aorta and immortalised using chick embryo extract (Kimes *et al*, 1976).

Latter experiments were performed using human adult mesenchymal stem cells (MSCs) provided by Professor Chris Boshoff (The Wolfson Institute for Biomedical Research, UCL, London, UK). All appropriate ethics committee approvals were in place at UCLH. Cells were isolated from the bone marrow aspirate using a Ficoll gradient (see below). The MSCs were selected on the basis of being anchorage dependent cells which were capable of attaching to polystyrene tissue culture flasks and negative for surface marker CD34. In contrast, bone marrow derived haemopoietic stem cells do not attach to polystyrene flasks and are CD34+ve.

The method used for MSC isolation was to take a fresh human 10 ml bone marrow aspirate, diluted it with 10 ml of phosphate buffered saline (PBS) (BioWhittaker, Walkersville, Maryland, USA) and then filter the resulting solution through a 40 micron filter. The filtrate was then layered on 20 ml of Ficoll and centrifuged at 1800 rpm for 30 minutes using a refrigerated centrifuge. Bone marrow mononuclear cells were removed from the Ficoll interface and pelleted by centrifugation (1,800 rpm for 30 minutes). The cell pellet was resuspended in 20 ml of PBS and centrifuged at 1,200 rpm for 10 minutes. For the final isolation of the MSCs, the cell pellet was resuspended in 10 ml of mesenchymal stem cell media, Mesencult (Stem Cell Technologies, Vancouver, British Columbia, Canada).

Both the rat and the human cell lines were grown in sterile polystyrene T-flasks (Corning, Corning, New York, USA], which were of the pretreated variety (negatively charged and hydrophobic surface) to aid cell attachment. The rat cell line was grown in supplemented growth media comprised of Dulbecco's Modified Eagle's Medium with 4.5 gL^{-1} glucose but without L-glutamine, (DMEM) (BioWhittaker, Walkersville, Maryland, USA), with 10% fetal bovine serum (FBS) (BioWhittaker, Walkersville, Maryland, USA), 2 mM L-glutamine (BioWhittaker, Walkersville, Maryland, USA), 100 U penicillin per ml with 100 µg streptomycin per ml

(BioWhittaker, Walkersville, Maryland, USA). The volume used was 30 ml in a T150 flask. The stem cell line was grown in identical T150 flasks (Corning, Corning, New York, USA) to the immortalised rat smooth muscle cells. The media was however specific for maintaining the stem cells in their multipotent phenotype. The media used was Mesencult (Stem Cell Technologies, Vancouver, British Columbia, Canada) supplemented with mesenchymal stem cell supplements (human) (Stem Cell Technologies, Vancouver, British Columbia, Canada), recombinant human fibroblast growth factor (rFGF, R&D Systems, Minneapolis, Minnesota, USA) and 100 U penicillin per ml with 100 µg streptomycin per ml (BioWhittaker, Walkersville, Maryland, USA). The volume of this supplement media used per T150 flask was 20 ml.

In collaboration with Julia Markusen (UCL), cell banks of both cells lines were produced and stored in cryovials (Nalgene, Nalge, Rochester, New York, USA) in liquid nitrogen in order to be able to perform reproducible experiments over a long period of time.

3.2 Cell preparation and cell culture methodologies

In order to produce adequate numbers of cells, for example a typical experiment requires 10^6 - 10^7 cells per ml of alginate solution, the cell lines were passaged using the following protocol.

A cryovial of banked cells was thawed and seeded into T150 flasks containing the appropriate supplemented media. Once the cells approached 80 - 100% confluence on the surface of the flask (viewed by light microscopy) e.g. approximately 3-5 days for the rat cell line and approximately 2-3 days for the stem cell line, the spent media was then drawn off using a pipette and the cell layer washed with 25 - 30 ml of phosphate buffered saline (PBS), (BioWhittaker, Walkersville, Maryland, USA) to prevent any residual proteins (e.g. from the FBS) interfering with the trypsin and thus reducing its enzymatic activity. Following rinsing, 6 ml of 0.25% trypsin in 0.03% EDTA (Sigma, St. Louis, Missouri, USA) was pipetted into the flask and by gently rocking the flask, spread over its growth surface in order to bring the trypsin into contact with the entire sheet of cells. After 5 - 7 minutes, the flask was manually tapped in order to dislodge the cells from the surface of the flask. In order to prevent cell membrane damage due to the non-specific protease activity of the trypsin, the reaction was quenched by immediately adding 12 - 18 ml of supplemented media and rocking gently to mix homogeneously. A 500 µL sample was then removed in order to count the number of live and dead cells and then to be able to extrapolate the result for the entire T-flask. At least three independent 100 µL samples with an equal volume of trypan blue dye (Sigma, St. Louis, Missouri, USA) in an Eppendorf tube (Eppendorf, Hamburg, Germany), were prepared by mixing thoroughly using the repeated action of a micropipetter.

After a brief vortex, a 20 µL sample was then removed and added to a freshly prepared

Improved Neubauer Haemocytometer slide with an in place cover-slip. The cover-slip was thoroughly cleaned before being applied to the haemocytometer with gentle pressure until Newton's rings were visible and remained visible during use, (Newton's rings are coloured interference fringes). The trypan blue dye works as an exclusion medium since the dye permeates all cells but only dead cells will retain the blue dye whereas live cells will exclude the dye and therefore will not permanently stain. Live cells therefore appear with a birefringent halo around them when viewed under a light microscope. Using a light microscope the grid etched on the Improved Neubauer Haemocytometer is easily discernable consisting of two sets of nine main squares each measuring 1 x 1 mm. Each of these main squares is subdivided into smaller squares each of which is 1/400 mm^2 in area.

By counting the number of live/dead cells, aided by a manual counter recorder, in the 10 squares, (the 4 corners plus 1 centre square of each of the two sets of 9 squares etched on the cytometer slide) and allowing for the dilution due to the addition of the trypan blue/EDTA solution, it is possible to estimate the cell density in the sample and hence extrapolate back to the original T150 flask. Since a properly applied cover-slip limits the height of the chamber to 0.1 mm, the volume contained in each square can be quickly calculated i.e. total volume of the 10 main squares is: 10 x 1 x 1 x 0.1 = 1 mm^3. Repeating the cell count and averaging was used to improve the statistical estimate for the original flask. Increased accuracy was also achieved using all 18 squares of the slide. It is essential to avoid all air bubbles plus the slide must have all main squares totally covered with the sample cell/trypan blue suspension. Furthermore, to get the best accuracy the cell solutions were diluted until the cell counts were in the range 15 - 50 cells per 1 mm^2 square. The convention by which counting cells touching/crossing the two sides next to the boundary line and not the cells touching/crossing the other two sides was adhered to. The accuracy of this means of estimating the total live/dead cell number in the original T flask will be reduced if the sampling technique is poor i.e. non homogeneously distributed cells e.g. clumping due to poor trypsinisation. Furthermore, if the sample is left for a period of time (greater than 15 minutes) even the live cells will unfortunately take up the dye. Individual T150 flasks at 80 - 100% confluence tended to contain 1 - 5 x 10^6 cells. The cells were either then added to alginate solutions to produce tissue engineering scaffolds or split into a number of fresh T-flasks in order to further expand the cell population. Typically a single flask would be split into 3 new T150 flasks and made up to an individual total flask volume of 30 ml of media by adding additional supplemented media. Flasks were then returned to the humidified incubators, set at 37°C containing 10% CO_2 (Galaxy S, R.S Biotech, Irvine, Ayreshire, UK).

Cell mixing with alginate needed to result in a totally homogeneous cell distribution, with no clumps and little (ideally zero) cell death. Furthermore, early range experiments had

demonstrated that final cell densities less than 10^5 cells per ml of alginate were distributed very sparsely in the finished scaffold i.e. allowing no cell-cell contact. Close proximity of the cells was deemed a prerequisite. This only occurred at 10^6 cells per ml of alginate and greater. Since the quenched trypsinised cell suspensions were typically $<2 \times 10^5$ cells per ml, direct addition to the alginate was not a possibility.

By knowing the approximate number of cells in the suspension (from Neubauer haemocytometry), the appropriate number of cells in suspension could be transferred into centrifuge tubes and centrifuged (Hutton Universal Centrifuge) at 100 g for 10 minutes. The supernatent was then carefully removed so as not to disrupt the cell pellet, this also removes any remaining trypsin, which would be undesirable in the final cell/scaffold construct. The pellet was then carefully resuspended to the desired volume by adding culture media or physiological saline (adding any polyvalent cations resulted in premature partial crosslinking of the alginate which was unacceptable). Likewise, excessive residual EDTA resulted in poor scaffold strengths due to the ion chelating nature of the EDTA on calcium ions which are essential for the integrity of the alginate hydrogel scaffold. Resuspension was performed using a micropipette and gentle repeated action.

3.3 Reagents and alginate solution preparation

Alginate solutions were prepared in the following manner. Physiological saline was initially produced by adding 9 gmL^{-1} of sodium chloride to water for injection (WFI - BioWhittaker, Walkersville, Maryland, USA) and then correcting the pH to approximately 7.4 using 1 M sodium hydroxide solution (Sterile filtered - Sigma, St. Louis, Missouri, USA). After adding the desired quantity of alginate powder to the physiological saline, the alginate required extensive mixing prior to autoclaving in order to obtain a homogeneous solution (alginate powder easily traps air to create "fish-eyes" which greatly hinder the mixing process).

Since the alginate was known to be non-sterile, prolonged mixing was thought undesirable as during this time any bacteria would rapidly replicate, thus increasing both the bacterial load and endotoxin level. Experiments with simple in line 0.2 µm syringe filters (Sartorius, Goettingen, Germany), on fully mixed alginate solutions lead to the retention of the long alginate chains within the filter. The resulting gels produced were extremely weak evidently being only produced using cross-linking of short alginate chains - not desirable for tissue engineering constructs requiring weeks/months to grow and mature to a point where the scaffold's function is replaced by cell synthesised extracellular matrix. To potentially reduce this loss of heavy chain, sequential filtration was carried out e.g. 1.2 µm followed by 0.8 µm before attempting the desired 0.2 µm size required to sterilise the alginate solution. However, this serial filtration failed to improve the strength of the final hydrogels. It was therefore

decided to autoclave the alginate/water for injection mixtures for 121°C for twenty minutes. This had the advantage of not requiring a prolonged mixing step since the alginate powder melts at approximately 90°C and goes into solution prior to reaching the 121°C sterilising step. This process is known to reduce viscosities of alginate (Vandenbossche and Remon, 1993), however, the effect upon the final alginate hydrogel scaffolds was not as deleterious as the in line filtration and therefore became the sterilising treatment of choice. Following autoclaving, all alginate solution were rolled on a roller mixer (SRT2 - Stuart Scientific, Redhill, Surrey, UK) to ensure homogeneity and allowed to cool to < 37°C prior to combining with cells.

Calcium chloride solutions were prepared by adding calcium chloride powder (Sigma. St. Louis, Missouri, USA), to physiological saline, pH corrected using 1M sodium hydroxide solution (Sigma, St. Louis, Missouri, USA), and then after thorough mixing, filter sterilised using a vacuum assisted 250 ml volume 0.2 μM Nalgene disposable filter, (Nalge Company, Rochester, New York, USA). Storage was at 4°C. Care was taken with storage of the calcium chloride powder as it is highly hygroscopic and therefore was kept in air tight containers at all times.

Calcium chloride solutions were prepared at different concentrations ranging from 0.5% to 2%, however, the majority of the research was performed at 0.5-1% concentration since concentrations below 0.5% resulted in highly variable gel strengths (on occasion not even forming a structural hydrogel). Concentrations above 1% appeared to have no obvious advantage. However, since calcium ions have a physiological effect on smooth muscle cells it was decided to limit the exposure - hence 1% was chosen. *In vivo*, human plasma contains calcium in three different forms; bound to protein (mainly albumin), complexed with citrate and phosphate and free ions. Only the free ion form is physiologically active. Thus of the total calcium plasma of 2.25 - 2.6 $mmolL^{-1}$ only 47% is physiologically active (1.1 - 1.2$mmolL^{-1}$). Since the calcium chloride preparation used was in fact calcium chloride (dihydrate) i.e. $CaCl_2 \cdot 2H_2O$, with a formula weight of 147.01, a 0.5%, 1% and 2% cross-linking solution contains 3.4 $mmolL^{-1}$, 6.8 $mmolL^{-1}$ and 13.6 $mmolL^{-1}$ respectively of free calcium ions.

3.4 Producing three-dimensional cell/alginate hydrogel structures

Three distinct three-dimensional cell/alginate structures were produced for experimental studies:

- Flat sheets.
- Round beads.
- Hollow tubes.

3.4.1 Flat sheet fabrication

Flat sheets were produced in the following manner. Round borosilicate glass cover-slips (BDH, Poole, Dorset, UK) of 13 mm in diameter were placed with forceps onto a flat block of stainless steel which had just been heated strongly with a blow-torch for 5 to 10 minutes. The cover-slips were left for approximately 30 seconds prior to being lightly sprayed with a 20% solution of calcium chloride (Sigma, St.Louis, Missouri, USA) in water for injection (Bio Whittaker, Walkersville, Maryland, USA) using a Badger B250-2 airbrush (Badger Air-Brush, Franklin Park, Illinois, USA). The aqueous solvent quickly evaporated leaving a thin film of calcium chloride on the cover-slips. Using sterile forceps, the cover-slips were then removed from the hot stainless steel block and being 13 mm in diameter could be easily dropped into the base of 24 well microwell plates, (Corning, Corning, New York, USA) with individual well diameters of 15.7 mm. Alginate only or homogeneously mixed cell-alginate solutions were then added, typically 500 µL of 1% alginate (dry weight/volume) in physiological saline. Care was taken to perform the removal of the coated cover-slip from the hot metal block to finally adding the alginate solution part of the process in an efficient manner since calcium chloride being highly hygroscopic easily attracts water from the surrounding air causing a wet film of calcium chloride solution to be present on the cover-slip and not the desired dry powder coating. The powder coating which was an opaque white in colour, stayed in place during the addition of the transparent alginate or cell-alginate solutions. By adding the alginate solutions using a micropipette carefully in a continuous action just above the centre of the glass cover-slip, the alginate solution would easily flow across the cover-slip creating a flat layer. Calcium ions from the coating then diffused into the liquid producing a hydrogel. The 24 well microwell plates were put into the humidified 37°C Galaxy S incubator for 20 minutes to aid this setting step. The sheets were then washed repeatedly with WFI and/or culture media e.g. adding 1 ml of solution and leaving for 5 minutes prior to pipetting it back off. Physiological saline was originally tried but this disrupted the hydrogels due to the presence of excess sodium ions competing with the calcium ions for the alginate cross-linking sites. The aim of the wash steps was to remove excess calcium chloride from the scaffold.

Sheets created in the above manner tended to adhere well to the glass cover-slips although on occasion separation would occur making the removal of wash solutions and later medium changes challenging. Also since the glass cover-slips were 13 mm in diameter compared to the 15.7 mm diameter of the wells, occasionally alginate solution would flow over the edge of the cover-slip and enter the area under the cover-slip, thus potentially trapping material in a physiological dead space e.g. poor mass transfer characteristics. However in the vast majority of experiments, surface tension prevented any unwanted flooding from occuring. The microwells with their clear glass cover-slip and transparent hydrogel sheet could easily be examined with a normal light microscope (Olympus 1 x 70 phase contrast microscope,

Olympus, Tokyo, Japan). Similar experiments were also performed with larger diameter round cover-slips and 12 well microwell plates.

3.4.2 Bead production

A basic overview of the preparation of cell/alginate solutions is depicted in Figure 3.1. In detail; cells were obtained by harvesting 80 - 100% confluent T150 flasks as previously described in Section 3.2. Known numbers of cells were pelleted (100x g for 10 minutes), the supernatant carefully withdrawn using a pipette and fresh supplemented media added to produce the desired cell/media volume. Thus it was possible to arrive at cell/media/alginate solutions with a final alginate concentration of 1% and a predetermined final cell density.

The desired cell densities aimed for were in the range of 10^5 - 10^7 cells per ml of cell/media/alginate solution, but the majority of bead experiments were in the 10^6 per ml to 10^7 per ml range. The cell/media/alginate was thoroughly mixed in a sterile 5 ml screw top polystyrene tube (Bibby Sterilin, Stone, Staffordshire, UK) by gentle swirling action using a micropipette and then rolled for 5 minutes prior to being drawn up into a 1 ml syringe (Becton Dickenson, Franklin Lakes, New Jersey, USA). All the air bubbles were carefully expelled prior to adding a 0.1 mm inside diameter syringe needle which had had its bevelled end previously machined off leaving a squared off tip to the needle. By holding the tip of the needle perpendicular to a bath (45 ml in a sterile 50 ml screw top polystyrene tube) (Corning, Corning, New York, USA) of 1% (weight/volume) calcium chloride in physiological saline and slowly depressing the syringe, small drops were produced. On falling a few mm from the truncated needle to the surface of the calcium chloride solution, the drops became more round (c.f. originally tear drop shape). On entering the solution the outer surface of the beads quickly cross-linked. In order to achieve complete cross-linking of the interior of the beads, the beads were left in solution for an extended period, typically 10 - 20 minutes during which time the 50 ml screw top container was sealed and gently rolled. After this cross-linking phase, the beads were rinsed. This task was completed by pouring the entire contents of the calcium chloride bath through a sieve, thus trapping the beads. The beads could then be put into a fresh container by inverting the mesh and gently tapping. Repeated washing was undertaken using supplemented culture media thus reducing excess calcium chloride levels.

Washed beads were then carefully added in pairs to 24 well microwells (Corning, Corning, New York, USA) containing 1 ml of supplemented culture media per well (as described in Section 7.1.1) using a sterile stainless steel "spoon". The microwells were then incubated at 37°C in humidified, CO_2 supplemented (10%) air. The beads produced varied in morphology, ideally round spheres were produced but often the beads had a more tear-dropped shape i.e. had a distinct tail. Another variant with manual production was a doughnut shape i.e. a ring

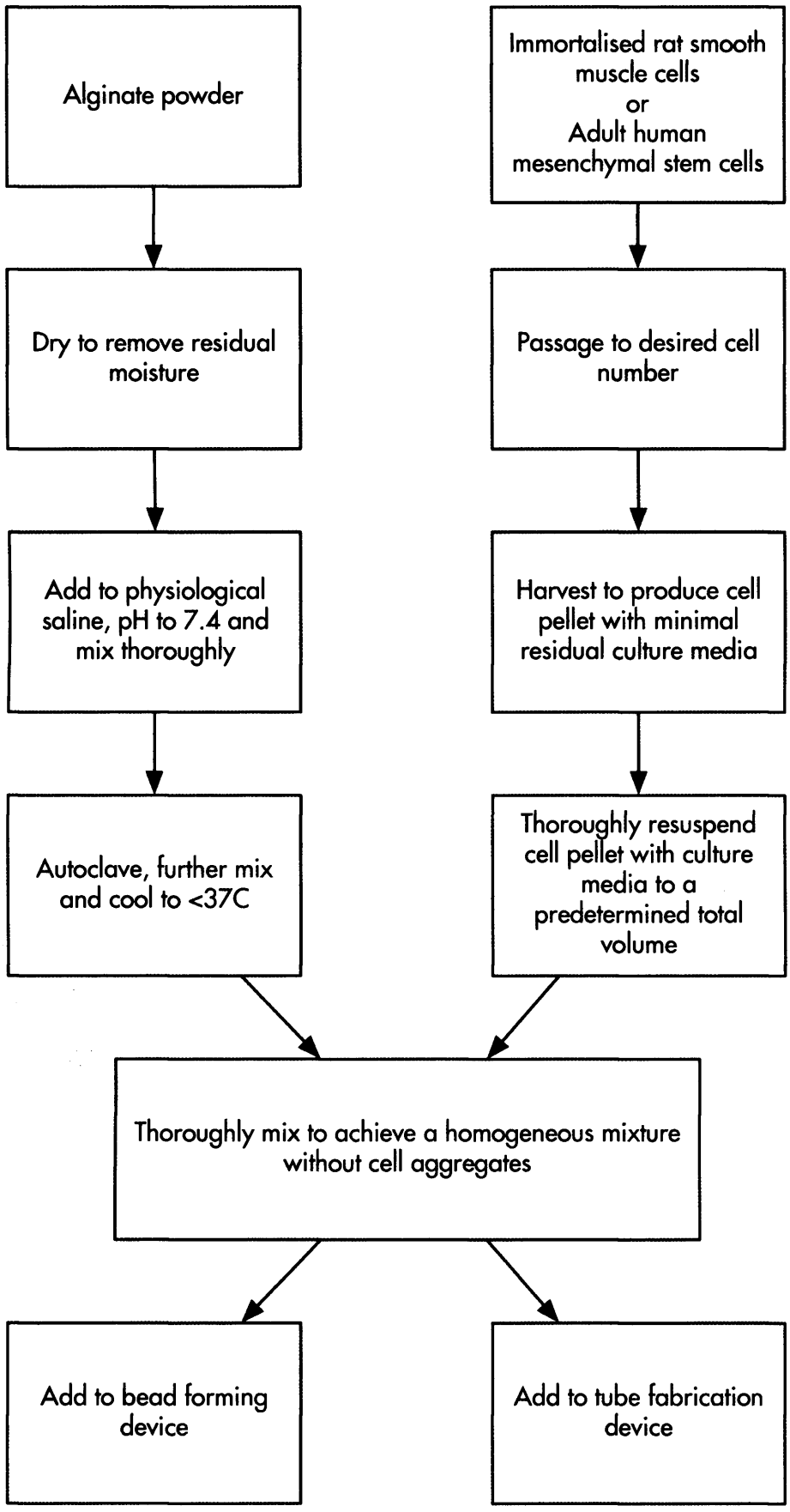

Figure 3.1

Overview of preparation of homogeneous cell/alginate mixtures.

with a hole in the centre. All the morphologies, however, had a similar starting volume e.g. the volume of each bead was fairly constant as its volume is determined by viscosity, needle orifice diameter and gravitational force, all of which stayed constant during a single manual production run.

The round beads when measured using a light microscope with a calibrated eye piece were in the order of 2.2 mm (+/- 0.5 mm) in diameter. Since thorough mixing was undertaken, it was assumed that the cell-alginate solution was reasonably homogenous in nature, thus the volume of the bead could be used to determine a bead's average cell load. For example, when using 10^6 cells per ml of cell/media/alginate to form beads of average diameter 2.2 mm each bead was estimated to contain on average 5,000 - 6,000 cells. This equates to approximately 28 - 33 cells per mm^3.

In order to make comparisons, a control well in the microwell plate was seeded with an approximate number of cells i.e. if 2 beads were being used, then approximately 10,000-12,000 cells were seeded per well. This equates to approximately 50 - 60 cells per mm^2. This results in similar cell:medium ratios for both the bead and microwell control experiments.

3.4.3 Tube fabrication

A basic overview of the preparation of cell/alginate solutions is depicted in Figure 3.1 and described in Section 3.2. The fabrication of cell/media/alginate hydrogel tubes deployed homogeneous mixtures of 1% Manugel alginate (ISP, Tadworth, Surrey, UK) in physiological saline, (0.9% sodium chloride, Sigma, St. Louis, Missouri, USA), in WFI (BioWhittaker, Walkersville, Maryland, USA) with a cell density of approximately 10^5 cells per ml were employed. A 1% calcium chloride solution (Sigma, St. Louis, Missouri, USA) in physiological saline was used as the cross-linking agent. Constructs were removed after 20 minutes and placed in fresh culture media in sterile Petri dishes (Bibby Sterilin, Stone, Staffordshire, UK). Incubation was at 37°C, humidified and 10% CO_2 atmosphere.

The protocol below is for the tube fabrication device whereby the float is activated by a pneumatically driven piston i.e. producing a cell/media/alginate hydrogel tube with an outside diameter of 9 mm, length 140 mm (i.e. dimensions determined by the particular glass tube chosen) and of the order of 0.25 mm hydrogel wall thickness (i.e. determined by the outer diameter of the piston within the glass tube). Cells were harvested as previously described, pelletted, resuspended to a known final volume with supplemented media and mixed carefully with 3% alginate solution (alginic acid salt from brown algae - Fluka, St. Gallen, Switzerland). Final concentrations were 2.7% alginate with a cell density of 10^6 ml^{-1} of cells/media/alginate. The device was used as described in Chapters 4 - 6 and Appendix 2. The concentrations of calcium chloride solution deployed ranged from 0.5 - 1%. Once

the cell/hydrogel tube was fabricated, the construct was left for a further 20 minutes in order to allow further cross-linking to occur prior to removing the glass tube/piston assembly from the device. This allowed the tubular construct to be withdrawn from the glass tube. The construct was placed in a sterile Petri dish (Bibby Sterilin, Stone, Staffordshire, UK) containing supplemented media. Because of the high alginate concentration and thick wall, the construct was easily handleable despite the 10^6 cells present per ml.

In the Petri dish, the 9 mm diameter tubes would collapse flat - like a fireman's water hose. Once flat, the tubes could be cut into a number of 7 mm in diameter discs using a specially fabricated 7 mm (inside diameter) "cookie cutter". Pressing the cutter on the collapsed tube resulted in 2 discs being produced (i.e. one from the upper most part of the tube wall and one from the lower most part). In this way each tube was theoretically capable of producing 40 discs, thus like the bead experiments, allowing parallel experimentation to be undertaken. Again, like the beads, 24 well microwell plates (Corning, Corning, New York, USA) were used each preloaded with 1 ml of fresh supplemented media. Care was taken to keep the tubes/disks submerged in fluid at all times since on exposure to air syneresis soon occurs i.e. water loss from the hydrogel leading to unwanted construct shrinkage.

The average number of cells in each disc was estimated from the cell density in the cell/media/alginate solution and the discs dimension i.e. 7 mm diameter. The average disc was calculated to have 9600 cells from an initial 10^6 cells per ml of cell/alginate solution. Again control wells were also produced matching the discs' cell number but containing no alginate, thus again matching the cell:medium ratio. Discs were incubated in 10% CO_2, humidified incubators at 37°C. Cells were also freed from the hydrogel using 0.1 M sodium citrate and cell numbers and viability estimated using trypan blue and Neubauer haemocytometry counts using light microscopy.

3.5 Alginate polymer/cell survival and proliferation studies

Cell/alginate homogeneous mixtures were prepared as previously described. Using the mixture, the Mark I tube forming device (i.e. float activated by a pump driven fluid) was used to create tubes of approximately 4 mm outside diameter and 12 cm in length from a 2% alginate (Fluka - St. Gallen, Switzerland) in physiological saline solution containing cells at a final concentration of 10^6 per ml. Cross-linking was carried out using 1% calcium chloride made up in physiological saline corrected to a pH of 7.4 with sodium hydroxide solution as previously described. The resulting tubes had a wall thickness of approximately 150 μm. Cross-linking was carried out for a total of 15 minutes prior to being rinsed with either supplemented media or physiological saline. The volume of rinsing agent used was either 1.5 ml, 12.5 ml or 125 ml. The rinsing agent was flushed through the hydrogel tube

whilst still *in situ* within the glass forming tube using a syringe driver (Harvard PHD 2000, Harvard Apparatus, Holliston, Maryland, USA) coupled directly to the base unit. The rates used were 1.5 $mlmin^{-1}$ (1.5 ml volume), 6.25 $mlmin^{-1}$ (12.5 ml volume) and 8.33 $mlmin^{-1}$ (125 ml volume). In order to count the cells and access their viability, the cells needed to be separated from the alginate hydrogel. Therefore, immediately following rinsing, sodium citrate solution (0.1 M) was flushed through the hydrogel tubes (still *in situ* in the glass forming tubes) using the Harvard PHD syringe driver and left until the tubes were fully dissolved prior to visual inspection using a light microscope. The glass forming tube and base unit when all the openings/ports are carefully stoppered off using small rubber bungs, can be easily mounted horizontally on a light microscope stage for viewing. Once the hydrogel tube was dissolved the resulting solution was expelled from the glass forming tube by removing all the stoppers, inverting the device and then gently pushing air through the device via a syringe inserted into the base unit. Cells were now counted and their viability assessed using trypan blue stain and Neubauer haemocytometry.

Control experiments were performed in parallel using identical cell numbers . The viability of these control cells was assessed following harvesting (trypsinisation from the T-flask) with no further manipulation i.e. only essential unit operations were performed to be able to obtain cells for viability assessment from a standard T-flask.

The A7r5 cells were rescued from the hydrogel using 0.1M sodium citrate as per Section 3.4.3.

3.6 Effect of media composition on cell survival and proliferation

Two different alginates were chosen for this particular experiment namely Fluka (alginic acid salt from brown algae - Fluka, St.Gallen, Switzerland) and Sigma (high viscosity alginic acid from macrocystic pyrifera [Kelp] - Sigma, St.Louis, Missouri, USA).

In order to have a comprehensive study, two three-dimensional structure types were constructed; discs from tubes and beads. Discs were made from tubes as per Section 3.4.3 and beads were produced as per Section 3.4.2. Overall there were six experimental conditions, all using 1% alginate weight/volume solutions. See Figure 7.5 for an overview of the experimental matrix. Experimental observations were carried out over a 16 day period.

3.7 GRGDY peptide synthesis

The initial batches of the GRGDY peptide were synthesised with the assistance of Dr. Patricia Zunszain in the Department of Chemistry at UCL. In brief, the synthesis of the pentapeptide deployed a Millipore 9050 OM peptide synthesiser, using standard FMOC resin based methodology and FMOC amino acids (Bachem, Bubendorf, Switzerland). In order to carry

out the peptide sythesis, both the arginine (R) and the aspartic acid (D) amino acids required side-protecting groups: Arg(Pfb) and Asp(otBu). After removal from the resin, these protective side groups were hydrolysed prior to the peptide being purified via preparative HPLC using a Vydac C18 (10 μm) 22 x 250 mm column (Grace Wydac, Columbia, Maryland, USA) and finally lyophilised and stored at 4°C.

3.7.1 GRGDY-alginate derivitisation

An overview of the derivitisation process is depicted in Figure 3.2 (reagent steps) and Figure 3.3 (dialysis steps). In detail; a 1% weight/volume solution of alginate (DMB pharmaceutical grade, Manugel, IAP, Tadworth, Surrey, UK) was prepared (allowing for the water content retained in the stock alginate powder) using 0.1 M MES buffer (Sigma, St. Louis, Missouri, USA) solution. This buffer was prepared using WFI (water for injection) (BioWhittaker, Walkersville, Maryland, USA) and 0.3 M sodium chloride solution (pharmaceutical grade, Sigma, St. Louis, Missouri, USA). The pH of the buffer was adjusted using 1M sodium hydroxide solution (pharmaceutical grade, Sigma, St. Louis, Missouri, USA) to pH 6.5. (This saline concentration and pH was the optimal conditions found by Mooney's group (Rowley *et al*, 1999 and 2001). The alginate was finally autoclaved at 121°C for 20 minutes in a bench top autoclave (Prestige Medical, Blackburn, UK), rolled (Stuart Scientific Roller Mixer SRT2) and allowed to cool to room temperature before use.

Initial experiments were performed using 1 mg of peptide per gram of alginate powder (dry weight). The other reactant ratios were: sulfo-N-hydroxysuccinimide (Sigma) (Sulpho-NHS) at 38 mg per mg of peptide and 1-ethyl-(dimethylaminopropyl)carbodiimide (Sigma) (EDC) at 67 mg per mg of peptide. These ratios were approximately the same as Rowley *et al* had previously described (Rowley *et al*, 1999). The EDC is a water soluble carbodiimide capable of forming amide linkages between amine containing molecules and the carboxylate moieties on the alginate polymer backbone. The co-reactant, sulfo-NHS, stabilises the reactive EDC-intermediate against a competing hydrolysis reaction, thus increasing the overall efficiency of the amide bond formation. The GRGDY pentapeptide was covalently bonded to the alginate polymer backbone via the terminal amine present on the peptide - see Figure 8.5 (Rowley *et al*, 1999). Both the EDC and Sulfo-NHS were made into solutions using WFI and then sterilised using a 0.2 μm in line filter (Sartorius, Goettingen, Germany). Wherever possible all manipulations were performed in a biological safety cabinet to try and protect experimental sterility (Gelman Sciences BH48 modified with a double HEPA filter). The Sulfo-NHS solution was added to the autoclaved alginate solution and thoroughly mixed by vigorous shaking prior to being rolled for 5 minutes. The EDC solution was then added and again thoroughly mixed and rolled for a further 30 minutes prior to adding the peptide which was predissolved just prior to use in WFI and filtered through a 0.2 μm filter.

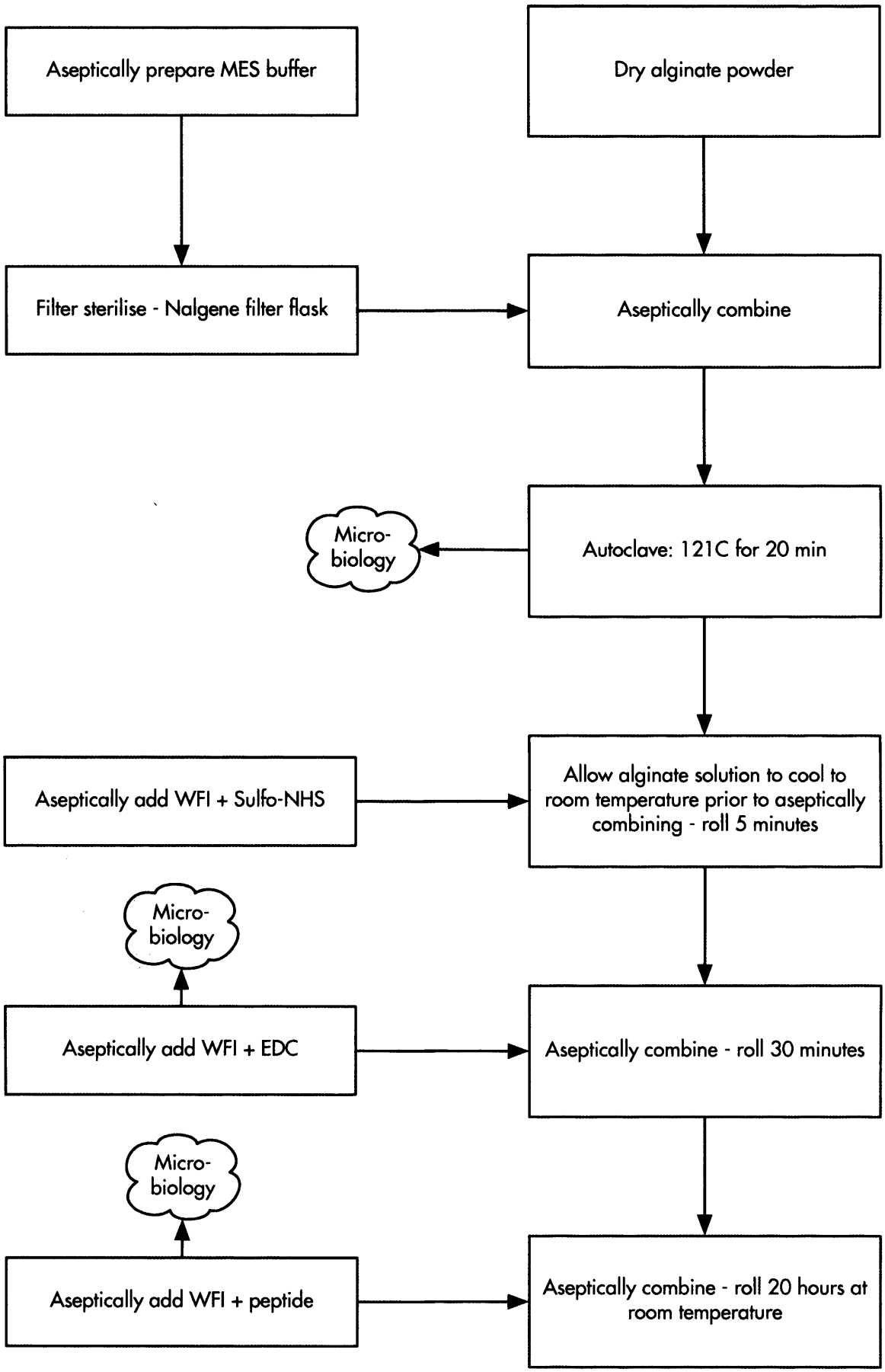

Figure 3.2

Overview of the aseptic preparation of derivatised alginate - Reagent stage + microbiology sampling points.

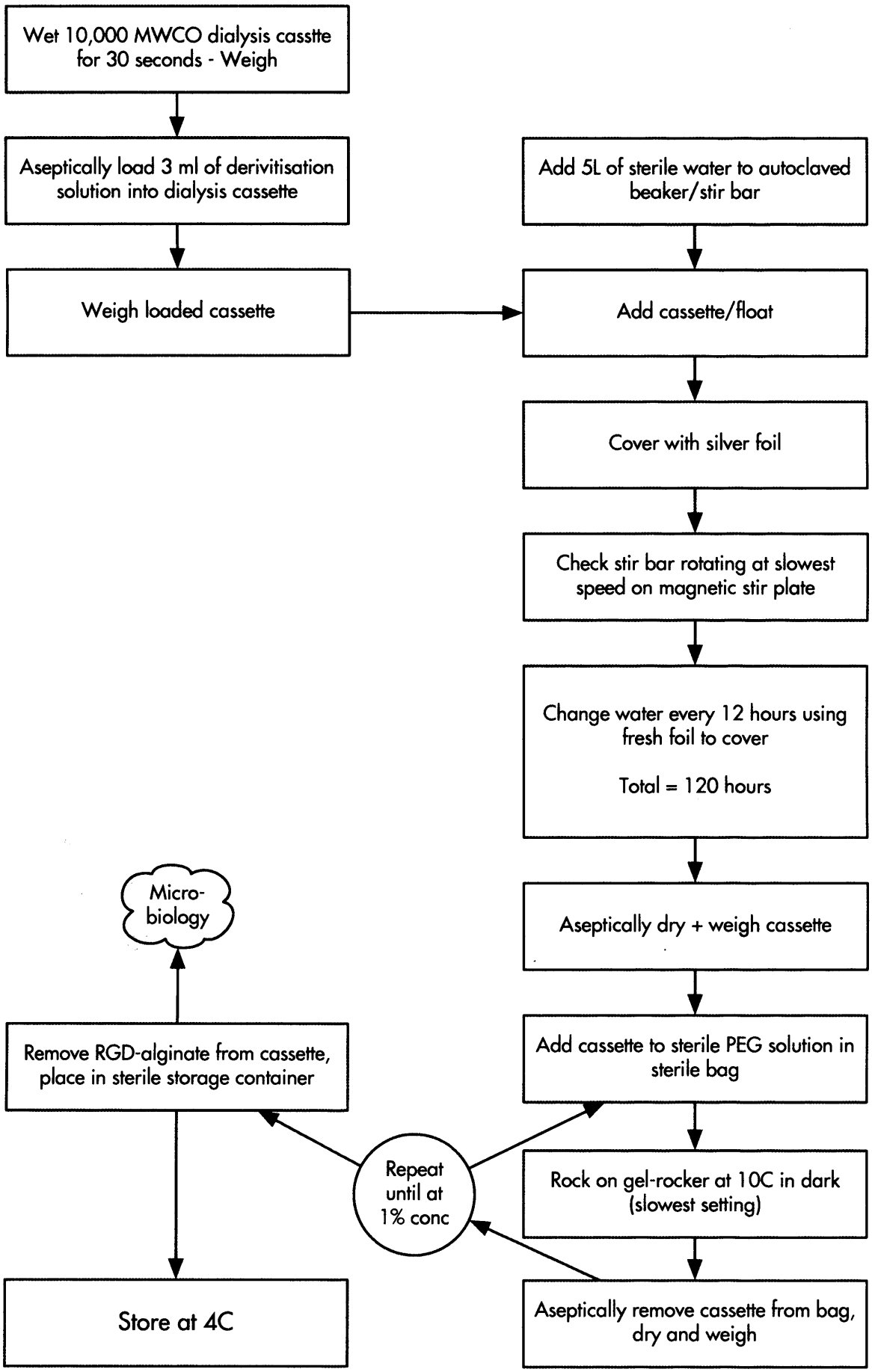

Figure 3.3

Overview of the aseptic preparation of derivatised alginate - Dialysis stage + microbiology sample point.

After combining all the reactant, including the peptide, the solution was then rolled for 24 hours. All the reactions were carried out at room temperature in light protected containers, i.e. aluminium foil applied to all containers. In order to remove excess reagents, the solutions were extensively dialysed using a molecular weight cut off (MWCO) of 3,500. Snake skin tubing (Pierce, Rockford, Illinois, USA) or Slide-A-Lyzer dialysis cassettes of maximum capacity 3 ml (Pierce, Rockford, Illinois, USA) supported by purpose made foam floats were operated in autoclaved reverse osmosis (RO) water in 5 L sterilised containers for a 48 - 96 hour periods at 4°C. During which time the RO water was stirred (magnetic bar/stirrer base - 211, Bibby, Stone, Staffordshire, UK) and replaced every 12 hours with fresh sterilised RO water. Care was taken to reduce possible contamination by keeping all the containers covered. This dialysis was carried out in total darkness apart from when changing the dialysis solution. After dialysis, activated charcoal (clinical grade - hydrochloric acid washed - Sigma, St. Louis, Maryland, USA) at 0.5 gm per 1 gm of alginate powder (dry weight) was added and mixed thoroughly prior to rolling for thirty minutes. Finally, in order to remove the charcoal plus any other impurities the solution was past through a ready prepared Celite Hyflo (acid washed diatomite filter aid - Celite, Lompoc, California, USA) column (sinter funnel) facilitated by a vacuum pump. This process took 3 - 6 hours depending upon the degree of agitation supplied to the mixture. The resulting solution was collected in a sterile flask and either stored immediately at 4°C or lyophilised using an Edwards Freeze Drier and then stored at 4°C. One other variation was to use polyethylene glycol (PEG) solutions (Slide-A-Lyzer concentrate solution - Pierce, Rockford, Illinois, USA) or PEG solid (35,000 MWt, Fluka, Buchs, Switzerland) to reconcentrate the dialysed samples to desired final concentrations (during the prolonged dialysis, water would enter the dialysis tubing/cassette thus diluting the alginate). Thus after dialysis, water could be drawn out in a relatively controllable manner using PEG either in solid form or in a Concentrated Solution (Slide-A-Lyser concentrating solution - Pierce, Rockford, IL, USA). The Concentrating Solution was poured into the small plastic bag provided and then the Slide-A-Lyzer Dialysis Cassette containing the derivitised alginate was added. The bag was then placed on a rocking table at it minimum movement setting. Using serial measurements obtained by carefully drying and accurately weighing the dialysis tube or cassette, the final concentration of the alginate could be controlled. Solutions of final concentration of either 1% or 2% were aimed at. This concentration step took 9 - 12 hours and was performed on a steady-state rocking table at approximately 10°C (purpose built cold room) in total darkness.

3.8 Imaging techniques

The additional imaging techniques included:

- Live/dead viability/cytotoxicity imaging.

3.8.1 Live/dead viability/cytotoxicity imaging

The live/dead viability/cytotoxicity assay kit (L-3224 - Molecular Probes, Eugene, Oregon, USA) has previously been demonstrated for use with cell/alginate beads (Read *et al*, 2001). This assay simultaneously positively identifies live from dead cells by using 2 probes. These probes measure 2 different aspects of cell viability namely intracellular esterase activity and plasma membrane integrity. Live cells are identified by the presence of intracellular esterase activity which is detected by the enzymatic conversion of nonfluorescent calcein AM to which cell membranes are permeable. Thus calcein AM is converted into fluorescent calcein in live cells only, thus staining them green when viewed using ultraviolet microscopy. Similarly dead cells fluoresce red when the second probe, ethidium homodimer-1 enters the membrane damaged cells and binds to nucleic acids thus increasing its concentration and therefore intensity (approximately 40x). Ethidium homodimer-1 is excluded by intact cell membrane (i.e. the same as for trypan blue stain). Bacteria and fungi, possible contaminants, are not affected by these probes i.e. there should be no false positives (Molecular Probes spec sheet MP 03224 24 January 2001).

Using the Molecular Probes kit it was possible to view both non-derivitised and derivitised alginate/cell constructs. For example using confocal microscopy it was possible to observe balled-up cells in derivitised alginate immediately after construction and then 12 - 24 hours later to observe the cells in the process of elongation throughout the structure.

4.0 Scaffold-cell combinations: Options and demonstration of principle

This chapter brings together the material selected with the options available for combining this material with cells and from the method selected puts forward a concept on how this may be achieved in a way that allows consistent preparation of many units of tissue.

4.1 Options

4.1.1 Scaffold seeding

Since a tissue engineered construct typically consists of a scaffold and cells, the first objective was to establish criteria for choosing the mode of scaffold seeding. There are two broad options for combining them:

- The scaffold can be fabricated first and then seeded
- Cells can be mixed with the scaffold material prior to or during scaffold fabrication

Both options have advantages and disadvantages, there now follows an analysis of the two approaches.

Fabricating the scaffold first allows a large host of materials and methods to be employed. Because the cells only come into contact with the finished scaffold, there is no need to be constrained to "cell friendly" conditions during fabrication. Thus fabrication can use materials which may require high temperature, extremes of pH and harsh chemicals e.g. polyglycolic acid (PGA) can only be melt moulded at temperatures in excess of 160°C. Provided the fabricated material is thoroughly washed and sterilised prior to cell seeding there are no difficulties. Furthermore, scaffolds made from many of the candidate materials e.g. PGA, polylactic acid (PLA) and PLA-PGA co-polymers can be easily stored prior to seeding. In contrast scaffolds created from pre-seeded material cannot be easily stored but must be used immediately. Suitable materials for preformed scaffolds include the thermoplastics discussed above plus natural polymers such as freeze-dried collagen (Butler *et al*, 1999) and fibronectin (Ahmed *et al*, 2000).

Seeding a preformed scaffold is a complicated task. Two difficulties arise. Firstly, it is essential to seed the scaffold homogeneously and secondly the cells must attach and migrate homogeneously throughout the material. Homogeneity and attachment are required in order for the cells to migrate through the scaffold, divide, differentiate and finally organise into the desired living structure. However, seeding preformed scaffolds usually involves adding cells suspended in culture media (Niklason *et al*, 2001). Seeding of preformed scaffolds has proven to be highly wasteful. Loses of a whole order of magnitude are not uncommon (Yacoub and Taylor, 2001). Ensuring that the cells are exposed to the scaffold in a homogeneous manner is "implied" by assuming that the cells are evenly dispersed in the culture media. This may not

be the case, e.g. because cells have a relative density just greater than media, they therefore have a tendency to settle due to gravitational force. Having the cells and the scaffold in close contact is the prerequisite for cell attachment. Assuming that cell attachment to the surface is even, the cells are then required to migrate evenly through out the porous scaffold in order to achieve a homogeneous cell-scaffold construct.

Alternatively, the cells can be mixed with the scaffold material prior to or during fabrication. Homogeneous mixing is essential and must be capable of being validated if a cGMP cell-scaffold construct is to be formed. Once again, the cells must remain evenly disbursed during the fabrication step. All the mixing and fabrication steps must not be hostile to cells e.g. high shear forces during mixing could result in cell damage. Dead cells would lead to unfavourable cell debris being released into the scaffold. Suitable materials for this cell premixing technique include collagen (Bell *et al*, 1991) and alginate (Kuo *et al*, 2001).

4.1.2 Sterility issues

Sterility is a major issue irrespective of which cell-scaffold construction is used, since tissue engineered constructs are currently likely to take weeks or months to fully form. Thermoplastics e.g. PGA can be sterilised by gamma irradiation post fabrication i.e. prior to cell seeding. However, natural polymers such as collagen need to be kept sterile throughout the fabrication process unless they are freeze-dried. Freeze drying allows gamma irradiation to be employed. However, this does change the nature of the polymer (Johnson *et al*, 1999 and Roe *et al*. 1992). In short, natural polymers need to be kept sterile at all times since both bacteria and sterilisation will degrade the polymer.

Long-term sterility and total number of unit operations (e.g. physical handling) are intrinsically linked to one another. Ideally handling must be kept to a minimum or avoided. One potential solution is to mix scaffold material and cells immediately prior to scaffold formation. Ideally the scaffold formation would be in a "device" which could also act as a bioreactor to grow and mature the fledgling construct, allow ease of monitoring and also act as the "delivery device" i.e. the first time the scaffold formation device is opened is in the operating theatre immediately prior to implantation into the patient.

4.1.3 Materials options

From an engineering process prospective, constructing a cell-scaffold from cells premixed with the scaffold material appears in principle to have a considerable number of advantages over the alternative method including:

- Being able to mix cells homogeneously in the material theoretically resulting in a scaffold that is uniformly seeded. Thus potentially easing validation of the seeded

scaffold

- Cell wastage is kept to a minimum since there is not the "hit and miss" attachment and migration into the scaffold problem
- Reduced culture times by achieving a high cell density within the material prior to fabrication end employing cells of exactly the right phenotype and maturity. Reducing culture times potentially leads to reduced contamination risk and lower inventory levels. The ideal situation would be where no culture time was required, i.e. cell density and their arrangement was near normal for artery, the scaffold sufficiently strong and most importantly, the ability of the cells to produce extracellular matrix optimised
- Bioactive molecules (e.g. to produce cell attachment or cell signaling effects) could also be incorporated homogeneously into the scaffold by premixing prior to fabrication
- Potential economic advantage due to reduced culturing times, less cell waste and inventory. This optimal situation fits the highly successful, "just-in-time" (JIT) manufacturing management philosophy (Cheng and Podolsky, 1996).

In order for the material to be suitable for combined cells-scaffold production, it must possess properties, which, allow a scaffold to be formed without harming the cell population; likewise the cell population must not substantially hinder the material from forming the desired scaffold e.g. too higher cell density (i.e. cells effectively "diluting down" the scaffold material).

The choice of material for premixed cell-scaffold fabrication is limited to those which can be fabricated into three-dimensional structures at "cell friendly" conditions, since mammalian cells are only capable of surviving in a narrow temperature range, they do not tolerate extremes of pH and are easily harmed by caustic chemicals. Some of the other major criteria include:

- Capable of being formed into a porous structure which has adequate strength
- Overall the material and its breakdown products must be non-toxic both *in vitro* and *in vivo*. Ideally, the scaffold material (and its breakdown products) should have totally left the construct prior to implantation
- The human body must be able to safely eliminate these molecules if still present at implantation
- Cell attachment ability may or may not be a prerequisite depending upon the cell type
- The material needs to breakdown in a predictable/controlled manner such that as the strength of the fledgling construct increases (due to the production of extracellular matrix) so the strength of the scaffold material decreases as it breaks down

- Preferably low cost
- Well characterised (Ideally with existing FDA/Conformité Européene [CE] approval)
- Ideally a wealth of publications in peer reviewed journals - i.e. existing skill base
- Easily mixable with cells and bioactive molecules
- Free from pathogens.

The suitable scaffold materials available to this particular project are presented in Figure 4.1 together with their characteristics matched against the above criteria. Other possible materials were not included if availability was an issue e.g. hyaluronic acid on account of cost.

4.2 Selected materials

Using the above criteria, sodium alginate was selected as the ideal scaffold material for further evaluation. Its major advantages being its cell friendly fabrication conditions coupled with its absent pathogenicity. Its major disadvantages being poor characterisation and known batch-to-batch variability. An unknown issue was whether cell attachment sites were essential with respect to smooth muscle cells. There is a vast wealth of scientific literature on virtually every other mammalian cell and its ability to be grown whilst encapsulated in alginate hydrogel (at the start of this research project, over 250 refereed journal articles have been published on cells successfully encapsulated in alginate beads). Furthermore, relatively simple chemical modification was possible if attachment sites were required (Rowley *et al*, 1999). Finally, alginate hydrogel beads had already been demonstrated to be able to successfully deliver bioactive molecules successfully e.g. encapsulated freeze dried vascular endothelial growth factor (VEGF) had been demonstrated to stimulate endothelial cells for a period of two weeks *in vitro*. (Peters *et al*, 1998).

4.2.1 Alginate options

Sodium alginate was chosen as a model scaffold material since it met the essential requirements (or could potentially meet the essential requirements by relatively easy chemical modified) and was easily available. Non-pharmaceutical grade (low cost) was chosen and only when required was pharmaceutical grade (high cost and short supply) utilised.

Alginate was supplied from four manufacturers - see Figure 4.2. From the figure, it can be seen that unfortunately most of the companies distribute very little technical data regarding their alginate products. Discussions with Neil Cruttenden at ISP Alginates (UK) Ltd (formerly Kelco) (Tadworth, Surrey, UK) revealed that this was due to large inter-batch variability, and companies when purchasing alginate from ISP would test samples from a number of different batches to evaluate if it met their specific requirements before purchasing a batch usually of

Characteristic	PGA	Collagen	Alginate
Wealth of relevant publications	✓	✓	✓ (Bead encapsulation)
Well characterised	✓	× (Inter-batch variability)	× (Inter-batch variability)
Inherent pathogens	×	✓ (Unless recombinant)	✓
Ease of mixing with cells	N/A	✓	✓
Cell friendly fabrication conditions	×	✓	✓
Porous structure	✓	✓	✓
Ease of cell attachment	× (Needs physical or chemical modification)	✓	× (Needs chemical modification)
Predictable degradation	×	✓	?
Non-toxic degradation products	Locally toxic	✓	✓
Cost	Low	Medium - Animal origin High - Recombinant	Low - Food grade Medium - Pharma grade High - Ultrapure

Figure 4.1

Potential scaffold polymers available to the research project together with their respective characteristics relevant to tissue engineering.

Manufacturer - Product	Manufacturers' Data			
	Viscosity	Molecular weight	Other relevant information	
ISP Alginates Surrey, UK				
Keltone LVCR	Low	-	-	
Keltone HVCR	High	-	-	
Manucol DH	Medium	-	-	
Manucol DMF	High	-	-	
Manugel DMB	High	-	-	
Sigma Dorset, UK				
A2158 Low Viscosity	Approx. 250 cP* (2% solution/25°C)	-	High M	
A0682 Low Viscosity	Approx. 250 cP* (2% solution/25°C)	-		
A2033 Medium Viscosity	Approx. 3,500 cP* (2% solution/25°C)	-		
A7128 High Viscosity	Approx. 14,000 cP* (2% solution/25°C)	-		
Pronova Oslo, Norway				
LVG	118 mPas s	189,000	73% G	GMP man-ufacture
MVG	287 mPas s	231,000	73% G	
LVM	148 mPas s	209,000	38% G	
MVM	200 mPas s	226,000	38% G	
Fluka St. Gallen, Switzerland				
71238	-	-	Purity grade: Immobilisation of microorganisms	
71240	-	-	-	

*[1 cP = 1 mPas s]

Figure 4.2

Summary of manufacturers' available data for the commercial sodium alginates (Compiled: 1999 - 2000).

several tons.

The viscosity of the final alginate solution is critical to key aspects of the entire process:

- Ability of the alginate to form a homogeneous solution
- Ease of cell-alginate mixing to obtain and retain a homogeneous solution
- Relative ease of constructing a desired three-dimensional shape and retaining the shape long enough to cross-linking with a polyvalent ion. Lower viscosity solutions require much faster times to cross-link compared to the more viscous solutions if the three-dimensional shape is to be faithfully retained

Viscosity of the alginate solution is determined by a number of factors including:

- Ratio of G:M monomers. High G:M ratio increases viscosity and strength e.g. Pronova MVM and MVG alginate have near identical molecular weights (226,000 and 231,000 respectively) but have different G:M ratios (19:31 and 73:27 respectively) resulting in different viscosities (200 c.f. 287 mPas respectively)
- Length of polyG sequences (Long polyG sequences increase viscosity and strength)
- Molecular weight. In aqueous solution, the alginate molecules are long flexible polymeric chains that are continually in motion. Viscosity is a measure of how difficult it is for these polymeric chains to slide past one another. The longer the chains the more difficult it is and hence an increase in viscosity is observed (e.g. both Pronova LVG and MVG alginates have a G content of 73% but LVG has a molecular weight of 189,000 and a viscosity of 118 mPas compared to MVG's higher molecular weight of 231,000 and a viscosity 2.4x larger at 287 mPas
- Polyvalent ions are present in the aqueous solution. By weight, ISP Alginates (U.K.) Ltd. has calculated that pure sodium alginate contains approximately 8% sodium and that pure calcium alginate also contains approximately 8% calcium. Furthermore, ISP claim that it is not possible to commercially produce alginates that are totally free from calcium and ISP's alginates typically contain around 0.2% calcium, the balance usually being made up with sodium i.e. a typical analysis would be in the region of 7.8% sodium and 0.2% calcium. Some of ISP's products intentionally contain a substantially higher level of residual calcium e.g. Kelset and Keltose. They do not contain enough calcium to make the products insoluble in water, however once these alginates are hydrated, the residual calcium that is present binds temporarily to the polymer chains and in doing so, brings about, in effect, an increase in alginate molecular weight. This effective increase in molecular weight gives an increase in viscosity. Conversely the addition of sequestrants to solutions made from alginates containing a relatively high level of calcium removes the calcium responsible for providing the added viscosity, and a viscosity loss is

observed. Sodium hexametaphosphate (Calgon) can be employed to remove the calcium that is providing the added viscosity. Therefore, "Calgon viscosities" are lower than crude viscosities. This difference in viscosity is referred to as "false viscosity" because the added viscosity does not come from the polymer itself but by manipulating the level of the alginate binding calcium ions present in the solution. The extent to which the sodium ions in an alginate solution are replaced by calcium ions is called "calcium conversion". Reducing the viscosity of alginate solutions using sodium hexametaphosphate has been employed to allow the solution to flow between parallel glass plates prior to cross linkage to form flat sheets as cell scaffolds (Rowley et a;. 1999 and Rowley *et al*, 2002)

- Percentage of alginate in the aqueous solution. The higher the percentage the higher the viscosity and vice versa
- Raising the temperature leads to a reduction in viscosity and vice versa
- Processing e.g. autoclaving alginate solutions decreases viscosity due to a permanent reduction in overall polymer chain length
- Increasing the density of cells in the alginate solution leads to an increased viscosity and vice versa
- Addition of binding sites to the alginate e.g. covalently bonding Glycine-Arginine-Glycine-Aspartic acid peptide (GRGD) also affects viscosity.

4.2.2 Cross-linking agent options

Monovalent cations are required to make alginates water-soluble. Multivalent cations form alginate salts that are insoluble i.e. the multivalent cations react with multiple alginates polymer chains and thus cross-link the molecules together. Therefore when multivalent cations are added to a sodium alginate solution they will replace the sodium ions from the alginate and cause it to precipitate out of solution. This "ion exchange" reaction is a vital property of alginate responsible for its ability to form fibres, films and hydrogels. To date scientists have successfully encapsulated cells with alginate using calcium, barium and strontium ions (Wideroe and Danielsen, 2001).

4.2.3 Sterility issues

Tissue engineering requires the culturing of cell-scaffold constructs for weeks or months. It is therefore essential that the cell-scaffold is sterile prior to this prolonged incubation period. Alginate from whatever source is never free of contamination (Cruttenden, 2001).

There are therefore two options:

- Add the cells to a "non sterile alginate" solution and then sterilise e.g. add antibiotic to the culture media. This has the disadvantage in that occult infections/antibiotic

resistant organisms could continue to survive. This option is therefore not feasible

- Add cells to sterilised alginate. Options for sterilising alginate include, gamma irradiating the powder, ultra high heat treatment (UHT) of an aqueous solution, autoclaving an aqueous solution and filter sterilisation through 0.22 μm membrane filters. Unfortunately all these approaches apart from filter sterilisation, denature the alginate e.g. fragment the polymer backbone resulting in lower viscosity solutions for a given alginate percentage (Smisrod and Skjak-Braek, 1990). Membrane filtration is only possible when using ultra pure very low viscosity alginates. Both UHT (Provided by ISP, Surrey, UK at 121°C for 1.5 seconds) and autoclaving have been used in this project. Raising the pH of the alginate to pH 7 - 8 has been reported to help reduce viscosity reductions due to autoclaving (Smisrod *et al*, 1990), this practise has been adopted throughout this research project.

4.3 Construct forming device: Concept and first prototype

4.3.1 Options

There are two basic ways to produce a hydrogel tube using a hardenable liquid (sodium alginate solution) and a hardening liquid (calcium chloride solution):

- Around another tube e.g. extruded around a mandrel
- Inside another tube e.g. formed on the inside surface of a barrel

The main advantage of the mandrel approach is that the newly formed tube is well supported along its length by the mandrel as it is formed. The delicate hydrogel tube (>90% water with a wall thickness in the order of a few hundred μm) can easily be handled whilst it is on the rigid mandrel. The alginate solution around the mandrel very quickly forms a hydrogel on contact with the calcium chloride solution. Following initial gelling there is a period of either swelling of the wall thickness +/- shrinkage of the overall tube diameter depending upon various parameters e.g. calcium chloride solution concentration, length of time exposed to calcium chloride solution, ratio of G:M monomers within the polymer and the presence of other cations e.g. sodium ions in the calcium chloride solution (affects gelling rate). Thus the newly formed alginate tube is in very close proximity to the mandrel. This is an advantage until flow is required down the centre of the tube. Since there is negligible space between the mandrel and the alginate tube, virtually no flow is possible between the two. The alginate tube must first be removed from the mandrel and coupled at each end in order to allow flow of a liquid along its length. This was found to have at least five major disadvantages:

- Removing the delicate alginate tube from the mandrel was difficult if one wanted to avoid damaging the tube (even more difficult if the tube is made from a premixed solution of live cells and alginate)

- Without a central mandrel the tube was unsupported and had a tendency to sag thus creating irregular flow within it as well as non-uniform forces along the tube
- Coupling the delicate hydrogel at either end was difficult without harming the construct
- Required multiple unit operations thus increasing risk of contamination
- In a commercial application, increasing the complexity of the task and increasing the risk of contamination potentially leads to increased cost.

A possible alternative is to create the alginate tube within another tube (barrel). As the alginate tube is formed the barrel provides both shape and support. Since the alginate tube tends to shrink, a space becomes available for addition flow of fluid around the outside of the tube i.e. between the tube and the barrel (not just down the central lumen). The "attachment " between the alginate tube and the barrel is by weak surface tension forces, which can be very easily overcome if desired. Due to these forces, after formation, because the tube receives support from the barrel, there is no tendency to sag. Furthermore, since there is space within and around the tube, if the tube ends are appropriately fixed as part of the formation process, no handling is required in order to install the tube within a fluid circuit. Overall the number of unit operations to arrive at a tube in a flow circuit is one. Furthermore, since the tube is "held" within the barrel potentially the barrel could act as a bioreactor for the cell-alginate construct as well as a "delivery device" which is not opened until it is required in the operating theatre. A patent covering the above has been filed (Mason and Town, 2002a) as well as a number of related patents (Mason and Town, 2002b; Mason and Town, 2003a; Mason and Town 2003b).

4.3.2 First prototype

To achieve the goal of creating an alginate hydrogel tube within a barrel a simple experiment was carried out. The equipment consisted of a barrel (15 cm glass tube with a 5 mm inside diameter), a piston (similar to a syringe piston) made of PTFE which fitted tightly into the bore of the barrel and a regulator element (a piece of Plasticine moulded into the shape of a bullet) which fitted into the barrel with a length of approximately 1 cm and a diameter of approximately 4 mm, see Figure 4.3. Thus there was an approximately 500 μm space all round the regulator element if it located centrally in the barrel. The barrel was positioned in an upright position. The piston was inserted from below until it was approximately 4 cm from the top of the barrel. Approximately 1 ml of 4% alginate solution (ISP Manugel in water) was added directly above the piston. The regulator element was gently dropped into the alginate solution, such that it was fully submerged with only its very top exposed. The piston was then swiftly drawn down the barrel stopping a few centimetres from the base of the barrel, see Figure 4.4. Since there is a gap between the regulator element and the barrel, alginate

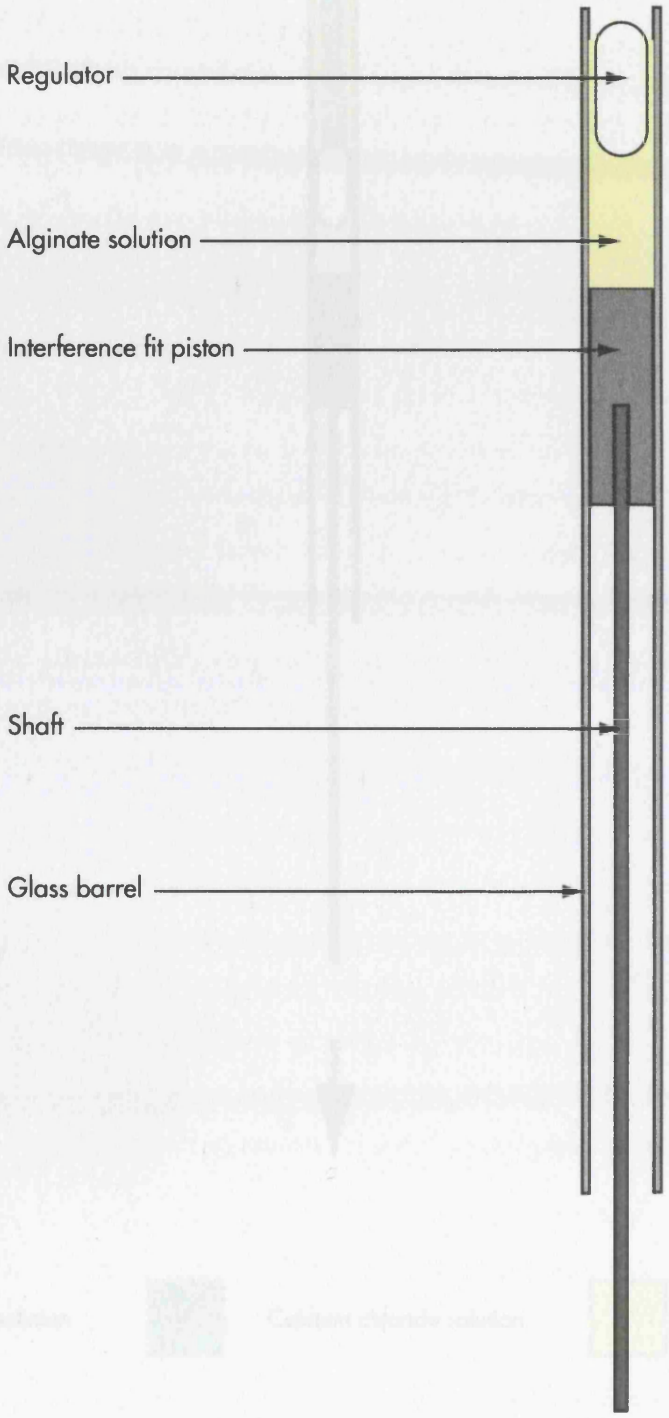

Figure 4.3

Tube-forming device - First prototype.

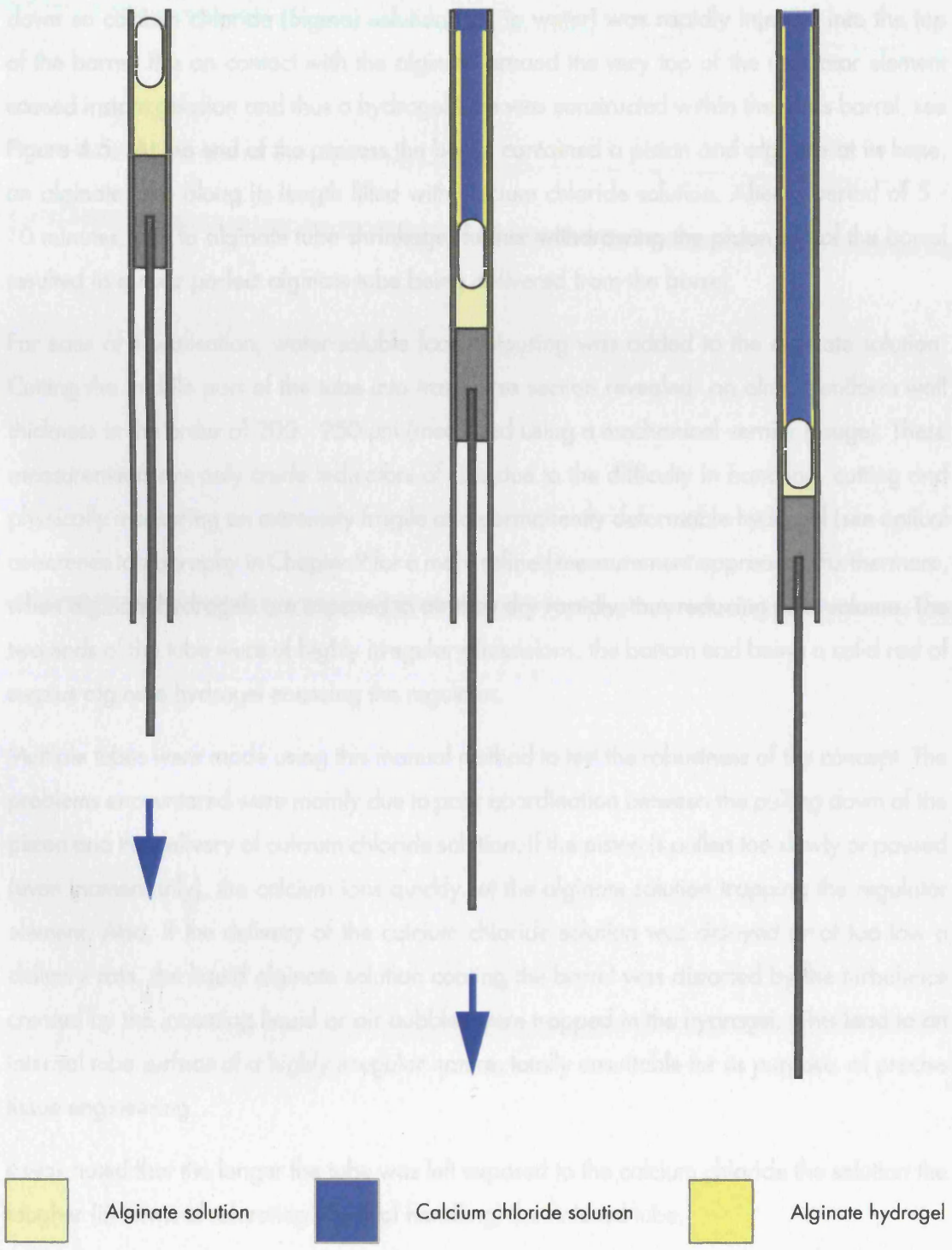

Figure 4.4

Schematic time progression in the formation of an alginate hydrogel tube.

↓ = Direction of travel of the piston relative to the barrel which is fixed

solution was deposited on the inside of the barrel along its length. As the piston was drawn down so calcium chloride (Sigma) solution (2% in water) was rapidly injected into the top of the barrel, this on contact with the alginate around the very top of the regulator element caused instant gelation and thus a hydrogel tube was constructed within the glass barrel, see Figure 4.5. At the end of the process the barrel contained a piston and alginate at its base, an alginate tube along its length filled with calcium chloride solution. After a period of 5 - 10 minutes, due to alginate tube shrinkage, further withdrawing the piston out of the barrel resulted in a near perfect alginate tube being delivered from the barrel.

For ease of visualisation, water-soluble food colouring was added to the alginate solution. Cutting the middle part of the tube into transverse section revealed an almost uniform wall thickness in the order of 200 - 250 μm (measured using a mechanical vernier gauge). These measurements are only crude indicators of size due to the difficulty in handling, cutting and physically measuring an extremely fragile and permanently deformable hydrogel (see optical coherence tomography in Chapter 9 for a more refined measurement approach). Furthermore, when alginate hydrogels are exposed to air they dry rapidly, thus reducing their volume. The two ends of the tube were of highly irregular dimensions, the bottom end being a solid rod of surplus alginate hydrogel encasing the regulator.

Multiple tubes were made using this manual method to test the robustness of the concept. The problems encountered were mainly due to poor coordination between the pulling down of the piston and the delivery of calcium chloride solution. If the piston is pulled too slowly or paused (even momentarily), the calcium ions quickly set the alginate solution trapping the regulator element. Also, if the delivery of the calcium chloride solution was delayed or of too low a delivery rate, the liquid alginate solution coating the barrel was distorted by the turbulence created by the incoming liquid or air bubbles were trapped in the hydrogel. This lead to an internal tube surface of a highly irregular nature, totally unsuitable for its purpose of precise tissue engineering.

It was noted that the longer the tube was left exposed to the calcium chloride the solution the tougher (in terms of tolerating physical handling) the finished tube.

Another point of interest was the degree of shrinkage both axially and longitudinally. Axial shrinkage gave the tubes an internal diameter in the order of 3.0 - 3.5 mm (measured by carefully passing a series of rods of known diameter down the tube). Longitudinal shrinkage was in the order of <0.5 cm per 10 cm length of barrel.

The Plasticine regulator was formed into a number of different bullet shapes, all of which gave similar results.

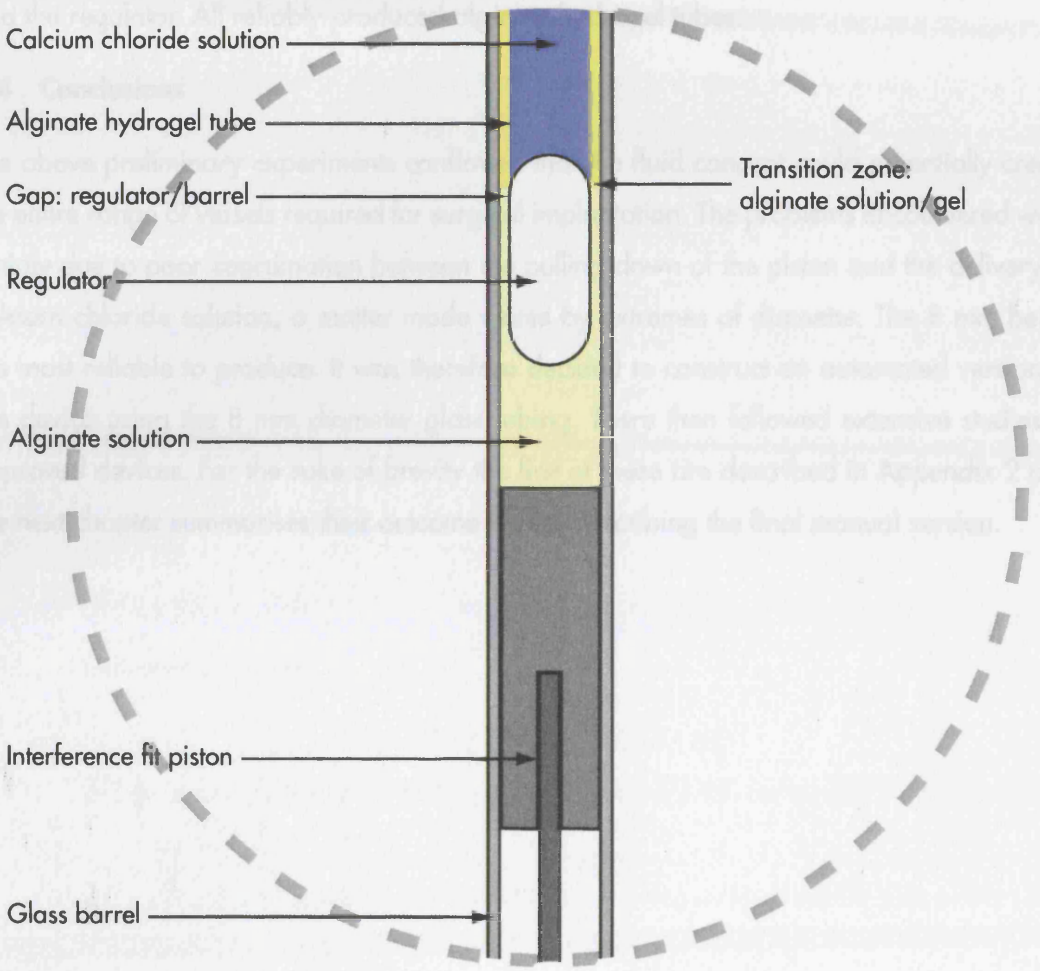

Figure 4.5

Transition zone: alginate solution meeting calcium chloride cross-linking solution and instantaneously setting to form a hydrogel.

The concept was then tried with glass barrels of various inside diameters, including 1.5 mm (equivalent in diameter to a medium size human coronary artery), 8 mm (equivalent in diameter to an human upper leg vessel) and 32 mm (equivalent in diameter to a human aorta) with matching pistons and appropriate sized bullet shaped regulator elements. Regulator elements were made either of Plasticine in the case of the 1.5 mm barrel or of PTFE which was used for the larger barrels with a barrel clearance of 500 μm all round between the barrel and the regulator. All reliably produced alginate hydrogel tubes.

4.4 Conclusions

The above preliminary experiments confirmed that the fluid concept could potentially create the entire range of vessels required for surgical implantation. The problems encountered were mainly due to poor coordination between the pulling down of the piston and the delivery of calcium chloride solution, a matter made worse by extremes of diameter. The 8 mm being the most reliable to produce. It was therefore decided to construct an automated version of the device using the 8 mm diameter glass tubing. There then followed extensive studies of improved devices. For the sake of brevity the first of these are described in Appendix 2 and the next chapter summarises their outcome before describing the final manual version.

5.0 Fluid driven tube forming device

The alternative to using a physical piston is to drive the movement of the regulator using fluid propulsion. The idea was to use the same major components i.e. precision bore barrel, regulator, alginate solution and calcium chloride solution, but in a different configuration in order to overcome the obstacles encountered with the piston driven device.

5.1 Fluid driven device prototype – solid regulator version

A prototype was designed and made which consisted of a 4 mm inside diameter borosilicate precision bore glass cylinder of 15 cm in length, see Figure 5.1. As before the device was to be used in the upright position. The base of the cylinder had a 2.5 cm Perspex cylinder added. This piece was machined such that it had, a strong interference fit to the outside of the glass barrel, allowed a syringe to be inserted into its base again creating an interference fit and had an internal "collar". All the interference fits were fluid tight. The purpose of the internal collar was to create a docking station with a relatively weak interference fit between the collar and the lower-most part of the regulator element's wall. Various bullet shaped regulators were machined from PTFE with outside diameters ranging from 3 - 3.8 mm (i.e. giving a regulator - barrel clearance of 200 - 1000 μm, resulting in a theoretical barrel coatings of 100 - 500 μm in thickness). All the regulators were 1 cm in length.

5.1.1 Operating sequence

The optimal operating sequence for this prototype consisted of:

1. Holding the barrel in the upright position with the Perspex cylinder at the base
2. Dropping the regulator down the barrel with interference fit part at the lower end
3. Applying a well fitting air line with a maximum pressure in the order of 3 p.s.i. to the top of the barrel. The air pushes the regulator into the collar and gives a fluid tight seal via a weak interference fit. Too much force and the regulator and collar became tightly jammed
4. Removing the air line
5. Using a modified 2 ml syringe with an extended needle (that reaches the length of the barrel), 1 ml of 2% alginate solution (ISP Manugel) was added carefully (in order to avoid air bubbles) to just above the regulator. By holding the tip of the syringe tightly against the side of the glass barrel, it is possible for the alginate to completely flow down and around the gap between regulator and barrel (i.e. displacing the air as the alginate flowed) thus leaving no trapped air

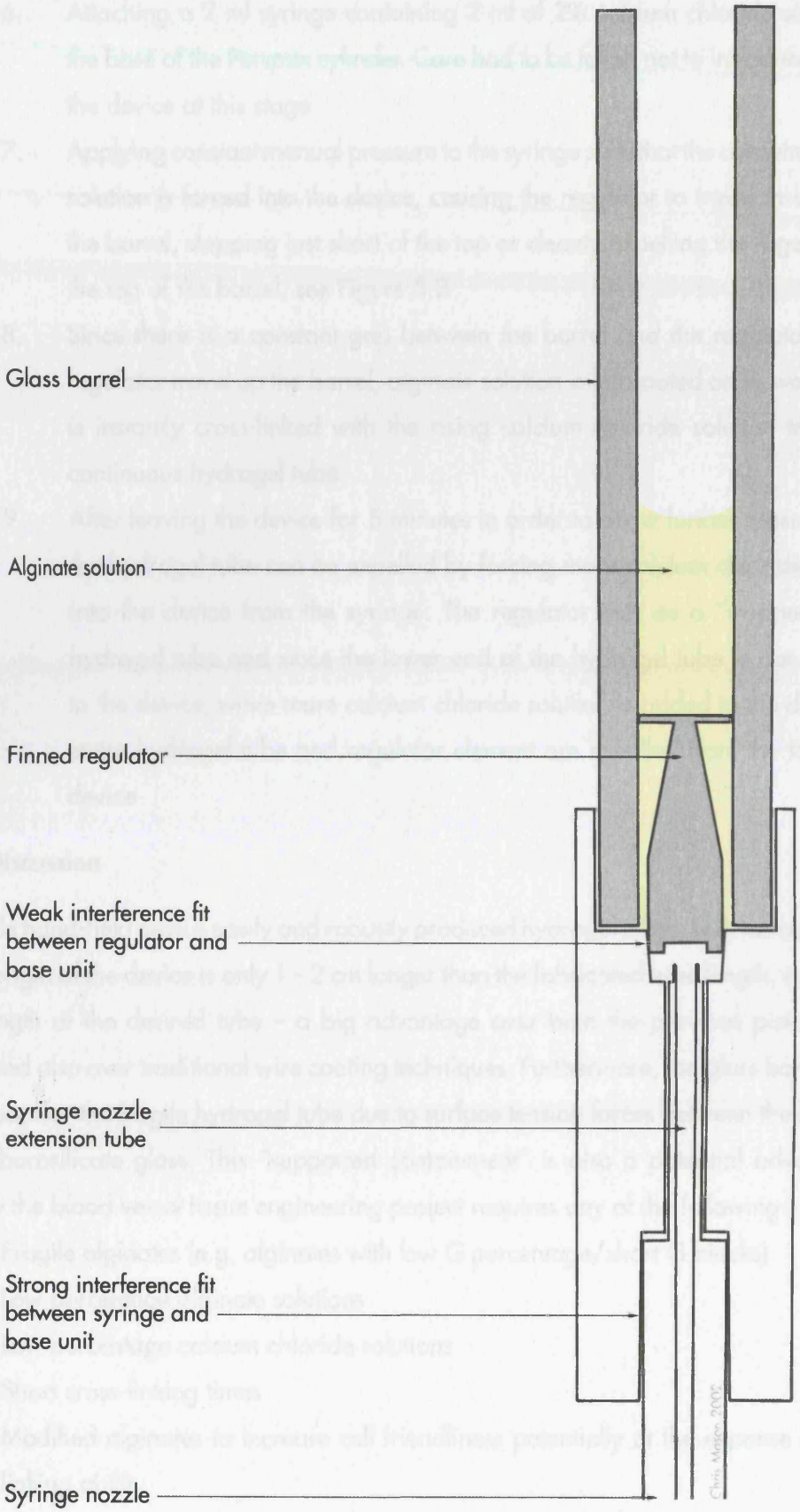

Figure 5.1

Fluid driven device - Prototype.

6. Attaching a 2 ml syringe containing 2 ml of 2% calcium chloride solution to the base of the Perspex cylinder. Care had to be taken not to introduce air into the device at this stage
7. Applying constant manual pressure to the syringe such that the calcium chloride solution is forced into the device, causing the regulator to travel smoothly up the barrel, stopping just short of the top or cleanly expelling the regulator out the top of the barrel, see Figure 5.2
8. Since there is a constant gap between the barrel and the regulator, as the regulator travel up the barrel, alginate solution is left coated on its wall, which is instantly cross-linked with the rising calcium chloride solution to form a continuous hydrogel tube
9. After leaving the device for 5 minutes in order to allow further cross linkage, the hydrogel tube can be expelled by forcing more calcium chloride solution into the device from the syringe. The regulator acts as a "stopper" in the hydrogel tube and since the lower end of the hydrogel tube is not attached to the device, when more calcium chloride solution is added to the device the entire hydrogel tube and regulator element are expelled from the top of the device

5.1.2 Discussion

This simple hand-held device easily and robustly produced hydrogel tubes, with the advantage that the length of the device is only 1 - 2 cm longer than the fabricated tube length, regardless of the length of the desired tube – a big advantage over both the previous piston driven method and also over traditional wire coating techniques. Furthermore, the glass barrel acted as a support for the fragile hydrogel tube due to surface tension forces between the hydrogel and the borosilicate glass. This "supported containment" is also a potential advantage if ultimately the blood vessel tissue engineering project requires any of the following:

- Fragile alginates (e.g. alginates with low G percentage/short G blocks)
- Low percentage alginate solutions
- Low percentage calcium chloride solutions
- Short cross-linking times
- Modified alginates to increase cell friendliness potentially at the expense of cross-linking ability
- Thin walled tubes
- Cells and/or bioactive molecules premixed with the alginate solution

This final point highlights a potential area of concern in general when premixing cells and a scaffold polymer. The problem is that the addition of cells even with negligible cell culture

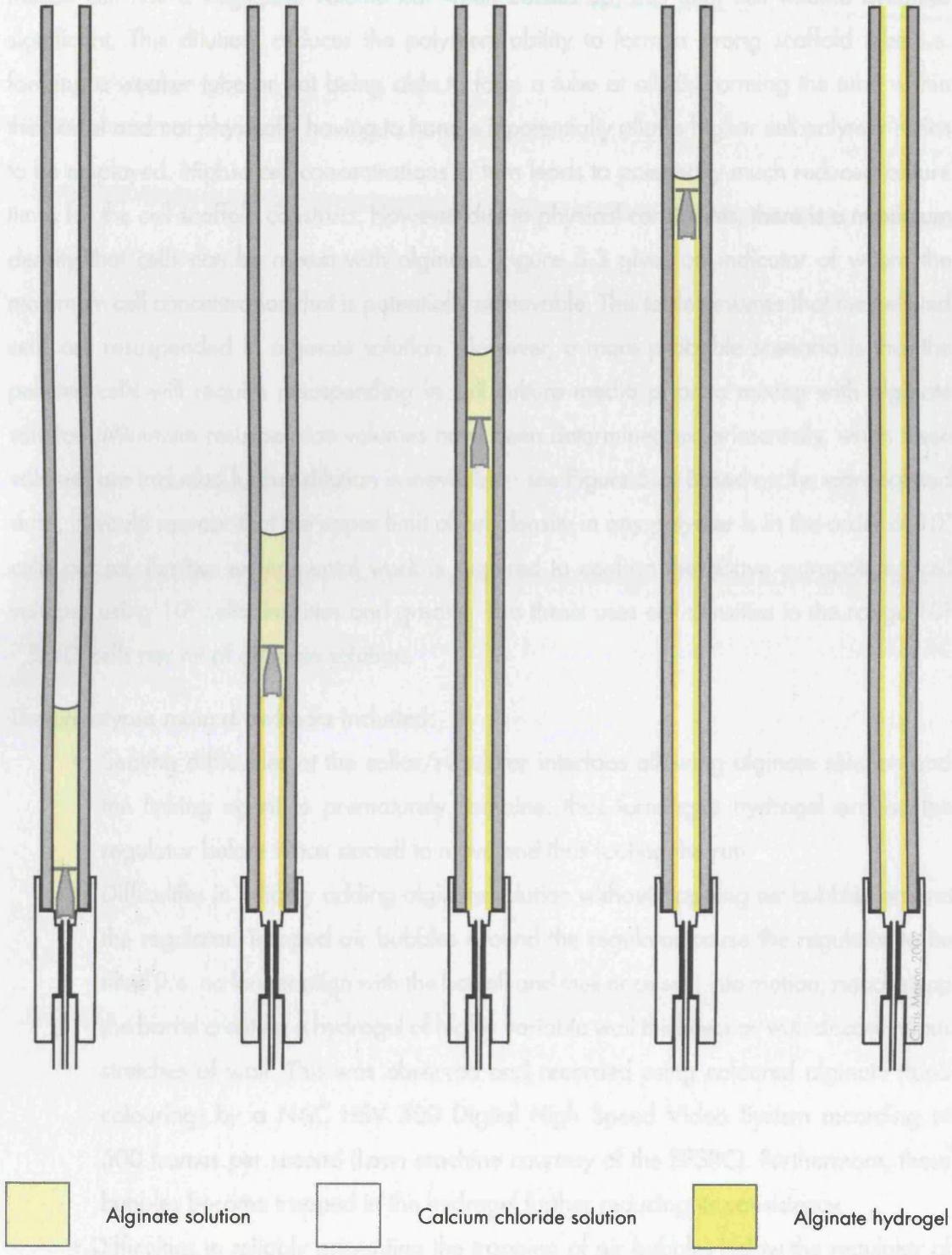

Figure 5.2

Production schematic of an alginate hydrogel tube from the loaded device to a finished tube with the regulator element having been expelled from the barrel.

media dilutes the polymer due to the physical volume of the cells themselves. Each smooth muscle cell has a negligible volume but when bulked up, this total cell volume becomes significant. This dilution, reduces the polymers ability to form a strong scaffold tube i.e. forming a weaker tube or not being able to form a tube at all. By forming the tube within the barrel and not physically having to handle it potentially allows higher cell:polymer ratios to be employed. Higher cell concentrations in turn leads to potentially much reduced culture times for the cell-scaffold construct. However due to physical constraints, there is a maximum density that cells can be mixed with alginate. Figure 5.3 gives an indicator of where the maximum cell concentration that is potentially achievable. This table assumes that the pelleted cells are resuspended in alginate solution. However, a more probable scenario is that the pelleted cells will require resuspending in cell culture media prior to mixing with alginate solution. Minimum resuspension volumes have been determined experimentally, when these volumes are included further dilution is inevitable - see Figure 5.4. Based on the extrapolated data, it would appear that the upper limit of cell density in any polymer is in the order of 10^7 cells per ml. Further experimental work is required to confirm the above extrapolated cell volumes using 10^8 cells densities and greater. This thesis uses cell densities in the range 10^5 - $5x10^7$ cells per ml of alginate solution.

The prototypes main drawbacks included:

- Sealing difficulties at the collar/regulator interface allowing alginate solution and the linking agent to prematurely combine, thus forming a hydrogel around the regulator before it has started to move and thus fouling the run
- Difficulties in reliably adding alginate solution without trapping air bubbles around the regulator. Trapped air bubbles around the regulator cause the regulator to be tilted (i.e. no longer align with the barrel) and thus once sent into motion, ricochets up the barrel creating a hydrogel of highly variable wall thickness or with discontinuous stretches of wall. This was observed and recorded using coloured alginate (food colouring) by a NAC HSV 500 Digital High Speed Video System recording at 500 frames per second (Loan machine courtesy of the EPSRC). Furthermore, these bubbles become trapped in the hydrogel further reducing its consistency.
- Difficulties in reliably preventing the trapping of air bubbles below the regulator of any size greater than the hole drilled into the underside of the regulator. Provided the trapped air did not protrude beyond the base surface of the regulator, it appeared to function correctly. However, if more air was present, then this excess air which is trapped below the regulator resulted in erratic regulator movement e.g. causing the regulator to travel only partially up the barrel before coming to a halt and letting the calcium chloride charge rush by it.

Approx. number of smooth muscle cells	Approx. volume of cells only when pelleted µL	Target cell concentration per ml of alginate solution	Approx. volume of alginate solution required to resuspend cells to 1 ml µL	Fraction of alginate solution in final 1 ml volume %
10^5	Unmeasurable	10^5	1,000	100.0
10^6	<10	10^6	990	99.0
10^7	75	10^7	925	92.5
10^8	750	10^8	250	25.0
10^9	7,500	10^9	Not possible	N/A

Figure 5.3

Potential cell concentrations in alginate solutions.

Experimental data was obtained using rat aortic smooth muscle cells (The European Collection of Cell Cultures (ECACC): A7r5 pelleted at 100 RCF (relative centifugal force) for 10 minutes and media drawn off using a pipette. These conditions produced easily resuspendable cells with greater than 97% viability. Cells were resuspended using a 500 µL pipette. The data for the target cell concentrations of 10^8 and 10^9 has been obtained by extrapolation.

Approx. number of smooth muscle cells	Approx. volume of cells only when pelleted µL	Approx. volume of culture media to fully resuspend cells µL	Target cell concentration per ml of alginate solution	Approx. volume of alginate solution required to mix with cells + culture media to achieve a 1 ml final volume µL	Fraction of alginate solution in final 1 ml volume %
10^5	Unmeasurable	50	10^5	950	95
10^6	<10	50	10^6	940	94
10^7	75	75	10^7	850	85
10^8	750	750	10^8	Not possible	N/A

Figure 5.4

Potential cell concentrations in alginate allowing for a media resuspension step.

Experimental data using rat aortic smooth muscle cells (The European Collection of Cell Cultures (ECACC): A7r5 pelleted at 100 RCF (relative centifugal force) for 10 minutes and media drawn off using a pipette. These conditions produced easily resuspendable cells in culture media with greater than 97% viability. Cells were resuspended using a 500 µL pipette. The data for the target cell concentration of 10^8 and has been obtained by extrapolation.

5.2 Fluid driven device prototype – Gas bubble regulator version

Having established that the fluid driven method was potentially a superior device to the previous piston driven prototype, refinement was now required to overcome the disadvantages. A very interesting observation was the air trapping had produced varying results in the prototype since an air bubble produces a discrete barrier between the alginate solution and the linking agent. A vital question needed answering – Was an air bubble alone capable of acting as a regulator element? To answer this essential question, a series of prototypes were produced to see whether or not a solid regulator was required. A non precision bore quartz glass tube with an inside diameter of 1.5 mm and 15 cm in length was used. Holding the tube in the vertical position, 0.25 ml of 2% alginate solution (ISP Manugel) was injected carefully into the base of the glass barrel. Covering the top (so as to create an air tight seal) prevented the alginate solution leaking out as the syringe was removed. A second syringe (2 ml) with 0.5 ml of air and 1.5 ml of 2% calcium chloride solution was attached to the base and the air tight seal removed from the top. Since air is lighter than the linking solution, on initially applying pressure to the vertical syringe, only the air is introduced into the glass barrel. This discrete air bolus is then followed by the liquid linking agent. Since the air bolus acted as a regulator element i.e. separating the main bodies of the alginate solution and calcium chloride solution, whilst still allowing alginate solution to coat the barrel where it could then be cross-linked immediately after the bubble had passed, a hydrogel tube was produced.

5.2.1 Initial conclusions

Repeated experiments at 1.5 mm (non-precision bore), 4 mm (precision bore) and 8 mm (precision bore) inside barrel diameters and varying quantities of air failed to reliably produce tubes of anything other than highly variable wall thickness. The proximal parts of the tubes were frequently of much greater thickness than the more distal parts. Variation in wall thickness was also more pronounced as the inside diameter of the glass barrel increased. However, on occasion an evenly walled tube (screened using a simple micrometer gauge) was produced. Overall from this series of simple experiments, the bubble regulator was indeed a possible option, however, the solid regulator produced much more reliable results for the same amount of experimental time.

The potential major advantages of a gas regulator over a solid regulator include:

- Reduced manufacturing time and costs
- Reduced number of unit operations
- No regulator to stick/jam
- Reduced chance of premature contact between the alginate and linking solutions
- No regulator to remove

A potentially suitable application for bubble regulators is where multiple short small-bore tissue constructs are required e.g. high throughput drug discovery. This is a potential area of convergence between ultra scale down, tissue engineering and high throughput screening. A simple experiment using a glass capillary tube (inside diameter 1.5 mm) robustly manufactured tubes when employing an air bubble as the regulator. This inside diameter of this capillary tube is less than for both 384 (4.5 mm) and 1536 (2.25 mm) microwell plates (Draft standards suggested by the Society of Biomolecular Screening 2002) making this a potential technology for a wide range of microwell sizes.

At this stage in the research it was decided to focus on the solid regulator approach.

5.3 Mark I design

Modifications to the fluid driven device were considered in order to overcome the three main difficulties encountered with the original solid regulator prototype:

- Failure to produce an adequate seal between the collar and the regulator
- Trapped air between the regulator and the barrel
- Excess air trapped under the regulator

A number of modifications were experimented with. These modifications cumulated in the Mark I version, which consisted of retaining the 4 mm inside diameter, 15 cm long borosilicate precision bore glass rod acting as the barrel but not the Perspex cylinder base. Instead a new cylinder base, a dual injector base was machined from polypropylene which had the benefit of allowing alginate solution to be introduced below the regulator, thus purging air out easily above it, see Figure 5.5 and Figure 5.6. The dual injector base consisted of a cylinder measuring 19 mm high by 22 mm in diameter. At its top protruded a small central stub measuring 6 mm high and 4.05 mm outside diameter. This stub allows the glass barrel to be attached to the base with a fluid tight seal just by pressing the stub firmly all the way into the glass tube. Careful machining of this interference results in perfect alignment of the glass barrel with the cylinder base.

A 1.55 mm hole was drilled through the body of the cylinder and out the base. Through this hole was pressed (strong interference fit) a stainless steel tube with an inside diameter of 1 mm and an outside diameter of 1.5 mm. This stainless steel tube became the injector nozzle.

This arrangement resulted in two concentric tubes i.e. a 4.05 mm outside diameter polypropylene hollow tube, with an inner stainless steel tube of 1.5 mm outside diameter protruding from the stub by 6 mm. A side port was drilled to allow a 2.5 ml syringe to be attached via an interference fit to provide a connection to the channel created between the outer polypropylene tube and the inner stainless steel tube. A similar base port was also

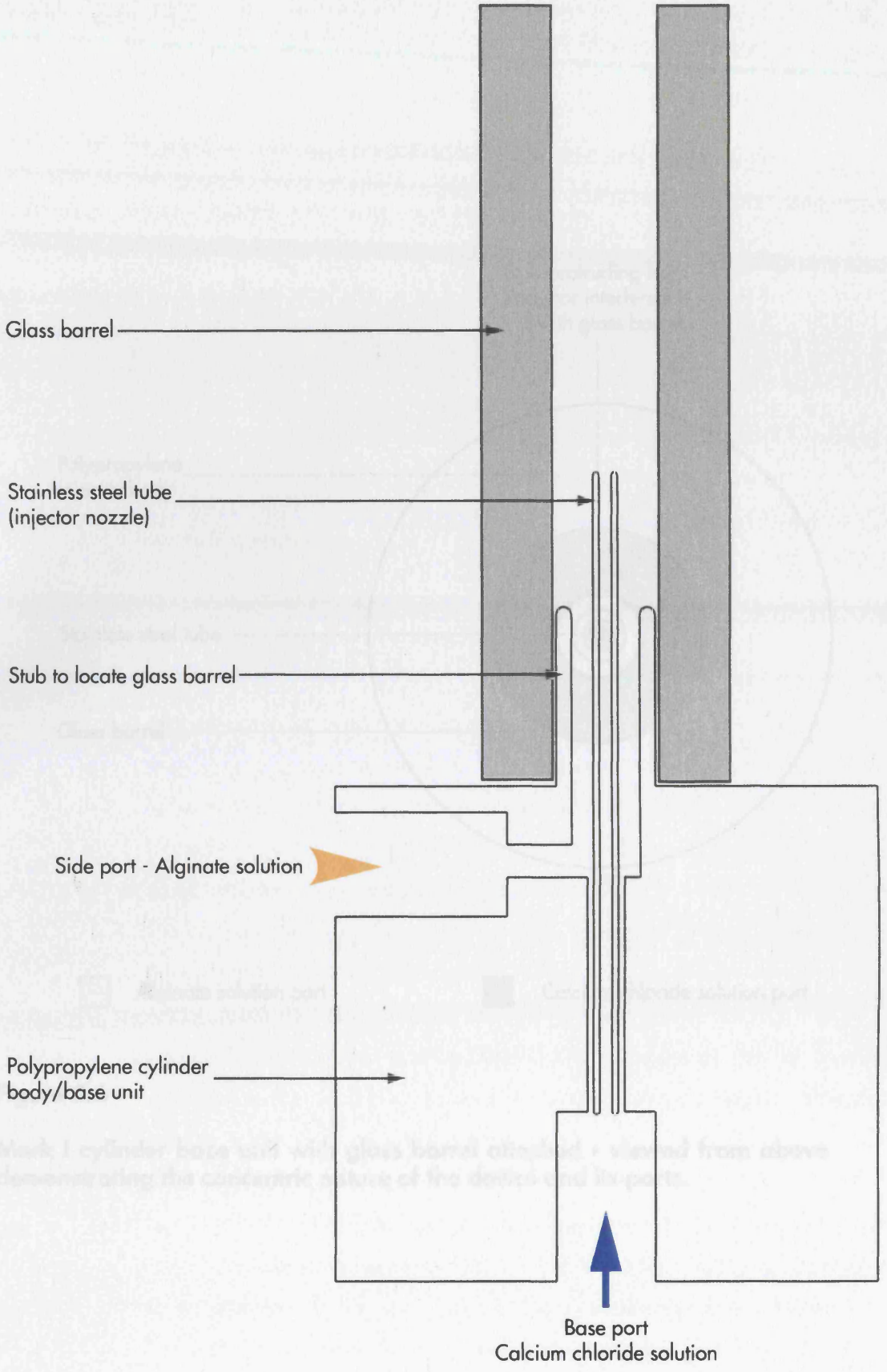

Figure 5.5

Mark I cylinder base unit with a short glass barrel attached - longitudinal section.

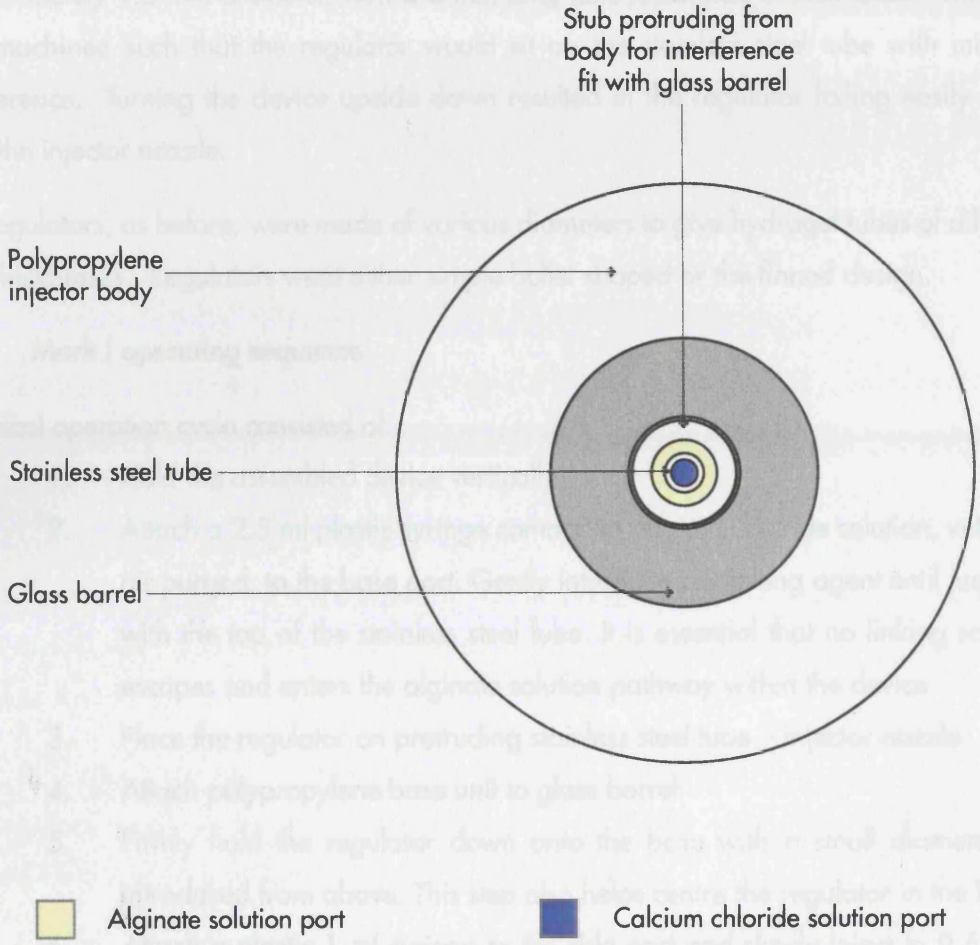

Figure 5.6

Mark I cylinder base unit with glass barrel attached - viewed from above demonstrating the concentric nature of the device and its ports.

drilled to allow connection to the lumen of the stainless steel tube.

The above arrangement allowed two discrete fluid delivery channels within the base unit:

1. Base port ⇒ injection nozzle [Calcium chloride solution]
2. Side port ⇒ channel around injection nozzle – [Alginate solution]

A series of different regulator elements were machined such that all were 1 cm tall and approximately 1.5 mm diameter, with a 6 mm long hole machined in their base. This hole was machined such that the regulator would sit on the stainless steel tube with minimal interference. Turning the device upside down resulted in the regulator falling easily away from the injector nozzle.

The regulators, as before, were made of various diameters to give hydrogel tubes of different wall thicknesses. Regulators were either simple bullet shaped or the finned design.

5.3.1 Mark I operating sequence

A typical operation cycle consisted of:

1. Hold the assembled device vertically
2. Attach a 2.5 ml plastic syringe containing calcium chloride solution, with any air purged, to the base port. Gently introduce the linking agent until just level with the top of the stainless steel tube. It is essential that no linking solution escapes and enters the alginate solution pathway within the device
3. Place the regulator on protruding stainless steel tube – injector nozzle
4. Attach polypropylene base unit to glass barrel
5. Firmly hold the regulator down onto the base with a small diameter rod introduced from above. This step also helps centre the regulator in the barrel
6. Attach a plastic 1 ml syringe to the side port and slowly inject in 0.6 ml of alginate solution. Care must be taken not to introduce or trap air and the regulator must be held firmly in place by the rod to stop it being displaced thus allowing premature contact of the two agents
7. Carefully withdraw the rod
8. Inject the calcium chloride solution via the base port into the device; this results in the regulator being forced off its stainless steel tube and being despatched up the glass barrel. Since alginate is left attached to the wall after the regulator has past, this is immediately cross-linked by the rising column of calcium chloride solution. In this way a hydrogel tube is created

By adding excess cross-linking agent the regulator could be expelled from the barrel driving the tube formation. This resulted a hydrogel tube supported by the glass barrel, which was

open at the top end and firmly attached at its base. This attachment consisted of an alginate plug extending all round the 6 mm of protruding stainless steel tube and extending back to the side port. With this attachment it was easy to add fluids via the base port e.g. additional calcium chloride solution, tissue culture medium etc. Unfortunately the side port where the alginate was introduced was blocked by cross-linked alginate. The calcium ions diffused slowly back through the alginate solution from the barrel to the port resulting in an excellent attachment for the tube at the expense of the loss to this port.

If a relatively strong hydrogel was produced e.g. 2% ISP Manugel, then 5 minutes after producing the tube, if the base was pulled away from the barrel, the hydrogel tube was delivered perfectly from the barrel firmly attached to the base unit.

This arrangement robustly produced tubes when using a variety of different alginates, alginate concentrators, calcium chloride concentration and regulator sizes.

Typically, high G alginates and /or high alginate concentrations (>2%) solutions produced tubes which could easily be delivered from the glass barrel. High M and low concentration solutions produced tubes, but these were invariably impossible to remove perfectly intact from the barrel even with additional help e.g. flowing calcium chloride solution down the barrel. To assist visualisation of the experiment, small quantities of glycerol based food colouring (Supercook (Leeds, UK)) or blue dextran (average molecular weight 2,000,000 – Sigma) was added to the alginate solution.

Early on it was discovered that scrupulous cleaning of the inside to the barrel, base unit and regulator was essential. Cross-linked alginate if allowed to dry was fairly resistant to removal from a surface, plus when wet was hard to visualise. The layers of alginate deposits caused two problems:

- Increased (and unwanted) interaction between the regulator and the stainless steel tube resulting in the regulator sticking.
- Irregularly decreased bore diameter which resulted in fouled runs.

Therefore, all components were washed in 4M sodium citrate solution prior to being dried using a compressed air source. The sodium citrate solution contained excess monovalent ions thus causing a phase shift from hydrogel (calcium alginate) back to the aqueous sodium alginate.

5.4 Conclusions

The above preliminary experiments with both the prototype and the Mark I manually powered and controlled fluid driven devices demonstrated that fluid drive was a feasible option for the production of alginate hydrogel tubes. The next chapter discusses the semi-automation

of this methodology to create an integrated system in order to achieve the goal of producing consistent cell/hydrogel tubular constructs.

6.0 Semi-automation of fluid driven device - Hydraulic drive

6.1 Design challenges, improvements and semi-automation

The manually powered fluid driven device consistently outperformed the pneumatic driven piston device in terms of the proportion of successful tube production runs (See Appendix 2). However, both approaches lacked tube consistency with respect to wall thickness and also premature "stalling" of the regulator in the barrel. Both these problems share a common aetiology, namely inconsistent propulsion mechanisms e.g. variable calcium chloride solution delivery rate. The challenge was therefore to semi-automate the fluid driven process in order to improve the consistency of results achieved manually. Accurately controlling the timing, rate and volume of the cross-linking agent entering the device was predicted to have a positive impact on tube quality and reproducibility, both important factors which had been poor to date. Unlike the pneumatic driven device whose performance was erratic in part due to the compressibility of its driving agent, air, a liquid driven device i.e. hydraulically operated suffers no such disadvantage.

Other important factors included:

- Overall wall thickness - In theory the wall thickness is directly proportional to the gap between the regulator and the barrel. However, the actual wall thickness may be different in size to the predicted for a number of reasons including the particular alginate solution's property of either shrinking or expanding as it cross-links.
- Tube length - Likewise the length of the tube formed is determined by a number of factors including, the volume of alginate solution loaded into the device, viscosity of the alginate solution, gap between regulator and barrel, volume of calcium chloride solution delivered and ultimately the length of the barrel.
- Inconsistent regulator travel - If calcium chloride solution "escapes" and enters the space between the regulator and the barrel, the alginate gels, and the regulator becomes stalled in the barrel and the calcium chloride solution flows up past the jammed regulator and makes direct contact with the bulk of the alginate solution thus gelling it in a highly irregular manner. The end result is a hydrogel tube being produced only until the regulator stalled. Causes of the "escape" of the calcium chloride solution include, non homogeneous alginate, trapped air bubbles, imperfect regulators, poor alignment e.g. due to the wear of polypropylene stub at the glass barrel interference fit surface (disassembly and reassembly of the device between runs and meticulous cleaning are absolutely essential between runs) and variable calcium chloride solution delivery.

6.2 Potential design solutions - Semi-automated Mark I version

Solutions to some of the above challenges were straight forward and quick to implement. These modifications were incorporated into the semi-automated Mark I device and its operating procedure. These changes included:

- Alginate was made homogeneous by careful premixing prior to autoclaving and further mixing immediately after autoclaving (whilst still warm) and again just prior to use. The most crucial step is the initial addition of the alginate powder to the water, physiological saline or buffer. This was best achieved by constant swirling of the flask as very small amounts of the powder were added in order to avoid clumping. Alginate powder does not dissolve quickly into solution. Further mixing was achieved using a roller bottle mixer but this does not resolve an initially poorly mixed solution. Alginate solutions were initially made using powder straight from the manufacturers container. However, later batches were desiccated for 48 hours prior to use thus removing excess water (e.g. ISP Manugel contains approximately 12% water by weight) in order to improve the direct comparisons between different alginates for a given percentage solution.
- Air bubble trapping was avoided by the careful addition of both alginate solution and calcium chloride solution into the device e.g. careful bleeding of the syringe and device prior to a tube production run.
- Regulators and polypropylene cylinder bases were accurately machined to avoid imperfections and precision bore borosilicate glass tubing was used extensively after thorough in-house checking (at least one batch of precision grade glass tubing was delivered with very poor tolerance control – requiring the manufacturer to remanufacture the mandrel the glass tube was made on). It was essential that base cylinder, glass barrel and regulator were all aligned at the start of a tube forming run. Wear of the polypropylene stub due to frequent disassembly and assembly caused both misalignment and reduction in the quality of the essential interference fit (i.e. to maintain a fluid tight seal plus hold the assembly together). If this design is retained, future work will require the cylinder base to be manufactured from a more durable material to overcome this wear issue.

The far more challenging area to resolve was that of erratic calcium chloride solution delivery. The components involved were the syringe driver and its electrical control system, syringe size and type and the path from the syringe to the stainless steel injector outlet. Two methods were selected to monitor the dynamic formation of individual tube constructs throughout their fabrication. [Complex fluid dynamic modelling was deemed outside the scope of this thesis, allowing a more visual based methodology to be adopted.] The techniques deployed were:

1. Digital high speed video imaging

2. Dynamic pressure recording

6.2.1 Digital high speed video imaging

The syringe driver chosen for semi-automating the calcium chloride solution delivery was a Harvard Apparatus PHD 2000 (High Power) lead screw type (Harvard Apparatus, Holliston, MA, USA). This is a microprocessor controlled syringe pump capable of driving two syringes in parallel (ranging from 0.5 μL - 140 ml) using a 1.8° incremental stepper motor. Its flow range can be set (depending upon the syringe chosen) from 0.0001 μL - 13.2 litres per hour). Rated at 65 Watts, it delivers an "average nominal force of 66 lbs". Its accuracy is claimed to be +/-1%, with a reproducibility of +/-0.1%. The syringe "pusher" travel rate ranges from 0.18 μm - 109 mmmin^{-1}. Due to the close proximity of the two syringes it is easy to link them together via a "T-piece" to double the maximum flow rate for a given "pusher" rate.

After a large series of initial experiments using plastic syringes ranging from 1 - 60 ml (1, 2.5, 5, 10, 20 and 60 ml) and also coupling the syringes via a T-piece at a range of delivery rates ranging from 1 - 212 mlmin^{-1}, using different viscosity alginate solutions, no reproducible results were obtained. The vast majority of runs failed to produce a tube. The most promising combination was a flow rate of 100 mlmin^{-1} (1.67 mlsec^{-1}), 60 ml Becton Dickinson Luer lock plastic syringe, 4 mm inside diameter barrel, 3.5 mm diameter regulator, 0.6 ml of 4% Fluka alginate solution and 2% calcium chloride solution in physiological saline at room temperature. However, even this combination had a tube production success rate of well under 50%. The problem consisted of near perfect runs punctuated by failures when using absolutely identical equipment, reagents and conditions including temperature. Wall thickness was measured using a simple mechanical micrometer once the tube was slit longitudinally. It is important to note that using exactly the same set of conditions except manually injecting the calcium chloride solution in a smooth manner resulted in a perfect tube virtually 100% of the time – the duration of production being of similar length of time. It was therefore decided to record individual runs using high speed digital video and then to watch the 'movies' generated in slow motion in order to better understand the high rate of failure and thus be able to make the appropriate modifications.

6.2.1.1 High Speed Camera Equipment

The apparatus consisted of a Mark I tube-forming device directly coupled to a vertically positioned Harvard Instruments PHD 2000 syringe driver. Directly behind the barrel of the Mark I device was positioned a clear Perspex rule behind which was mounted a sheet of matt white card. Illumination was provided using simple bench lamps, one on each side. A NAC HSV 500 Digital High Speed Video system (NAC Image Technology Inc., Tokyo, Japan) was positioned directly in front of the glass barrel such that the base of the Mark I device could just

be seen in the lower most part of the view finder with a further 140 - 150 mm of glass barrel occupying the remainder of the view finder. An overall barrel length of 20 cm was used in order that the regulator was 'still in play' i.e. making a hydrogel tube at the very top of the image. The camera was set to record at its maximum of 500 'frames' per second (fps) these images were stored as .tiff files (tag image file format - Adobe Systems). The NAC camera was kindly loaned by the Engineering and Physical Science Research Council (EPSRC).

Alginate solutions were produced using different alginate concentrations (ISP - Manugel) in physiological saline, thoroughly mixed using a roller mixer and then autoclaved. Immediately after autoclaving i.e. whilst still hot, food colouring dye was added to the solutions and then further mixed on the roller mixer in order to improve the homogeneity of the solutions. A 1% calcium chloride solution was produced using physiological saline and its pH adjusted to 7.36 - 7.40.

A standard Mark I tube-forming device was used including polypropylene regulators with diameters ranging from 3.6 - 3.9 mm (increasing in a 0.1 mm incremental manner). All experiments were performed at room temperature.

The experimental sequence of events commenced with the Mark I device being carefully loaded and put into position as described above, the high speed camera was manually triggered followed by the immediate manual starting of the syringe driver. The NAC camera's maximum record time at 500 fps was 5 seconds. Each completed film run thus produced 2,500 .tiff files (individual .tiff files were approximately 500 Kb in size). Each run's data was in turn burnt to a CD-ROM for later processing.

The .tiff images were subsequently processed in two distinct ways:

1. 'Movie' generation
2. Individual 'still' analysis

6.2.1.2 'Movie' generation

'Movies' were produced by linking all the .tiff images together to produce an AVI file (Audio Video Interleave, the file format for Microsoft's Video for Windows standard). Initially, this was performed using an IBM compatible PC, in two steps using PicaView (ACD Systems - www.acdsystems.com) to convert the .tiff files into JPEG format (Joint Photographic User Group) and then stringing the JPEG's together using AVI Constructor (www.aviconstructor.com) to form a continuous AVI 'movie'. This produced informative AVI's regarding the overall movement of the regulator and the coloured alginate column directly above it. Unfortunately this software combination had a number of major drawbacks including; poor data compression, poor replay management e.g. speed control, and very slow processing times. Having seen the

potential value of building AVI's from the data and needing to be able to quickly process the tube-forming runs, the software was switched to Adobe Premier 6/6.5 (Adobe Systems, San Jose, CA, USA). Premier is a professional package design for the production and editing of digital video. Using this software, .tiff images could be linked together to produce a high quality continuous 'movie' of each run. The resulting AVI's were 20 - 30 Mb in size (a large reduction from the original 1 - 1.5 Gb of .tiff files). Premier allowed the frame rate to be controlled. The original shooting rate was 500 fps, the Premier 'movies' were produced to run at 15 fps i.e. approximately 3% of the original speed. Furthermore image resolution was optimally preserved by Premier being able to retain the .tiff file at its original size of 496 x 332 pixels. These slow motion 'movies' when played back either using the Premier built-in viewer or for simplicity, Apple QuickTime Pro (Apple, Cupertino, CA, USA), both allowed very detailed viewing. These AVI's demonstrated the overall characteristics of an individual tube forming run including:

1. Overall movement of the regulator and alginate column e.g. did the regulator travel all the way to the top in a smooth and controlled manor or did it travel in a staccato manor
2. Indication on whether a run was successful or failed. If a tube was formed then the region below the regulator was a pale blue/green (due to the colouring agent which had been added to the calcium chloride solution) extending continuously from the injector nozzle. The nozzle itself was always in a region of slightly darker blue due to the alginate 'plug' formed in the region just below the base of the regulator in its loaded position. When a tube run failed, this light blue colouring was virtually absent
3. Allowed accurate timing of events due to both the slow motion and viewer forward/reverse control. Both viewers have built-in timers. By accurately locating both the start and the finish of each run the 'movies' could be cropped to just contain the tube-forming run and not the excess prior to after the run, thus reducing AVI file size and improving playback
4. Demonstrated additional unexpected information e.g. very small air bubbles were trapped under the regulator as it travelled up the barrel. These revealed an area of high turbulence immediately under the regulator base. Ricochetting of the regulator was also occasionally observed

6.2.1.3 Individual 'still' analysis

Individual 'stills' were analysed by processing discrete .tiff files. By locating the exact start points of each run using the AVI 'movie', it was possible to quickly locate the actual .tiff file immediately prior to the regulator moving. This .tiff file subsequently became the reference

point for both time and regulator position i.e. the position of the stationary regulator at time zero.

Each .tiff file was processed in the following manner using Adobe Photoshop 6 or 7 (Adobe, San Jose, CA, USA). The .tiff file was opened in the image window which had both a grid and rulers. It was quickly apparent that on some of the runs the Mark I tube-forming device was not absolutely vertical. This was digitally corrected by rotating the image so that the glass barrel became parallel with the vertical grid lines. The maximum rotation required by any run was 1.25°, the majority of runs required no correction. Using the grid function, a redefined zero point was set at the midpoint of the uppermost edge of the Mark I device (x = 0, y = 0). The measuring process was performed at the base of the regulator, tip of the regulator and air/alginate interface using the scroll function at the 1600x enlargement. By placing the cursor exactly over the centre of the pixel at the point of interest, Photoshop displays the x and y coordinates in mm for the actual image. Care was taken to have a value of x = 0 (long central axis of the device) at all measuring points since both the top of the bullet and the air/alginate interface are curved. Since x = 0 is the approximate midline, this should approximate to the inflection point of the curves. Finally each .tiff was cropped to show just the device and ruler and saved as a native Photoshop file (.psd file). These .psd files were later directly imported into Adobe Illustrator 10 (Adobe, San Jose, CA, USA) a vector graphics piece of software which is tightly integrated with bit-map imaging capability of Photoshop, to create the chronological sequences and saved as native Illustrator files (.ai files). See Figure 6.1 for a sample of two time points 0.45 seconds apart (225 frames separate the two images).

Initially every 100th .tiff was processed (i.e. 0.02 of second intervals). However it as soon apparent that the very first part (0 - 0.05 seconds) of the run required further investigation and therefore shorter time intervals of sampling were used during this period.

The data generated was processed using a computer spread AppleWorks 6 (Apple, Cupertino, CA, USA) From the data, graphs were drawn using Adobe Illustrator 10.

6.2.1.4 Data processing

Each .tiff image has a computer generated file number which places the image precisely in its overall sequence. Since each .tiff has a displacement of 0.002 seconds from its immediate neighbour it was easily possible to calculate the time displacement for each file.

Finally, all the distances were adjusted to a common reference point which coincided with the very base of the regulator in the loaded position. This position is the theoretical start of the actual hydrogel tube that is produced (i.e. not the plug of alginate hydrogel which attaches

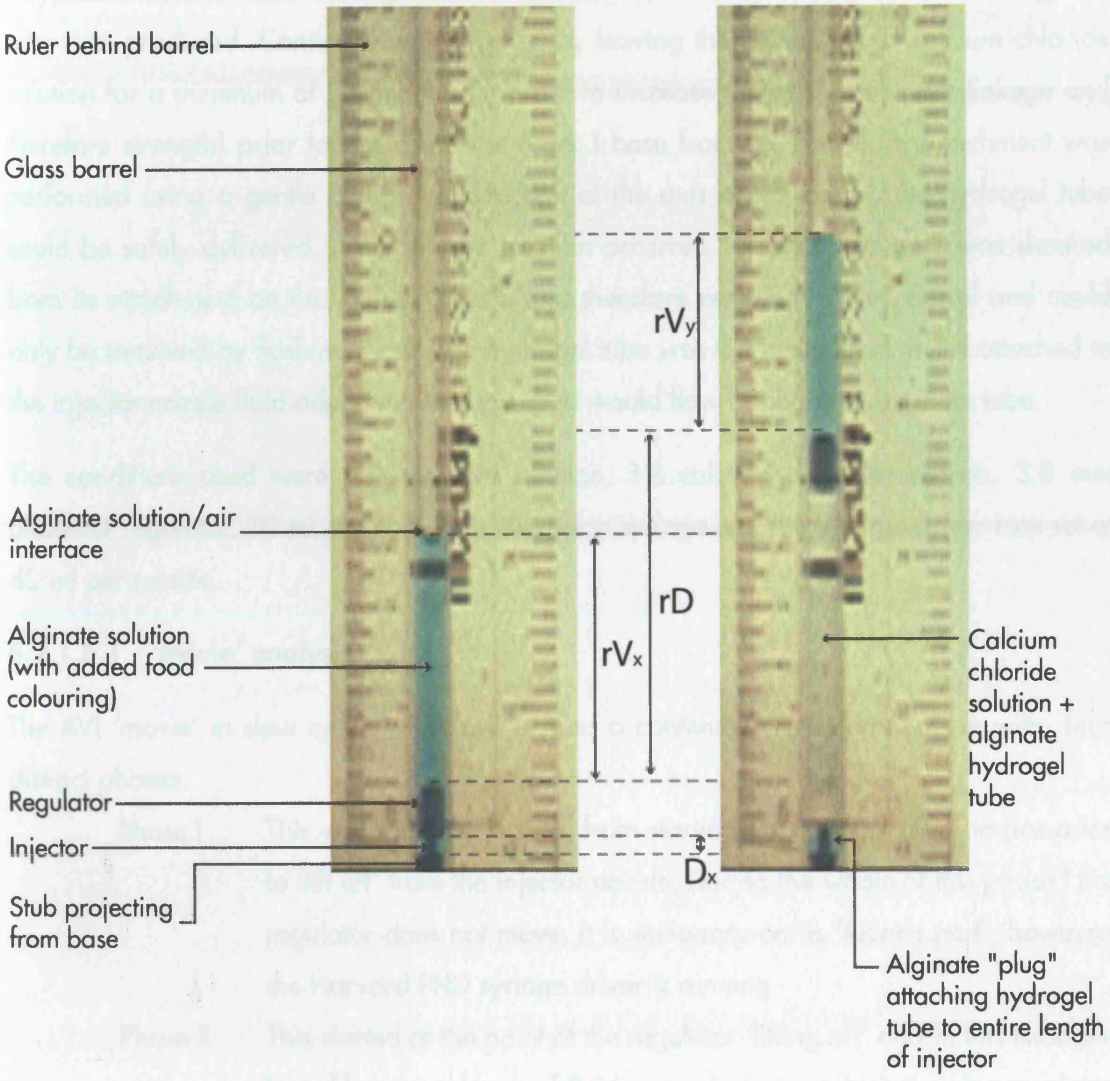

Figure 6.1

Two sample images from one tube production covered by 225 frames (0.45 seconds apart) images.

The first image is shortly after the opening snap - the injector is just becoming exposed (D_x). The second image shows the run at a known time later when the regulator has travelled a further distance (rD) and the volume of coloured alginate above the regulator has decreased from rV_x to rV_y

the base of the tube to the stainless steel injector rod which is below the regulator). The data was then plotted in a graph.

6.2.1.5 Typical successful tube-forming run

A typical successful tube-forming run is described below during which a continuous alginate tube was produced. Continuity was checked by leaving the device full of calcium chloride solution for a minimum of 20 minutes (in order to increase the degree of cross-linkage and therefore strength) prior to detaching the Mark I base from the barrel. If detachment was performed using a gentle pull in the direction of the axis of the barrel, the hydrogel tube could be safely delivered. If any excess rotation occurred, the hydrogel tube was sheared from its attachment on the injector nozzle and therefore remained in the barrel and could only be removed by flushing it out. The hydrogel tube was then inspected. If still attached to the injector nozzle fluid added via the base port would flow through the alginate tube.

The conditions used were: 4% alginate solution, 1% calcium chloride solution, 3.8 mm diameter regulator, 10 ml plastic Becton Dickinson syringe and the syringe driver rate set at 40 ml per minute.

6.2.1.5.1 'Movie' analysis

The AVI 'movie' in slow motion (15 fps) showed a continuous tube forming run with four distinct phases:

- Phase I — This was the time interval from starting the syringe driver to just prior to 'lift off' from the injector nozzle. During the whole of this phase I the regulator does not move, it is stationary on its 'launch pad', however, the Harvard PHD syringe driver is running
- Phase II — This started at the point of the regulator 'lifting off' and in this example lasted for a maximum of 0.05 seconds during which time the regulator travel no more than 7 mm from its loaded position.
- Phase III — This was a brief period (in this example < 0.01 seconds) which consisted of an almost instantaneous halt of the regulator prior to entering the fourth and final phase.
- Phase IV — This final phase continued until the regulator went out of camera shot

In this example, the cumulative time for the final three phases was 2.2 seconds. Each of the individual phases is covered in more depth in the paragraphs below:

Phase I

By definition, no movement was observed nor too was there any movement of the air/ alginate interface i.e. there is no discernable leakage of calcium chloride solution 'around'

the regulator prior to 'lift off'. Any leakage would lead to a premature exposure of the two reagents and a failed run.

Phase II

The regulator was seen to rapidly rise in the barrel forcing the alginate solution column above it to also rapidly rise. Phase II included a short part of the run where the regulator is in contact with the uppermost part of the stainless steal injector nozzle plus a short distance above it.

Phase III

This transition phase appeared to be a short (<0.01 second) linking the rapid velocity first phase to the slower velocity fourth phase. It is a period of extremely rapid deceleration where the regulator almost appears to come to a complete halt before entering the final phase.

Phase IV

The longest phase which lasted approximately 2 seconds before the regulator left the field of view. During this phase tiny air bubbles, less 500 μm in diameter were seen travelling randomly around at high speed just under the regulator as is travelled up the barrel. These tiny air bubbles could possibly have come from a tiny volume of air trapped in the internals of the Mark I but this is most unlikely as the system was thoroughly bled prior to positioning the regulator and final assembly of the device. More likely it was from the small pocket of air trapped inside the regulator where it interacts with the stainless steel injector nozzle. The air possibly left the regulator due to rapid pressure changes in the calcium chloride solution which was propelling the regulator. The volume of air trapped in the regulator was negligible since the total space into which the stainless steel injector nozzle fits is less than 20 μL and virtually all of this air was expelled as the regulator was carefully lowered onto the injector since the two components fit together in a close but loose manor i.e. there was minimal interference between the two components. The injector nozzle was filled to its opening with calcium chloride solution prior to regulator positioning.

6.2.1.5.2 'Stills' analysis

The series of individual 'stills' from the successful run had their data plotted in a graph with distance/length plotted on the y axis with time on the x axis - see Figure 6.2. The position of the air/alginate interface and regulator were plotted - see Figure 6.3. This graph like the AVI 'movie' had the same four distinct phases.

Phase I

From the experiment, the duration from starting the syringe driver to lift off is unknown. Therefore the start of phase II is the origin of the graphs.

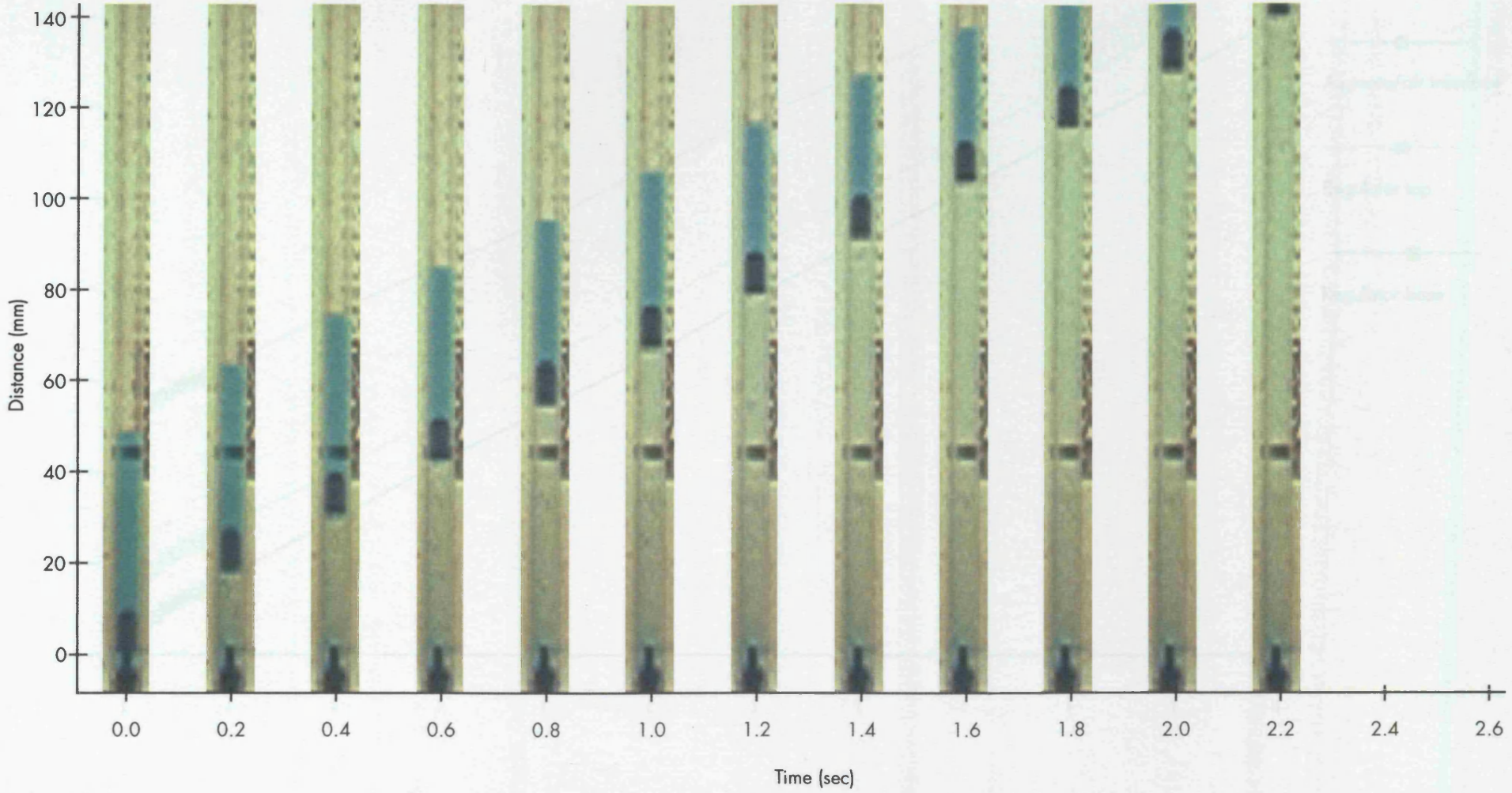

Figure 6.2
Stills selected at discrete time points (0.2 seconds apart) during the course of a typical successful tube forming run.
(Labelling as per Figure 6.1)

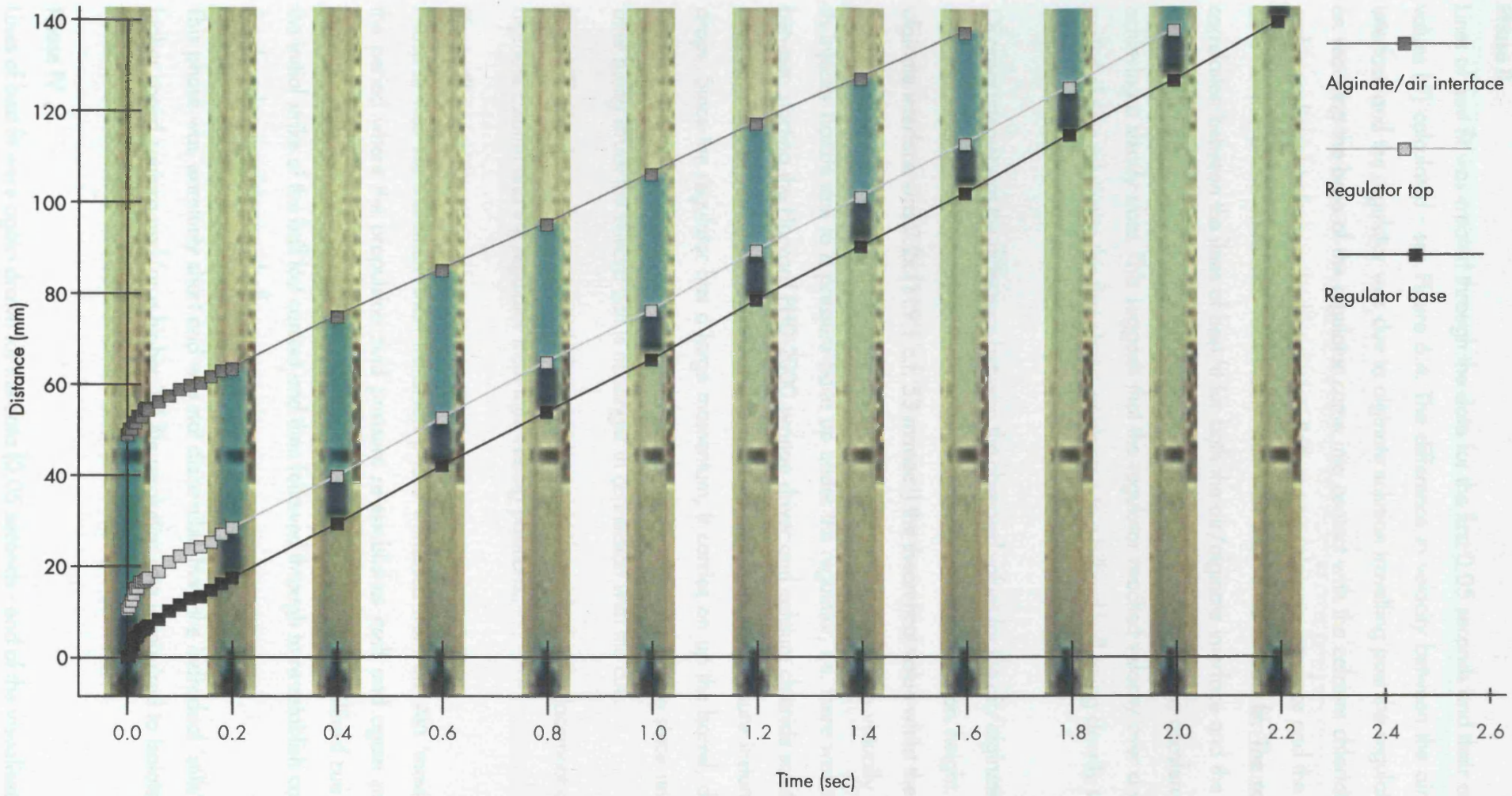

Figure 6.3
Graph of distance against time for the alginate/air interface and regulator overlaid on Figure 6.2.
(Labelling as per Figure 6.1)

Phase II

Lines of best fit was created through the data for the first 0.05 seconds and their correlation values (r^2) calculated - see Figure 6.4. The difference in velocity between the air/alginate interface and the regulator was due to alginate solution travelling past the regulator, which on reaching the base of the regulator came into contact with the calcium chloride solution and cross-linked to form a hydrogel tube. Both the air/alginate interface and the regulator data for this phase correlated reasonably well with their lines of best fit. The reasonable correlation between the lines of best fit for both the air/alginate interface and the regulator suggest that the velocity during this period was relatively constant i.e. no acceleration, thus achieving a steady-state. This suggests that the regulator reached velocity over a very short period of time relative to this first phase, analogous to a billiard ball being cleanly struck with a billiard cue.

Of great interest was the difference between the observed values for the air/alginate interface and the regulator compared to the theoretical calcium chloride solution height. The air/alginate interface was 2.2x (119.1 c.f. 53 $mmsec^{-1}$) the theoretical value whilst the regulator was 2.8x (147.9 c.f. 53 $mmsec^{-1}$). This suggests that the regulator was virtually 'fired off' its injector nozzle due to a pressure build up under the regulator, i.e. there was a time lag between starting the Harvard PHD 2000 syringe driver and calcium chloride solution being injected into the Mark I device. When the regulator 'lifts off' the pressure instantaneously drops. Since the regulator has a large momentum, it carries on up the barrel, despite the reduced propulsion pressure. The billiard cue analogy again holds true since immediately after being struck the billiard ball is no longer in connection with the cue.

In conclusion phase II was a period of extremely rapid change in the displacement of both the alginate column and the regulator from their resting positions.

Phase III

Phase III was the extremely short transition phase witnessed from the AVI 'movie'. It was the period where the propulsion fluid pressure re-establishes itself and again propels the regulator and the head of alginate solution above. It is as though the billiard cue had after the initial strike of the ball lost contact and then followed through to re-establish contact with the deccelerating/stopped ball.

This phase was extremely short and was not discernible from the individual 'stills'. Either a higher speed camera and/or a higher .tiff file resolution rate is required to isolate this brief event.

Phase IV

Lines of best fit were again drawn for the data (0.05 seconds - end of the visualised run) and

Location	Gradient = Average velocity mmsec^{-1}	Correlation (r^2)
Air/alginate interface	119	Acceptable (0.942)
Top of regulator	148	Acceptable (0.903)
Theoretical top of $CaCl_2$ column	53.0	N/A

Figure 6.4

Phase II average velocities for a successful tube forming run generated from digital high speed video imaging data.

Location	Gradient = Average velocity mmsec^{-1}	Correlation (r^2)
Air/alginate interface	49.5	Excellent (0.999)
Top of regulator	56.9	Excellent (0.999)
Theoretical top of $CaCl_2$ column	53.0	N/A

Figure 6.5

Phase IV average velocities for a successful tube forming run generated from digital high speed video imaging data.

their correlation values (r^2) calculated - see Figure 6.5. As in phase II the regulator velocity was greater than the air/alginate interface velocity. It was approximately 14.9% faster which is less than the phase II similar comparison of 24.1%.

All of the best fit lines correlated excellently with the data. This was highly suggestive that the velocity of all the components during this fourth phase were constant. This phase lasted 2.2 seconds and thus made up the majority of the tube-forming run time (97.7%). The length of hydrogel tube formed during this phase (excluding cross-linking changes e.g. shrinkage) was 111.6 mm.

As in phase II, the observed velocities of both the air/alginate interface and the regulator were different to the theoretical calcium chloride solution column height but to a much lesser extent - see Figure 6.6. The acceptable correlation with the best fit lines during phase II and the excellent correlation with the best fit lines during phase IV suggest that the velocity transition takes place during phase III i.e. the average velocity of phase II 'shifts' to the lower velocity of phase IV, since no acceleration/decceleration is seen during these phases (dv/dt is a straight line for both graphs).

If phase III was analogous to the billiard ball being restruck by the cue, then phase IV is analogous to the cue remaining in contact with the ball at all times. It is as if the ball were being pushed against a constant resistance and cannot break away from the cue as it had done on initially being struck (phase II). The resistance in the tube-forming system being the head of alginate solution above the regulator plus the forces exerted by the alginate solution as it passed around the regulator.

The difference between phase II and phase IV was that the former required considerably more propulsion force (pressure) to start the system moving from rest, whilst in phase III, the regulator and the alginate column above it are probably moving and only required a change in velocity. Thus overshoot of the regulator was observed in phase II but not in phase IV.

The difference between the air/alginate velocity and the theoretical calcium chloride column height velocity was probably due to back pressure in the system due to the extra work required to push the regulator and alginate column compared to the free flowing aqueous system used to verify the syringe drivers stated performance. The back pressure effectively dropped the delivery volume from the pre-set 40 $mlmin^{-1}$ to 37.3 $mlmin^{-1}$, a 6.7% reduction.

6.2.1.6 Varying alginate concentrations

The above experiment was repeated using identical conditions but using different concentrations of alginate in order to be able to compare the effect of viscosity on the process. Alginate solutions (1%, 2%, and 4% Manugel) were made up as before.

Location	Phase II velocity mmsec^{-1}	Phase II velocity as a % of theoretical $CaCl_2$ velocity	Phase IV velocity mmsec^{-1}	Phase IV velocity as a % of theoretical $CaCl_2$ velocity
Air/alginate interface	119	225%	49.5	93%
Top of regulator	148	279%	56.9	107%

Figure 6.6

Comparison of phase II and IV average velocities for a successful tube forming run generated from digital high speed video imaging data.

The measurements, data manipulation and calculations for each different viscosity alginate solution were performed in exactly the same manner as that described above. The data was averaged from three successful runs for each alginate concentration. The same phase nomenclature has been used.

6.2.1.6.1 'Movie' analysis

Provided the run was a successful run i.e. an alginate tube was produced which stretched the length of the visible (to the camera) part of the barrel, all the AVI 'movies' were very similar in overall appearance to the 4% alginate run described above. (Failed runs were of totally different appearance and will be dealt with in detail later, this next part of this chapter will only be concerned with successful tube-forming runs.)

The AVI 'movies' did reveal differences in duration for both specific phases as well as the duration of the overall run for the different alginate concentrations. As before there was still the rapid velocity phase II followed by an extremely brief phase III transition followed by a smooth phase IV. Phase I again demonstrated no discernable leakage of calcium chloride solution prior to regulator 'lift off'. This typical sequence of events seems to be the hallmark for a successful tube production run.

6.2.1.6.2 'Stills' analysis

Looking at the individual .tiff files as before allowed precise measurement of the events described above.

Phase I

For all the different alginate concentration there was no discernable increase in the height of the air/alginate interface until the regulator 'lifted off', nor was a clear layer observed in the region of the regulator at any time.

Phase II

Phase II lasted in the order of 0.05 seconds for all the sample alginates. Precise determination of the end of phase II was difficult to find from the 'stills'. Certainly no phase II lasted longer than 0.05 seconds. Plotting a distance against time graph for the air/alginate interface and using lines of best fit together with calculating its correlation value (r^2) suggested that for all the samples a dramatic slowing of velocity (change in gradient) occurred no later than 0.05 seconds. An r^2 value in the order of 0.95 was taken as the cut off point, thus the time points were reduced until approximately this value was reached.

The average values for the air/alginate interface are shown in Figure 6.7. Likewise the data was used to find the average regulator velocity. The average regulator volume is shown in

Alginate concentration	Average velocity for phase II air/alginate interface n = 3 $mmsec^{-1}$	r^2	Phase II air/alginate interface velocity as a % of theoretical $CaCl_2$ velocity
1%	186	>0.95	351%
2%	170	>0.96	321%
4%	119	>0.94	225%

Figure 6.7

Comparison of the average velocities of the air/alginate interface during Phase II of a successful tube forming run deploying alginate solutions of different concentrations.

Alginate concentration	Average velocity for phase II air/alginate interface n = 3 $mmsec^{-1}$	r^2	Phase II regulator velocity as a % of theoretical $CaCl_2$ velocity
1%	180	>0.95	340%
2%	191	>0.96	359%
4%	146	>0.90	276%

Figure 6.8

Comparison of the average velocities of the regulator during Phase II of a successful tube forming run deploying alginate solutions of different concentrations.

Figure 6.8. The lines of best fit correlated well with the data, with all the r^2 values exceeding 0.9.

Phase III

As previously described for the 4% alginate solution, the Phase III was extremely short and of similar character.

Phase IV

Results for the three different alginates were near identical to the Phase IV results for the original 4% alginate (see Figure 6.5) with average air/alginate interface and regulator velocities approximately identical to the theoretical calcium chloride solution velocity.

6.2.1.7 Description of a typical failed tube-forming run

Characteristically the hallmark of a failed tube-forming run was that the regulator would lift off and then slow or completely stall in the barrel. This resulted in calcium chloride solution escaping past the regulator and thus coming into contact with the alginate in an uncontrolled manor. Understanding why runs failed is crucial to producing the essential robust process required for future clinical material.

6.2.1.7.1 'Movie' analysis

The run described below is a typical example of a failed run. The conditions were all identical to the previously described successful tube production run including the alginate concentration (4% Manugel), regulator diameter (3.6 mm) and syringe driver flow rate setting (40 $mlmin^{-1}$). The measurements, data processing and calculations were performed in exactly the same manner. The same phase nomenclature has been used.

An overall view of the AVI 'movie' in slow motion (15 fps) showed the regulator smoothly lifting off from the base unit. Immediately the regulator was seen to ricochet of the barrel walls as it made its way up. By approximately 0.5 seconds from the start of movement, an extremely thin clear layer could just start to be seen above the regulator instead of the dark blue of the dyed alginate solution. This thin layer was presumably calcium chloride solution which had escaped up passed the regulator i.e. a backflow. The amount of calcium chloride solution above the regulator increased slowly over approximately the next 0.3 seconds to a few millimetres in height. Turbulence was easily seen in this evolving layer due to traces of the dyed alginate mixing with it. At approximately 0.8 seconds into its journey the regulator slowed abruptly whilst the clear calcium chloride layer above increased rapidly. The regulator carried on slowly up the tube in a staccato manner whilst ricochetting from side to side. The total time for the run from 'lift off' to the regulator leaving the field of view completely was in excess of 2.5 seconds (compared to the successful run under the same conditions which was

2.2 seconds).

Examining the individual phases observed during the AVI 'movie' revealed great differences to the successful run except for phase I.

Phase I

As for the successful run there was no increase in the length of the alginate column until the regulator 'lifted off'. This suggests that the later failure was unlikely to have been caused by calcium chloride solution leaking between the regulator and injector nozzle prior to 'lift off'.

Phases II, III and IV

Following 'lift off' there was a visibly slow journey up the barrel by the regulator with no discernible phase III i.e. phase II blended into phase IV with no visible change in velocity. Phase IV was abruptly ended by a rapid deceleration in the regulators velocity. After this 'terminal event' the alginate-calcium chloride cross-linking zone was above the regulator and not at its trailing edge. Thus from approximately 0.8 seconds into the run, the regulator was propelled through the alginate gel precipitated above it, hence the highly staccato ascent from this moment on.

Previous unrelated experiments have demonstrated that a very irregular shaped 'tube' can be produced even when no regulator element is present provided the flow is moderately slow (10 - 20 $mlsec^{-1}$), however, as the velocity of the linking agent increases, the more common occurrence was that the two reagents mixed and no precipitate was formed thus leaving an empty barrel. These previous observations possibly explain the two different alginate-calcium chloride interactions which were observed:

1. The initial mixing of the calcium chloride solution with the alginate solution above the regulator. The alginate probably failed to cross-link due to the high turbulence which was observed in the region immediately above the dome at the top of the regulator.
2. The AVI 'movie' showed that once sufficient calcium chloride solution had accumulated above the regulator, the turbulence at the alginate~calcium chloride interface was much reduced. This was because the alginate~calcium chloride interface was now clear of the very turbulent zone immediately above the dome of the regulator. This reduced turbulence led to hydrogel precipitation and hence the staccato regulator movement as it tries to break through this rapidly forming barrier just ahead of it.

6.2.1.7.2 'Stills' analysis

Stills were selected at 0.2 second intervals and were combined into a time-distance study

- see Figure 6.9 for a typical sequence of stills for a failed run. The collection of sequential images relate extremely well to the above detailed description of the 'movie'. Detail; analysis of this data failed to add any further clarity to the 'movie' data.

6.2.1.8 Conclusions

The AVI's suggested that the most crucial moment in the process is the lift off of the regulator – "opening snap". Factors affecting this opening snap include the syringe driver, coupling of syringe to injector, fit between stainless steel tube injector and regulator, viscosity and head of alginate i.e. alginate level above the regulator, calcium chloride solution flow rate and syringe size used. These issues were each addressed and modifications where appropriate were incorporated into the semi-automated Mark II device and its operating procedure.

Since the Harvard PHD syringe driver produced flow rates comparable with the successful manually produced hydrogel tubes it was decided to persist with this driver. Furthermore, a thorough check of the market showed this to be one of the highest calibre units available. After checking its accuracy (by accurately weighing volumes of water delivered by the device and observing a very high agreement between the machine set value and the weight of water delivered over a recorded time period) it was decided to strip and rebuild the device exactly to the manufacturer's specifications since this information gave no indication about the initial volume delivered (i.e. at the opening snap) and the device in question had already had a fairly hard life. The mechanical part of the device consisted of a series of gear wheels and one toothed drive belt, all of which were stripped and reassembled in a manner aimed at reducing backlash in the device. Backlash was a possible cause for an irregular opening snap. The belt assembly had the most attention since this potentially could produce the most backlash in the device. It was noted that should the rebuild not cure the opening snap problem then replacing the belt set up with gear wheels was an option in order to reduce backlash. After the rebuild the accuracy of delivery was checked as before. Finally, all experiments were performed only after the pusher had moved a short distance in the driving (c.f. filling) direction in order to minimise any backlash in the drive mechanism and also to try to standardise the direction of deformity in the plastic syringe seal into the fluid delivery position.

All couplings between the device and the syringe were made either of Perspex or stainless steel in order to prevent wall distortion. Luer lock fittings were used wherever possible. The length and shape of the coupling appeared to be a factor but not the main factor. A straight coupling over 2 - 3 cm in length appeared to be better than a shorter coupling or coupling the device directly to the syringe. This is possible due to turbulent boundary layer effects persisting leading to non laminar flow in the device. The inlet length for laminar flow [L] to be re-established can be calculated from the equation:

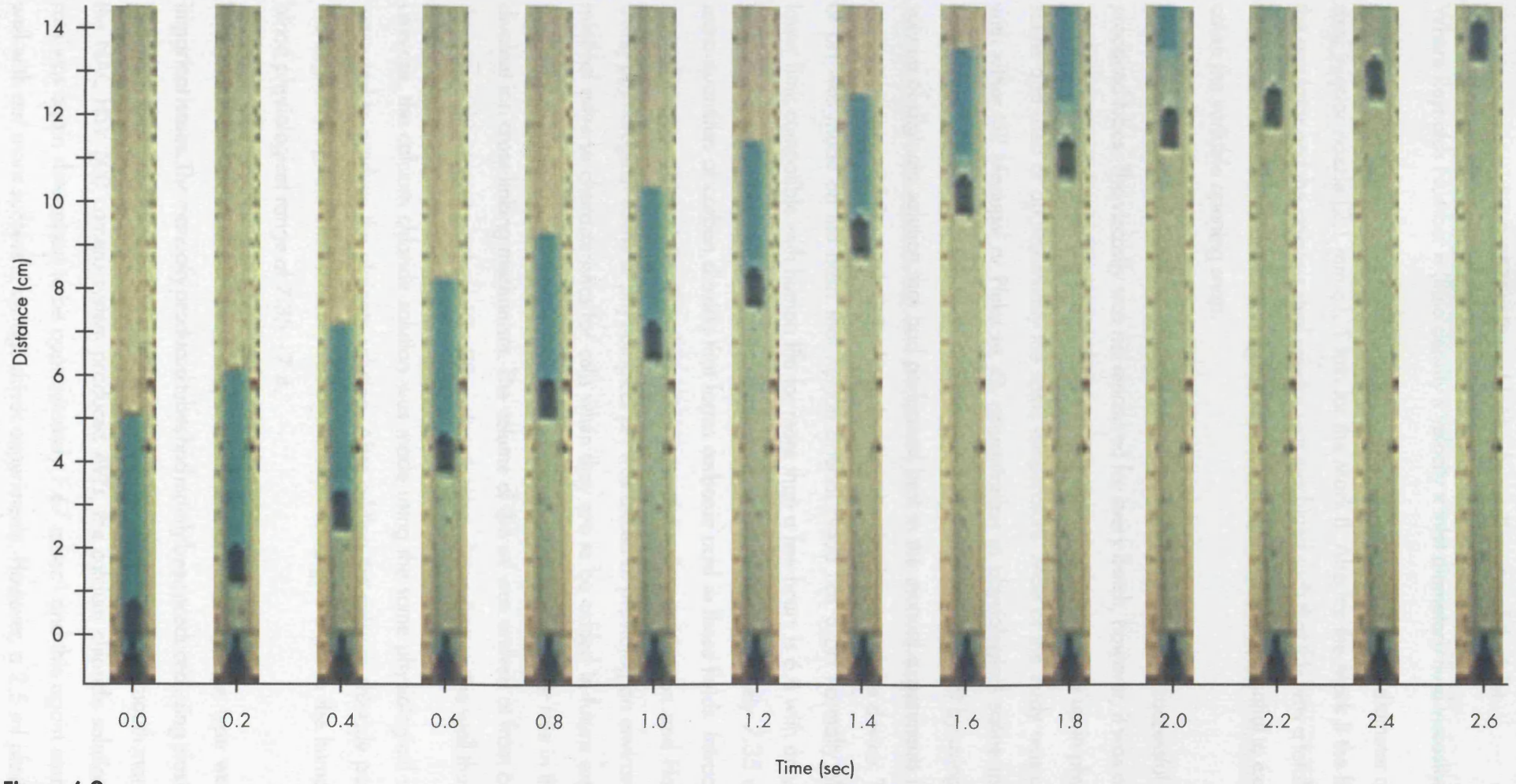

Figure 6.9
Stills selected at discrete time points (0.2 seconds apart) during the course of a typical failed tube forming run.
(Labelling as per Figure 16.1)

$$L = 0.0575 \times \text{Reynolds Number} \times \text{diameter of the inlet}$$

Where Reynolds Number = (fluid density x velocity x inlet diameter)/fluid viscosity.

As a direct consequence, the Mark II version was designed with a larger diameter of stainless steel injector nozzle (2.1 mm c.f. 1 mm for the Mark I). Also for the Mark II the fit between the regulator and the stainless steel injector was machined such that this was a totally loose fit with no discernable interference. Any friction here was perceived as potential to exacerbate/ cause the variable opening snap.

The percentage of alginate in solution was kept exactly as for the successful manually produced tubes. The viscosity was not measured for every batch, however, it was assumed to be relatively constant for a given percentage of a specific alginate made up in physiological saline and used at approximately the same temperature. Most of the study was carried out with either ISP Manugel or Fluka at 4% concentration in physiological saline made up to between pH 7.35 - 7.4. The head of alginate solution was kept constant by using the same volume of alginate solution that had performed best in the manual experiments i.e. 0.6 ml per experiment. Of the 6 ml, 0.5 ml was lost into the dead space of the device. The choice of pH was made on the basis that human arterial blood has a pH normally of 7.4 (The lower limit compatible with human life for more than a few hours is 6.8 with an upper limit of 8.0). Venous blood and interstitial fluids have a pH of approximately 7.35 due to the extra quantities of carbon dioxide that forms carbonic acid in these fluids. Intracellular pH normally ranges from 6.0 - 7.4 depending upon the cell type (Guyton and Hall, 2000). Using physiological saline at physiological pH was aimed at providing an environment with minimal adverse characteristics for cells when they are to be added in future experiments. Furthermore, both pH and monovalent cation concentration play a major role in the calcium divalent ion cross-linking mechanism. The volume of 0.6 ml was arrived at from calculation, the aim at this stage to make a 10 - 30 cm length tubes depending on the wall thickness.

Likewise, the calcium chloride solution was made using the same physiological saline that was used to produce the alginate solution. After adding the calcium chloride powder and thorough mixing, the final solution was again adjusted to give a pH in the human arterial blood physiological range of 7.35 – 7.4.

The calcium chloride solution flow, coupled with the choice of syringe type were clearly important issues. The manually produced tubes had mainly been produced using plastic Beckton Dickinson Plastipak 2.5 ml syringes injecting in 2 ml in a controlled and smooth manner. From the NAC HSV 500 camera system produced AVI's, the calcium chloride solution injection rate was again determined to be approximately 1.67 $mlsec^{-1}$ and this again corresponded well with our more successful syringe driver experiments. However, a 2.5 ml plastic syringe

in the syringe driver failed to be able to deliver at this desired rate – the maximum flow rate deliverable by the pump with a 2.5 ml syringe is 0.13 $mlsec^{-1}$. The maximum flows for the PHD 2000 syringe driver is tabulated in Figure 6.10. All flows are in $mlsec^{-1}$ since the device typically only requires a few ml to produce a hydrogel tube e.g. a 20 cm long tube with a 4 mm outside diameter requires less than 10 ml of calcium chloride solution. From the data, it can be seen that only the 20 ml syringe doubled up, 60 ml, 100 ml and 140 ml syringes could deliver at the speeds required (i.e. 1.67 $mlsec^{-1}$). However, 2 x 20 ml syringes failed to perform as well as 1 x 60 ml syringe both set ups delivering calcium chloride solution at the same rate. The reason being that the hydraulic pressure being generated by the syringe driver reduces as the syringe piston diameter increases. The approximate values were provided by the manufacturer of the syringe driver (Harvard Apparatus) - see Figure 6.11.

The pressure that a syringe pump can generate is a function of the force of the pump, diameter of the syringe and the overall set up e.g. syringe stiction and tubing diameter. Average pump pressure is calculated by dividing the average pump force (30 Kg for the PHD 2000 High powered version) by the surface area of the syringe piston. If two syringes are used the their respective surface areas are summed. Harvard Apparatus advised that:

- Higher pressures may be achieved at minimum speed and lower pressures at maximum speed
- Pump speed and force are inversely proportional

Given the ease and relatively low cost of supply of 50/60 ml plastic syringes compared to the bigger syringes, it seemed an obvious choice to continue with this syringe size. Two 20 ml syringes did not seem to perform as well. This could possibly be due to turbulence created by the two flows meeting at the T-junction, however, the theoretical average pump pressures are very similar due to the near identical piston surface areas (2 x 20 ml – 575 mm^2 c.f. 1 x 50/60 – 519 mm^2). The larger syringes (with their bigger piston diameters) have the advantage of running at lower pusher speeds for the same output and therefore more force is generated by the fluid. Another probable benefit of the larger diameter syringes is that since they deliver the same volume of linking solution per unit time a slower syringe driver pusher speed is required and therefore the period of time required to accelerate to this lower speed is less. Since this period of time is closely linked to the critical opening snap, this plays a significant role in whether a tube run is successful or not.

A comparison of syringe driver pusher speeds is tabulated in Figure 6.12. Thus using the Beckton Dickinson 50/60 syringes required the PHD 2000 syringe driver to work at its totally capacity in order to deliver the required 1.67 $mlsec^{-1}$ of calcium chloride solution, whilst the Saco and Sherwood Medical largest syringe offerings due to their large piston surface areas required much slower pusher cruise velocities to deliver identical volumes over the same

Syringe size ml	Maximum flow rate $ml sec^{-1}$	Maximum flow rate achievable when coupling 2 identical size syringes together via a non-deformable T-piece $ml sec^{-1}$
1	0.06	0.11
2.5	0.13	0.26
5	0.36	0.73
10	0.53	1.05
20	0.91	1.83
50/60	1.78	3.56
100	3.04	6.08
140	3.68	7.36

Figure 6.10

Maximum flow rates for the Harvard PHD 2000 syringe driver when used in combination with either a single syringe or two identical sized syringes coupled together in parallel via a stainless steel T-piece.

Syringe piston diameter mm	Nearest equivalent Becton Dickinson syringe size ml	Average pump pressure bar
Single syringe		
<5	1	>69
10	2.5	32.8
15	10	14.6
25	50/60	5.2
Comparison: Single vs. dual syringes		
1x 23	1x 25	5.4
2x 23	2x 25	2.7

Figure 6.11

Comparison of various syringe piston diameters with average pump pressure for the Harvard PHD 2000 syringe driver.

(Data - Harvard Apparatus)

Manufacturer/ syringe model	Piston diameter mm	Required volume injected $mlsec^{-1}$	Pusher speed $mmsec^{-1}$	Fraction of maximum speed of PHD 2000 syringe driver* %
Beckton Dickinson Plastipak 50/60	25.7	1.67**	3.2**	>100
Lux Bloc 50 ml	26.7	1.67	2.98	94
Saco 100 ml	34.9	1.67	1.75	55
Sherwood Medical 140 ml	38.4	1.67	1.43	45

Figure 6.12

Comparison of syringe driver pusher speeds for four different manufacturer's largest syringes.

*The PHD 2000 syringe driver has a maximum pusher speed of 3.17 $mmsec^{-1}$

**Only just achievable given the PHD 2000's maximum pusher speed

period of time.

6.3 Dynamic pressure recording studies

Prior to constructing an semi-automated Mark II system, it was decided to investigate further the perceived number one problem - the opening snap. i.e. the precise moment that the pusher in the syringe driver started to move coupled to the action of the regulator via a continuous column of liquid in a rigid tubular system (i.e. a non compressible linkage). It was therefore decided to study the pressure in the semi-automated Mark I system during the process of making a hydrogel tube.

6.3.1 Materials and methods

The semi-automated Mark I system comprised of; the PHD 2000 syringe driver was set up in a vertical position such that when a syringe was installed its opening was upper most. The syringe was coupled via a Luer fitting to a pressure transducer which was in turn coupled to the device i.e. the pressure transducer was in the direct path of the fluid going to the injector. The distance between the syringe nozzle outlet and the injector was significantly greater (90 mm) than the minimum optimal length (20-30 mm) for this path due to the length of the AD Instruments pressure transducer fixing device.

The pressure transducer was an AD Instruments (Castle Hill, Australia) MLT844 device. It is a piezo-resistive device designed for measuring animal intravascular arterial and venous pressures via an indwelling vascular catheter. Its working range is minus 20 to plus 300 mmHg. The transducer signal was amplified by connecting up to an ADInstuments ML110 bridge amplifier. The ML110 is a single channel bridge amplifier with an claimed accuracy of +/- 1% and is capable of low pass filtering (1 - 2000 Hz in 8 steps) which is important for filtering out background signal. The bridge amplifier was connected to an ADInstruments PowerLab 4S Precording unit. This unit is capable of recording from 0 - 200,000 samples per second continuously to disk with further high and low pass filtering capability if required. The PowerLab was connected via a universal serial bus (USB) to an Apple Macintosh PowerBook G3 233 MHz computer running ADInstruments Chart software. This software allows the computer to act as a digital chart recorder that can simultaneously record and display data in real time, at a sampling rate of up to 200,000 per second.

At the start of the experiment the pressure recording system was calibrated using a mercury sphygmanometer at 0 and 300 mmHg. A series of experiments were carried out using the following standard equipment, reagents and conditions: a 4 mm diameter 20 cm long precision bore borosilicate glass barrel, a Mark I device, 3.5 mm diameter 1 cm long regulator, 2% calcium chloride solution (normal physiological saline at pH 7.4), room temperature

(approximately 21°C), calcium chloride solution flow rate of 100 $mlmin^{-1}$, Fluka alginate solutions were prepared in normal physiological saline at pH 7.4 and 0.6 ml of alginate solution was injected per experiment. Syringe types and alginate solution concentrations were then varied.

6.3.2 Results

All the experiments performed produced a characteristic pressure trace over time, see Figure 6.13 for a typical trace. Figure 6.14 depicts major components of the characteristic traces with the associated labelling of the trace defined in Figure 6.15.

Standard plastic Becton Dickinson 50/60 ml syringes were initially tried with 3% alginate solution. The resulting pressure traces were highly variable, but did have the characteristic overall shape described above. Keeping everything else the same, the plastic syringe was substituted with a Lux Bloc (Italy) glass 50 ml syringe with Luer lock fitting. The subsequent traces were all near identical in both overall shape and magnitude – a unique and highly reproducible fingerprint was observed for that set of conditions. Measurement of the wall thickness with a micrometer gauge after slitting the tube longitudinally revealed a wall thickness of approximately 200 μm at selected points along its length. Furthermore, the glass syringe runs worked 100% of the time with no regulator stalling. It would appear that a major component of the previously experienced reproducibility was due to stiction in the plastic syringes i.e. the deformability of the plastic seal against the wall of the syringe. Another factor may have been the slight out of alignment of the syringe driver pusher and the plunger shaft of the syringe. A plastic syringe plunger is only supported in its syringe body by the seal whereas a glass syringe plunger is supported along its entire length thus preventing pivoting at the seal.

Having established glass syringes as the new "gold standard" further pressure experiments were only carried out using the same Lux Bloc glass syringe. These included varying the alginate percentages. Three different percentages were; 1%, 2% and 3% and all in physiological saline at pH 7.4. All had unique and highly reproducible fingerprint pressure tracings. See Figure 6.16 for a summary of the results and Figure 6.17 and Figure 6.18 for graphical representation.

6.3.3 Discussion

Closer examination of the data for each of the four different sets of experiments above suggested that:

1. Becton Dickinson 50/60 ml plastic syringe – 3% alginate solution

Overall the data was extremely variable. Opening snap pressures were on average much

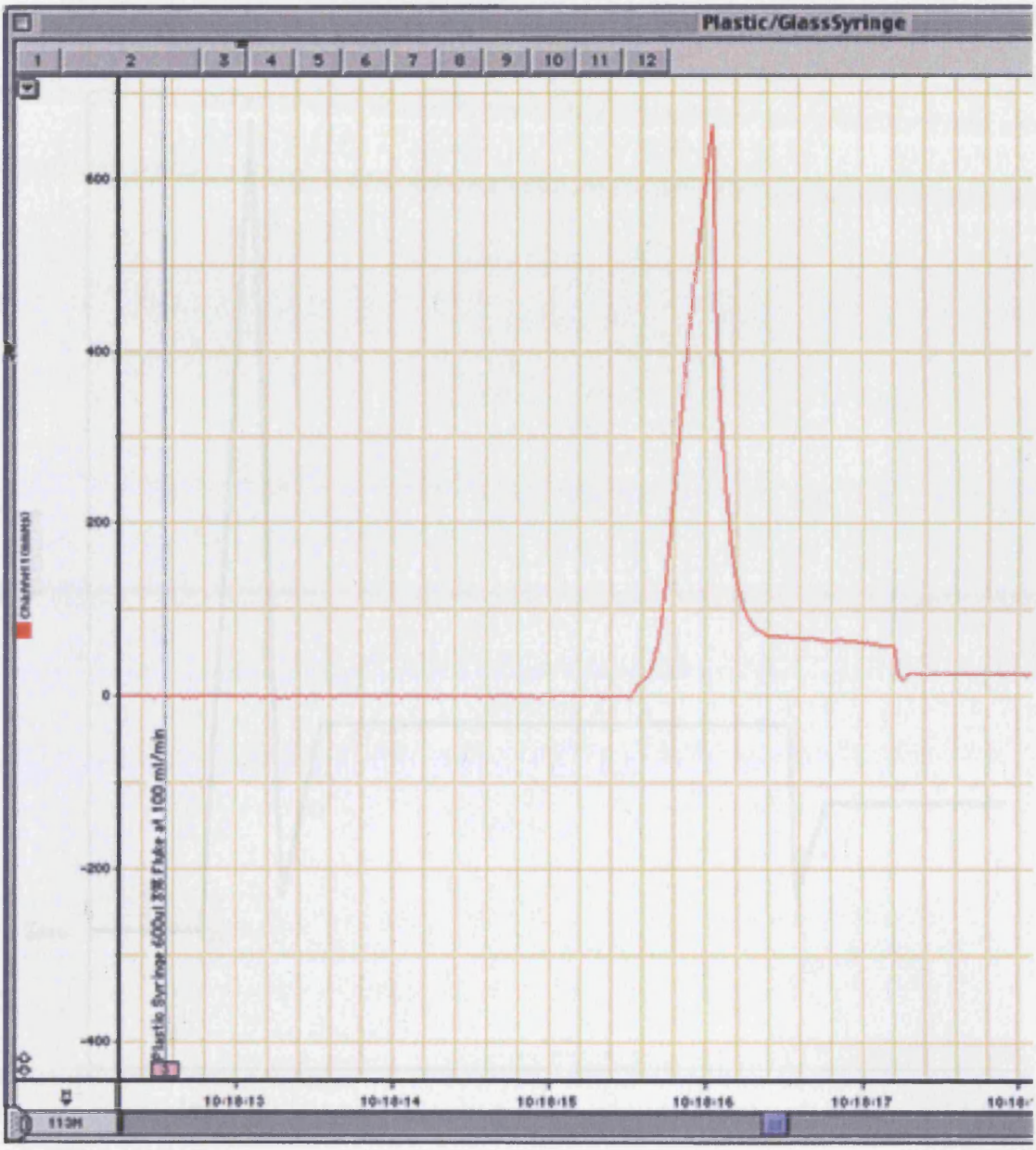

Figure 6.13

Example of a typical pressure trace recorded using the ADInstruments system (Apple OS 9.2 screen shot).

Pressure is recorded on the y axis against time on the x axis. Particular example is for a 50/60 ml Beckton Dickinson Plastipak syringe injecting calcium chloride solution at 1.67 $mlsec^{-1}$ in order to cross-link 3% Fluka alginate solution.

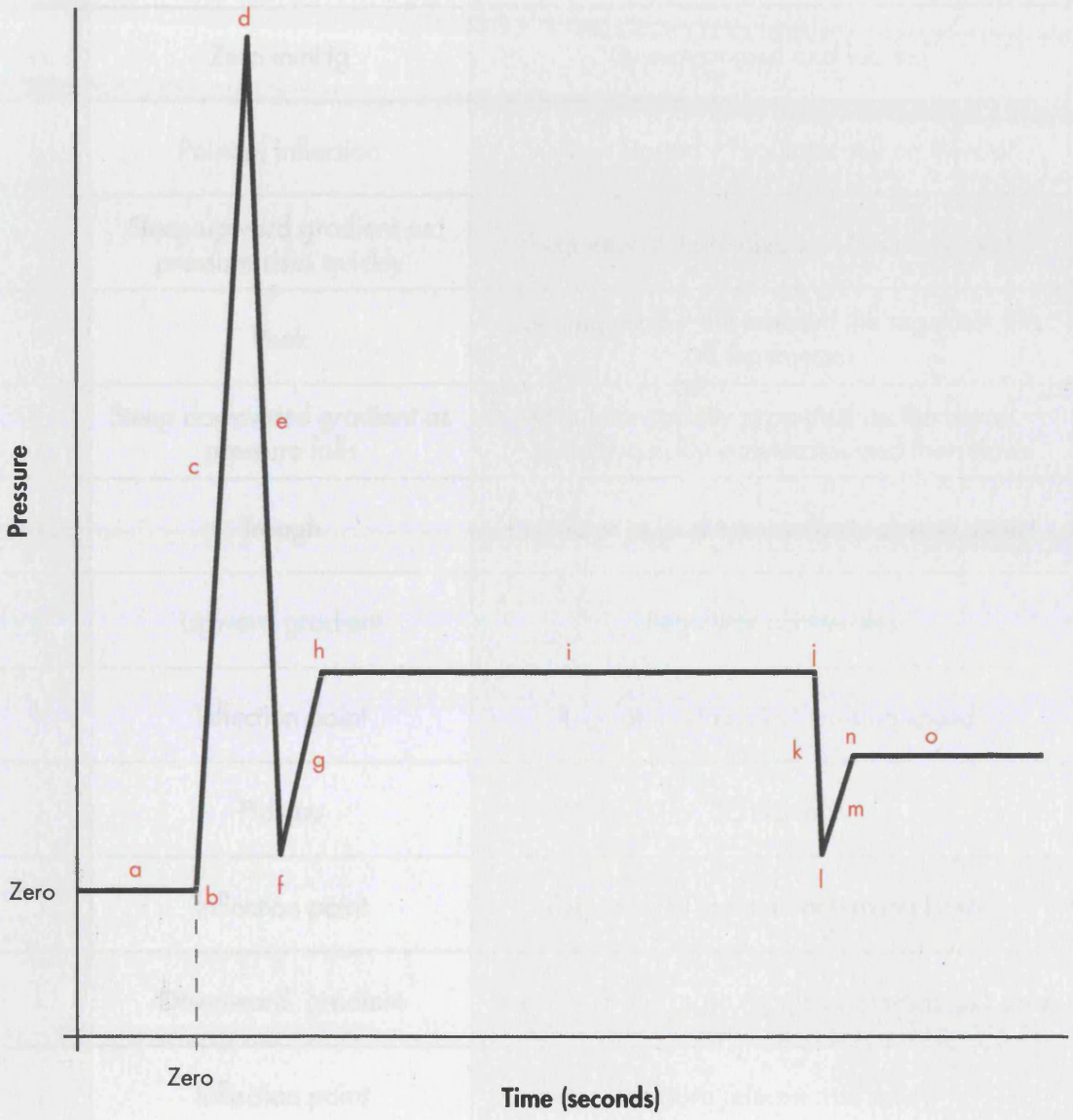

Figure 6.14

Schematic of a charachteristic pressure trace against time for a complete tube forming run.

See table - Figure 6.15 for explanation of labels.

Letter	Description of graph	Position or action of regulator
a	Zero mmHg	System primed and loaded
b	Point of inflection	Syringe started – regulator still on injector
c	Steep upward gradient as pressure rises quickly	Regulator still on injector – No movement
d	Peak	Opening snap – the moment the regulator lifts off the injector
e	Steep downward gradient as pressure falls	Regulator rapidly propelled up the barrel – initially quickly accelerates and then slows
f	Trough	Regulator at its slowest velocity during ascent
g	Upward gradient	Regulator accelerates
h	Inflection point	Regulator attains its "cruising speed"
i	Plateau	"Cruising"
j	Inflection point	Regulator at moment of leaving barrel
k	Downward gradient	Pressure drops as no regulator element in barrel
l	Inflection point	Pressure release overshoot
m	Upward gradient	Stabilisation of system
n	Inflection point	Return to new baseline pressure level
o	Plateau	Plateau (above zero mmHg) due to retained column of calcium chloride solution in the device

Figure 6.15

Labelling for characteristic pressure trace depicted in Figure 6.14.

Experimental conditions	Number of runs (n)	Range of point d (First peak) [Opening snap] mmHg	Average of point d (First peak) mmHg	Range of duration of run (points j minus b) secs	Average duration of run (points j minus b) secs	Range of integral value under the curve from points b - j	Average of integral value under the curve from points b - j
50/60 ml plastic B-D syringe – 3% alginate	6*	149 - >300**	N/A	1.65 - 3.29	2.11	92 - 249	171
50 ml Lux Bloc glass syringe – 3% alginate	6	165 - 168	167	1.51 - 1.54	1.53	87 - 90	89
50 ml Lux Bloc glass syringe – 2% alginate	3	60 - 61	60	1.54 - 1.58	1.56	71 - 76	74
50 ml Lux Bloc glass syringe – 1% alginate	3	57 - 60	58	1.56 - 1.61	1.59	70 - 75	73

* Only successful runs are included out of the 10 runs performed in total – 4 of which failed

** Values out of calibrated range

6.16

Summary of the AVInstruments system generated data.

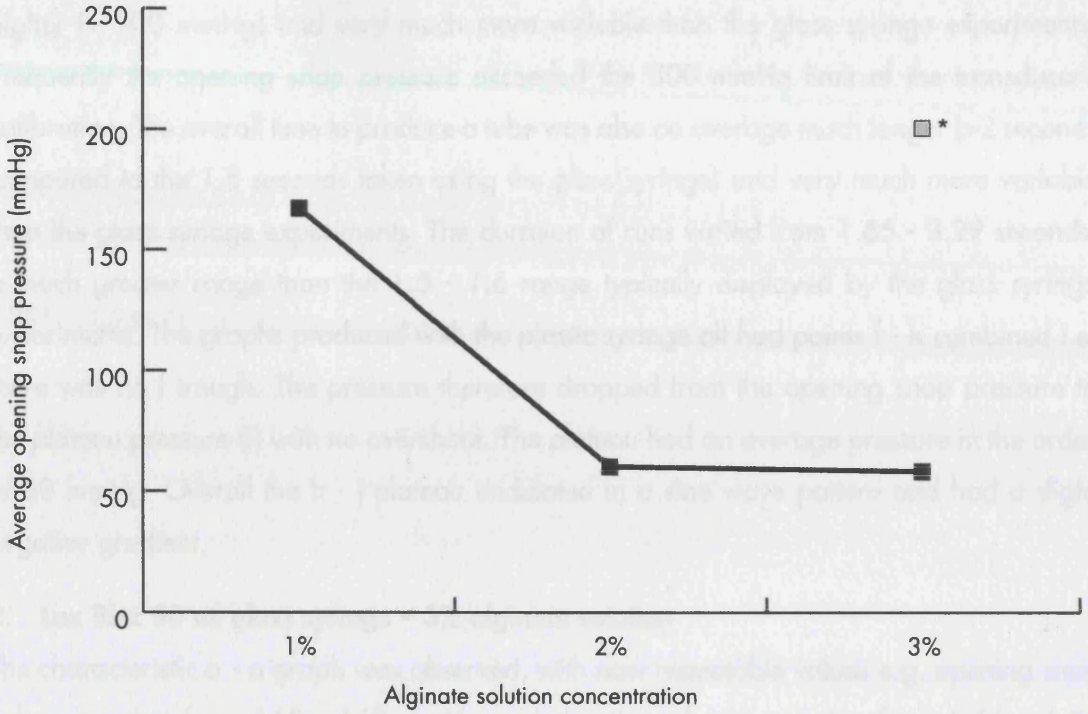

Figure 6.17
Average opening snap pressure with respect to alginate solution concentration.

* Minimum value

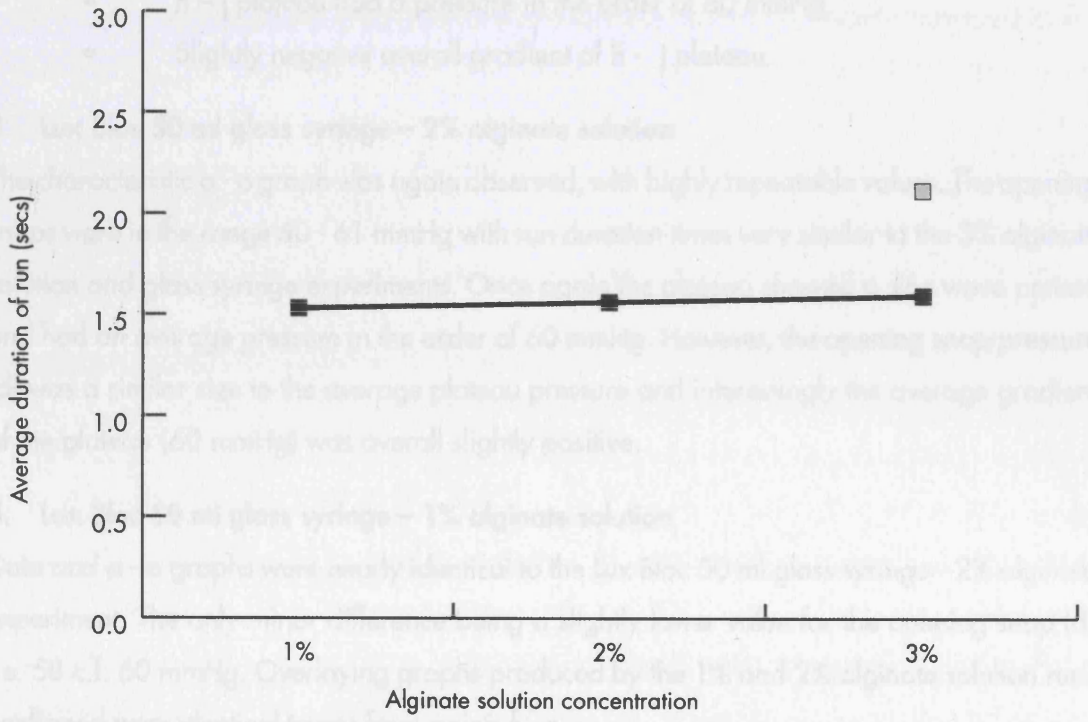

Figure 6.18
Average duration of tube forming run with respect to alginate solution concentration.

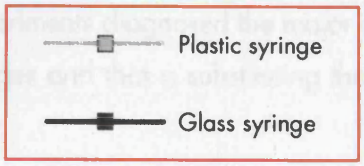

higher (> 200 mmHg) and very much more variable than the glass syringe experiments. Frequently the opening snap pressure exceeded the 300 mmHg limit of the transducer's calibration. The overall time to produce a tube was also on average much longer (>2 seconds compared to the 1.5 seconds taken using the glass syringe) and very much more variable than the glass syringe experiments. The duration of runs varied from 1.65 - 3.29 seconds, a much greater range than the 1.5 - 1.6 range typically displayed by the glass syringe experiments. The graphs produced with the plastic syringe all had points f - h combined i.e. there was no f trough. The pressure therefore dropped from the opening snap pressure to the plateau pressure (i) with no overshoot. The plateau had an average pressure in the order of 60 mmHg. Overall the h - j plateau undulated in a sine wave pattern and had a slight negative gradient.

2. Lux Bloc 50 ml glass syringe – 3% alginate solution

The characteristic a - o graph was observed, with now repeatable values e.g. opening snap values ranging from 165 - 168 mmHg and duration of runs ranging from 1.51 - 1.54 seconds. These values are much tighter grouped than for the equivalent plastic syringe values. Similarities to the plastic syringe date included:

- h – j plateau showed a sine wave pattern.
- h – j plateau had a pressure in the order of 60 mmHg.
- Slightly negative overall gradient of h - j plateau.

3. Lux Bloc 50 ml glass syringe – 2% alginate solution

The characteristic a - o graph was again observed, with highly repeatable values. The opening snaps were in the range 60 - 61 mmHg with run duration times very similar to the 3% alginate solution and glass syringe experiments. Once again the plateau showed a sine wave pattern and had an average pressure in the order of 60 mmHg. However, the opening snap pressure (d) was a similar size to the average plateau pressure and interestingly the average gradient of the plateau (60 mmHg) was overall slightly positive.

4. Lux Bloc 50 ml glass syringe – 1% alginate solution

Data and a - o graphs were nearly identical to the Lux Bloc 50 ml glass syringe - 2% alginate experiment. The only minor difference being a slightly lower value for the opening snap (d) i.e. 58 c.f. 60 mmHg. Overlaying graphs produced by the 1% and 2% alginate solution runs confirmed near identical traces from points f - o.

6.3.4 Conclusions

The dynamic pressure experiments diagnosed the major cause of the erratic performance to be due to the plastic syringes and that a substituting the plastic syringe by a glass syringe improved reliability greatly.

The viscosity of the alginate solution was a major factor affecting the opening snap pressure, with a major transition from 2% to 3% (60 c.f. 167 mmHg). 1% and 2% showed no real difference.

The ideal pressure trace would probably be a square wave i.e. a very rapid rise in pressure, followed by a plateau, followed by a rapid fall in pressure. See Figure 6.19 which uses the same labelling as Figure 6.14 for consistency.

Presently, only the plateau and the rapid drop in pressure have been demonstrated by the system using the Lux Bloc syringe system. The 1% and 2% Fluke alginate solutions best approximate to the ideal square wave graph in that their opening snap pressure is very similar in value to the plateau and both have the "ideal" h - o part of the curve.

6.3.5 Future Work

On the basis of the conclusions drawn from both the digital high speed video imaging and the dynamic pressure recordings, the semi-automated Mark II system was designed and fabricated - see Section 6.4. However, to more fully understand the dynamics of the various semi-automated fluid driven devices in the future it will be necessary to simultaneously combine continuous pressure recording and high speed digital imaging and correlate the data, for example, to precisely locate the position of the regulator in time and space compared to the pressure trace. This probably is best done using a second channel on the AD Instruments PowerLab, so that a high speed camera can record simultaneously with the pressure recorder. This may better elucidate whether the sine wave pattern superimposed on the h - j plateau is real or an artefact. Also simultaneous pressure and flow rate monitoring would also be of great value e.g. using a Transonic flow rate detector (Transonic Systems, Ithaca, NY, USA) which can be plugged directly into the AD Instruments PowerLab system.

Finally, it may be possible that by better understanding of the pressure trace and achieving a high level of reproducibility that the trace could be used in real time to predict whether a particular hydrogel tube is of an acceptable quality during its fabrication rather than trying to image the entire tube for flaws post production. The expensive component, the transducer e.g. AD Instruments MLT844 Pressure Transducer (>£400) merely clips onto a disposable Perspex/plastic part of the circuit e.g. AD Instruments MLA844 Disposable Clip-On Blood Pressure Domes (<£7) to get the readings. By incorporating this low cost disposable part into the bioreactor circuit allows not only tube production monitoring but also intraculturing pressure monitoring of the sealed bioreactor e.g. pulsatile flow monitoring.

[One other option which was successfully trialed but not incorporated into the final Mark II System was to control the pressure above the alginate solution. For example, it was possible to

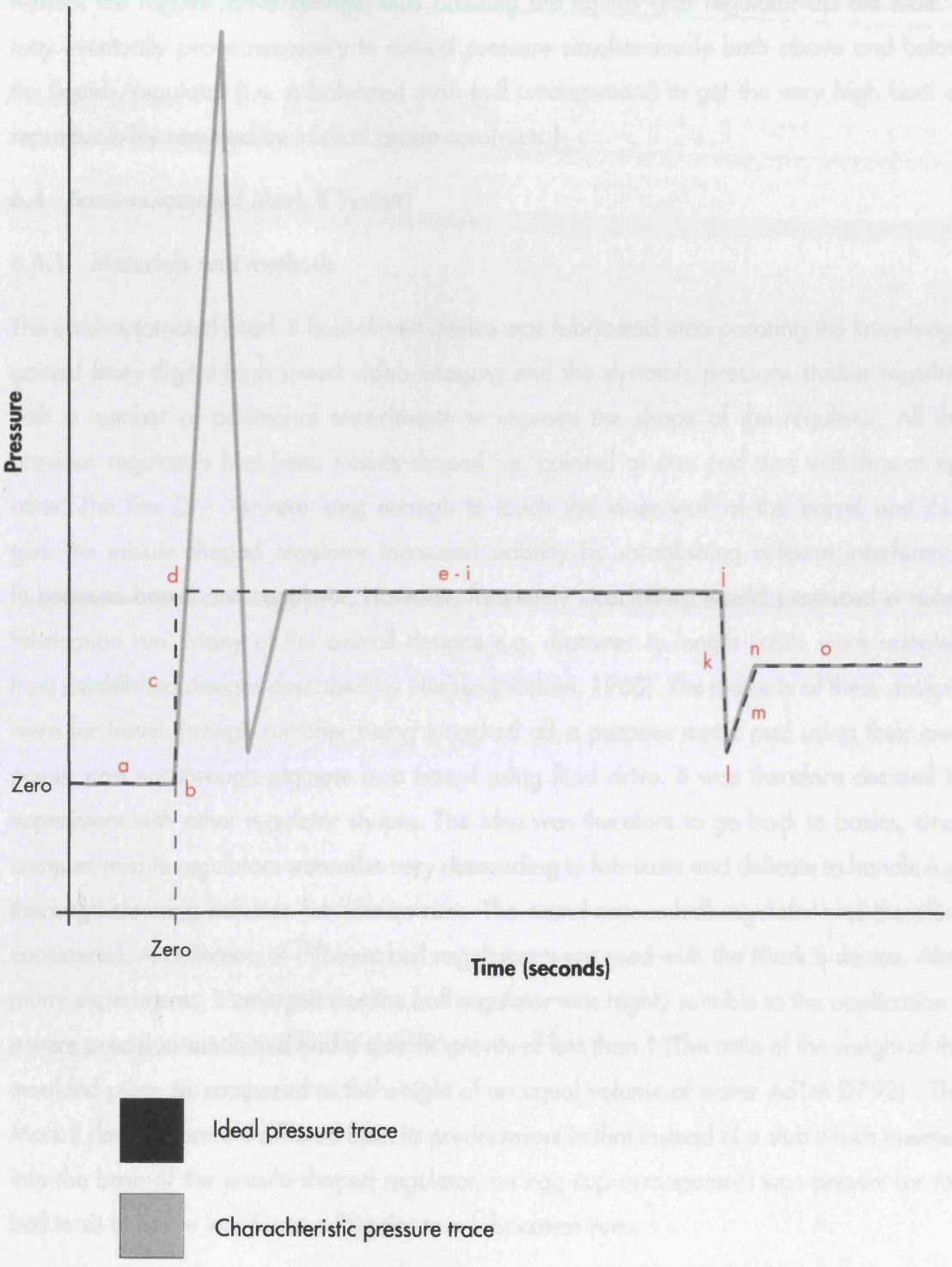

Figure 6.19

Schematic of a ideal pressure trace against time - characteristic pressure trace in background for comparison.

(Labelling is exactly the same as for Figure 6.14).

produce a tubular construct by just applying a negative pressure above the alginate solution without the regular drive syringe, thus drawing the liquids and regulator up the tube. It may eventually prove necessary to control pressure simultaneously both above and below the liquids/regulator (i.e. a balanced push-pull arrangement) to get the very high level of reproducibility required for clinical grade constructs.]

6.4 Semi-automated Mark II System

6.4.1 Materials and methods

The semi-automated Mark II fluid driven device was fabricated incorporating the knowledge gained from digital high speed video imaging and the dynamic pressure studies together with a number of additional experiments to improve the shape of the regulator. All the previous regulators had been missile-shaped i.e. pointed at one end and with fins at the other. The fins (3 - 4) were long enough to touch the inner wall of the barrel and thus give the missile shaped regulator increased stability by establishing a loose interference fit between barrel and regulator. However, frequently ricocheting would produced a failed fabrication run. Many of the overall designs e.g. diameter to length ratios were adapted from established designs described by Nielsen (Neilsen, 1960). The majority of these designs were for travel through air after being launched off a purpose made pad using their own power and not through alginate in a barrel using fluid drive. It was therefore decided to experiment with other regulator shapes. The idea was therefore to go back to basics, since complex missile regulators were also very demanding to fabricate and delicate to handle e.g. thorough cleaning between fabrication runs. The round cannonball regulator was therefore considered. A collection of different ball regulators were used with the Mark II device. After many experiments, it emerged that the ball regulator was highly suitable to the application if it were precision-made and had a specific gravity of less than 1 (The ratio of the weight of the moulded piece as compared to the weight of an equal volume of water ASTM D792) . The Mark II device therefore differed from its predecessors in that instead of a stub which inserted into the base of the missile-shaped regulator, an egg-cup arrangement was present for the ball to sit in (loose interference fit) prior to a fabrication run.

The ball regulators used were 3.4 mm diameter high density polyethylene (HDPE) and 3.175 mm diameter polypropylene (Precision Plastic Ball Company, Ilkey, West Yorkshire, UK). Both types were precision manufactured to +/-10 μM. Of particular importance was their specific gravity which was 0.96 and 0.92 respectively (earlier attempts with precision-made balls of denser materials had all conclusively failed including polystyrene (1.05) and nylon (1.01)). The reagents were 1% solutions of sodium alginate (Manugel DMB) made up in physiological saline and 2% calcium chloride solutions.

Figure 6.20 shows a photograph of the complete Mark II system with Figure 6.21 being a close-up view of the base unit demonstrating the ball and egg-cup arrangement. Aside from the use of a ball regulator, the only other significant diversion from the Mark I device was the use of a Saco 100 ml glass syringe instead of the original 60 ml plastic Becton Dickinson syringe resulting in the requirement for far slower syringe pusher speeds (45% less - see Figure 6.12). The device was used in an identical manner to the Mark I except that the syringe driver was run at $20 ml min^{-1}$ thus reducing the pusher speed further. Dynamic pressure recording studies had suggested that slower pusher speeds lead to improved inter-run consistency.

Experiments were carried out with a rule attached directly behind the glass barrel (as per the digital high speed video imaging experiments), known volumes of alginate solution with added colouring to aid viewing were loaded into the device using either a 0.5 or 1 ml precision ground glass syringe (Hamilton, Reno, NV, USA) and a tube then fabricated. The distance to the exact point that the ball just started to brake through the air/alginate interface (i.e. at the point that the alginate solution reservoir above the regulator was exhausted) was recorded. A number of the runs were also imaged using the high speed video equipment as before to confirm consistency of regulator progress within the barrel. Finally a small number of samples were imaged using optical coherence tomograpy (OCT) to confirm consistent wall dimensions - see Chapter 9. This final piece of research with the Mark II semi-automated system was in collaboration with Garr Chau (UCL).

6.4.2 Results and discussion

Figure 6.22 shows the data for different volumes of alginate solution (200 - 800 µL) and the maximum length of tube that was fabricated when using the 4 mm inside diameter barrel/3.4 mm regulator combination. The graph shows a highly linear relationship over the entire range of values. When extrapolated, the graph cuts the x axis at 87 µm, this figure represents a combination of the physical dead-space in the device's base unit plus the contribution from the plug of alginate around the egg-cup securing the tube (The switch from a stub/missile to a ball/egg-cup arrangement not only improved tube consistency but also greatly improved tube attachment at its proximal end). Further experiments were performed to study the effect of different ball sizes (see Figure 6.23) and different barrel diameters (see Figure 6.24). All the experiments resulted in linear relationships between the volume of alginate used and the maximum length of the resulting tube suggesting a consistent wall thickness (this was later confirmed for a number of samples using OCT - see Chapter 9). The lines of best fit for each distinct set of barrel/regulator combination however all had different gradients reflecting the rate the alginate solution flowed past the regulator as it travelled up the barrel. This difference in rate of flow past the regulator results in tubes of different wall thickness. Thus by changing the barrel/regulator combination alginate constructs of different diameter and wall thickness

Figure 6.20

Semi-automated Mark II System.
(Photographer: Dave Sayer - © The Wellcome Trust Medical Photographic Library - 2005)

Figure 6.21
Semi-automated Mark II device - base unit only.
Left-hand image - Empty egg-cup. Right-hand image with ball regulator *in situ*.
(Photographer: Dave Sayer - © The Wellcome Trust Medical Photographic Library - 2005)

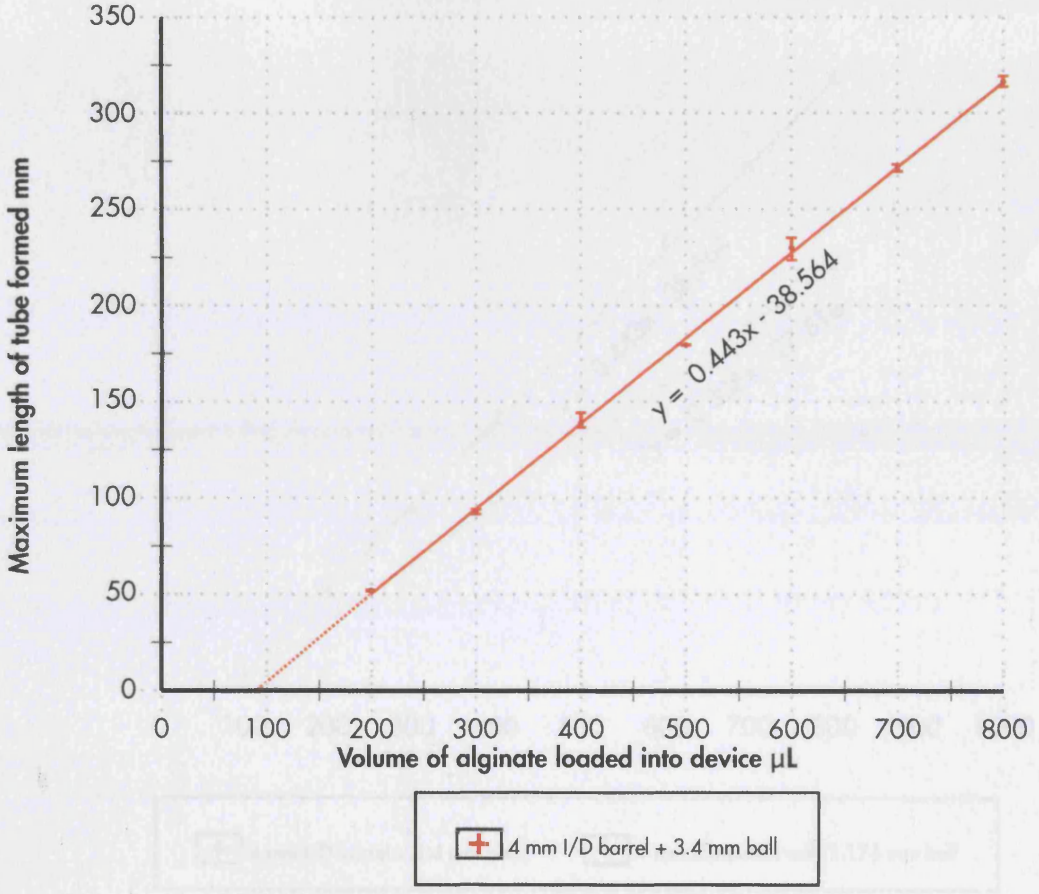

Figure 6.22

Graph of data generated using the combination of a 4 mm inside diameter barrel and 3.4 mm regulator ball (n = 21) demonstrating the linear relationship between the quantity of alginate loaded into the device and maximum length of tube formed.

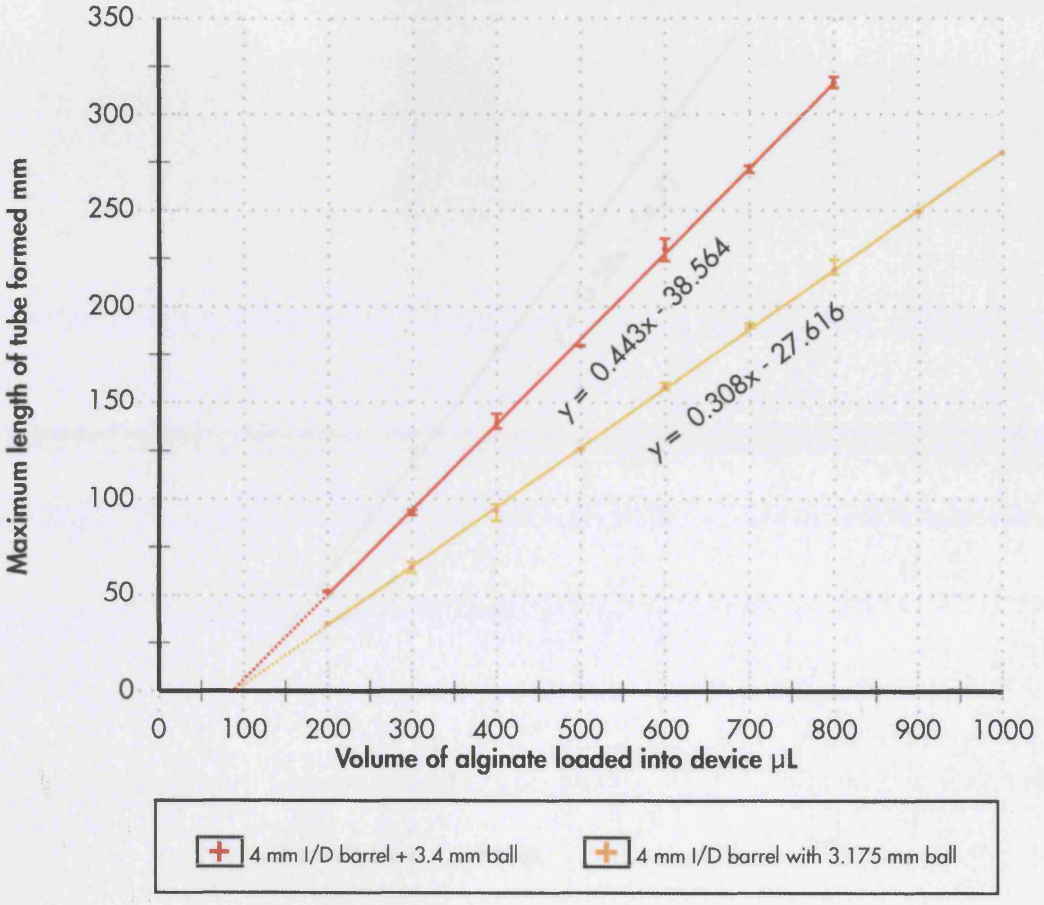

Figure 6.23

Graph indicating the effect of change in regulator ball diameter when the barrel dimensions remain constant.

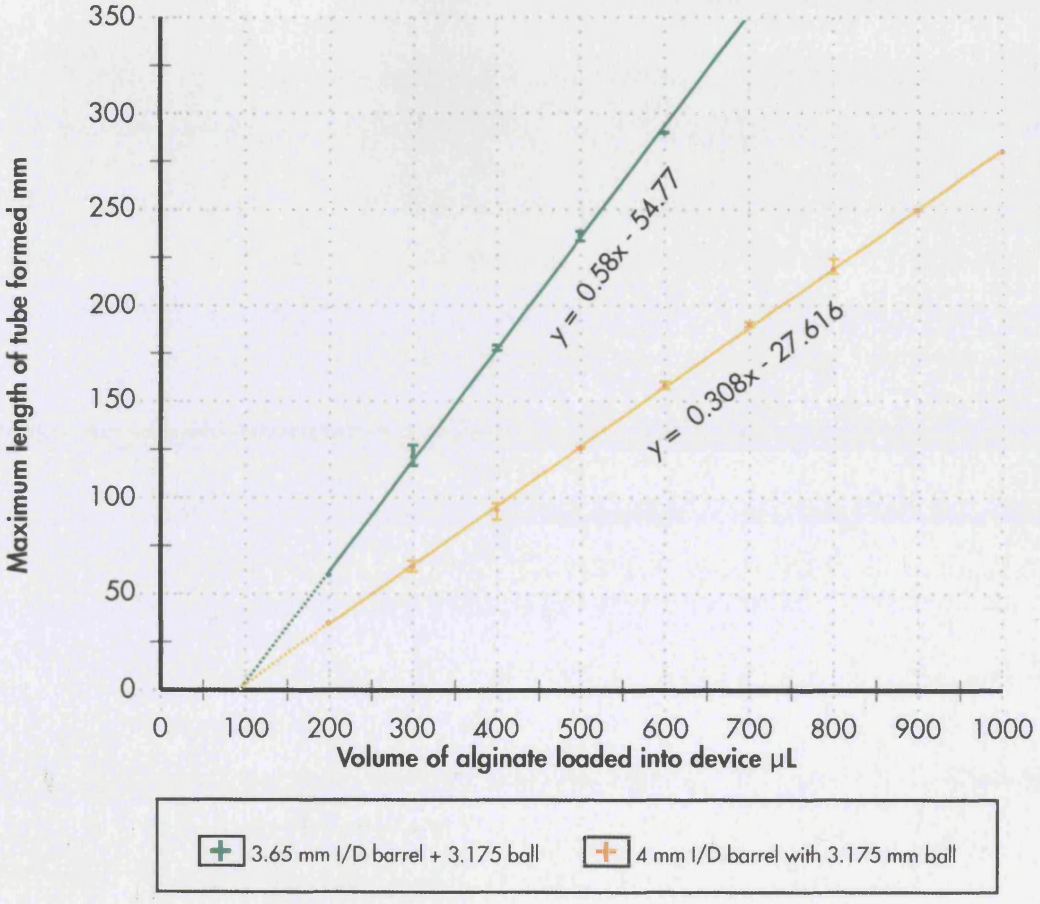

Figure 6.24

Graph indicating the effect of change in internal diameter of the barrel when the ball regulator dimensions remain constant.

can be constructed. Overall the Mark II system greatly improved the fabrication success rate (approaching 100%) and tube physical consistency regardless of inside tube diameter and/or regulator ball diameter.

7.0 Cell - alginate constructs

7.1 Overview

One of the aims of this thesis was to produce constructs consisting of a homogeneous distribution of cells and supporting polymer matrix in contrast to the almost universal tissue engineering approach of adding cells to a preformed scaffold e.g. Niklason *et al*, 1999. This approach tends to result in an incomplete, non-homogeneous distribution plus large amounts of cell wastage - only approximately 10% of the cells enter a preformed tubular scaffold, (Taylor, 2000). Also in order to be easily automated, one potential option is that all the stages prior to the actual homogeneous cell/polymer construct being fabricated are fluid in nature.

In order to successfully produce a tissue engineering construct from cells premixed with a polymer prior to scaffold formation, the following criteria with regard to the cells must be met:

1. Cells must be viable after the three-dimensional scaffold formation process is complete. Furthermore they must not be permanently damaged e.g. permanent change of phenotype
2. Anchorage dependent cells must be capable of interacting with the scaffold material after the formation process e.g. attach, elongate and correctly orientate
3. Cells must be capable of interacting with one another after the formation process
4. Mass transfer of nutrients, dissolved CO_2/O_2 and intercellular messenger signals must be adequate
5. Cells must be capable of synthesising normal extracellular matrix
6. Adequate strength of extracellular matrix must be achieved prior to predictable/ controlled polymer degradation

Since artery was the chosen tissue for the project, the strategy adopted was to attempt to grow a uniform tube composed of vascular smooth muscle and extracellular matrix which could then be seeded with endothelial cells. A series of experiments was therefore planned to evaluate the potential to grow smooth muscle cells or potential smooth muscle cells (stem cells) in alginate and also to evaluate the potential to use these cells mixed with alginate solution in the tube fabrication devices i.e. the float activated by a pneumatically driven piston device, the float activated by hand driven fluid device and the float activated by pump driven device.

The initial choice of smooth muscle cells included: commercial immortalised animal cell lines, commercial human non-immortalised cell lines and human or animal explants. The choice of

stem cells included both embryonic and adult stem cell again of human or animal origin.

Probably for the near future, autologous explants will be the cell lines of choice for the clinic for most organs apart from possibly skin. In the long term, the ideal might be "genetically modified universal non-immunogenic cell lines". The disadvantages of using explant material at this stage in the research is the lack of reproducibility between explant material. Human explant material available for basic research can only be obtained as "clinical surplus" from surgical operations, provided proper ethical permission is obtained beforehand. Such material is therefore not in large supply and only limited numbers of cells can be obtained for culturing. Furthermore, using such cells, only a finite number of passages is possible (Grunwald *et al*, 1983). This effectively means that only a few experiments per patient sample would be possible and since there is known to be significant variability between individuals' cells, reproducibility of experiments would be limited.

Commercial human non-immortalised cells lines are an option since the cells are obtained from a cadaver which allows a much greater number to be harvested. Unfortunately these cell lines are relatively expensive and again the cell type of interest, smooth muscle cells do not possess long term vigorous growth over multiple passages.

The option chosen for initial experiments was an immortalised animal cell line. Whilst being better in terms of cost, safety and availability, two distinct drawbacks were present:

- Immortalised cells behave differently to their non immortalised form, plus there is a potential to mutate further between passages
- Animal cells behave differently to human cells

Overall, however, the choice of an immortalised cell line does provide a potentially excellent model for the above work. The plan was to start with such a cell line and then progress on to human non-immortalised cell lines and/or stem cells.

Later, using the alginate tube forming devices described previously, a series of cell based experiments were performed using either immortalised rat smooth muscle cells or human adult mesenchymal stem cells (MSCs). Whilst the above cell types were selected on the basis that the project was to grow coronary artery, in fact all hollow organs (excluding bone) are predominantly composed of smooth muscle cells and extracellular matrix with a layer of epithelial cells (endothelium in the case blood vessels) on their lumen wall, i.e. there is a common architecture between hollow visceral organs. Thus, a universal platform technology is potentially possible for all soft tissue tubular structures e.g. gastrointestinal tract and urinary tract.

A generalised overview of the experimental procedure is depicted in a flow chart - see Figure

3.1. The materials and methods are fully described in Chapter 3. Some of the extended time course experiments were conducted with Julia Markusen (UCL).

For all the experiments (bar 1 preliminary experiment), one of two cell lines has been employed:

- Immortalised rat embryonic smooth muscle cells
- Adult human mesenchymal stem cells

7.1.1 Immortalised rat embryonic smooth muscle cells

Initial experiments were performed using an immortalised rat smooth muscle cell line - A7r5 (American Type Culture Collection, Manassas, Virginia, USA. Catalogue Number CRL-1444). A7r5 is a rat embryonic smooth muscle cell line derived from thoracic aorta and immortalised using chick embryo extract (Kimes and Brandt, 1976). Kimes and Brandt minced thoracic aortas and then placed them in media containing 20% fetal calf serum (FCS) and 2% chicken embryo extract (CEE) and incubated at 37°C. After these primary cultures had become nearly confluent, they were enzymatically dissociated in to single cell suspensions. These cells were then replated in fresh culture dishes. After 40 - 90 minutes, approximately 90% of the cells had become attached to the dish. The floating cells were aspirated and transferred to a new dish where they were allowed to attach to the dish and to grow to confluency. They were then passaged again. Each successive passage of these cells was accomplished in an identical manner until the increased multiplication rate of the cells in the culture indicated that a cell line had become established. This method of obtaining muscle cell lines is known as "selective serial passaging" and is based on the observation that for some types of muscle cells, fibroblasts and endothelial cells have a faster rate of attachment to the surface of tissue culture flasks than myoblasts (Yaffe, 1968 and Blondel *et al*, 1971). Once a cell line had emerged, the CEE was omitted from the medium. From each cell line, individual clonal cell lines were subsequently obtained including cell line A7r5, by isolating colonies derived from single cells. Cell line A7r5 was reported to have been grown under continuous cell culture conditions for over one year with no change in morphology, biochemistry or physiology properties. Characterisation of A7r5 suggested that A7r5 was a muscle cell line due to electrophysiological studies (capable of generating overshooting action potentials) and biochemical studies (synthesis of creatine phosphokinase-MM isoenzyme c.f. the BB dimer found in fibroblasts and neurones plus the ratio of myokinase:creatine phosphokinase activity is comparable with other established muscle cell lines, (Kimes and Brandt, 1976)). With this data and because the A7r5 line was derived from aorta, Kimes and Brandt therefore hypothesised that the cell line was smooth muscle. Their hypothesis was further supported by ultrastructural studies of internal cellular architecture including visualising the presence of bands of thin filaments (6 - 8 nm) orientated in parallel to the long axis of the cell - a feature

commonly observed in smooth muscle both *in vivo* and *in vitro*. However, the studies did reveal that the contractile mechanism of the cells appeared to be underdeveloped and at no stage did Kimes and Brandt witness cell contraction. A7r5's ultrastructure also set it aside from both cardiac and skeletal muscle. Interestingly, later studies by other researchers have elicited contraction of A7r5 cells (Fultz *et al*, 2000 and Fultz and Wright, 2003).

The A7r5 cell line was chosen because it was an immortalised well characterised adult rat aortic cell line with over 300 published papers (Ovid Medline search from 1966 to 2001), plus being immortalised it would provide more reproducible cell growth over multiple passages which would reduce inter-experimental variation such as would occur with explant material. It is only possible to perform a few limited experiments with cells obtained from original patient material due to smooth muscle cell's limited potential to divide. Furthermore the ATCC A7r5 cell line was certified free of various pathogens. The morphology of the commercially available A7r5 cells has been described as "fibroblastic" (ATCC specification sheet) and "flat 'ribbon-like' cells differentiating to parallel arrays of spindle shaped cells" (European Collection of Animal Cell Cultures - specification sheet for A7r5 in their collection - ECACC 86050803).

7.1.2 Adult human mesenchymal stem cells

The human adult mesenchymal stem cells (MSCs) were kindly provided by Professor Chris Boshoff and his group (The Wolfson Institute for Biomedical Research, UCL, London, UK). The MSCs were surplus clinical material obtained from bone marrow aspirates from live related donors of patients awaiting bone marrow transplants following high dose chemotherapy treatment. All the appropriate ethics committee approvals were in place at UCLH. MSC cells were isolated from the bone marrow aspirate using a Ficoll gradient as described in Section 3.1. The MSCs were selected on the basis of being anchorage dependent cells which would attach to polystyrene tissue culture flasks and negative for surface marker CD34. In contrast, bone marrow derived haemopoietic stem cells do not attach to polystyrene flasks and are CD34+ve. The rationale for using MSCs was that unlike explant material their vigour to grow and divide over multiple passages was better, although not infinite (Kobune *et al*, 2003 and Zimmermann *et al*, 2003). The aim of using MSCs was to add them to the alginate solution, produce a homogeneous mixture prior to forming a homogeneous tube and then to correctly orientate/align the stem cells prior to permanently differentiating them into smooth muscle cells, ideally coronary artery smooth muscle cells. [Provisional data had suggested that it was possible to switch MSC's in a three-dimensional alginate matrix into smooth muscle using preconditioned media and a patent filed (Mason *et al*, 2003)]

7.1.3 Cell and polymer mixing

In order to produce adequate numbers of A7r5 and MSC cells, for example, a typical experiment required 10^6 -10^7 cells per ml of alginate solution, the cell lines were cultured using the techniques described in Sections 3.1 and 3.2. Known quantities of cells in known volumes of culture medium were added to known volumes of alginate solutions to produce desired cell/alginate concentrations.

A basic requirement, was that the cell mixing with alginate process needed to result in a totally homogeneous cell distribution, with no clumps and little (ideally zero) cell death. Furthermore, early range-finding experiments had demonstrated that final cell densities less than 10^5 cells per ml of alginate were distributed very sparsely in the finished scaffold i.e. allowing no cell-cell contact. Close proximity of the cells was deemed a prerequisite. This only occurred at 10^6 cells per ml of alginate and greater. The techniques employed to produce cell concentrations greater than 10^6 cells per ml of alginate are described in Section 3.2. Final mixing was by using the repeated action of a manual micropipette. This final step does not lend itself to robust reproducibility and is highly operator dependant. Therefore other options were sought.

An alternative to using a micropipette to create a homogeneous cell/alginate solution is a static mixer e.g. Kenics mixer. This type of mixer consists of a series of elements within a tube. The helical mixing elements direct the flow of material radially toward the tube walls and back to the centre. Additional velocity reversal and flow division results from combining alternating clockwise and counter clockwise elements, thus increasing mixing efficiency. The greater the number of elements the greater the degree of mixing. The advantage of this system is that it is an in-line mixing system (ideal for automation) and the device produced shear forces which are very low and therefore theoretically cell friendly. A Kenics mixer of 192 mm in length, 4.8 mm O/D, 3.5 mm I/D made of surgical grade stainless steel containing 32 elements (Chemineer Kenics, North Andover, Massachusetts, USA - Part number 37-03-075) was tried. However, whilst its mixing ability was never in doubt its construction was not suitable for multiple cell experiments in quick succession. The reason being that the elements are sealed (welded) into the 22 gauge tube thus making thorough cleaning and sterilisation between runs impossible. Furthermore, the volume lost by being retained in the device and its associated tubing was unacceptable (>1 ml, equating to > 10^6 cells lost per experiment). Whilst in the long term static mixers may well be the way forward since they can be put in-line with the tube forming device and since at present no simple plastic sterile disposable versions were available, it was decided to continue with the manual cell/alginate mixing using a micropipette and gentle aspiration and keep reviewing the availability of sterile disposable static mixers.

(As of early 2004, disposable static mixers have become available from: TAH Industries

(Robbinsville, New Jersey, USA). The smallest diameter device in their range is a 2.36 mm element diameter device with either 8 or 12 elements resulting in retained volumes of 0.07 ml and 0.1 ml respectively). Individual mixing elements are also available from TAH, allowing a bespoke mixer to be fabricated.)

7.1.4 Alginate Polymer

A variety of different manufacturers' alginate products has been obtained as potential candidate polymers during the course of developing the alginate tube forming devices. These alginates therefore continued to be used for the cell/alginate work since the tube forming device development and the cell/alginate research experiments were running in parallel.

The choice of aqueous solvent was limited by certain key parameters including being cell friendly and maintaining scaffold integrity. Typically, alginate powder was added to physiological saline in final concentrations ranging from 0.5 - 6%. Ideally the lowest alginate concentration that produces the desired structural strength needs to be used since it has been shown that increasing alginate concentration decreases diffusion across the hydrogel (Martinsen *et al*, 1992). Preliminary experiments had demonstrated that if water for injection (WFI - BioWhittaker, Walkersville, Maryland, USA) was used instead of physiological saline, then upon mixing the alginate solution and cells, cell lysis would quickly ensue. This was due to the hypotonic nature of the solution relative to the cell cytoplasm. PBS with or without calcium ions/magnesium ions, (Dulbecco's Phosphate Buffered Saline, DPBS) (BioWhittaker, Walkersville, Maryland, USA), was also originally tried since it had the correct osmolarity and pH; but when DPBS alginate solution came into contact with the calcium chloride cross-linking agent, the calcium was precipitated thus reducing available calcium ions for cross-linking and therefore significantly weakening the hydrogel construct. Furthermore, calcium insoluble precipitates are undesirable in the construct since calcium has a physiological effect on smooth muscle cells e.g. causes them to contract. This effect is not desirable during the proliferation and growth phase as it is necessary for the smooth muscle cells to spread out i.e. elongate in order to form good cell-cell interactions throughout the construct.

The reagents and alginate solution preparation techniques are described in Section 3.3.

7.2 Producing three-dimensional cell/alginate hydrogel structures

Three distinct three-dimensional cell/alginate structures were produced for experimental studies:

- Flat sheets
- Round beads
- Hollow tubes

Studies on these three-dimensional constructs included cell survival assays (trypan blue dye or live/dead viability/cytotoxicity kits (Molecular Probes L-3224, Molecular Probes, Eugene, Oregon, USA) cytology and optical coherence tomography.

7.2.1 Flat sheets

The simplest of the structures produced were flat sheets. These structures either had cells embedded in them or cells added immediately after the gels had totally set. These sheets were primarily used in order to study the interaction between the polymer surface and the cells e.g. attachment. The sheets were produced by the method described in Section 3.4.1.

7.2.2 Beads

The next more complicated three-dimensional structure produced was alginate/cell beads i.e cells immobilised in alginate beads. Cell encapsulation using alginate has a long and rich literature (Martinsen *et al*, 1989).

Virtually every mammalian cell has been encapsulated, although the literature at the time did not include any references to smooth muscle cells for reasons which later become apparent, (Uludag *et al*, 2000). The potential advantage of bead studies was that the three-dimensional structures have embedded cells whilst using minimal material, effectively a microscale down version of the desired tube experiments e.g. 600 µL of alginate will produce one 25 cm tube with a wall thickness of approximately 150 µm (allowing for losses within the tube forming device). Whereas the same 600 µL will produce well over 100 beads of approximately 2 mm in diameter (also allowing for losses within the bead making device). Thus effectively 100 parallel experiments can be performed with the same 600 µL sample volume. The manual bead fabrication technique is described in Section 3.4.2.

The potential drawbacks to beads produced manually using a small bore needle and syringe include possible mass transfer problems due to the distance from the bead's surface to centre plus manually fabricated beads lack uniformity of shape and size. After experimenting with a range of needle sizes it appeared that the smallest diameter bead which could be manufactured using the manual technique was 2 mm +/- 20%. It was therefore decided to switch to an automated method built in collaboration with Dr. Julian Mason (Kingston University, Kingston, Surrey). All later experiments were performed with an automated bead forming devices since beads could be made in the range 100 µm and upwards. This reduction in bead diameter improved mass transfer through the individual beads whilst also allowing increased numbers of parallel experiments to be performed for a given volume of cell/alginate solution.

In order to assess the number of cells contained in the beads plus also their variability it was essential to be able to free them from the alginate. Placing beads in 0.1 M sodium

citrate (Sigma, St. Louis, Maryland, USA) resulted in the excess number of sodium ions competing with the far fewer calcium cross-linking ions resulting in the alginate hydrogel quickly becoming a liquid once again, thus releasing the cells. Once freed, the cells were counted using the Improve Neurbauer Haemocytometer as previously described in Section 3.2. The ratio of live:dead cells was important in determining the viability of the cells. It is worth noting that the trypan blue stain dye only reflects the status of the cell membrane and not any long term detrimental changes which may have taken place e.g. commencing apoptosis. Possible ways to monitor this include DNA microarrays and/or two-dimensional protein gel electrophoresis (Boshoff, 2003). Finally, the culture media used for these microwell experiments was typically the supplemented media previously described or αMEM (minimal essential media with ribonucleasides and deoxyribonucleasides) (Gibco-BRL, Gathersburg, Maryland, USA). This alternative media was used following a personal communication with Dr Clare Seldon (2000) who had had extensive experience in the encapsulation of liver cells in alginate whilst fabricating extra-corporal liver assist devices (Seldon *et al*, 1998 and Seldon *et al*, 1999 and Seldon *et al*, 2000 and Khalil *et al*, 2001) and with whom we briefly collaborated.

7.2.3 Tubes

Since the aim of the research was to produce tissue engineered vessels it was essential to produce cell/media/alginate hydrogel tubes. All the devices previously described (excluding the initial powder spraying research - which for the sake of brevity is not included in this Thesis) were used in all their various forms as they evolved. The first preliminary studies were performed with Professor Ian Charles and his group (The Wolfson Institute for Biomedical Research, UCL, London, UK) using their genetically engineered tetracycline-inducible nitric oxide generating cell line (T-Rex 293 clone 22). This is a human transformed primary embryonal kidney cell line (Xu *et al*, 2002). The nitrite concentration of the surrounding growth medium was used as a reflection of the nitric oxide (NO) produced by the cells. The nitrite concentration was determined using the Greiss reaction (1% sulfanilamide, 0.1% n-1-naphthylene diamine dihydrochloride). Absorbance was then measured at 540 nm using sodium nitrite as a standard. The tube fabrication process used the original device, whereby the float is activated by a pneumatically driven piston, the method is described in Section 3.4.3. The combination of the 9 mm inside diameter/14 cm long glass forming tube together with an 8.5 mm diameter regulator was used. The control consisted of T-Rex 293 clone 22 cells encapsulated in manually produced alginate beads (1% Fluka) - made from the same batch of homogeneously mixed cells and alginate as that used to fabricate the tubes. The identical cross-linking conditions were employed (1% calcium chloride solution for 20 minutes). After fabrication the tubes were cut using a scapel blade into approximately 1 cm long sections.

At three time points, 24, 48 and 96 hours, the NO induction agent, tetracycline was added to the media of both the tubes and the beads and the NO levels determined. Whilst the cells encapsulated in the beads produced measurable levels of NO, the cells in the tubes did not. These very preliminary studies quickly demonstrated that tubes with cells in could be fabricated, however, the process appeared to possibly interfere with their biochemistry. A repeat set of similar experiments resulted in the same conclusions. In all the experiments, the morphology (light microscopy with no staining) of the encapsulated cells appeared identical with no obvious areas of cell death/necrosis. The difference between the beads and the sections of tubes may have been the result of the beads being efficiently optimised for the conditions (the conditions used were the standards used in Professor Charles' lab at that time). The sections of tube contained 10 - 20x more cells and alginate than the individual beads they were compared to. The rationale was that at this elevated level an NO reading should be easily obtainable. However, in hindsight, it may well have been that the quantity of media the sections were placed into (1 ml per well - the same as the beads) was inadequate in terms of both the nutrient supply as well as the dilution of residual calcium ions left in the construct after the washing steps.

Later experiments in our own laboratories aimed to build on this modest start continued to use the tube forming device whereby the float is activated by a pneumatically driven piston in order to produce a cell/media/alginate hydrogel tube. Section 3.4.3 describes the fabrication. Alginate tubes containing cells were constructed with an outside diameter of 9 mm, length 140 mm (i.e. dimensions determined by the particular glass tube chosen) and with a wall thickness in the order of 0.25 mm (determined by the outer diameter of the regulator within the glass tube). Both tubes and discs cut from tubes were studied. Care was taken to keep the tubes/disks submerged in fluid at all times since on exposure to air syneresis soon occurs i.e. water loss from the hydrogel leading to unwanted construct shrinkage. Rehydration (imbibition) is not an option because whilst the alginate hydrogel might swell to its former dimensions, the encapsulated cells are likely to have suffered irreversibly. Despite cell damage due to the handling and the cutting of the discs, overall the discs are potentially a better and closer analogue to the tubes than beads.

Using a bespoke 7 mm inside diameter "cookie cutter" an exact 7 mm diameter disc could be cut (see Section 3.4.3). The average number of cells in each disc could therefore be estimated from the cell density in the cell/media/alginate solution and the discs dimension i.e. 7 mm diameter. The average disc was calculated to have 9600 cells from an initial 10^6 cells per ml of cell/alginate solution. Again control wells were also produced matching the discs' cell number but containing no alginate. Discs were incubated in 10% CO_2, humidified incubators at 37°C. Cells were also finally freed from the hydrogel using 0.1 M sodium citrate and cell

numbers and viability estimated using trypan blue and Neubauer haemocytometry counts using light microscopy.

The results are displayed in Figure 7.1 (cell proliferation over time) and Figure 7.2 (cell viability over time). From Figure 7.1 it can be seen that the total cell number for the discs stayed constant with time, i.e. on average approximately 7300 (+/- 40%) cells per disc, this contrasts strongly with the initial lag phase and then exponential proliferation phase observed in the control (cell in a T-flask). The average of 7,300 cells per disc compares reasonably favourably in terms of order of magnitude with the estimated number of 9600 cells per disc based on the cell density in the cell/alginate solution prior to tube formation. This 24% average difference is probably due to a combination of factors including, potentially incomplete cell and alginate mixing, poor tube construction with respect to consistent wall thickness (a problem if cell aggregates persist and particularly with the early forms of the tube fabricating devices), and possible sampling errors.

Visually the discs appeared unchanged over the 9 day study, also the discs retained their integrity throughout. These observations suggest that the discs were not significantly degrading due to the presence of divalent ions in the culture media over the time course of the experiment. Degradation of the discs would lead to cell losses. The possible explanations for the constant cell number can be explained in 2 possible scenarios:

1. The cell proliferation rate exactly matched the rate cells were lost due to alginate hydrogel degradation and releasing the encapsulated cells
2. The discs stayed intact and the cells failed to proliferate

Scenario 1 is unlikely due to the architecture and integrity of the discs remaining constant throughout. Furthermore, the cells remained tightly balled-up (i.e. spherical) throughout the experiment. For anchorage dependant cells, without attachment and elongation within the matrix, it is highly unlikely that cell proliferation can occur. "In tissue engineering, cell adhesion to a surface is critical because adhesion precedes other events such as cell spreading, cell migration and often differentiated cell functioning" (Saltzman, 2000).

Scenario 1 is further unlikely when the viability studies are taken into account (see Section 7.3). Scenario 2 is therefore the most likely explanation of the constant cell number observed in each disc over the 9 day period. In contrast, the control cells (i.e. cells not immobilised in alginate), proliferated in an exponential manner after a short (1 - 2 days) lag phase. This extended lag phase was probably due to the cells being seeded at too low a density for the surface area of the T flask; by approximately 2 orders of magnitude. It is normal for freshly seeded cells to enter a brief lag phase immediately after seeding during which time they attach, elongate and then re-enter the cell cycle. This lag is typically less than 24 hours if cells

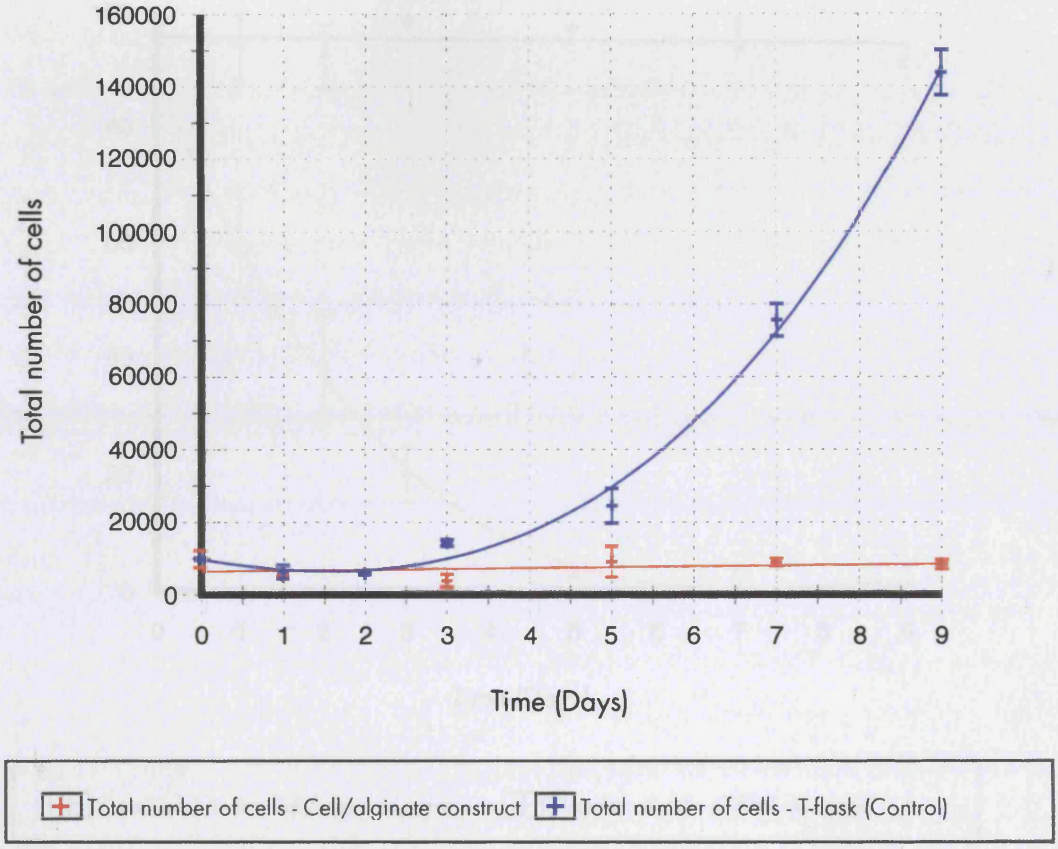

Figure 7.1

Total cell numbers for A7r5 immortalised rat smooth muscle cells encapsulated in alginate hydrogel 7 mm diameter discs cut from tubular constructs over a 9 day time period.

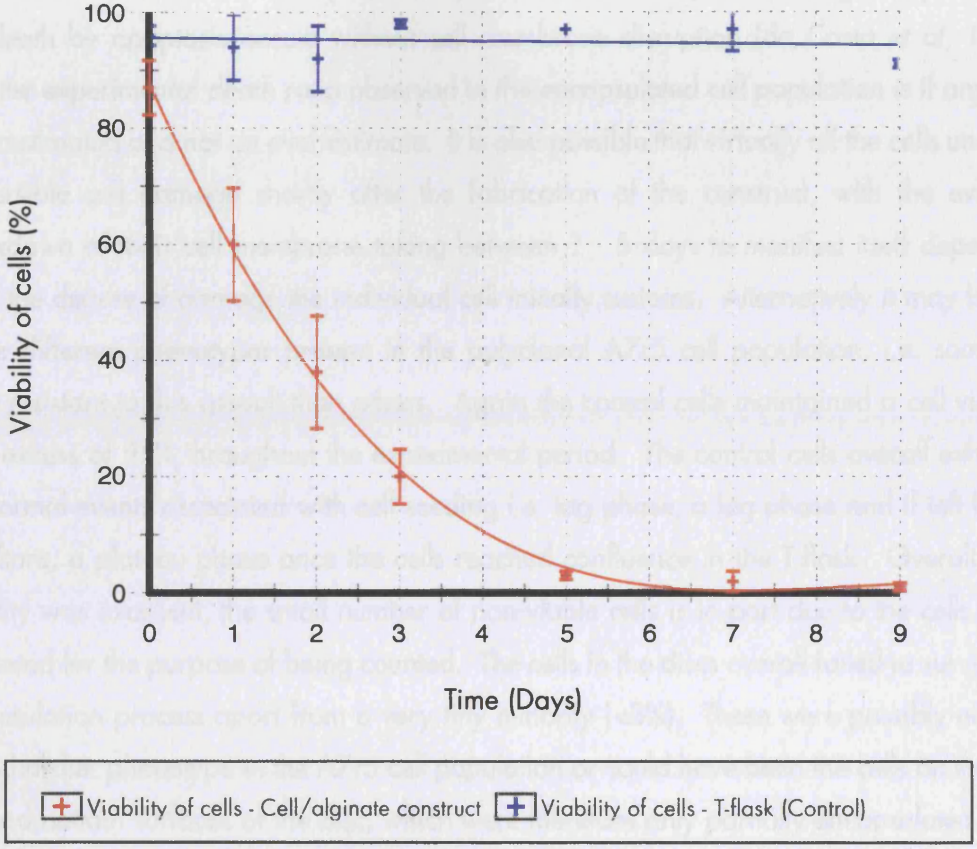

Figure 7.2

Viability of A7r5 immortalised rat smooth muscle cells encapsulated in in alginate hydrogel 7 mm diameter discs cut from tubular constructs over a 9 day time period.

are seeded at an appropriate density (Freshney, 2000).

Figure 7.2 shows that the viability of the cells that were encapsulated in alginate decreased to zero over a six day period whilst the control cells in T-flasks retained their viability throughout the 9 day period. The viability was assessed by comparing the number of trypan blue stained cells versus the number unstained. This assay measures cell membrane integrity. A drawback to this approach is that loss of cell membrane integrity occurs late on in the event of cell death. Thus there is a tendency to over estimate the viability of cells e.g. the process of cell death by apoptosis occurs without cell membrane disruption (da Costa *et al*, 1999). Thus the experimental death ratio observed in the encapsulated cell population is if anything underestimated and not an over estimate. It is also possible that virtually all the cells undergo irreversible cell damage shortly after the fabrication of the construct, with the eventual breakdown of their cell membrane taking between 1 - 5 days to manifest itself depending upon the degree of damage the individual cell initially sustains. Alternatively it may be due to the different phenotypes present in the polyclonal A7r5 cell population, i.e. some are more resistant to this assault than others. Again the control cells maintained a cell viability of in excess of 95% throughout the experimental period. The control cells overall exhibited the normal events associated with cell seeding i.e. lag phase, a log phase and if left longer in culture, a plateau phase once the cells reached confluence in the T-flask. Overall, their viability was excellent, the small number of non-viable cells is in part due to the cells being harvested for the purpose of being counted. The cells in the discs overall failed to survive the encapsulation process apart from a very tiny minority (<3%). These were possibly either a much hardier phenotype in the A7r5 cell population or could have been the cells on the very top and bottom surfaces of the disc, which were therefore only partially encapsulated in the alginate hydrogel and therefore enjoyed better media supply and mass transfer.

7.3 Alginate polymer/cell survival and proliferation studies

From the results obtained in Section 7.2, the essential question needing to be answered was whether alginate solution/hydrogel and the actual formation of a three-dimensional structure had an adverse effect on the smooth muscle cells, since the published literature did not include reference to smooth muscle cell encapsulation in alginate. The basic experiment undertaken was to mix cells homogeneously with alginate solution, produce a tubular construct cross-linked with calcium chloride solution, rinse and then to immediately release the cells from the hydrogel using sodium citrate solution. Full details are provided in Section 3.3 with the results recorded in Figure 7.3.

In order to be able to identify the effect of individual aspects of the tube forming process (i.e. cell harvesting including centrifugation, mixing with alginate solution, exposure to calcium

Rinse solution	Total rinse volume (ml)	Cell viability following release from cell/alginate tubular contructs - Trypan blue exclusion assay
Supplemented media	1.5	92%
	12.5	89%
	125	87%
Physiological saline	1.5	85%
	12.5	N/A
	125	N/A
Harvested control cells - No alginate/calcium chloride	-	96%

Figure 7.3

Results of cell viability studies for A7r5 immortalised rat smooth muscle cells immediately following release from cell/alginate hydrogel tubular constructs using sodium citrate solution. Cell/alginate constructs were fabricated and rinsed with different volumes and different rinse solutions to remove excess calcium chloride cross-linking solution.

chloride solution - the cross-linking process and finally being exposed to 0.1 M sodium citrate), a collection of control experiments was undertaken in parallel using 24 microwell plates. Microwell plates were used since the tube forming device will only work if all the components of the steps in the process are undertaken and since the controls were designed to have selected component(s) omitted, microwell plates were the only way forward. In order to keep the total volumes identical, supplemented media was used to substitute for the omitted component(s). See Figure 7.4 for an overview of the experimental set.

Control experiments were performed in parallel using identical cell numbers, see Section 3.3. In brief, the viability of these control cells was assessed following harvesting (trypsinisation from the T-flask) with no further manipulation i.e. only essential unit operations were performed to be able to obtain cells for viability assessment from a standard T-flask. The viability of these control cells after trypsinisation and the addition of trypan blue was 96%. No data was possible for both the higher volume saline rinses as with both experimental conditions the calcium cross-linked hydrogel dissolved due to the presence of excess sodium ions. It is likely that even the 1.5 ml saline wash as well as the supplemented media wash caused an element of tube dissolution. The cross-linking solution of 1% calcium chloride equates to a calcium ion concentration of 6.8 $mmolL^{-1}$. In contrast the supplemented media has a calcium ion concentration of 1.6 $mmolL^{-1}$ (0.018%). Likewise, supplemented media contains other polyvalent cations whereas physiological saline contains only monovalent cations and hence strongly affects calcium ion cross-linking by out competing the calcium ions with monovalent sodium ions.

The A7r5 cells were rescued from the hydrogel using the previously described sodium citrate technique. Cells rescued after undergoing the various different conditions created by the omission of the various unit operations/component(s) differed little in their overall viability with an overall range of 85 - 92% survival. Unfortunately, it is impossible to make a conclusion with respect to the difference in wash solutions i.e. supplemented media versus physiological saline due to the physiological saline degrading effect on the hydrogel, however, it would appear from the smallest volume (1.5 ml) that supplemented media was better with respect to cell survival than physiological saline. Increasing the volume of supplemented media used for washing did not improve cell survival. In fact, it appeared to slightly decrease cell survival. It would therefore appear that a short wash step with 1.5 ml of supplemented media was the best option since increasing the volume of media made no improvement. Since the total volume of the 12 cm long glass tube, with a 4 mm diameter, is approximately 1.5 ml and the dead space in the device base is approximately 100 µL, this gives a total volume of 1.6 ml in the total device. Given that the alginate is a 1% mixture and that the cell pellet was < 100 µL after centrifugation, this gives an approximate fluid volume in the complete device,

	Control - Experimental conditions	Cells pelleted by centrifugation	Cell pellet resuspended in media prior to homogeneous mixing with alginate solution	Processed through tube forming device	Cross-linked with calcium chloride solution	Cells released from cell/alginate hydrogel construct using sodium citrate solution
Fully fabricated cell/alginate hydrogel tubes	N/A	✓	✓	✓	✓	✓
Controls	No $CaCl_2$ cross-linking step	✓	✓			✓
	No $CaCl_2$ cross-linking + no sodium citrate release steps	✓	✓			
	No $CaCl_2$ cross-linking, no sodium citrate release step no pelleting, resuspension in culture media + mixing with alginate solution	✓				
	Cells harvested only - no further manipulations					

Figure 7.4

Experimental design array for examining the effects of omitting different unit operations required to form a cell/hydrogel construct on A7r5 immortalised rat smooth muscle cell viability.

with cell/alginate hydrogel tube *in situ*, of approximately 1.5 ml. Thus the 1.5 ml wash step approximately reduced the calcium chloride to 50% of its original strength i.e. approximately 3.7 $mmolL^{-1}$, (taking into account the 1.6 $mmolL^{-1}$ of calcium ions in the supplemented media). It is surprising therefore that this level is compatible with a high level of cell survival i.e. over 3x the physiological level of free calcium ions. Cell survival is in part due to calcium ions being involved in the cross-linking of the hydrogel, plus a number being bound to proteins e.g. FBS and thus since no longer in a free ionic form unable to enter the cell and cause damage, much the same way as albumen in human plasma acts as a reservoir of bound calcium ions. The binding of calcium ions to plasma proteins *in vivo* renders the calcium ions physiologically inactive. Only when they are released are they again biologically active.

Further work on this area needs to include the crucial experiments to quantifying where the calcium ions are i.e. what percentage are free and therefore physiologically active and what percentage are protein bound or alginate bound and therefore physiologically inactive. The 12.5 ml and 125 ml wash steps represent a 6.8 fold and 75.6 fold dilution of the calcium ions since the wash was a single continuous flow through the device. This approximation again takes into account the calcium content of the media. The resulting calcium ion concentrations for the 12.5 ml and 125 ml wash step were; 2.2 $mmolL^{-1}$ and 1.7 $mmolL^{-1}$ respectively. However, their flow rates were higher than 6.25 $mlmin^{-1}$ for the 12.5 ml wash volume and 8.33 $mlmin^{-1}$ for the 125 ml wash volume. Investigation of flow rate may therefore also be an important factor for cell survival.

7.4 Effect of media composition on cell survival and proliferation

It was suggested by an early collaborator, Dr Clare Seldon (Department of Medicine, Royal Free Hospital, Hampstead, Middlesex, UK) that the choice of media was a critical factor in encapsulated cell survival. This opinion was based upon her extensive research on encapsulated liver cells for extracorporal liver assist devices (Seldon *et al*, 1998 and Seldon *et al*, 1999 and Seldon *et al*, 2000 and Khalil *et al*, 2001). The suggestion was to use αMEM with ribonucleasides and deoxyribonucleasides (Gibco-BRL, Gathersburg, Maryland, USA) with DMEM (Dulbecco Modified Eagles's Medium with 4.5 gL^{-1} glucose and without L-glutamine) as a control. The respective media were used throughout one or other arm of the experiment i.e. cell suspension prior to mixing with alginate solution, as wash media and culture media during the incubation phase with, in one instance, daily refeeds of fresh media (following removal of the spent media).

Two different alginates were chosen for this particular experiment namely Fluka (alginic acid salt from brown algae - Fluka, St.Gallen, Switzerland) and Sigma (high viscosity alginic acid from macrocystic pyrifera [Kelp] - Sigma, St.Louis, Missouri, USA).

In order to have a comprehensive study, two three-dimensional structure types were constructed; discs from tubes and beads. Discs of 7 mm in diameter, were made from tubes as per Section 3.4.3 and beads were produced as per Section 3.4.2. Overall there were six experimental conditions, all using 1% alginate weight/volume solutions. See Figure 7.5 for an overview of the experimental matrix.

Experimental observations were carried out over a 16 day period, the viability results are graphically represented in Figure 7.6 (cell proliferation over time) and Figure 7.7 (cell viability over time). Both graphs demonstrate the same general trends regardless of the experimental conditions. On day zero, i.e. immediately post fabrication of the constructs, all the experimental conditions had cell viabilities greater than 90% using 0.1 M sodium citrate solution (Sigma, St.Louis, Missouri, USA) to free the cells and the trypan blue exclusion assay to assess viability. However, after this initial time point, all the constructs in both αMEM and DMEM media underwent a near exponential decline in viability until by day 16 the survival range was less than 10% for all the experimental conditions. Over this 16 day period, in a highly similar manner to the experiment described in Section 7.2, no cell proliferation was observed with the individual beads containing a constant number of cells (approximately 10,000 - 12,000 cells per 2.2 cm in diameter bead).

There was, however, a difference in the rate of decline between experimental conditions using αMEM and DMEM. Cells in DMEM suffered a far faster rate of death (i.e. membrane disruption) than the cells in αMEM. Interestingly the Sigma beads undergoing daily refeeds with αMEM performed far worse than all the other experimental conditions, and not better as was hoped.

In conclusion, αMEM did reduce the rate of cell death, but did not prevent it nor did it trigger cell proliferation. Dr Clare Seldon had found αMEM to provide the ideal survival and proliferation media for hepatocytes encapsulated in alginate (Seldon *et al*, 1998 and Seldon *et al*, 1999 and Seldon *et al*, 2000 and Khalil *et al*, 2001), however, it appeared not to be the solution for the immortalised rat smooth muscle cells, A7r5. Both liver cells and smooth muscle cells have been reported to form spheroids (Bjorkerud *et al*, 1994).

The disc from the tube leg of the experiment performed in a fairly average manner with respect to the beads. It was thought that using a disc with a maximum thickness of 250 μm might fare better than a 2.2 mm diameter bead i.e. 0.125 mm versus 1.1 mm for mass transfer at the very centre of the construct.

7.5 Conclusions

Overall, despite an extensive literature on the successful encapsulation in alginate of a very

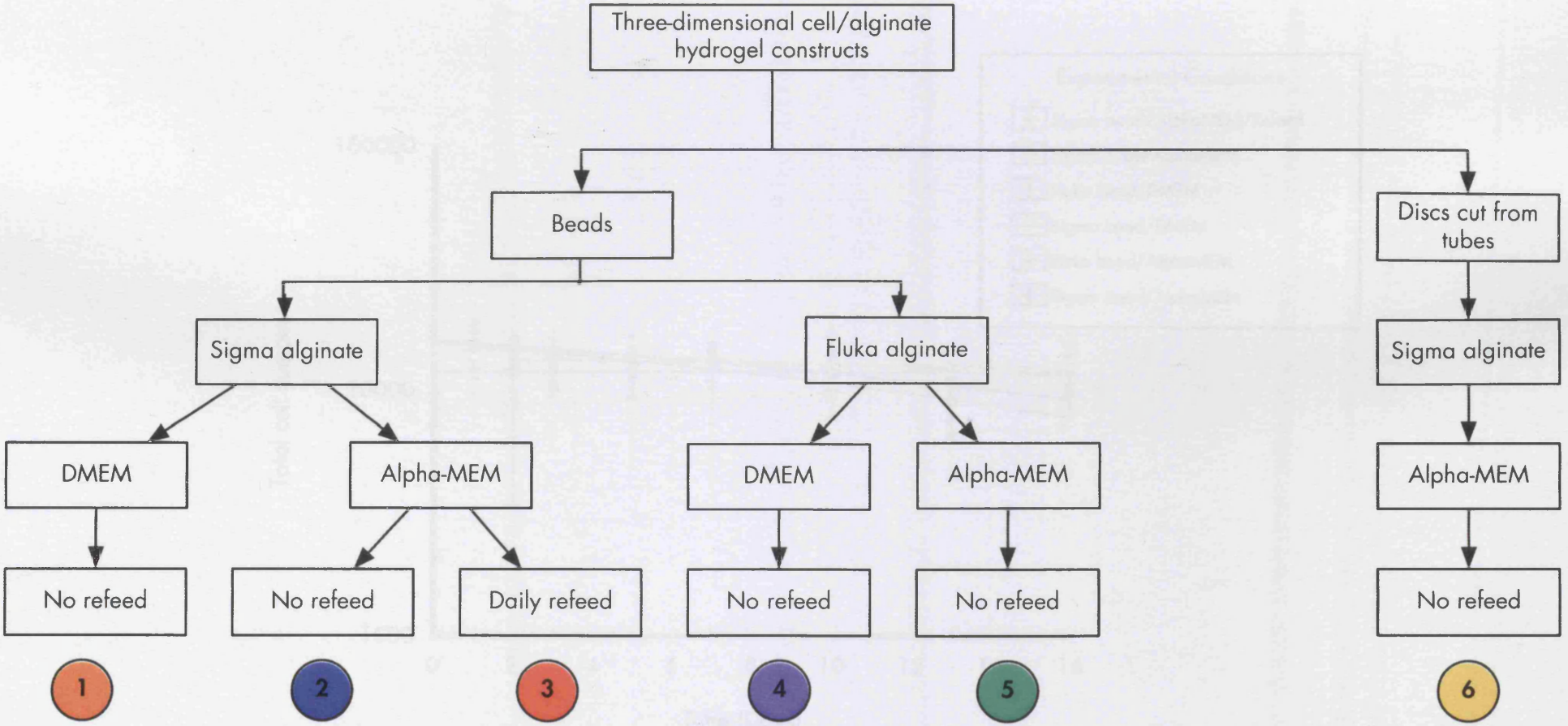

Figure 7.5

Overview of the six different experimental conditions with the different constructs, alginates, media and refeeding regimens (Colour coding of the six conditions as per Figures 7.6 and 7.7).

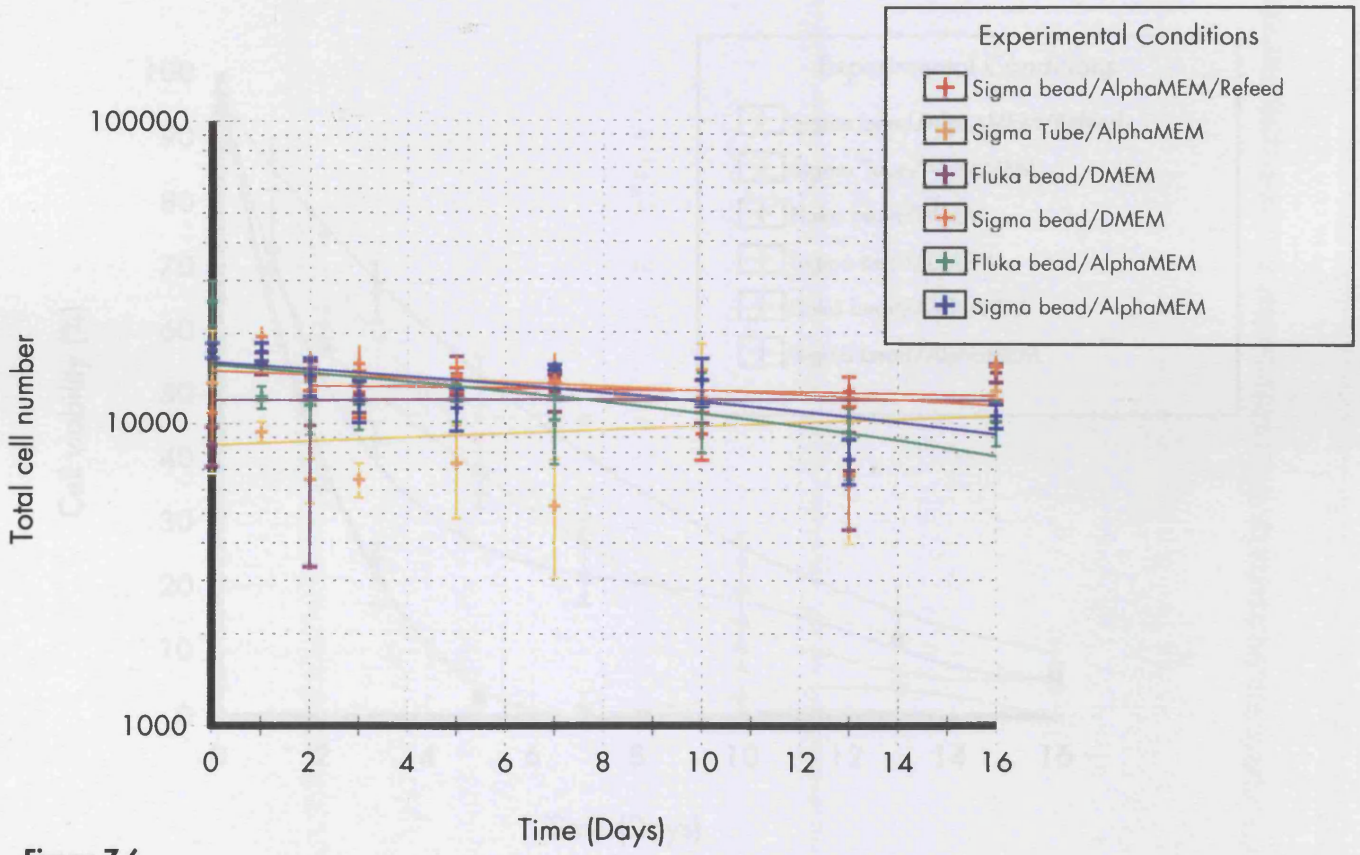

Figure 7.6

Total A7r5 immortalised rat smooth muscle cell number for 6 different experimental conditions with different constructs, alginates, media and refeeding regimens.

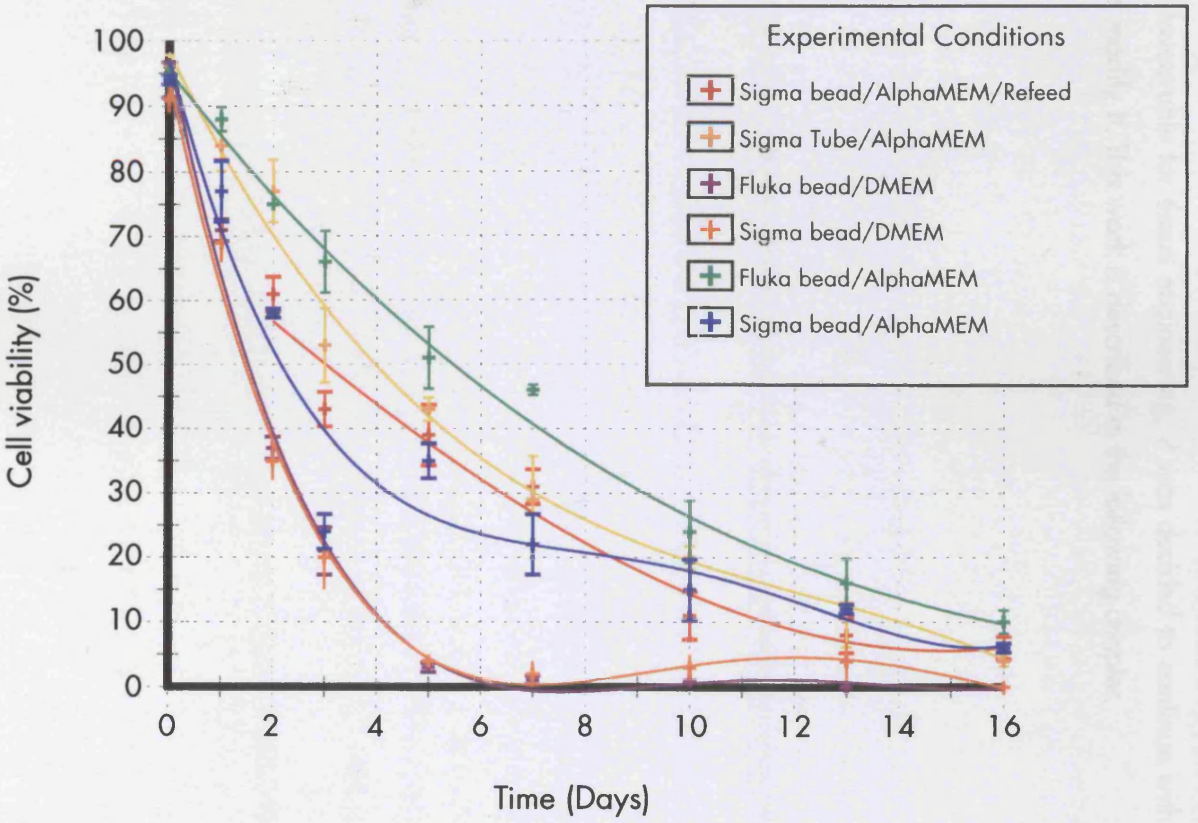

Figure 7.7

A7r5 immortalised rat smooth muscle cell viability for 6 different experimental conditions with different constructs, alginates, media and refeeding regimens.

wide range of mammalian cell types, it was concluded from the above research that alginate was not able to support either A7r5 immortalised rat smooth muscle cell or the human adult mesenchymal stem cell attachment, which is considered an essential prerequisite for their survival in both two and three-dimensional constructs. It is possible that the rat cell line may not be truly representative of non-immortalised human cells (although the A7r5 cells attached easily to tissue culture flasks), additional experiments with human explant vascular smooth muscle cells would resolve this issue. Overall, since alginate did have many of the properties deemed favourable for tissue engineering, it was decided to continue with alginate but to chemical modify it. This work is described in the following chapter.

8.0 Controlling cell-alginate interaction

From the data in Chapter 7, it became apparent that alginate hydrogels could not support smooth muscle cell activity. Other researchers have observed the need for alginate to be modified in order for the final hydrogels to have cell attachment sites (Smentana, 1993). The introduction of anchorage sites within the hydrogel scaffold is required to promote not only attachment, but cell migration, proliferation and specific gene expression (Hynes, 1992, Yagi *et al*, 1993, Price, 1997 and Rowley *et al*, 1999). Furthermore due to the hydrophilic nature of alginate, cell adhesion molecules from the culture medium are also unable to become deposited on the alginate's surface - a process known to facilitate anchorage dependant cell attachment (Smentana, 1993).

One recent example is by Chung in South Korea (Chung *et al*, 2002). Chung reacted galactosylated chitosan with alginate forming a highly porous three-dimensional sponge which provided specific cell attachment sites for hepatocytes. Galactose is know to be a specific adhesive ligand for the asialoglycoprotein receptor found on the surface of hepatocytes. Hepatocytes like smooth muscle cells are also anchorage dependent cells.

Smooth muscle cells when harvested from the T150 flasks, using trypsin as described previously in Chapter 3, became spherical in shape i.e. balled-up cells. If placed back in a T150 flask with media, over the first 6 hours the balled-up cells will attach and spread out into a more smooth muscle "spindle" shape morphology. This occurs because the commercially available T-flasks are either pretreated with a thin layer of suitable material to encourage cell attachment e.g. collagen, fibronectin, poly-D-lysine (Bicoat T150 flasks, Beckton Dickinson, Bedford, MA, USA) or made negatively charged and hydrophobic (Corning, Corning, New York USA).

It is interesting to note that several authors have observed this balled-up appearance for other attachment cells prior to observing proliferation within alginate hydrogels e.g. fibroblasts (Shapiro and Cohen, 1997). However, unlike fibroblasts, neither smooth muscle cells nor adult mesenchymal stem cells have been observed to proliferate or to produce extracellular matrix whilst in their balled-up state during the course of this project. One possibility is that vascular smooth muscle only rarely proliferates in a three-dimensional construct/tissue and then only as part of a pathological process (e.g. atherosclerosis) (Gordon *et al*, 1990). Furthermore even in pathological processes e.g. neointimal hyperplasia after vascular injury, cell hypertrophy (increase in individual cell size) rather than hyperplasia (increase in cell numbers) is observed. Likewise *in vivo*, human mesenchymal stem cells when entrapped in a tissue requiring repair/regeneration only demonstrate clonal expansion "under a strong and persistent selective pressure", furthermore such replication is "known to be infrequent and a

slow event" (Wang *et al*, 2002 and Preston *et al*, 2003).

Attempts in the present study to overcome this lack of attachment sites on the native alginate included seeding at maximal cell density, adding known cell attachment polymers to the alginate prior to setting and modifying the alginate by adding specific cell attachment sites.

8.1 Increasing the cell density

The rationale for increasing cell density is that if the density of cells were high enough then cell-cell contact would be achieved homogeneously throughout the cell/hydrogel construct. Close virtual cell-cell contact is the normal arrangement through out the human body at all stages in human development. For tissue engineering this approach has a great advantage, namely reduced construct growing times. Bulking patients' cells up to high numbers is already a commercially automated process e.g. Cellmate and SelecT (The Automation Partnership, Royston, Hertfordshire, UK). There are currently in excess of 70 Cellmates employed worldwide. Using very high densities of cells initially to fabricate the construct would reduce the need for cell proliferation within the matrix therefore potentially reducing the period for which the construct needs to develop. Furthermore, since it is highly desirable to have the polymer creating the scaffold totally removed prior to implantation in the body, having more cells and therefore less alginate for a given volume also is an advantage. Finally, more cells could potentially produce increased volume of extracellular matrix earlier, thus reducing the structural demands upon the scaffold and again potentially reducing the amount of scaffold polymer required in the initial construct.

The difficulty in the laboratory is in producing adequate cell numbers using typical laboratory T-flasks and incubators. In reality the maximum cell densities achievable were 10^8 cells per ml of alginate. No improvement in cell elongation and proliferation was seen at this order of magnitude and higher orders were not practical. It is, however, an area of research that does require further investigation because of the advantages listed above plus recent research has suggested that in terms of thickness, the number of cells that individual blood vessels are composed of at birth is retained throughout life. It is therefore possible that this may be true in tissue engineering i.e. that for a certain cell density no further cell proliferation is possible.

Interestingly, since the above work was performed, Cohen's group has demonstrated that the more dense the seeding of hepatocytes in alginate mats, the better the cells survive and proliferate. For example, a change from a cell seeding density of 0.28×10^6 cells cm^{-3} to 5.7×10^6 cm^{-3} resulted in a change from almost total cell death by day 7, to maintained viability for the same time period in the denser seeded mat (Dvir-Ginzberg *et al*, 2003). Likewise Osiris Therapeutics (Baltimore, MD, USA) have demonstrated that increased MSC seeding densities leads to increased contact inhibition of proliferation and increased cartilage (extracellular

matrix) production suggesting that the MSCs were exhibiting a chondrogenic commitment. The suggestion made was that there is an inverse relationship between proliferation and differentiation (Kavalkovich *et al*, 2004)

8.2 Adding cell attachment polymers to the alginate solution

If alginate lacks cell attachment sites, then one option is to mix the "inert" alginate solution with a cell friendly polymer which naturally contains such sites. Similar work with collagen and other extracellular molecules incorporated into various hydrogels has previously been attempted (Carbonetto *et al*, 1982, Woerly *et al*, 1993 and Civerchia-Perez *et al*, 1980). Type I collagen was chosen for this project, since it is a liquid and therefore could be easily mixed with alginate and is already extensively used in tissue engineering e.g. Weinberg *et al*, 1985. Collagen is also phylogenetically well preserved and there is little human immunological response to animal collagens, hence the FDA approval of bovine collagen as the scaffold material for Apligraf (Organogenesis, Canton, Massachusetts, USA). Alginate composites have previously been produced using hyaluronic acid combined with alginate. These gels were prepared by allowing calcium ions to diffuse into homogeneous acid/alginate mixtures. Overall, the mechanical strength of the alginate was improved, but no cell interaction studies were performed (Oerther *et al*, 1999a and Oerther *et al*, 1999b).

8.2.1 Collagen only matrices

Initial experiments were performed using collagen only in order to assess the ability of the immortalised rat smooth muscle cells to proliferate in a three-dimensional collagen structure. Later experiments involved the homogeneous mixing of the alginate and collagen prior to setting.

Type I collagen extracted from rat tail (First Link (UK) Ltd, Brierley Hill, West Midlands, UK), was selected on the basis that this particular supplier's collagen was starting to be investigated by other groups, including Professor Sir Magdi Yocoub's group at The Heart Science Centre, Harefield Hospital, Middlesex, UK. However, these groups were using the collagen as dry mats and then adding cells similar to the original work of Bell in the 1970's and 1980's (Coulomb *et al*, 1984). Instead, the experiments performed for this project involved adding the cells directly to the collagen and then setting the cell/collagen construct prior to adding cell culture media and incubation. On this occasion for the purposes of clarity, the experimental method for this bank of experiments is described below (rather than in the materials and methods chapter - Chapter 3) since the reasoning, methodology, chose of reagents and results are extremely intertwined.

The rat tail type I collagen was supplied sterile (chloroform treated) and pre-dissolved in

acetic acid (0.6%) in order to keep the pH below 7, since above pH 7 the collagen will set, i.e. adding alkali causes the collagen to cross-link and thus retain its shape. However, unlike alginate, the cross-linking process takes minutes allowing further mixing and manipulation of the collagen before final setting is achieved. The concentration of collagen in each batch was in the order of 2 $mgml^{-1}$ with interbatch variability approaching +/- 10%. Typically a collagen sheet was produced by initially adding 400 µL of collagen solution to 50 µL of 10x Eagles Minimum Essential Media (EMEM) (BioWhittaker, Walkersville, Maryland, USA) and homogeneously mixed using a pipette. The 10x concentration media was employed for 2 reasons. Firstly, to arrive at the correct concentration for the final solution volume of approximately 500 µl thus producing suitable media and pH conditions for the cells. Secondly, the EMEM contains a pH indicator, phenol red. Phenol red at the correct concentration i.e. a final concentration of 1x, allowed the careful titration from the initially bright yellow i.e. acidic collagen solution to bright pink as the solution became more alkali due to the controlled addition of 1 M sodium hydroxide solution (Sterile filtered - Sigma, St. Louis, Missouri, USA), thus allowing the collagen to cross-link. Care must be taken not to exceed a pH of 7 since at higher pHs collagen will also not set. The final titration point was taken to be where a permanent colour change to pink occurred. In order to determine the exact volume of sodium hydroxide solution required to set the collagen but not to overshoot, different volumes of 1 M sodium hydroxide solution were placed in the wells of 24 microwell plates (Corning, Corning, New York, USA), (range 37.5-50 µL in 2.5 µL steps) prior to adding 450 µL of collagen/ EMEM mixture and then again thoroughly mixing. Immortalised rat smooth muscle cells A7r5 had been harvested as previously described, centrifuged into a pellet, the supernatant removed and then resuspended in supplemented media containing 10% FBS (BioWhittaker, Walkersville, Maryland, USA), 60U penicillin ml^{-1} combined with 60 µg streptomycin per ml (BioWhittaker, Walkersville, Maryland, USA) plus additional glucose (Sigma, St. Louis, Maryland, USA) to a final concentration of 3.3 $mgml^{-1}$. To each collagen/EMEM/NaOH mixture was added 50 µL of the cell/αMEM or cell/DMEM suspension. The resulting solution in each well was homogeneously mixed using a fresh pipette prior to placing the microwell plate in a 37°C incubator with 10% CO_2 for 10 minutes in order to accelerate the collagen setting process plus to provide a more favourable environment for the cells. The initial concentration of the rat tail collagen was 2.16 $mgml^{-1}$ (0.216% weight/volume), after dilution with EMEM, cells and sodium hydroxide solution the final concentration was in the order of 1.6 $mgml^{-1}$ - i.e. 0.16% weight/volume (c.f. the typical alginate experiment of 0.5-6% alginate dry weight/volume). This concentration of collagen was similar to the concentration used by Organogenesis to provide the bovine collagen scaffold for Apligraf (Kemp, 2003b). The cell density in the collagen sheets prior to setting was 10^6 cells ml^{-1} i.e. identical to previous alginate experiments, therefore each well had an estimated cell volume of 0.5 x

10^6. By comparison the density of 10^6 cells ml^{-1} was approximately four times that used to make Apligraf. Interestingly once the cells were seeded, the Apligraf construct was reported to contract to a volume of approximately 10% of its original size i.e. giving a collagen density of 16 $mgml^{-1}$ and a cell density of approximately 3.75×10^6 per ml. The disproportionate increase in cell density was due to a proliferation rate of approximately 1.5 cell population doublings over the 7 day period (Kemp, 2003b).

After cross-linking of the collagen in the microwells was complete, 1 ml of supplemented media was added to each well. Like alginate, set collagen is transparent thus allowing easy visualisation of the encapsulated cells using light microscopy. Control microwells with no collagen/EMEM/NaOH were seeded at a density of 9.6×10^3 cells per microwell and again made to up a final volume of 1 ml per well with the supplemented αMEM or DMEM. From previous range finding experiments without cells, it was known that 1 M sodium hydroxide in the range 37.5-50 µL was adequate (but not excessive) to set the 450 µL of collagen/EMEM solution. The addition of the cells to the mixture made no difference to the setting, however, it was observed that different sodium hydroxide volumes did result in gels of different physical characteristic and morphology when viewed using light microscopy. A summary of the results is given in Figure 8.1. In all the microwells, by the end of the first twenty four hours, the balled-up smooth muscle cells had elongated throughout the encapsulation matrix. These day 1 results suggest that the cells are not unduly harmed during the scaffold fabrication process including the range of pHs (6.5 - 12) that the cells are initially exposed to on the addition to the collagen/EMEM/NaOH solution for approximately 15 minutes during the mixing and setting phase prior to the addition of the 1 ml of supplemented αMEM or DMEM which retained its red colour throughout the process, i.e. confirming the cultures were within an acceptable physiological pH range. On day 1 there was no visible shrinkage of the collagen. However, by day 3, shrinkage had become evident at the lower sodium hydroxide setting concentrations and especially in the 37.5 µL sodium hydroxide set scaffold. Shrinkage would appear also to compromise the ability of the sheets to retain the cells in their elongated state, the scaffold appeared to have collapsed leaving the cells without a firm structure to attach to. Possibly this observation reflects that the cells were too vigorous in their attachment and elongation and the scaffold was too weak because the cells physically collapsed the scaffold as they tried to elongate - a possible mismatch (a similar problem has recently been reported by Langer's group involving human embryonic stem cells and Matrigel (Levenberg *et al*, 2003). Interestingly at the higher sodium hydroxide concentrations, whilst shrinkage was not observed, the cells also return to their balled-up state, again possibly suggesting that the collagen sheet had lost strength possibly due to excess alkali. Overall the optimum setting conditions appeared to have been in the range 42.5 - 45.0 µL of sodium hydroxide

Time point	1M NaOH volume (µL)	pH prior to addition of cells/medium	Cell-collagen sheet characteristics	Cell morphology
Immediately post fabrication	37.5	6.5	Fully set construct with same diameter as microwell - i.e. no shrinkage	Round balled up cells distributed through out the construct
	40	6.8		
	42.5	9.0		
	45	10.5		
	47.5	11.5		
	50	12.0		
Day 1	37.5	6.5	No change from immediately post fabrication	Cell elongation - smooth muscle appearance
	40	6.8		
	42.5	9.0		
	45	10.5		
	47.5	11.5		
	50	12.0		
Day 3	37.5	6.5	Shrinkage +++	Returned to balled up state
	40	6.8	Shrinkage +	
	42.5	9.0	No change from immediately post fabrication	Remain elongated
	45	10.5		
	47.5	11.5		
	50	12.0		Balled up
Day 5	37.5	6.5	Shrinkage +++	Balled up
	40	6.8	Shrinkage ++	
	42.5	9.0	Shrinkage +	
	45	10.5	No change from immediately post fabrication	Elongated
	47.5	11.5		
	50	12.0		Balled up

Figure 8.1

Summary of results for cell-collage constructs using different quantities of collagen setting agent - 1M NaOH solution.

solution. Having established that the A7r5 rat smooth muscle cells were capable of spreading within a three-dimensional sheet of rat collagen the experiment was repeated except with the substitution of varying amounts of collagen solution for alginate solution.

8.2.2 Composite collagen-alginate matrices

Composite collagen/alginate gels were produced using 4% alginate (Fluka, St. Gallen, Switzerland) in physiological saline prepared in solutions in order to arrive at a final concentration of 1% alginate in the final composite gel. However, the option of a higher concentration stock solution for the collagen was not available and hence the final collagen concentration in the final composites was reduced from the previous 1.6 $mgml^{-1}$ to 1.25 $mgml^{-1}$ (a 21.9% reduction). In order to minimize the reduction in collagen composition the volume of αMEM or DMEM media used to resuspend the pelleted cells after harvesting fully was minimized. Finally, to achieve setting of the composite polymer it was necessary to perform the various cross-linking steps in a very precise order, as all other combinations proved not to work.

The only order of adding the individual components found to produce a set collagen/alginate scaffold containing cells was: collagen solution, 10x EMEM, 4% alginate solution, sodium hydroxide solution, cells in supplemented αMEM media and finally calcium chloride solution once the collagen had set. Prior to adding each component except the calcium chloride solution (as this would have disrupted the freshly set collagen gel) thorough mixing was performed using a pipette in order to produce homogeneous mixtures. The final composition had a ratio of dry alginate powder:collagen protein of approximately 8:1. Thus the majority of the construct was alginate with the collagen acting as a fortifying agent.

This final mixture resulted in a rat cell density of 4.2×10^5 cells ml^{-1}. 300 μL samples of this final mixture was placed into individual microwells, resulting in each well containing an estimated 1.3×10^5 cells. The microwell plate was then placed into a 37°C incubator with 10% CO_2 for 10 minutes in order to set the collagen solution. Finally 1 ml of calcium chloride cross-linking solution was added to each well for a further 10 minutes. Calcium chloride solutions at different concentrations (0.1%, 0.5% and 1%) in physiological saline were used. After 10 minutes the calcium chloride in physiological saline was carefully removed using a pipette and replaced with 1 ml of supplemented media for a further 10 minutes in order to dilute the remaining calcium chloride solution and buffer the excess 1 M sodium hydroxide solution prior to it being drawn off and replaced once again with fresh supplemented media (αMEM or DMEM).

The controls consisted of either identical mixtures except supplemented DMEM media or physiological saline was added in place of the calcium chloride solution (since physiological

saline was used to make up the calcium chloride solutions), or cells were seeded into the microwells with no composite scaffold components present. Cells were seeded at a density of 1.3×10^5 per well. All the wells had a final volume of media of 1 ml. The microwell plates were finally returned to the 37°C humidified 10% CO_2 incubator. The morphological progress of the cells and scaffold shrinkage was observed as before using simple light microscopy.

On day 1, cells in both the controls (supplemented media, physiological saline) were no longer balled-up but elongating in the same manner observed in the previous collagen only scaffold experiment. The 0.1% calcium chloride cross-linked scaffold exhibited a small minority of cells which were elongated but the vast majority remained balled-up. In both the 0.5% and 1% calcium chloride cross-linked scaffold, all the cells remained balled-up. Repeat observations over a 2 week period revealed no change from the day 1 cell morphology observations, except cell proliferation was observed in both the control conditions - see Figure 8.2. Shrinkage over the time course was only observed in the scaffolds not exposed to calcium chloride cross-linking agent (i.e. the controls with physiological saline or supplemented media) and this was only observed from day 10. However, the shrinkage observed was minor compared to the shrinkage observed in the lowest concentration sodium hydroxide cross-linked collagen only sheets produced in Section 8.2.1. An extended version of this experiment (20 days) was later carried out with similar results including extensive cell attachment, elongation and proliferation in the control collagen-alginate sheets - see Figure 8.3.

Calcium chloride solution (at any concentration between 0.1% -1%) would therefore potentially appear to act in two different areas:

1. To have a protective factor with respect to composite scaffold shrinkage. Shrinkage would therefore not appear to be a factor when considering why the higher (0.5% + 1%) calcium chloride solution cross-linked scaffolds failed to show cell elongation
2. To have an adverse effect with increasing concentrations of calcium chloride solutions on A7r5 cell attachment, elongation and proliferation despite the presence of "cell friendly" collagen within in the composite matrix material

The experiment did, however, possibly suggest that at low calcium chloride concentrations (0.1%) it was possible to fabricate a collagen/alginate composite scaffold with embedded cells with some degree of success i.e. a small minority at the cells left their rounded-up state post harvesting and spread out/elongated into the surrounding composite matrix with similar morphology to the cells in the collagen only scaffold. However, following elongation no cell proliferation was observed.

The results possibly suggest that alginate is an inert player i.e. it does not behave in

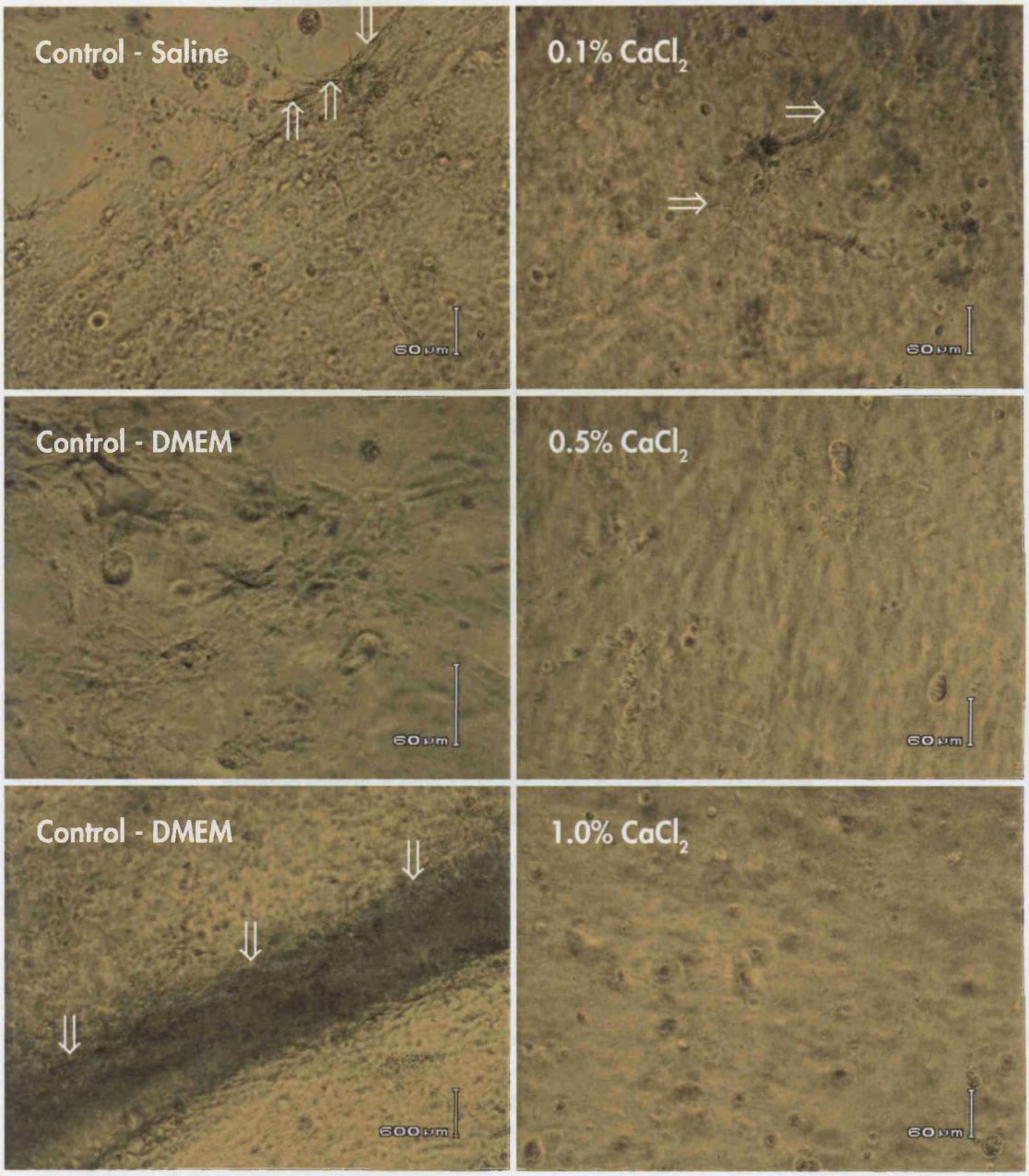

Figure 8.2

Collagen-alginate matrices - Day 14 results.

The control conditions demonstrated good cell attachment and elongation for the A7r5 immortalised rat smooth muscle cells in the collagen-alginate matrix. Under the control conditions, only a few balled up cells were seen whilst the majority were elongated within the matrix. However, the 0.1% $CaCl_2$ condition showed only a very small number of cells making attachment and elongation (⇒). Cell-matrix interaction was not seen at the higher $CaCl_2$ concentrations where all the cells remained balled up. The progressively receding edge of the collagen-alginate hydrogels can be clearly seen in the control conditions images (⇓) as too can be seen the elongated cells which appeared to be attached to both the gel and the exposed surface of the microwell thus straddling the gap (⇑).

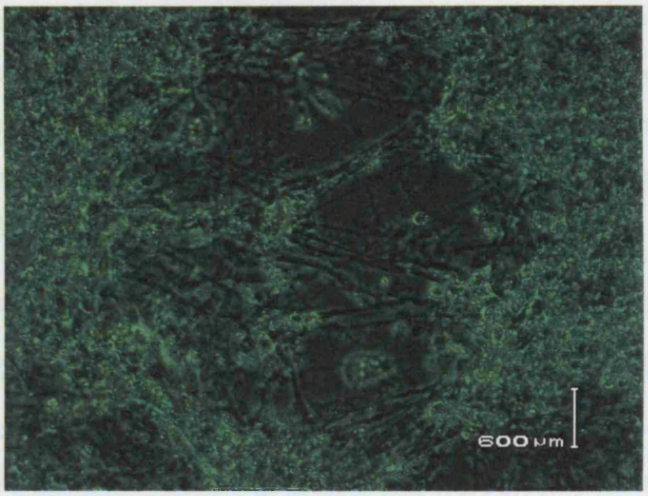

Figure 8.3

Collagen-alginate matrix - Day 20.

A typical example of the high level of interaction observed between the A7r5 immortalised rat smooth muscle cells and the collagen-alginate matrix in the absence of $CaCl_2$ solution being added to the set hydrogel prior to the wash stage of the fabrication process. Attachment, elongation and migration can be observed in the image, whilst evidence of proliferation can be inferred from the high number of cells present relative to the original seeding density of 4.2×10^5 ml^{-1} of matrix.

a deleterious way towards the rat smooth muscle cells. The provision of attachment sites is evidently of real benefit in order to coax the smooth muscle cells into spreading out in the scaffold - the first step on the way to possible proliferation. However, the experiments had demonstrated the complexity of fabricating cell/scaffolds using an alginate/collagen composite. This complexity did not lend itself to the tube device process which was already progressing well in parallel towards making consistent tubular constructs using just alginate solutions. The experiment demonstrated that the A7r5 immortalised rat cells were not of an abnormal phenotype which was incapable of elongating in a three-dimensional scaffold due to, for example, the immortalisation technique or extended culturing they had undergone. It was therefore decided that having established that A7r5 were capable of elongation when encapsulated inside a three-dimensional structure the logical way forward would be to not use a composite but to chemically modify the alginate (i.e. return to a single polymer but one which was modifiable readily to allow cell attachment).

8.3 RGD-alginate scaffolds

Whilst alginate solutions with their rapid cross-linking times were ideal for tube and bead formation, their lack of cell attachment properties was a major disadvantage. Keeping the alginate in a solution was an absolute prerequisite since a solution containing cells lends itself to the desired process of automation. It was therefore deemed necessary to modify the alginate such that it remained a liquid, unlike the collagen/alginate composites which required a "collagen-presetting stage".

8.3.1 GRGDY-alginate

The tripeptide arginine-glycine-aspartic acid (RGD) is a common sequence found in extracellular proteins e.g. collagen, fibrinogen and laminin. Cell-RGD adhesion is mediated by transmembrane cell surface receptors called integrins which recognise and bind directly to the RGD site. RGD not only controls cell attachment but also other important cell activities e.g. differentiation, by allowing the transduction of signals from the extracellular matrix to the interior of the cell. Pierschbacher and Ruoslahti were some of the earliest researchers to demonstrate the importance of RGD for the adhesion of anchorage dependent cells in tissue culture (Piersbacher and Ruoslahti, 1984). Because RGD is highly important in the process of cell adhesion, synthetic RGD motifs have been immobilised on a large number of inert polymers with the aim of making the resulting RGD-polymer cell friendly. Polymers which have been modified with RGD motifs include PTFE (Massia and Hubbell, 1991a, polyurethane (Lin *et al*, 1994), PEG (Drumheller and Hubbell, 1994), PEG-diacrylate (Mann and West, 2002) and PVA (Matsuda *et al*, 1989). The addition of the RGD motif to these inert synthetic polymers has led to cell attachment which would otherwise not occur or only occur to an

exceedingly limited degree.

A thorough literature search revealed that Mooney's group at the University of Michigan, USA, had successfully attached an GRGDY peptide covalently to an alginate using carbodiimide chemistry, cross-linked the derivatised alginate and then grown mouse skeletal myoblasts (skeletal muscle precursors) on its surface. The cells failed to grow on the unmodified control alginate (Rowley *et al*, 1999). Rowley and Alsberg later repeated a variant of this work in two subsequent paper, (Rowley and Mooney, 2001 and Alsberg *et al*, 2002), but again only demonstrated cells growing on the surface and not within the three-dimensional structure. Partly this was due to the method of cross-linking chosen i.e. instead of using calcium chloride solution which is extremely fast acting, Rowley used calcium sulphate as a water-based slurry directly added to the alginate. Calcium sulphate is very insoluble in aqueous solution unlike calcium chloride. The alginate solution/calcium sulphate slurry mixtures were then cast between parallel glass plates to set which took minutes/hours to complete i.e. not readily suitable for cell encapsulation since the cells would be exposed for a prolonged period to calcium sulphate, if encapsulated within the alginate/calcium chloride slurry.

It was therefore decided to modify the Mooney approach in order to retain the rapid calcium chloride cross-linking process which lay at the heart of the evolving tube making device.

For the preliminary GRGDY experiments the Rowley protocol was initially followed nearly exactly with only minor changes apart from the major change in the choice of cross-linking agent, but this proved to be totally unsatisfactory in that cells failed to perform any better than alginate alone either on the surface or in the three-dimensional structure. The basic protocol consisted of attaching cell adhesion ligands to the alginate backbone using carbodiimide chemistry.

Alginates are linear unbranched polymers composed of two different monomers 1-4-linked β-D-manuronic acid (M unit) and α-L-guluronic acid (G unit) - see Figure 8.4. Alginates are not random copolymers of M + G units, but, depending upon the particular type of seaweed they are derived, consist of blocks of G or M units or exactly alternating residues i.e. GMGMGM... It is the G units that are responsible for the cross-linking process with divalent ions such as calcium chloride, creating "ionic interchain bridges" and hence hydrogels between alginate chains. Using Rowley's protocol, alginate was chemically modified using a water soluble carbodiimide, 1-ethyl-3-(dimethylaminopropyl) carbodiimide (EDC) (Aldrich, Sleinheim, Germany), to activate the carboxylate groups on the G monomers, which were then able to react with the amine terminal of the cell attachment ligand (GRGDY - Gly-Arg-Gly-Asp-Tyr) to form amide bonds - see Figure 8.5. A co-reactant N-hydroxy-sulfosuccinimide (Sulfo-NHS) (Aldrich, Sleinheim, Germany) was used to stabilise the reactive EDC-intermediate

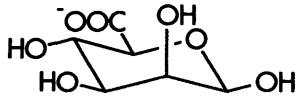

M monomer ($^4C_1$)

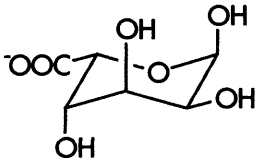

G momomer ($^1C_4$)

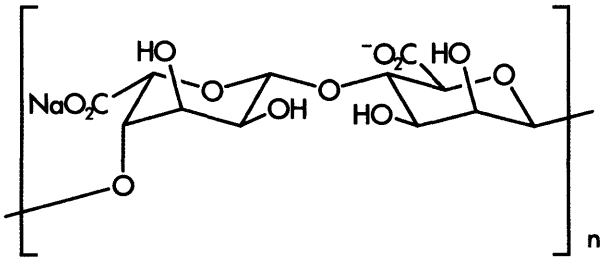

-M-G- polymer unit

Figure 8.4

Alginate M ((1,4) linked β-D-mannuronic acid) and G (α-L-guluronic acid) monomers and their covalent bonding within alginate polymer in an -M-G- repeat unit.

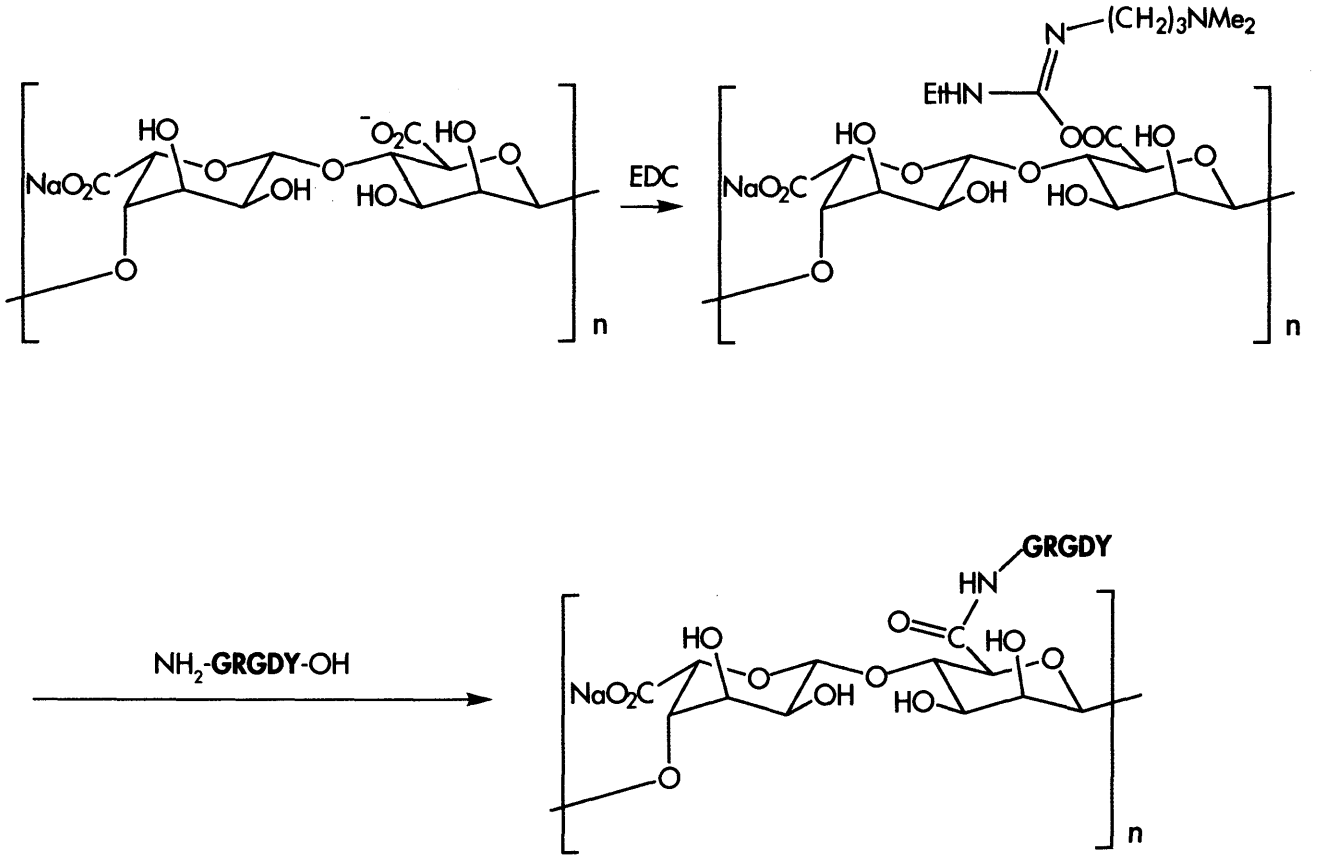

Figure 8.5

Covalent attachment of the pentapeptide GRGDY to a G monomer in an -M-G- repeat unit of alginate using carbodiimide chemistry.

The EDC reacts only with the G (α-L-guluronic acid) monomer to form an o-acylisourea intermediate (stabilised by the presence of sulfo-NHS) prior to reacting with the GRGDY pentapeptide.

(o-acylisourea) against a competing hydrolysis reaction thus improving the efficiency of the overall coupling reaction. Sulfo-NHS was used in preference to NHS since NHS is virtually insoluble but they behave identically with respect to their stabilising action.

The initial batches of the GRGDY peptide were synthesised with the help of Dr. Patricia Zunszain in the Department of Chemistry at UCL using a Millipore 9050 OM peptide synthesiser - Section 3.7. After the preliminary proof of principle experiments were successful, the peptide was purchased commercially from Neosystem Group SNPE (Strasbourg, France). This additional source provided the necessary total volume of peptide required to progress the project forward at a reasonable pace. The commercially supplied material was certified 95% pure and supplied in 11 mg lyophilised aliquotes in sealed glass vials.

Since sterility is vital, it was decided to check the reagents prior to derivitisation. In a preliminary experiment, peptide, Sulfo-NHS and EDC had all been made up under sterile conditions with WFI but not then sterile filtered. Alginate solutions had been autoclaved. To test the sterility of the above reagents, mammalian cell culture media was inoculated with freshly made samples of the above individual solutions and incubated at 37°C. At 4 days no growth was observed. However, as a further precaution it was decided to 0.2 μm filter the reagents (excluding the alginate) to ensure maximum possible sterility since future experiments would proceed for weeks and months, and 100% sterility was therefore absolutely essential. The alginate was not filtered since it was too viscous for a 0.2 μm filter also since it had been autoclaved and had never raised any sterility issues in previous experiments was considered sterile. The vast majority of experiments described in this thesis were performed with a batch of ISP Manugel DMB which upon autoclaving appeared to be rendered sterile, however, later batches of Manugel alginates were shown to contain a bacteria resistant to autoclaving. The resistant bacteria was purified with assistance from Dr. Vanya Gant and Mike Wren (Centre for Infectious Diseases, UCLH, London). The purified samples were sent to the Central Public Health Laboratory (Specialist and Reference Microbiology Division, Health Protection Agency, Colindale, London) for final identification. The organism was identified as Bacillus licheniformis. The reason for the later batches containing Bacillus licheniformis is unknown. Discussions with ISP failed to resolve the issue. The scientific literature contains reports regarding the effects of sterilisation on the properties of commercial alginates but not whether total sterility had been achieved (Leo *et al*, 1990, Vandenbossche *et al*, 1993 and Wong *et al*, 2001).

Bacillus licheniformis is a gram-positive, motile, spore-forming, anaerobic rod bacteria. It is well known to be thermophilic in nature (Alvarez-Macarie *et al*, 1999, Wu *et al*, 1993, De Bartolomeo *et al*, 1991 and Palop *et al*, 1996). Commonly found in soil where it leads a saprophytic existence it is also found in various human food products including diary

products (Chopra and Mathur, 1984). Information regarding Bacillus licheniformis in relation to human safety is however limited. Food poisoning by Bacillus licheniformis is well described (Mikkola *et al*, 2000 and Salkinoja-Salonen *et al*, 1999). Other pathologies are also described including persistent bacteraemia (blood poisoning), prosthetic aortic valve endocarditis and indwelling catheter infections (Hannah and Ender, 1999, Santini *et al*, 1995 and Blue *et al*, 1995). The ISP Manugel batches testing positive for Bacillus Licheniformis were either destined for the manufacture of food stuffs (batch number: 200792) or destined for the manufacture of pharmaceuticals (batch number 281011). Studies by Souw and Rehm have shown that Bacillus licheniformis isolated from alginate readily degrade alginate (Souw and Rehm, 1975). Spores of bacteria liceniformis have been reported to have temperature resistance of 135°C (Janstova and Lukasova, 2001) and hence the inability to achieve sterility with standard autoclaving (121°C for 20 minutes). Furthermore, this particular bacteria has been demonstrated to be resistant to a wide range of sterilisation techniques including microwaves (Wang *et al*, 2003).

The first derivitisation experiments were performed using 1% weight/volume solutions of Manugel DMB alginate as per Rowley (Rowley *et al*, 1999). After combining all the reactants, the solution was then rolled for 24 hours. All the reactions were carried out at room temperature in light protected containers. In order to remove excess reagents, the solutions were extensively dialysed (see Section 3.7.1). After dialysis, activated charcoal was added and mixed thoroughly prior to rolling for thirty minutes. Finally, in order to remove the charcoal plus any other impurities the solution was past through a ready prepared Celite Hyflo (acid washed diatomite filter aid - Celite, Lompoc, California, USA) column (sinter funnel) facilitated by a vacuum pump. This process took 3 - 6 hours depending upon the degree of agitation supplied to the mixture. The resulting solution was collected in a sterile flask and either stored immediately at 4°C or lyophilised using an Edwards Freeze Drier and then stored at 4°C. One other variation was to use polyethylene glycol (PEG) solutions (Slide-A-Lyzer concentrate solution - Pierce, Rockford, Illinois, USA) or PEG solid (35,000 MWt, Fluka, Buchs, Switzerland) to reconcentrate the dialysed samples to desired final concentrations, since during the prolonged dialysis, water would enter the dialysis tubing/ cassette thus diluting the alginate. Using serial measurements obtained by carefully drying and accurately weighing the dialysis tube or cassette, the final concentration of the alginate could be controlled - there was found to be a straight line relationship between time and water removed from the cassette (data not shown). Solutions of final concentration of either 1% or 2% were aimed at. This concentration step took 9 - 12 hours and was performed using a steady-state rocking table at approximately 10°C (purpose built cold room) in total darkness.

As with non-derivatised alginate, the GRGDY-alginate could be readily cross-linked with a 1% calcium chloride solution to form beads, sheets or tubes. Also these three-dimensional constructs could be easily dissolved using sodium citrate solution (Sigma, St. Louis, Missouri, USA).

Experiment were performed using exactly the same techniques to produce tubes, beads and sheets as were performed for the non derivatised alginates in Chapter 7. Subsequent examination of the constructs included, trypan blue exclusion assay, live/dead viability/ cytotoxicity kit (L-3224 Molecular Probes, Eugene, Orogon, USA), phase contrast microscopy, histology and cytology.

8.3.1.1 GRGDY-alginate sheets

GRGDY-alginate sheets were fabricated as per Section 3.4.1. All the initial sheet experiments with the ratio of alginate (dry weight):peptide:SulphoNHS:EDC of 1 gm:1 mg:38 mg:67 mg (i.e. as per Rowley (Rowley *et al*, 1999), failed to show any improvement over the standard non-derivatised alginate in terms of cell attachment to their surface. One difference was that the quantity of uronic acid in the particular alginate chosen, Manugel DMB (ISP, Tadworth, Surrey, UK) had to had be estimated. Manugel DMB is high in the G monomer (ISP data sheet) and therefore produces high strength gels. Rowley (Rowley *et al*, 1999) used ProNova MVG (Norway) which was also high in G residues, so it seemed sensible to start with the same ratio of reactants since Rowley had optimised the reagents for this particular alginate using radiolabelled ^{125}I-GRGDY as a tracer molecule. Therefore after the early experiments failed with Manugel it was decided to try two different approaches.

Firstly different alginates (including ProNova MVG) and in parallel different ratios of reactants were examined. Fluka alginate (Fluka, Buchs, Switzerland) was also tried as this had a good history in mammalian cell encapsulation. This was the alginate being used successfully by Professor Charles' group in The Wolfson Biomedical Research Institute, UCL to encapsulate modified hybridoma cells (Xu *et al*, 2002) with whom early work with tubes had been carried out. However, at the alginate:peptide:sulphoNHS:EDC (A:P:S:E) ratio of 1 gm:1 mg:38 mg:67 mg (1000:1:38:67) no attachment or elongation of cells was observed.

A series of experiments were undertaken to optimise the A:P:S:E ratio. Since there was uncertainty with respect to the exact uronic acid content of both the Fluka and the Manugel alginates, was decided to keep the SulfoNHS:EDC ratio as per Rowley (Rowley *et al*, 1999), but then to alter the other ratios. The experiments were repeated using Fluka standard grade and Manugel DMB alginates using the following A:P:S:E ratios: 1000:1:38:67, 1000:10:380:670 and 1000:50:1900:3350 which are abbreviated to 1x, 10x and 50x respectively - see Figure 8.6. The positive control used was cells seeded directly in microwells i.e. no alginate. The

	Reagent ratios - A:P:S:E ratios (weight/weight)			
Abbreviated name	Alginate (Dried powder) (A)	GRGDY peptide (P)	Sulpho-NHS (S)	EDC (E)
1x	1000	1	38	67
10x	1000	10	380	670
50x	1000	50	1900	3350
Negative control	1	0	0	0
Positive control (Cells seeded directly onto microwells)	0	0	0	0

Figure 8.6

Ratios of reagents (weight/weight) used to produce GRGDY derivatised alginates and the positive and negative controls.

negative control was unmodified autoclaved alginate i.e. no exposure to peptide, SulphoNHS or EDC. After derivitisation, the alginates were then lyophilised for 48 hours at -70°C at 10^{-1} mbar (Edwards Freeze Dryer Modulo with a Savant Two Stage VP100 vacuum pump). The derivatised alginate powders where then reconstituted in WFI (BioWhittaker, Walkersville, Maryland, USA) back to 1% final solutions. Sheets of the four alginates (negative control, 1x 10x and 50x) where formed in microwells (as per Section 3.4.1) including thorough rinsing with supplemented medium. Immortalised rat smooth muscle cells (A7r5) were added to each well at a density of approximately 3×10^5 cells per well. The media volume in each well was topped-up to a total of 1 ml with additional supplemented media. The microwell plates were placed in a 37°C, humidified incubator with 10% CO_2 atmosphere. The constructs were observed for 5 days using light microscopy.

The 1x and 10x performed no better than the negative control i.e. no elongation was observed over the 5 day period. However, the 50x demonstrated a small minority of cell attachment and elongation. Manual time interval photography revealed that in a minority of instances cells were elongating towards one another on the surface of the GRGDY-hydrogel and in one instance making actual contact across an initial 60 - 80 µL gap - see Figure 8.7. The positive control (cell/no alginate) cells attached and proliferated as normal.

The indentical experiment with the negative control, 1x, 10x and 50x derivatised alginates were repeated but omitting the lyophilisation step. This step was omitted as it was thought that the degree of control was insufficient with the Modulo Edwards freeze dryer e.g. no available temperature or moisture probes, therefore it was impossible to assess the extent of drying whilst in progress. Furthermore, this step was seen as a high risk for contamination e.g. bacteria. Leaving it out, however, meant that the derivatised alginates produced were considerably less than 1% dry weight/volume. Typically they were in the order of 0.5% due to the dialysis water being taken up by the dialysis tubing or cassette during the long dialysis phase of the process.

However, derivatised alginate sheets at approximately 0.5% were fabricated from 1x, 10x and 50x reagent conditions. This experiment demonstrated only at the 50x level a significant improvement in cell attachment and elongation in that it was now the majority of cells attaching and elongating. The 50x Manugel out performed the 50x Fluka derivatised alginate. Cell attachment and proliferation was similar in appearance to the positive control (cells/no alginate) i.e. appeared to be approaching 100% of the cells. The 10x alginates also demonstrated a weak degree of cell attachment and elongation (similar to the original 50x lyophilised alginate experiment).

Sheets were also made with derivatised Pronova MVG alginate (1, 10, 50x) i.e. the same

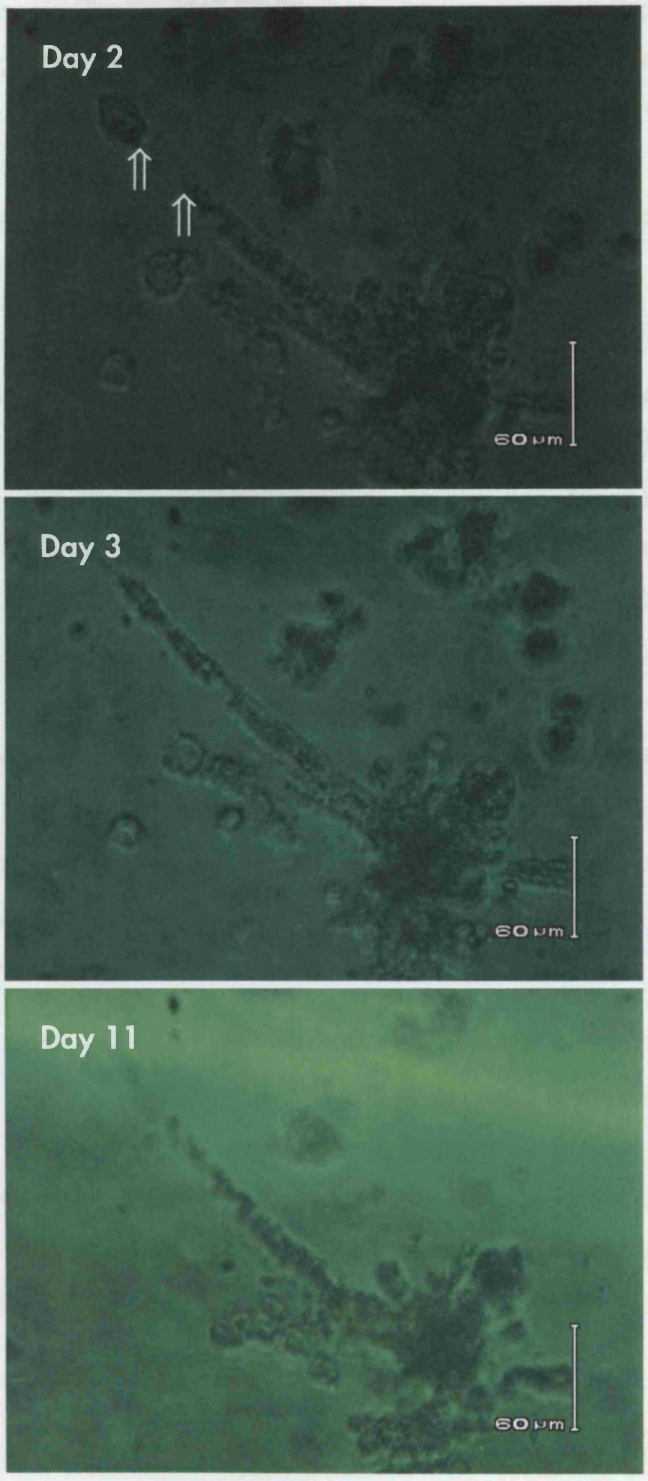

Figure 8.7

Cell interaction with GRGDY-alginate preformed sheet over an 11 day period.

Serial time-point images showing the interaction of A7r5 immortalised smooth muscle cells on a preformed sheet of 50x GRGDY-Fluka alginate gel. Two days after being seeded, cells can be seen to have attached and then to have elongated and migrated across a gap (⇑) and remain in location over a further 8 days.

alginate used by Rowley (Rowley *et al*, 1999). Again the lyophilisation step was omitted. Once again, the 50x performed best but with only a minority of cells attaching and elongating. The 10x also demonstrated a very small degree of biological activity, whilst the 1x and negative control showed no activity. In the positive control the cells attached and proliferated as normal. The differences between these results and Rowley's may have been due to alginate inter-batch variability.

Finally it was decided to explore if there was a difference between alginate with a high G content versus alginate with a high M content. Gels made with high G content tend to be far stronger than their high M counterparts, a factor which may well be crucial when fabricating larger tissue-engineered constructs. Sheets were made from derivatised Manugel DMB (high G) and Fluka cell culture grade (high M) alginates at the 1x, 10x and 50x concentration ratios. A representative selection of the results is contained in Figure 8.8 which shows the positive control (microwell plate - no alginate), 10x high G, 50x high G and 50x high M conditions. In the first 24 hours, the A7r5 cells were able to quickly interact i.e. attach, elongate and migrate on the sheets fabricated from 50x alginate regardless of whether the alginate was high G or high M in composition. At 10x concentrations the vast majority of the cells failed to attach and remained balled up. The 1x concentrations showed no evidence of cell interaction (data not shown). Overall the 50x high G Manugel DMB was observed to be better at interacting with the A7r5 cells.

In all the sheet experiments performed, attachment and elongation occurred in the first 12 - 24 hours after cell seeding. From these initial sheet experiments it was decided to discontinue any lyophilisation step until better derivatised alginates were produced i.e. excellent cell attachment in three-dimensional structures prior to lyophilisation. Then once good biological activity was achievable, to investigate the lyophilisation process further in order to retain the derivatised alginate's bioactivity.

8.3.1.2 GRGDY-alginate beads

As before in Chapter 7, in order to allow a wider range of experiments, beads were also manufactured with the derivatised alginates. The methods of bead production are described in Section 3.4.2. Experiments were either performed with the dilute derivatised alginate (i.e. immediately post dialysis) or with a more concentrated version following exposure to polyethylene glycol solution or solid to bring the concentration back to approximately 1% prior to adding the cells. A series of experiments were performed fabricating beads and sheets from the same batches of 1x, 10x and 50x derivatised alginates. Initially A7r5 immortalised rat smooth muscle cells were employed however after extensive studies there was no evidence that the A7r5 cells elongated when encapsulated in the GRGDY-alginate despite evidence of

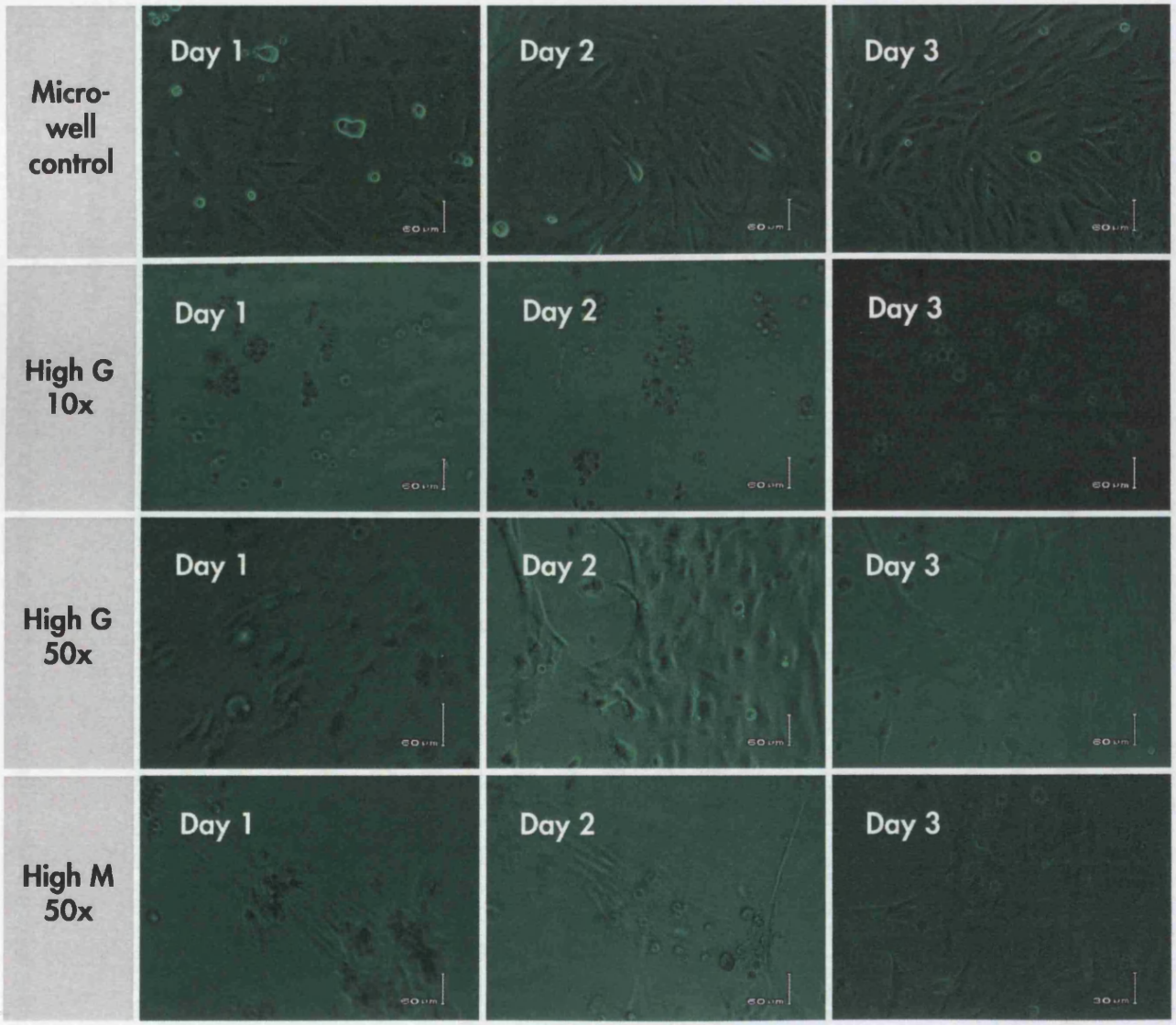

Figure 8.8

Comparison of derivatised alginates.

In the first 24 hours A7r5 cells were able to quickly interact i.e. attach, elongate and migrate on sheets fabricated from 50x alginate regardless of whether the alginate was high G or high M in its composition. At 10x concentrations the vast majority of cells failed to attach and remained balled up. The 1x concentrations showed no evidence of cell interaction (data not shown). Overall the 50x high G Manugel DMB was observed to be best at reproducibly interacting with the A7r5 cells.

good interaction between the A7r5 cells and the surface of sheets made from the same batch of matrix. The sheets and beads were fabricated one after another over the period of a few minutes. Some of the extended time course experiments were conducted with Julia Markusen (UCL).

Deploying human mesenchymal stem cells (c.f. immortalised rat smooth muscle cells) in the bead experiments, there was excellent correlation between cell interaction on the surface of the sheets and elongation and networking of the cells within the beads. Selected images from a typical MSC bead and sheet experiment are shown in Figure 8.9, in this experiment, derivatised alginate was compared directly with non-derivatised alginate in order to check whether MSCs could interact with non-derivatised alginate. In the first 24 hours MSCs were able to quickly interact with the Manugel DMB 50x GRGDY-alginate i.e. attach, elongate and migrate, on both the surface of the sheets and within the beads, whilst in the derivatised beads, intercellular networking can also be observed. On the non-derivatised alginate sheets there was no cell interaction, instead the cells were seen to aggregate into clumps by day 1 which were lost by day 3 leaving just a few unattached cells. There was no cell elongation observed within the non-derivatised alginate beads - this result is fully consistent with the previous A7r5 work. Parallel live/dead viability/cytotoxicity assays (L-3224 - Molecular Probes, Eugene, Oregon, USA) were performed as per Section 3.8.1. They revealed a very high percentage of live cells (fluoresce green under ultraviolet light c.f. red when dead) in both the derivatised and non-derivatised alginate beads (the Day 7 bead images in Figure 8.9 are examples of this assay).

Having established that the MSCs required GRGDY peptide to be present (not an unsurprising result given that the MSCs are selected from the rest of the bone marrow cells on the basis of being anchorage dependent cells), a series of experiments was performed to optimise the type of alginate and alginate:peptide:sulpho-NHS:EDC ration (A:P:S:E ratio). This experiments suggested that 50x GRGDY Manugel DMB performed best. Figure 8.10 shows the results of a typical experiment carried out during this optimisation phase comparing 1x, 10x and 50x GRGDY-Manugel DMB alginate, again there is a good correlation between the sheets and the beads for a given reagent concentration with respect to MSC interaction. In Figure 8.10, both the 50x GRGDY sheets and beads showed extensive elongation and migration of the MSCs by day 4. In comparison, the MSCs did not interact with the 10x GRGDY sheets, remaining balled up or aggregating into loose clumps. A very small minority of cells did however interact weakly with the 10x GRGDY beads mainly close to the surface of the bead. At the lowest concentration, 1x GRGDY, the MSCs did not interact with either the sheets or the beads (data not shown).

Since the 50x GRGDY-Manugel DMB combination performed significantly the best with

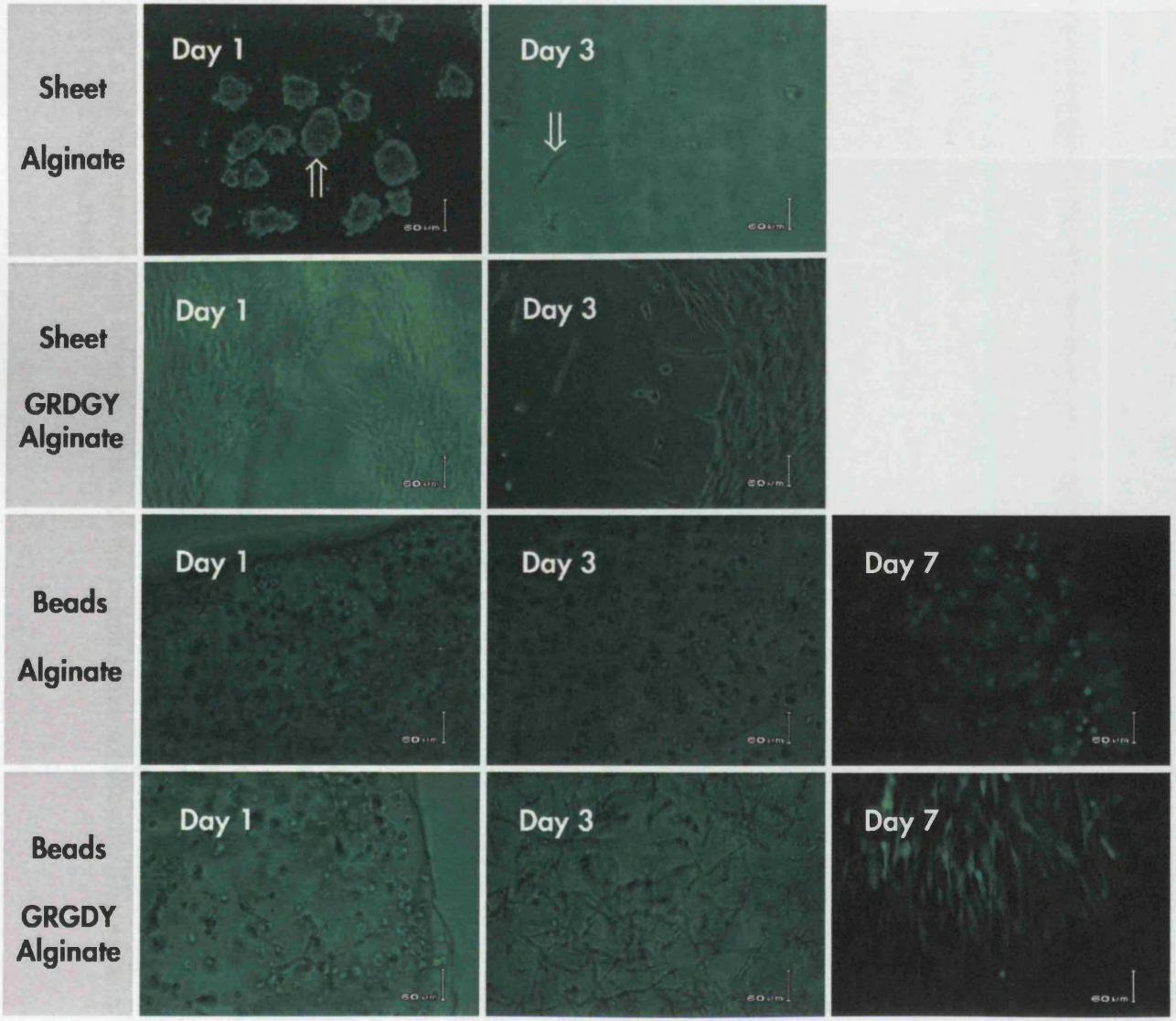

Figure 8.9

Comparison of the interaction of adult MSCs with derivatised and non-derivatised alginates on sheets and in beads.

In the first 24 hours the MSCs were able to quickly interact with the Manugel DMB 50x GRGDY-alginate i.e. attach, elongate and migrate, on both the surface of the sheets and within the beads. In the derivatised beads, intercellular networking can also be observed. On the non-derivatised alginate sheets there was no cell interaction, instead the cells were seen to aggregate into clumps by day 1 (⇑) which were lost by day 3 leaving just a few unattached cells. Likewise there was no cell elongation observed within the non-derivatised alginate beads. (N.B. Debris is marked ⇓)

Live/dead viability/cytotoxicity assays (L-3224 - Molecular Probes, Eugene, Oregon, USA) revealed a very high percentage of live cells (fluoresce green under ultraviolet light c.f. red when dead) in both the derivatised and non-derivatised alginate beads (Day 7 bead images are examples of this assay).

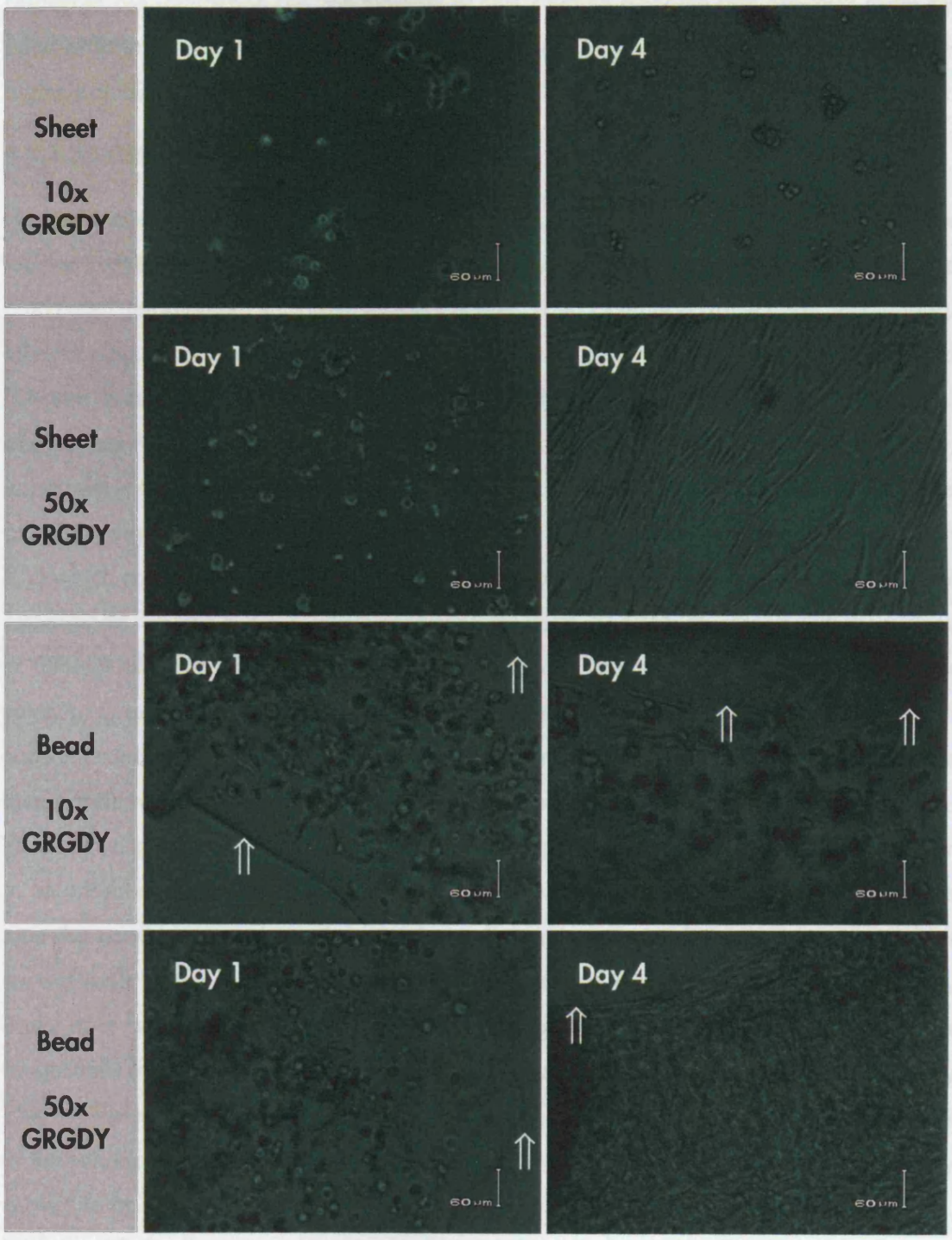

Figure 8.10

Comparison of human adult MSC interaction with sheets and beads made from Manugel DMB using different derivatisation reagent concentrations (1x, 10x and 50x).

Both the 50x GRGDY sheets and beads showed extensive elongation and migration of the MSCs by day 4. In comparison, the MSCs did not interact with the 10x GRGDY sheets, remaining balled up or aggregating into loose clumps. A minority of cells did however interact weakly with the 10x GRGDY beads. At the lowest concentration, 1x GRGDY, the MSCs did not interact with either the sheets or the beads (data not shown). (The edges of the beads are marked ⇑).

respect to cell interaction (i.e. the majority of MSCs would elongate and network) in all the bead experiments, it was decided to continue with this combination for all the future GRGDY-alginate studies.

8.3.1.3 GRGDY-alginate tubes

Having established the optimum conditions in beads, GRGDY-alginate was used to produce tubular constructs using both the float activated by the hand driven fluid device and the automated pump driven fluid devices, see Chapter 5 and Chapter 6 respectively. Preliminary tube forming experiments used a sterilised 4 mm inside diameter glass tube and a sterilised 3.4 mm float with 50x GRGDY Pronova MVG alginate (preparation process described above) and A7r5 cells at 10^5 per ml. These experiments were performed either prior to, or, in parallel with the bead experiments i.e. before the conclusion that A7r5s were not capable of interacting within the GRGDY-alginate but after both the collagen experiments (Section 8.2) which confirm that A7r5s could interact within a three-dimensional matrix and the sheet experiments (Section 8.3.1.1) which confirmed the ability of A7r5s to interact with the surface of GRGDY-alginate. This mixture was cross-linked with sterile filtered 1% calcium chloride solution. Cross-linking time was 10 minutes and then the tubes were flushed through with supplemented media. The entire tube forming apparatus including the construct *in situ* was then transferred to a humidified, 10% CO_2 37°C incubator. At daily intervals the tubes were flushed through with fresh medium which was pre-equilibrated by being left in the incubator in an unsealed container. This experiment was continued for up to one month. During this time the constructs could be viewed using a light microscope although the 1.6 mm thick curved walls of the 7.2 mm diameter glass fabrication tube meant that viewing was only really at its best when totally perpendicular to the glass tube (very small viewing angle) or tangentially (i.e. at the very edge), otherwise cells appeared extremely distorted. Being only able to view at these locations required the glass tube to be rotated in order to assess the state of the entire construct wall at a given point along the its length. Overall viewing tangentially proved to be the preferred option and this is reflected in the images in the various figures. With the A7r5 cells encapsulated in the GRGDY-alginate, a very small number of cells were seen to elongate and this appeared to only happen in the extraluminal gap (i.e. between the construct and the inner wall of the glass tube). No elongation was observed within the actual construct (a result consistent with the A7r5-GRGDY-alginate bead experiments). The cells which elongated in the extraluminal space may have left the construct due to slight hydrogel disintegration and then floated onto the glass wall where they became attached. However, an experiment seeding cells (i.e. with no alginate scaffold) directly into glass tubes failed to show cell attachment over similar periods of time.

Performing the above tube experiment with MSCs and refeeding the constructs either once

or twice per day did show cell-GRGDY-alginate interaction. Figure 8.11 shows selected time points from the first 22 days of such a study whilst Figure 8.12 shows more magnified images of the crucial day 1 and day 2 period when the cells are starting to attach and orientate. In Figure 8.12, both the images are of exactly the same location on the construct. The day 1 image is very difficult to interpret but possibly contains cells starting to interact with the derivatised alginate i.e. elongating but in a totally random and disorganized manner. However, by day 2, the cells have become orientated and aligned in the construct parallel to the long axis of the construct. The aligned cells appear to be to a maximum thickness of 4 - 6 cells deep and arranged in an overlapping pattern (for comparison, the observed arrangement was very similar to that found histologically in normal smooth muscle *in vivo*). In Figure 8.11, the day 3 - 17 images shown are also in approximately the same location in the same construct. The alignment and depth of the aligned cells appears to remain approximately constant for the first 7 - 11 days but later in the series the "growth" appears to continue but to be more disorganised. In addition to the collective "growth" in the construct, discrete cell aggregates appear to be forming by day 17 which become mature by day 22. It is possible that these aggregates are extraluminal i.e. between the construct and the inner wall of the glass tube and formed from cells shed from the construct as the GRGDY-alginates gel starts to degrade.

The tube experiments described above were re-fed by bolus i.e. refeeding medium at discrete time intervals. *In vivo*, bolus refeeding never occurs, nutrient is always continuously delivered by the pulsed circulatory system. Ideally a blood vessel bioreactor probably needs to be pulsatile flow (Niklason *et al*, 2001), however, it is generally agreed that at the very least it must have flow. It was therefore decided to construct a simple flow circuit where by fresh media continuously flowed through the glass tube containing the construct. The system was a total loss system i.e. culture media was not recirculated after passing through the construct. The circuit consisted of a syringe driver (Harvard PHD 2000) positioned outside the incubator with a 60 ml plastic syringe (Becton-Dickinson) filled with supplemented media. The syringe was linked to the 4 mm I/D glass tube using 1.6 mm I/D sterilised silicon tubing via an adaptor to the device's base unit to accommodate the small tube size. An excess length of silicon tubing was used in order to allow approximately 0.5 m to be inside the incubator where due to the nature of the material, the temperature, O_2 and CO_2 would all equilibrate with the incubator prior to the media entering the construct. A visible change in media colour was noted between the medium upon immediately entering the CO_2 incubator compared to when the medium entered the construct. The open end of the glass tube had another piece of sterile tubing added to its end in order to allow spent media to be collected in a sterile glass beaker. It was decided to set the syringe driver to give a flow rate compatible with approximately 3 media changes in a 24 hour period i.e. 0.2 $mlhr^{-1}$, since the fabrication device has a total

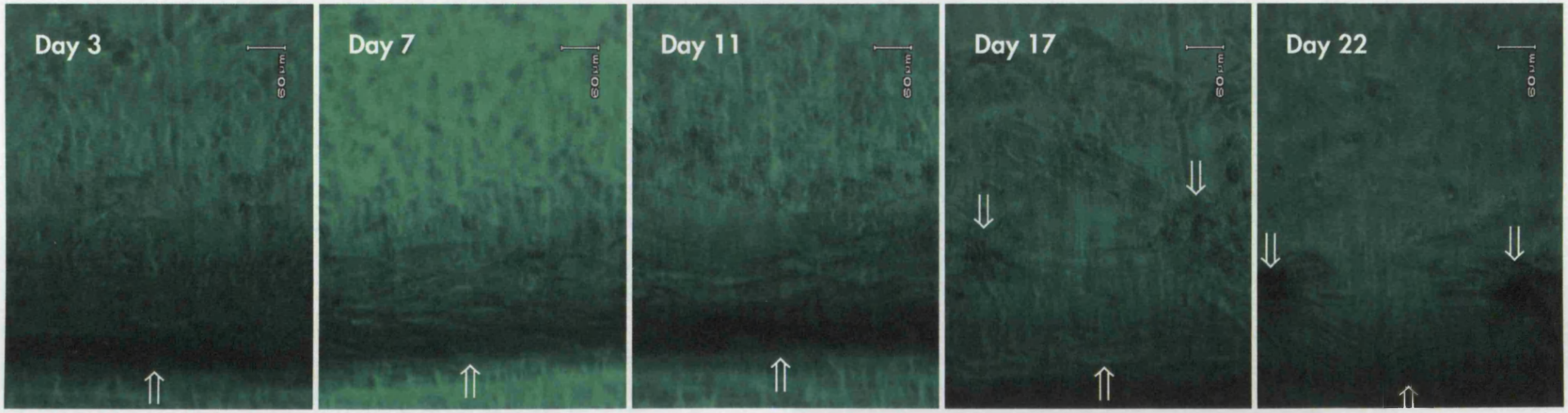

Figure 8.11

Time series for human adult mesenchymal stem cells encapsulated in a 50x GRGDY-Pronova MVG alginate tube viewed with a light microscope whilst in situ in the glass walled bioreactor.

The images are taken at the inner edge of the glass tube which both fabricated the construct and is now acting as its bioreactor (marked ⇑). At this location, a tangential view of the inner glass wall of the tube is observed that by previous experiments had been found to be one of the optimum positions for obtaining good views despite the lensing effect due to the curvature of the wall of the glass tube (data not shown). Thus by rotating the glass tube around its longitudinal axis it was possible to sequentially image the entire construct. The day 3 - 17 images shown are all in approximately the same location in the same construct. By day 3, the cells start to be seen to be elongated and aligning in the construct parallel to the long axis of the construct. The day 7 image shows these aligned cells to be to a depth of up to 4 - 5 cells thick and in an arrangement similar to that found histologically in normal smooth muscle in vivo. Later in the series the "growth" appears to continue but to be more disorganised. In addition to the collective "growth" in the construct, discrete cell aggregates appear to be forming by day 17 which become mature by day 22. It is possible that these aggregates are extraluminal i.e. between the construct and the inner wall of the glass tube and formed from cells shed from the construct as the GRGDY-alginates gel starts to degrade (aggregates marked ⇓).

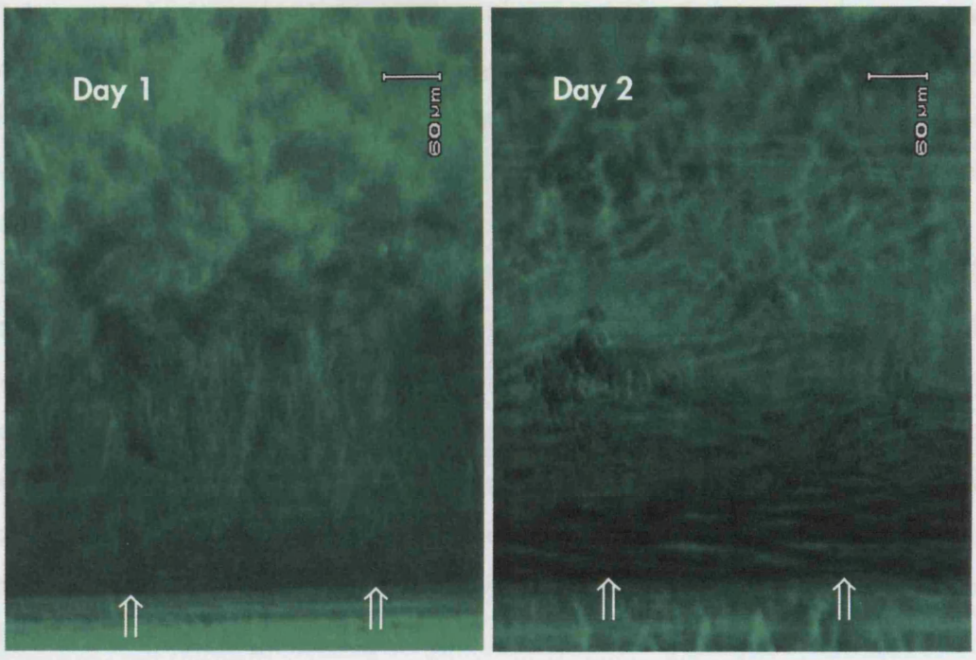

Figure 8.12

Enlarged images of cell alignment in the first two days of culture following fabrication of a tubular construct of human adult mesenchymal stem cells encapsulated in GRGDY-Manugel DMB alginate viewed in situ in the bioreactor.

Both images are of exactly the same location on the construct. The day 1 image is very difficult to interpret but possibly contains cells starting to interact with the derivatised alginate i.e. elongating but in a totally random and disorganized manner. However, by day 2, the cells have become orientated and aligned in the construct parallel to the long axis of the construct. The aligned cells appear to be to a maximum thickness of 4 - 6 cells deep and arranged in an overlapping pattern very similar to that found histologically in normal smooth muscle in vivo. (The inner edge of the glass tube is marked ⇑).

volume of approximately 1.5 - 1.6 ml allowing for dead space in the base unit. In addition to the regular controls, bead controls were also produced. Figure 8.13 shows selective images from this experiment which compared the interaction of human adult MSC in beads and tubes made from Manugel DMB using different derivatisation GRGDY peptide concentrations (1x, 10x and 50x) but maintaining all the other reagent concentrations constant. In all the different concentration GRGDY beads there is extensive elongation and networking of the MSCs by day 7. In comparison, on day 1 there is some elongation of cells into a random arrangement within the tube matrix which becomes more orientated by day 7. However, unlike the beads which maintained (or increased) their cell densities, the density of cell in the tube declined possible due to GRGDY-alginate degradation. This degradation may have been higher than the earlier bolus refeeding experiments due to the continuous feeding regimen washing away the Ca^{2+} cross-linking ions faster. A similar experiment in shown in Figure 8.14 which also contains a time series for adult human MSCs encapsulated in a 50x GRGDY-Manugel DMB alginate tube. On day 1, the majority of cells are starting to elongate into a patchy random network which by day 9 appears to be more densely packed, almost continuous and to have some degree of alignment with the long axis of the glass tube. This orientation is continuing on day 12 with overall the packing arrangement appearing to be fairly homogeneous along the length of the construct. Clearly more work is required to study the effect of continuous flow and its rate on GRGDY-alginate degradation.

Overall the MSC-50x tubular constructs displayed similar cell elongation and networking to the beads with the addition of the beginnings of regular aligned cell orientation in the long axis of the construct. For artery a circumferential (as opposed to longitudinal) alignment is probably preferred since this is the arrangement in normal artery *in vivo*.

8.3.2 Alternatives to using GRGDY for derivatising alginate

It was decided not to limit the derivitisation purely to the covalent bonding of only the pentapeptide GRGDY to the alginate, but to also look at other alternatives. GRGDY is a relatively short peptide with the functional motif RGD which couples with cell surface integrins e.g. $\alpha_5 \beta_1$ which is the most abundant β integrin on proliferating smooth muscle cells (Hunt *et al*, 2002). However, due to of the motif's small size and length in addition to its distance (1 x glutamine residue) from the large alginate backbone, it was decided to produce alginate derivatives with the functional RGD motif spaced away from the backbone, in order to potentially increase the accessibility of the RGD motif to the cells. The spacer itself may also have an effect on the RGD binding site in terms of it efficiency to bind cells. For example, Ruoslahti and Pierschbacher have demonstrated that the amino acids surrounding the RGD motif greatly affect the receptor-ligand specificity, an effect brought about by their influences on the conformational shape of the RGD receptor site (Ruoslahti and Pierschbacher, 1987).

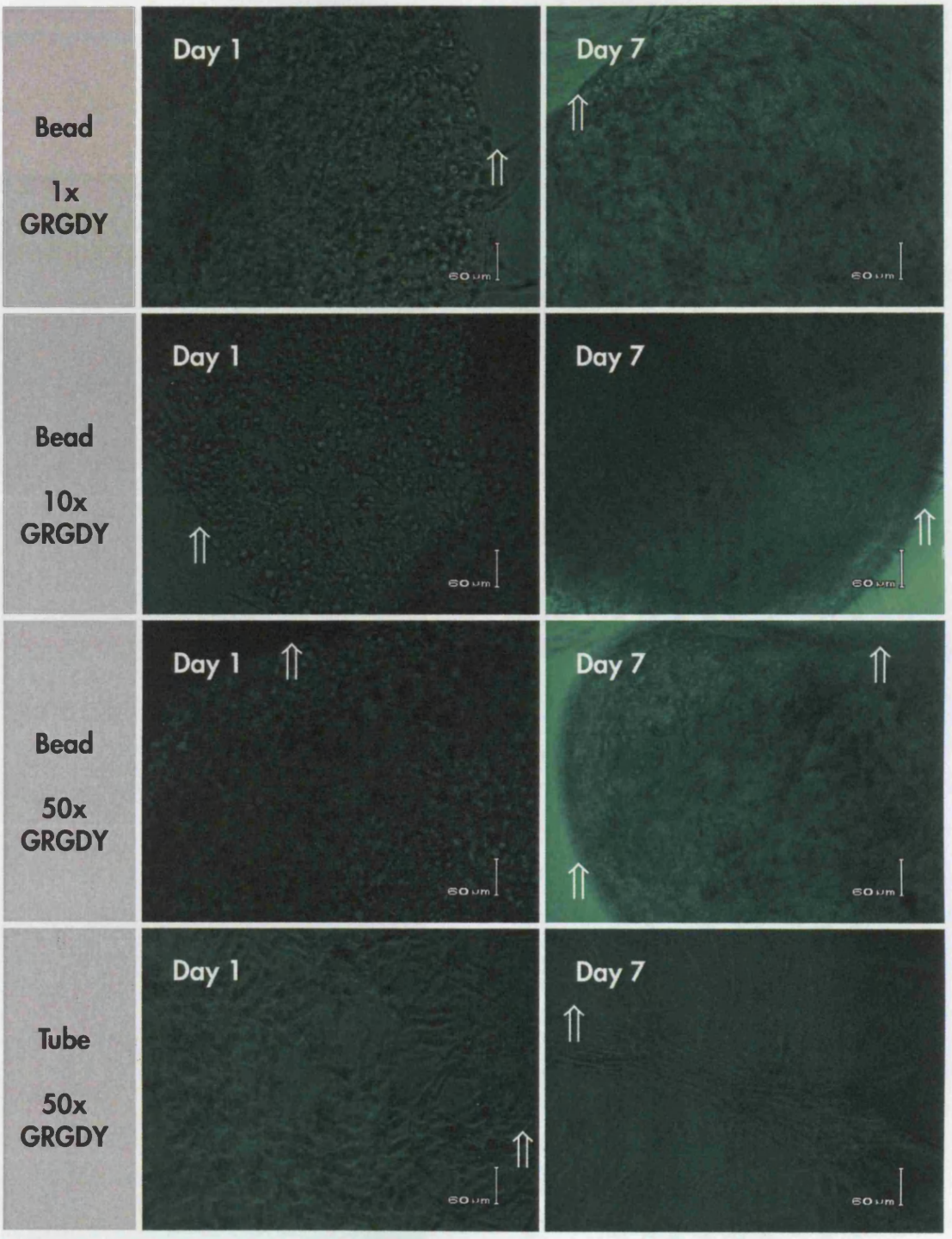

Figure 8.13

Comparison of human adult MSC interaction in beads and tubes made from Manugel DMB using different derivatisation GRGDY peptide concentrations (1x, 10x and 50x) but maintaining all other reagent concentrations constant.

In all the different concentration GRGDY beads there is extensive elongation and networking of the MSCs by day 7. In comparison, on day 1 there is some elongation of cells into a random arrangement within the tube matrix which becomes more orientated by day 7. However, unlike the beads which maintained (or increased) their cell densities, the density of cell in the tube declined possible due to alginate degradation. (The edges of the beads are marked ⇑)

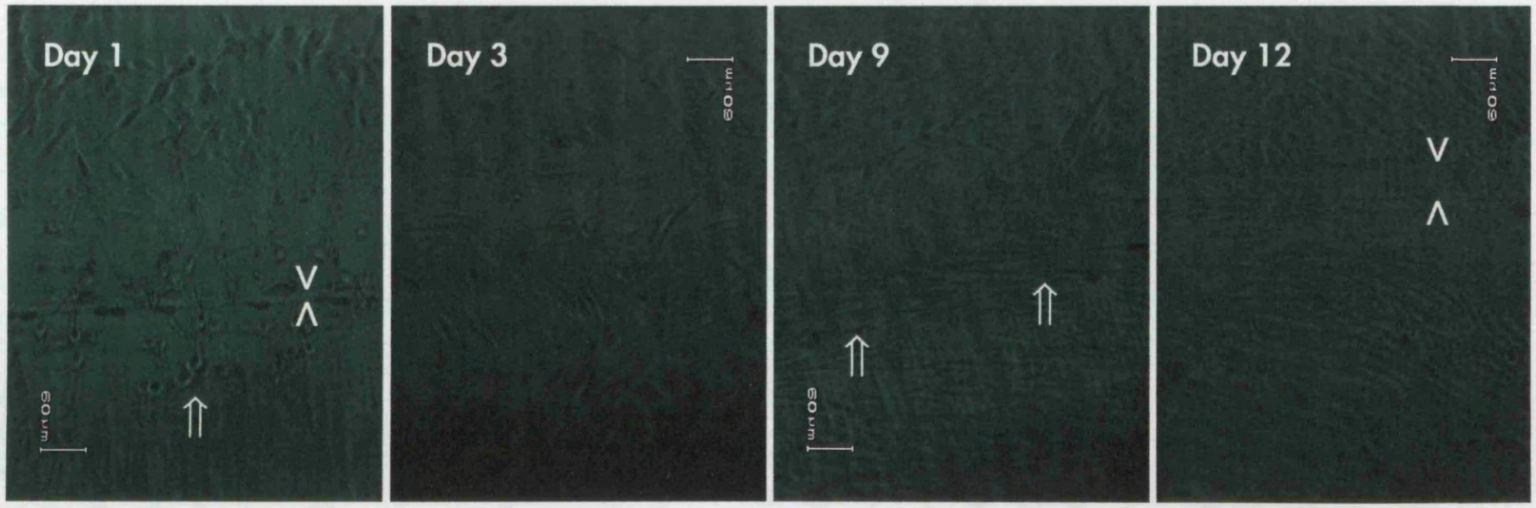

Figure 8.14

Time series for adult human MSCs encapsulated in a 50x GRGDY-Manugel DMB alginate tube viewed with a phase contrast light microscope whilst in situ in the glass walled bioreactor.

The orientation of all the images is such that the glass tube wall is at the their lower end (where included marked ⇑). However, the Day 1 and 9 images are taken at the inner edge of the glass tube which both fabricated the construct and is now acting as its bioreactor; whilst day 3 and 9 images were obtained more towards the midline of the tube to try and capture from another perspective the widespread cell orientation occurring within the tubular construct. The trade-off of this viewing location is unfortunately increased distortion due to the lensing effect of the glass walled tube. The horizontal parallel lines present in both the day 1 and 12 images are imperfections (scores) in the glass' surface which occasional occur when the mandrel is removed from the precision bore glass tube after its extrusion (marked > <). Balled up cells occupying the scores on day 1 but by day 12 these cells are no longer present, presumably they fail to attach and die or are washed away on changing the medium. On day 1, the majority of cells are starting to elongate into a patchy random network which by day 9 appears to be more densely packed, almost continuous and to have some degree of alignment with the long axis of the construct. This orientation is continuing on day 12 with overall the packing arrangement appearing to be fairly homogeneous along the length of the construct.

Two approaches were used, namely adding extra glutamine residues (GGGGRGDY) and adding a polyethylene glycol spacer (PEG), (PEG_4-GRGDY and PEG_4-RGDY). Altering the specific RGD motif was not undertaken since it has been shown that single amino acid substitutions dramatically reduces the biological activity of the peptide (Ruoslahti, 1996).

8.3.2.1 GGGGRGDY-alginate

The octapeptide GGGGRGDY-alginate had previously been covalently bonded to alginate by Rowley (Rowley and Mooney, 2001). Rowley had successfully demonstrated myoblast differentiation on the surface of preformed GGGGRGDGY-alginate hydrogels. Our aim was to examine its potential with respect to smooth muscle cells (and later adult mesenchymal stem cells) when the cells are embedded in a precise three-dimensional shape.

GGGGRGDY was obtained from Neosystem Groupe SNPE (Strasbourg, France) in a lyophilised form in 10 mg aliquotes. Using the carbodiimide chemistry described in Section 3.7.1 this peptide was covalently bonded to the alginate backbone. However, whereas the reaction for the previous GRGDY attachment was relatively straightforward, the longer peptide derivative posed greater problems; presumably due to its greater length. The resulting compounds were unsatisfactory because the GGGGRGDY-alginate would become irreversibly set during the dialysis stage. Attempts to reverse the setting process e.g. trying to dissolve the hydrogels in high concentration sodium citrate (1 M) for lengthy periods (>24 hours), failed to breakdown the gels. The reason for the gel setting during the dialysis step is unknown and informal discussions with Dave Mooney failed to resolve the issue. However, it would appear that the cross-linked GGGGRDGY compound produced was covalently bonded, hence the inability to be broken down by the sodium citrate. When small pieces of the GGGGRGDY gel were placed in Microwells with A7r5 cells and supplemented culture media a small number of cells attached and elongated. The majority, however, failed to attach and settled on the bottom of the microwell where they attached and readily proliferated.

8.3.2.2 Polyethylene glycol-GRGDY-alginate

The rational behind the polyethylene glycol spacer was again to increase the ligand accessibility, but instead of using additional amino acids (glutamine residues) the plan was to use polyethylene glycol (PEG). Using PEG has several key advantages (Halstenberg *et al*, 2002, Eiselt *et al*, 1999 and Shin *et al*, 2002):

- Ease of chemical modification e.g. good control over PEG chain length
- Inert with respect to cell attachment
- Flexible molecule and therefore potentially allows better ligand accessibility
- Low cost of production relative to "amino acid spacers"
- Biocompatible e.g. not immunogenic

There was also a literature to draw on of previous researchers who had worked with PEG and the RGD motif including Drumheller and Hubbell, 1994, Eiselt *et al*, 1999 and Halstenberg *et al*, 2002.

It has been demonstrated by Houseman, that for a fixed density of an attachment peptide, altering the spacer length can be expected to alter the degree of cell attachment and interaction, (Houseman and Marksich, 2001).

Another advantage of using PEG is that the amino acids on either side of the RGD motif (i.e. the glutamine residue (G) and the tyrosine residue (Y) in Section 8.3.1) have a direct influence on receptor-ligand interaction and specificity, (Ruoslahti *et al*, 1987). Therefore by using a PEG spacer with GRDGY motif used in Section 8.3.1, it was possible to directly compare the derivatised alginates knowing that the RGD's receptor-ligand specificity was theoretically unchanged unlike GGGGRDGY, where the extra glutamine residues may have a direct action on the RDG interaction site.

Tetraethyleneglycol-GRDGY (PEG_4-GRDGY) was prepared in collaboration with Ros Selfe/ Dr. Alethea Tabor in the Department of Chemistry at UCL. Using the same carbodiimine chemistry described in Section 3.7.1, this PEG_4-GRDGY peptide was covalently bonded to alginate (1% ISP Manugel - Pharmaceutical grade in 0.1 M MES buffer made up with 0.3 M sodium chloride solution in WFI, final pH adjusted using sodium hydroxide (pharmaceutical grade) to pH 6.5). Reactions were set up such that the final peptide densities were 10 mg and 50 mg of GRGDY motif per gram of PEG_4-GRDGY-alginate. Controls of 10 mg and 50 mg GRGDY-alginate were produced in parallel (as per Section 8.3.1) in order to allow exact comparison between linker and non linker GRGDY. Both beads containing cells and sheets for cell surface studies were prepared from the PEG_4-GRDGY-alginate and the controls as previously described in Section 3.4.1 and Section 3.4.2.

Overall the use of PEG_4-GRDGY-alginate gave good results. The bead experiments using adult mesenchymal stem cells at a final density of 10^5 -10^6 cell ml^{-1} of scaffold material demonstrated cell elongation for both the linker and non linker alginate. Figure 8.15 shows the results from an experiment to the compare human adult MSC interaction in beads made from Manugel DMB using different derivatisation GRGDY peptide methods of attachment (PEG4 linker versus non-linker) at different concentrations (1x, 10x and 50x). In the 50x concentration GRGDY and PEG_4-GRGDY alginate beads there was extensive elongation and networking of the MSCs by day 2. Both the 10x conditions showed a moderate degree of cell interaction, whilst the 1x conditions failed to support cell interaction (data not shown). Once again the 50x concentration was clearly superior, however there was no obvious advantage of having the PEG_4 linker present.

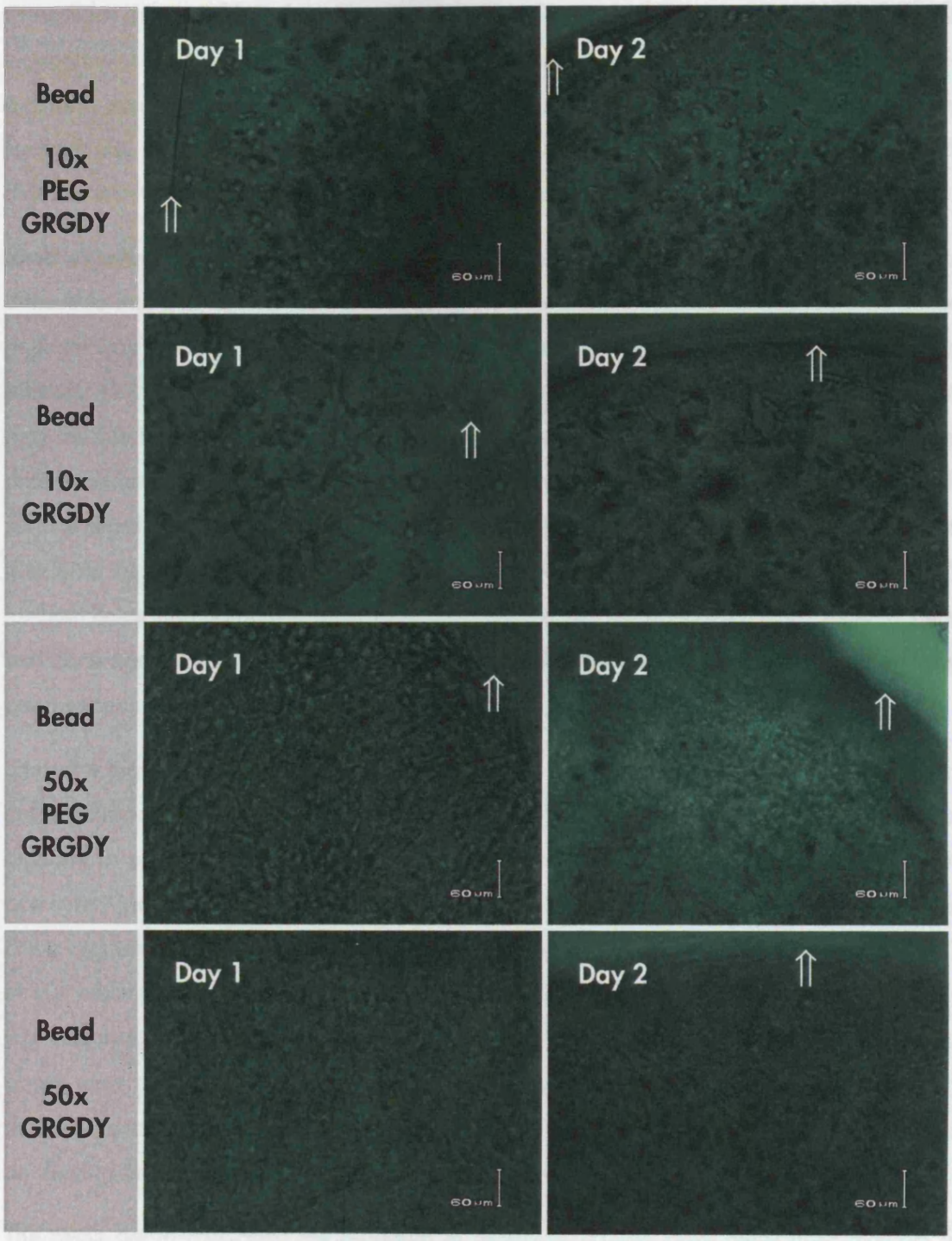

Figure 8.15

Comparison of human adult MSC interaction in beads made from Manugel DMB using different derivatisation GRGDY peptide methods of attachment (PEG_4 linker versus non-linker) and concentrations (1x, 10x and 50x).

In the 50x concentration GRGDY and PEG_4-GRGDY alginate beads there was extensive elongation and networking of the MSCs by day 2. Both the 10x conditions showed a moderate degree of cell interaction, whilst the 1x conditions failed to support cell interaction (data not shown). Once again the 50x concentration was clearly superior, however there was no obvious advantage of having the PEG_4 linker present (The edges of the beads are marked ⇑).

Overall for this set of bead experiments, for a given peptide density, considerably more cell elongation was observed in the non linker peptide-alginate than in the linker PEG-peptide-alginate. Also, the number of cells elongating increased as the peptide concentration increase for both the linker and non-linker alginates, i.e. 10 mg of motif per gram of derivatised alginate was inferior in cell interaction than the 50 mg per gram version.

Sheet experiments using the same PEG-peptide-alginate had less substantial results and are difficult to interpret due to technical problems with the sheet making process e.g. the linker alginate was prone to trapping air bubbles which made interpreting light microscope studies difficult. Air bubble trapping had not been a problem with linkerless alginates and the effect may be due to the change in viscosity or surface tension. However, overall there was little difference between the linker and non linker alginates with both appearing to support cell surface attachment and spreading. However, once again the linker was out performed by the non-linker alginate in terms of cell elongation. Likewise, the higher density peptide (50 mg) for both linker and non-linker out performed the lower density peptide (10 mg). Overall there was once again good correlation with respect to MSC interaction between the sheet and the bead experiments.

Since the higher density peptide had demonstrated a superior performance with respect to cell attachment and elongation, it was decided to increase the concentration of the derivatised alginate in solution. This would not change the overall peptide:alginate ratio, but might potentially increase the overall activity of the motif in the scaffold. In order to concentrate the linker-alginate and the control alginate, freeze drying was undertaken for 24 hours at -70°C at 10^{-1} mbar (Edwards Freeze Dryer Modulo with a Savant Two Stage VP100 vacuum pump), which reduced the overall volume by approximately 50%. Identical cell experiments to the above were performed with these lyophilised PEG_4-GRDGY-alginates, which demonstrated that this concentrating step greatly reduced biological activity which only partially returned on diluting the compound back to its original volume with WFI prior to adding the cells.

The result again confirmed the reduction in biological activity once derivatised alginate is flash frozen with liquid nitrogen and then placed in a freeze dryer. Interestingly the ability of the concentrated material to cross-link and form beads, gels and tubes appeared unchanged except stronger constructs were produced as would be expected by using higher concentration alginate solutions.

8.3.2.3 PEG_4-RDGY-alginate

In order to further understand the relationship between the RGD motif and its surrounding environment, i.e. the glutamine (G) and tyrosine (Y) residues on either side of the RGD motif, it was decided that instead of using the pentapeptide GRDGY to use just the quadrapeptide

RGDY component plus the linker. Glutamine and tyrosine are both amino acids with uncharged polar side chains. Because of their uncharged nature, these amino acids tend to be relatively hydrophobic and as such are usually found on the inside of the proteins they help form. (Albert *et al*, 1989). It was decided to investigate the loss of the first glutamine residue since PEG_4-RDGY is slightly easier to produce than PEG_4-GRGD. This PEG_4-quadrapeptide peptide was also made in collaboration with Ros Selfe/Dr. Alethea Tabor in the Department of Chemistry at UCL.

Therefore linker-RGDY, (PEG_4-RGDY), was covalently bonded to alginate and formed into beads with cells encapsulated and sheets as per PEG_4-GRDGY experiments described in Section 8.3.2.2. Non linker GRGDY controls were produced in parallel. Overall a very similar result to the linker GRGDY alginate was achieved i.e. cell attachment and elongation was facilitated but once again at a lower level than that of plain GRGDY-alginate. Figure 8.16 shows the results of an experiment to compare adult human MSC interaction in beads made from Manugel DMB alginate using PEG_4-RGDY with GRGDY as the cell attachment motif at 1x, 10x and 50x concentrations. The 10x and 50x concentration conditions showed good cell interaction by day 2 - 3, whilst no cell interaction was observed in the 1x concentrations (data not shown). Interestingly over the course of 5 days, there was little difference in the cell networks between any of the 10x or 50x concentrations. This results obtained using PEG_4-RGDY-alginate suggests that the amino acid glycine may potentially not be required at the N-terminus of the RGD sequence for cell attachment although more research is required to evaluate this fully including the comparison of PEG_4-RGDY-alginate with PEG_4-GRGDY-alginate.

8.4 Conclusion

Experiments performed with non derivatised alginate consistently lacked evidence that the cells were attaching or proliferating with the result that the cells stayed balled-up until they eventually died. Increasing the cell density to 10^8 cells per ml of alginate solution also made no difference despite the greater cell density bringing the cells into closer contact with one another but still less tightly packed than they would be in normal tissue. Possibly raising the cell concentration further may have merit since this would produce closer cell packing and therefore promote direct cell-cell contact and interaction. Close virtual cell-cell contact is the normal arrangement in the human body (Radisic *et al*, 2003). The final cell packing arrangement is vital for smooth muscle to function as an organ. *In vivo*, smooth muscle the organ, is composed of elongated smooth muscle cells (each of which is enclosed by a basal lamina and a network of reticular fibres (collagen type III)), blood vessels and nerves. The basal lamina and the network of reticular fibres constitute the endomysium, the function of which is to combine the force generated by each smooth muscle cell into a concerted action

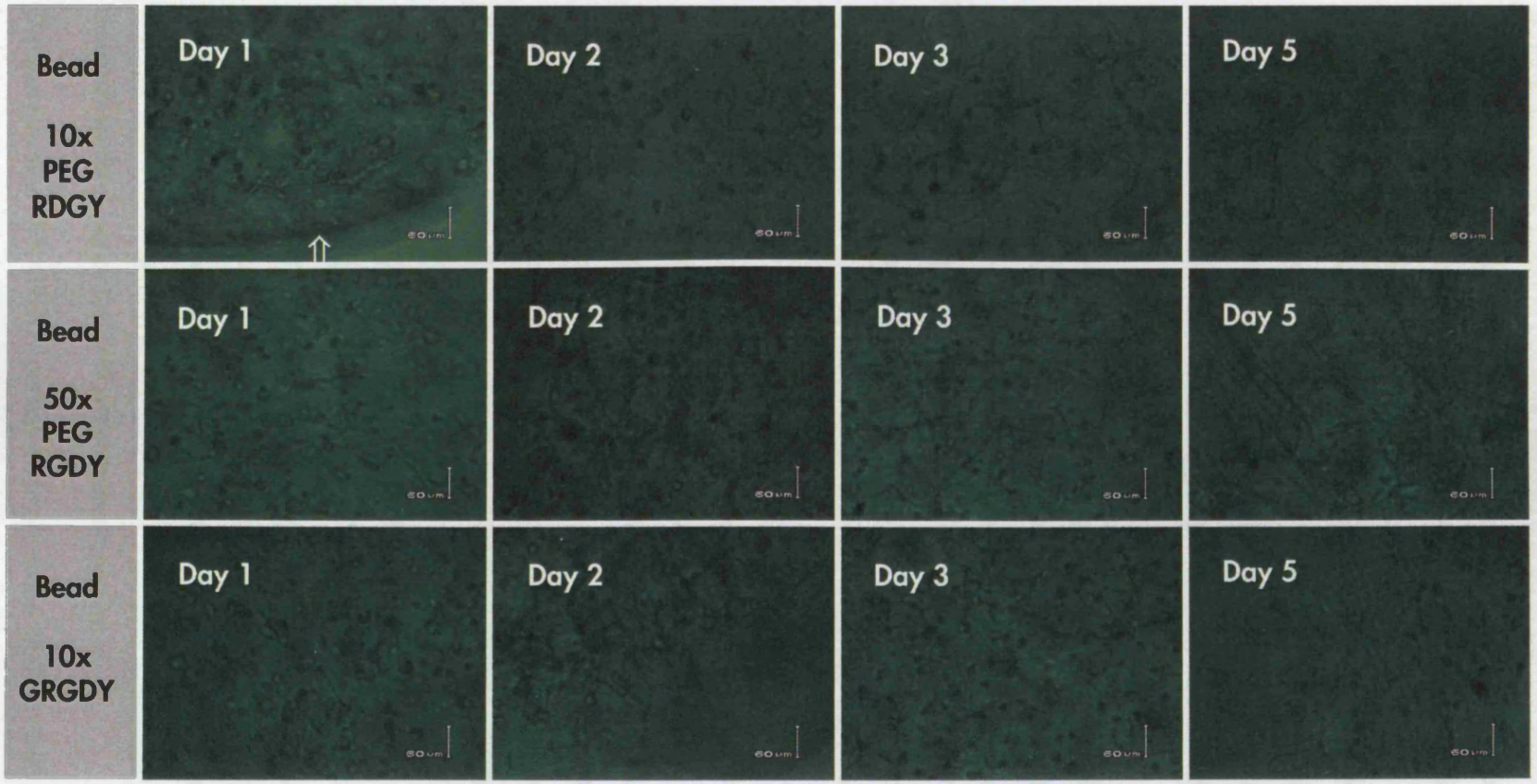

Figure 8.16 Comparison of adult human MSC interaction in beads made from Manugel DMB alginate using either PEG_4-RGDY or GRGDY as the cell attachment motif at either 1x, 10x or 50x concentration.

All the 10x and 50x concentration conditions showed good cell interaction by day 2 - 3. No cell interaction was observed in the 1x concentrations (data not shown). Interestingly over the course of 5 days, there was little difference in the cell networks between any of the 10x or 50x concentrations. (Edge of bead where shown marked ⇑)

e.g. arterial vasoconstriction. *In vivo*, smooth muscle cells are fusiform in shape i.e. they are largest at their midpoints (which contains the nucleus) and taper toward their ends. To achieve the closest packing possible, the cells line up in parallel with the narrow part of one cell lying adjacent to the broad part of neighbouring cells. In this close packed arrangement, the smooth muscle cells can function as a syncytium (Junqueira at al, 1986). *In vitro*, given the above close packing arrangement *in vivo*, smooth muscle cell density may be critical. It may be that there is a very precise cut off point i.e. cell densities below a certain value are still too dispersed to elongate and proliferate. This is analogous to the cut off seen with adult stem cells in GRGDY-alginate where there was little (if any) cell elongation at concentrations below 10^6 cells ml^{-1} and ideally 10^7 cells ml^{-1} was required to produce elongation in the majority of the cell population.

The other possible concern was that although the cells were capable of elongating and proliferation in single layer of flat sheets on the surface of T-flasks, they were not capable of elongating in a three-dimensional encapsulated environment. The collagen only matrix experiments therefore provided evidence that the A7r5 immortalised rat smooth muscle cell line (despite possible phenotype irregularities due to the immortalisation process) was still able to elongate in a three-dimensional scaffold, provided there were the necessary cell attachment sites.

The addition of alginate to the collagen prior to setting suggested that the alginate did reduce the degree of attachment but not totally. The collagen-alginate experiments were not, however, optimised but were solely conducted to confirm if the A7r5 smooth muscle cells could elongate in the presence of alginate hydrogel in the light of the negative data in Chapter 7. Optimisation was not performed since the alginate-collagen setting protocol does not easily lend itself to the tube production process for three main reasons. Firstly, the long setting times are not compatible with the fast gel forming times required of our particular device. Alginate solution becomes a hydrogel (at least at its boundary) in fractions of a second, whereas the collagen-alginate gels required minutes. Secondly, there was significant batch to batch variability with the commercially supplied collagen solutions. Thirdly, the collagen solutions despite being stored at 4°C "aged" such that there were significant differences between the setting time of different experiments, even from the same batch of collagen just due to short periods of storage (days/few weeks) e.g. later experiments from the same batch would demonstrate total loss of their cell attachment properties.

The derivitisation with GRGDY pentapeptide produced alginates with the first indication that both A7r5 immortalised rat smooth muscle cells and human adult mesenchymal stem cells could elongate on a two-dimensional matrix made from derivatised alginate. However, only the MSCs were capable of interacting when encapsulated in the same matrices. The reason

for the non-correlation between the MSCs and the A7r5s is not clear but may relate to the immortalisation process the embryonic rat cells originally underwent to create this immortalised cell line. Whilst Mooney and colleagues had demonstrated the ability of myoblasts to attach to the surface of GRGDY-alginate (Rowley *et al*, 1999 and Rowley and Mooney, 2001), the experiments with both beads and tubes demonstrated the three-dimensional application of a modified version of this approach. It is the ability to produce homogeneously seeded three-dimensional structures with viable cells which is key to tissue engineering.

The experiments to distance the attached functional RGD motif from the alginate backbone suggest that this area needs further work both in producing satisfactory octapeptide GGGGRGDY and also optimising the PEG linker length. Once this optimisation is complete, it will then be possible to directly compare the distanced RGD motif with the current "gold standard" GRDGY-alginate. The preliminary data suggests that the presence of the spacer does adversely effect the ability of the RGD motif to interact with the MSCs.

The experiment using just PEG_4-RGDY-alginate suggests that more work is required to better understand the minimal requirement for cell attachment. There was insufficient experimental evidence to conclude whether RGDY is better that GRGDY as the attachment motif. However, it is potentially possible that just RGD-alginate is all that is required. If this was the case, then this would significantly reduce both the complexity and cost of the method of derivatising alginate such that MSCs (and potentially other suitable anchorage dependent cells e.g. primary smooth muscle cells) can attach and elongate.

Finally, the difficulty in freeze drying the derivatised products i.e. the near total loss of biological activity, suggests that the peptide may be becoming permanently denatured by the process. This area needs focusing on since freeze drying normally represents an excellent means of storing such material.

8.5 Future work

The main areas to consider are:

1. Increasing the cell density to test the hypothesis that closer cell-cell distances leads to greater cell-cell contact and interaction, this in turn leads to cells attaching to one another or producing extracellular matrix (ECM) which allows cell-ECM-cell attachment and then proliferation. It raises the important question, is cell proliferation required at all in the maturing tissue engineering construct? If cells could be added at high enough densities though, not so high that the scaffold cannot maintain integrity, then if no further, or minimal, proliferation was required, then this could potentially reduce individual bioreactor time (and possibly therefore cost) by effectively transferring all the

cell bulking to the first part of the process, i.e. prior to mixing with alginate solution. The biotechnology industry already has a number of tried and tested methods for economically bulking-up attachment cells e.g. Cellmate and SelecT from The Automation Partnership (Royston, Hertfordshire, UK) and Cell Factories from Nunc (Roskilde, Denmark)

2. If it not possible to create constructs with near *in vivo* cell:synthetic extracellular matrix ratios, then cell proliferation within the developing construct will be essential. Given that both smooth muscle cells and human mesenchymal stem cells are potentially not natural replicators *in vivo* (Gordon *et al*, 1990, Wang *et al*, 2002 and Preston *et al*, 2003), it may be necessary to find low cost reagents capable of causing controlled proliferation e.g. ouabain which has been demonstrated to stimulate proliferation of vascular smooth muscle cells. Ouabain is an endogenous compound with an enormous scientific literature (>18,000 publications since 1966) (Abramowitz *et al*, 2003)
3. An alternative strategy could be to use fibroblasts - a cell type that is well known to proliferate whilst encapsulated in alginate. Thus a potential alternative option to the differentiation of autologous MSCs into vascular SMCs might be to transdifferentiate allogeneic non-immunogenic fibroblasts. Non-immunogenic fibroblasts are readily available from neonatal foreskin and have already been successfully deployed in FDA approved products including Apligraf (Organogenesis, Canton, MA, USA). Whilst the transdifferentiation of fibroblasts into myelofibroblasts occurs in a number of common and well described pathological process e.g. hypoxia induced vascular remodelling (Short *et al* 2004, Stenmark *et al* 2002) and corneal wound healing (Funderburgh *et al* 2001), transdifferentiation into vascular smooth muscle has not yet been demonstrated. However, recent research based on animal embryological studies by Prof. Karen Hirschi's group at Baylor College of Medicine (Houston, Texas, USA) has suggested that this may be possible (Hirschi, 2004)
4. Another cell option might be to use immortalised cells since all the arteries tissue-engineered to date have required extensive culturing in the order of months (Niklason *et al*, 1999 and L'Heureux *et al*, 1998). This excludes the paediatric applications of Shin'oka - where because of their short length and the very young age of the patients, the scaffolds were seeded with cells on the actual day of surgery (Matsumura *et al*, 2003). However, adult somatic cells can only divide a finite number of times before undergoing replication senescence (growth arrest). This is mainly due to the progressive shortening

of the cells' telomeres with each cell division. This eventually progresses to a critical length which triggers senescence (Sedivy 1998). Depending upon the number of cells in the initial sample/biopsy, SMCs may be required to proliferate for at least 45–60 population doublings to produce a mechanically robust artery *in vitro* (McKee *et al*, 2003). Bovine, porcine, human fetal and human neonatal cells possess lengthy telomeres, and therefore can divide extensively in culture before entering the senescence phase; this has shown to be more than adequate to be able to successful engineer arteries *in vitro* (McKee *et al*, 2003). However, adult human SMCs, a potential source of cells to create clinical constructs can only proliferate *in vitro* to a maximum of 10 – 30 population doublings before undergoing senescence (Bierman, 1978 and Bonin *et al*, 1999). Furthermore in human SMCs it has been demonstrated that their proliferation capacity is inversely proportional to age (Grunwald *et al*, 1983), an undesirable fact given that the majority of patients requiring coronary artery bypass surgery will be over 50 years of age.

Human MSCs have also been shown to behave in a similar manner to SMCs with growth arrest at approximately 20 population doublings (Kobune *et al*, 2003 and Zimmermann *et al*, 2003). The limited replication life-span of both human adult SMCs and MSCs may therefore prove to be a real "show stopper" for their use in the construction of tissue-engineered arteries.

One solution to this problem may be to produce immortalised cell lines from either MSCs or SMCs. An established method of creating an immortalised adult human cell line is to elongate the telomeres using the enzyme telomerase. (Nakamura and Cech, 1998) Telomerase is a ribonucleoprotein which in man is assembled from a telomerase RNA subunit (hTR) and a telomerase reverse transcriptase subunit (hTERT) (Collins and Mitchell, 2002). All human somatic cells express hTR, but not hTERT, and thus lack the necessary telomerase activity required to maintain telomere length (Collins and Mitchell, 2002). However, genetic modification to restore the expression of hTERT in human cells has been demonstrated to restore telomerase activity and thus prevent senescence (Bodnar *et al*, 1998). Recently both human MSCs and SMCs have been immortalised using hTERT restoration methodology (Okamoto *et al* 2002, Kobune *et al*, 2003 and McKee *et al*, 2003).

5. The optimisation of the derivatised alginates. All the derivatised alginates produced to date require rigorous optimisation to ensure acceptable levels of batch to batch variability. This optimisation would need to start with the thorough characterisation of the initial alginate. Alginate is a natural polymer

produced from seaweed with highly variable composition in terms of its G and M monomer make-up. Batch to batch variability is therefore a potential problem unless the material can be characterised. Furthermore, the alginate needs thorough purification. At present, even the pharmaceutical grade alginate contains unwanted trace elements including lead and arsenic plus bacterial and fungal contaminants. Whilst some necessary characterisation is performed by the alginate producers which was adequate for proof of principle experiments, this is now inadequate for future progress.

6. Future work also needs to include demonstrating the optimal density of cell attachment motif to achieve cell attachment and proliferation. Options to determine this include using known concentrations of specific monoclonal antibodies to the RGD site to compete with the cells for attachment sites. Too few RGD motifs and the matrix will not support cell attachment, too many may be a hindrance to cell elongation (similar to being embedded in cement), detrimentally affect calcium cross-linking or be financially prohibitive.
7. Determination of whether a PEG spacer is beneficial and if so, what is the optimum length. Too short and there may be no real benefit (possibly the case for the PEG_4-GRGDY and PEG_4-RDGY experiments). Too long and potentially because of its innate flexibility, the PEG linker could fold back onto the alginate backbone thus reducing the accessibility of the RGD motif.
8. Thorough investigation of the uronic acid residue component of the chosen alginate is required. Rowley *et al* used ^{125}I-GRGDY as a tracer molecule which could then be detected in lyophilised ^{125}I-GRGDY-alginate using a gamma counter (Rowley *et al*, 1999).
9. Determination of the best cell attachment motif to bond to the alginate. Could it be just RGD alone or is RGD even the best motif? This work will require the use of a non-sense control peptide (Alsberg *et al*, 2002). An issue specific to coronary artery smooth muscle cells is the emerging evidence to suggest that coronary smooth muscle cells differ significantly from non cardiac smooth muscle cells. (Shi *et al*, 1996, Scott *et al*, 1996 and Christen *et al*, 1999). These differences include integrin expression i.e. the very receptor the RGD motif is binding to. The integrin adhesion molecules consists of heterodimers of non covalently linked α and β subunits. There are (as of 2001) at least 16 α and 8 β different subunits. (Davenpeck *et al*, 2001). For blood vessel the β_1 and β_3 integrin families are both involved in the regulation of vascular cell functions and pathology (Luscinskas and Lawler, 1994, Sanders, 1994 and Shattill, 1995). Of all the integrins expressed on vascular smooth muscle cells

$\alpha_5 \beta_1$ is thought to be the most important for its functioning and proliferation potential e.g. $\alpha_5 \beta_1$ plays an important role in vascular smooth muscle cells changing from a contractile to an extracellular matrix synthesising phenotype (Hedin and Thyber, 1987). Furthermore, in vascular smooth muscle cells $\alpha_5 \beta_1$ mediates the assembly of fibronectin matrix assembly, which is an essential precursor for proliferation (Mercurius and Morla, 1998). This last role of $\alpha_5 \beta_1$ is probably due to it being the primary fibronectin receptor in vascular smooth muscle cells. (Takada *et al*, 1987). Pathologically, another integrin $v_5 \beta_1$ has been suggested as a key modulator in arterial narrowing due to smooth muscle cell remodelling. (Yee *et al*, 1998 and Yee and Schwartz, 1999).

However, whilst $\alpha_5 \beta_1$ plays an important role in vascular smooth muscle modulation, it is not clear whether $\alpha_v \beta_1$ also play a role, albeit to a slightly less degree. The integrin $\alpha_v \beta_1$ binds to a host of vascular extracellular matrix proteins including vibronectin and fibronectin. (Brown *et al*, 1994). Like $\alpha_5 \beta_1$, $\alpha_v \beta_1$ has also been demonstrated to be involved with fibronectin matrix assemble (essential precursor to vascular smooth muscle proliferation) plus cellular migration and proliferation. (Charo *et al*, 1990, Wu, 1997 and Slepian *et al*, 1998). Another integrin, $\alpha_v \beta_3$ has been implicated in the pathological process of arterial narrowing e.g. neointimal hyperplasia following arterial injury. This is the undesirable narrowing of arteries due to individual smooth muscle cells expanding in size in response to mechanical stimuli or trauma. (Stouffer *et al*, 1998). Furthermore, competitively blocking $\alpha_v \beta_3$ integrins after arterial trauma reduces the resultant neointimal hyperplasia. (Srivatas *et al*, 1997).

Davenpeck, (Davenpeck *et al*, 2001), has demonstrated that porcine coronary artery smooth muscle cells express few $\alpha_5 \beta_3$ integrins compared to human coronary artery smooth muscle cells. However, Davenpeck suggests that the up-regulation of $\alpha_5 \beta_3$ by coronary smooth muscle cells may be a prerequisite to their proliferation. This example alone demonstrates the importance of identifying and understanding the different integrins and their functions in different smooth muscle cell types. Of interest to this project is the difference between coronary artery smooth muscle cells and possible sources of these cells. Whilst ultimately we require a normal coronary artery for CABG surgery, it will be essential to understand the precise phenotype and behaviour of the actual autologous cells available to produce such a vessel. To this end, the scaffold with its cell attachment sites may be key. Experiments with specific

integrin binding sites e.g. CRRETAWAC (cysteine-arginine-glutaminc acid-threonine-alanine-tryptophan-alanine-cysteine) which is specific for α_5 β_1 (Koivunen *et al,* 1994), may well help resolve which integrins are required for cell attachment and/or proliferation of the chosen autologous cell type. Finally, it may be essential to switch the encapsulated cells into the desired cardiac artery smooth muscle cell phenotype prior to implantation if, for example, neointimal hyperplasia is not to ensue.

9.0 Optical coherence tomography

For tissue-engineered products to become first-line therapies in routine clinical practice, they will need to be both more effective than conventional therapies whilst demonstrating a high degree of safety. This will require the constructs to be produced in a highly reproducible and economic manner. This will necessitate constant monitoring techniques to be employed which need to be both non invasive, non harmful to the developing tissue construct and cost effective.

The technology chosen for this project to achieve the potential for continuous non invasive, non harmful monitoring is optical coherence tomography (OCT). It is believed to be one of the earliest deployments of OCT in tissue engineering. Prior applications include various clinical applications, namely ophthalmic (viewing pathological progressive eye disease e.g. macular degeneration, the leading cause of blindness in those aged over 55 in the Western World), new clinical applications (e.g. determining cancerous changes in oesophageal tissue *in vivo*) and examining industrial coatings. Its application to this project includes the monitoring of vessel wall thickness plus some very preliminary data on flow through the construct whilst *in situ* (Mason *et al*, 2004a, Mason *et al*, 2004b).

9.1 Background on OCT

OCT represents a paradigm shift over conventional optical light microscopes employing advanced photonics and fibre optic technology. It is capable of high resolution, cross-sectional imaging of materials and biological tissues. OCT is frequently described as the optical equivalent of ultrasound scanning (USS) (Schmitt, 1999, Tadrous 2000 and Fujimoto *et al*, 2000). This analogy is made since OCT involves shining a beam of near infrared light into tissue and then sensing the magnitude and depth of any light reflected back (back reflection or back scatter i.e. the light equivalent of acoustic echo), (Tadrous, 2000) from the structures within the tissue.

Professor James Fujimoto at MIT, the principle proponent of OCT, believes it is best for illustrative purposes to describe the visualisation of the operation of OCT by thinking of a light beam as being composed of short optical pulses, however, in reality whilst OCT can be performed using short pulse light, most OCT system actually use continuous wave short coherence length light (Fujimoto *et al*, 2000). The following account therefore uses this "short optical pulse" model when describing the various unit operations that make up OCT.

With USS, the relatively slow speed of sound allows the detection of the tissue's structures by measuring directly the time of flight of individual pulses of sound from the emitter to the target and back to the receiver. The velocity of sound in water is in the order of 1500 $msec^{-1}$ whereas

the velocity of light in water is in the order of 3×10^8 msec^{-1}. Because the velocity of light is many orders of magnitude greater, such direct measurement even using the most advanced electronics is not possible. Since distance or spatial information can be determined from the time delay of reflected light (i.e. equivalent to echo delay in USS) by using the formula:

$$\text{Reflected light delay} = \frac{\text{Distance travelled by reflected light}}{\text{Velocity of light}}$$

Thus the measurement of distances or spatial dimensions on the 100 μm scale (a typical scale for USS) has an echo delay in the order of 100 nsec (100×10^{-9} seconds) for sound. However, when employing light and resolving at the 10 μm scale (a typical scale for OCT) the reflected light delay is in the order of 30 fsec (130×10^{-15} sec). Since femtosecond timing is not possible using direct electronic detection, an alternative technology is employed. The technology is based on Michelson interferometry, an idea which resulted is German born Albert Michelson (1852 - 1931) receiving a Nobel Prize for Physics in 1907 (Kyle and Shampo, 1981). Michelson's technique when deployed by OCT (termed low-coherence optical interferometry) indirectly measures the reflected light delay and the intensity of this back scattered light by comparing it to light from the same source that has travelled a known reference path length and time delay. In terms of Fujimoto's simplified model, low coherence light is made up of a number of pulses of light, each pulse lasting for an identical period of time. The time duration of the individual pulses is known as the coherence length of the light source. Overall, the shorter the coherence length of the light source, the better the final resolution of the particular OCT device.

OCT in its simplest form involves a pulse of low coherence light being split into 2 equal parts, see Figure 9.1. One half of the beam is sent to the specimen being investigated and the other half to a reference mirror. Light reflected back from the specimen is combined with the light reflected back from the reference mirror and detected by a photo detecting diode coupled to a computer to store and process the data. By moving the reference mirror, the path length travelled by both the beams of light can be made identical, i.e. to within the coherence length of the particular light source. When this occurs, the two beams will have their light waves in phase, so called constructive interference. The position of the reference mirror when constructive interference occurs is therefore an indirect measure of the depth within the specimen from which the light was reflected back. The magnitude of the constructive interference effect is a measure of the strength of the reflection (Tadrous, 2000). Thus the reflected light delay and the intensity of the backscatter from structures within the specimen can be indirectly measured by detecting and demodulating the interference output of the

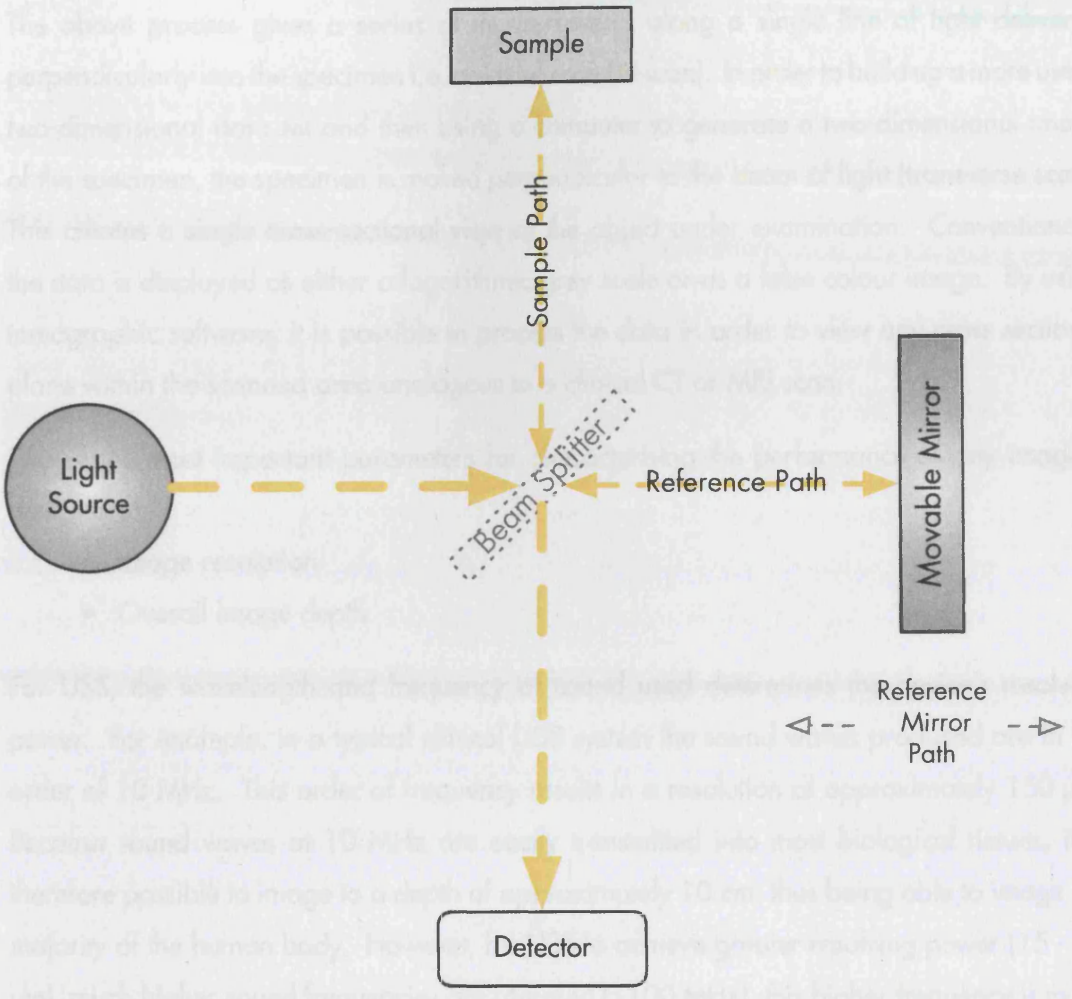

Figure 9.1

Principle of Michelson interferometry.

Interferometry works on the principle that when two light waves in exactly identical phase coincide with one another amplification will occur, however, if they are in exactly the opposite phase, they will cancel one another out.

Light from the light source is divided into two paths by the beam splitter (half-silvered mirror); one to the sample and one to the reference mirror. This light is reflected back from both the sample and the reference mirror, recombined prior to reaching a detector.

If the two path lengths differ by a whole number of wavelengths, constructive interference will occur resulting in a strong signal at the detector, whereas if they differ by exactly half a wavelength, the outcome will be destructive interference and no light will reach the detector. Thus the depth dimension of the sample is explored by scanning the optical path difference (OPD). The maximum interference signal is obtained for an OPD = 0. A reflective depth profile (A-scan) is obtained by axial scanning. This means changing the OPD by moving the mirror back in the reference path (Podoleanu *et al*, 2004).

interferometer while scanning the reference path length.

The above process gives a series of measurements along a single line of light delivered perpendicularly into the specimen i.e. an axial scan (A-scan). In order to build up a more useful two-dimensional data set and then using a computer to generate a two-dimensional image of the specimen, the specimen is moved perpendicular to the beam of light (transverse scan). This creates a single cross-sectional view of the object under examination. Conventionally the data is displayed as either a logarithmic grey scale or as a false colour image. By using tomographic software, it is possible to process the data in order to view any cross sectional plane within the scanned area analogous to a clinical CT or MRI scan.

Two of the most important parameters for characterising the performance of any imaging device are:

- Image resolution
- Overall image depth

For USS, the wavelength and frequency of sound used determines the device's resolving power. For example, in a typical clinical USS system the sound waves produced are in the order of 10 MHz. This order of frequency results in a resolution of approximately 150 μm. Because sound waves at 10 MHz are easily transmitted into most biological tissues, it is therefore possible to image to a depth of approximately 10 cm, thus being able to image the majority of the human body. However, for USS to achieve greater resolving power (15 - 20 μm), much higher sound frequencies are required (>100 MHz), this higher frequency is much less easily able to penetrate the body (maximum of a few mm). Thus, there is a trade-off between resolution and tissue penetration. In contrast, OCT has far higher resolving power than USS, being able to resolve structures down to 1 μm in size and is sensitive to differences in refractive index between different tissue structures (Fujimoto *et al*, 2000). Unfortunately, light unlike sound, is highly scattered by tissue and thus limits penetration to a maximum of approximately 4 mm (Fujimoto, 2003b).

Since its invention, OCT has had a very rapid adoption by the clinic. The technique was first demonstrated *in vitro* by Fujimoto in 1991 (Huang *et al*, 1991). Two years later the first *in vivo* OCT imaging was performed in humans (Fercher *et al*, 1993 and Swanson *et al*, 1993). By 2000, at the New England Eye Centre alone over 10,000 patients had benefited from this imaging modality. Today over 1600 hospitals have OCT machinery installed (Fujimoto, 2003a) To date, OCT's main clinical applications have been in the field of ophthalmology e.g. macula degeneration, an incurable eye disease which affects more than 10 million Americans (Drexler *et al*, 2003). However, its clinical role is now extending into many other areas including cardiovascular disease (Brezinski *et al*, 1996), oncology (Fujimoto

et al, 1995), dermatology (Welzel, 2001, gastrointestinal medicine (Brand *et al*, 2000), respiratory medicine (Yang *et al* 2004), neurology (Boppart *et al* 1998c) and dentistry (Otis *et al*, 2000). Effectively, OCT is producing an optical equivalent (optical biopsy) of the former traditional surgical excision biopsy but in real time. By being able to resolve down to 1 μm, the method offers the histopathologist a potential alternative to conventional histology and cytology. Furthermore, in comparison to conventional excision biopsy, light biopsies are far safer and much less painful, being totally non-invasive (OCT does not require direct contact unlike USS which requires close contact including the presence of optical coupling gel). Since these images are in real time, diagnosis is immediate as too can be necessary advice to the surgeon e.g. providing information that all of a cancer has been removed (excision margin). In current clinical practise OCT can resolve structures in the region of 2-4 μm (Boppart *et al*, 1998a and Bouma *et al*, 1995 and Boppart *et al*, 1997 and Fujimoto *et al*, 1995 and Fujimoto *et al*, 1998), not yet as good as conventional light microscopy, but adequate to distinguish tissue morphology. However state-of-the-art research devices can easily resolve individual animal cells and to be further able to distinguish nucleus from cytoplasm with some degree of intranuclear detail (Tadrous, 2000). However, in development are OCT systems using short pulse $Ti:Al_2O_3$ lasers which generate coherence lengths of approximately 2 optical cycles which produce resolution in tissue *in vivo* approaching 1 μm (Drexler *et al*, 1999 and Boppart *et al*, 1998b). At this level of resolution even cell and organelle membranes are clearly visible. At present femtosecond lasers are not an option clinically due to their high cost (over $250,000) and complexity. However, the OCT industry is being greatly aided in its research and development by the giant global telecommunications industry with its similar demands for lower cost light sources and optic fibre cables.

It was against the above background of a fast developing technology with the ability to already perform high resolution *in situ in vivo* light biopsies that it was decided to evaluate if OCT has a role to play in the automation of tissue engineering and in the monitoring of the fabrication of substitute artery in particular.

In terms of application to vascular studies, OCT has already started to demonstrate its potential for imaging blood vessels both *in vitro* and *in vivo*, including Fujimoto's research group who had been the first to successfully image microvascular tissue (Brezinski *et al*, 1997). Since this preliminary work, *in vivo* vascular applications started to be reported (Brezinski *et al*, 1997, Brezinski, 2002, Kehlet *et al*, 1999, Nelson *et al*, 2001, Barton *et al*, 2001 and Wong *et al*, 2002). The uses to date have included the three-dimensional visualisation of blood vessels to assist in assessing the efficacy of laser therapy for port-wine stain birth marks (Kehlet *et al*, 1999, Nelson *et al*, 2001). In order to treat port-wine stains it is necessary to permanently and significantly reduce the blood flow to the lesion. This is performed using laser therapy to

create irreversible microthrombus formations in the vessels to and from the lesion. However, if the position and number of the relevant vessels is unknown then a common result is incomplete or unacceptable clinical outcomes. However, when optical Doppler tomography (ODT) was used as the imaging device, the efficacy of the laser treatment could be observed in real time. ODT combines laser Doppler flow studies with OCT, thus it is possible to visualise the vessel and the actual reduction in blood flow through the vessel to the specific lesion.

Animal work has demonstrated that OCT has a potential role in improving the efficiency of photothermal coagulation beyond the realm of real time monitoring of port-wine stain laser therapy (Barton *et al,* 2001). Wong has demonstrated that sub-surface blood vessels can be easily visualised in the skin of rats *in vivo* (Wong *et al,* 2002). Wong reported that by using ODT it was easily possible to visualise cross-section and vessel diameter as well as bidirectional blood flow velocity. Local haemostatic interventions including sclerosant injections, heat probes and lasers were observed for their ability to permanently stop blood flow in the visualised vessels. These observations were later confirmed by conventional histologically.

In order to further improve the usefulness of OCT/ODT, contrast agents are being studied in order to enhance the image analogous to barium contrast agents and conventional X-ray to visage soft tissue e.g. barium meal to image the gastro-intestinal tract. One promising contrast agent for OCT is microbubbles injected into the lumen of the vessel(s) being examined (Barton *et al,* 2002). Microbubbles are already employed in clinical USS to enhance blood vessels images (Correas *et al,* 2001).

The ability of OCT to resolve the structure of blood vessels has been demonstrated during the surgical repair of small blood vessels following trauma (Culberton *et al,* 1990 and Wyrick and Stern, 1992). OCT has proven capable of providing the surgeon with real time images of the subsurface and the lumen of the vessel being repaired i.e. intra-operative monitoring which would otherwise be impossible using a conventional operating microscope. The preliminary *in vitro* work was once again performed in Fujimoto's laboratory (Boppart *et al,* 1998c). Using OCT it is possible to view an artery's morphology i.e. lumen, tunica interna, tunica media and tunica adventitia.

9.2 Preliminary Investigations - Kent OCT Device

Since OCT was being used to demonstrate its potential in the field of vascular structures and flows, it was decided to evaluate its feasibility for tissue engineering. Professor Fred Fitzke at the Institute for Ophthalmology, London, UK, kindly agreed to allow this preliminary work to be undertaken on his research/clinical based OCT device (Kent OCT) at The Institute for Ophthalmology. The Kent OCT unit was designed and built as a pure research unit by Dr.

Adrian Podoleanu and Professor David Jackson both of the University of Kent (Canterbury, UK). The principle is depicted in Figure 9.1 A brief description of the basic Kent device now follows. Light from a pigtailed super luminescent diode of wavelength 850 microns was injected into a single-mode directional coupler, which transmits a percentage of the optical power into the sample arm. Light in the sample arm was propagated through a phase modulator. Light subsequently travelled via a microscope objective, entered an orthogonal scanning mirror pair and passed through a converging lens, 6 cm in diameter with a focal length of 60 mm, which brought the light to convergence at the lens of the human or animal model. The reference beam, which also emerged from the single mode directional coupler, was of much higher power than the signal beam and was directed via two sequential microscope objectives and mirrors to the detectors, The two mirrors were mounted on a computer controlled translation stage, which could be moved continuously at a constant speed or discretely in steps. Polarisation controllers were mounted in both the sample arm and in the reference arm. Two photo detectors, collected the returned optical signals and their outputs were applied to the two inputs of a differential amplifier. The signal was then demodulated and subsequently applied to a variable scan digital frame grabber. Since the Kent device was built solely for *in vivo* ophthalmology studies, many of the components e.g. directional coupler, polarising controller, microscope objective, orthogonal scanning mirror pair and a converging lens were mounted on the chin rest used to accommodate the patient's head (Above description adapted from the original description in Podoleanu *et al*, 1998).

Because the device was primarily designed for imaging the posterior chamber of eyes of either small rodents for research purposes or humans for diagnostic/monitoring purposes; the basic set up was not ideal for examining long tubular structures compared with the near roundness of eye balls. It therefore required an adaptor device to be designed and manufactured in order to place the tube to be visualised in an upright position at a distance from the light emerging from the "half mirror" of approximately +/-1 mm the same position as an *in vivo* eye would be positioned. Without this adaptor the device had too little gross adjustment. Furthermore, the adaptor had to hold the tube assembly perfectly still (i.e. vibration free), hence it was bolted to the main optic bench supporting the OCT device, otherwise adjusting the reference mirror to obtain the necessary constructive interference would have been impossible.

9.2.1 Materials and methods

Alginate tubes were produced using both the very early pneumatic driven piston device/float regulated device as well as the first of the pump driven fluid/regulator devices - During this period of time, the far superior pump driven fluid/ball regulator device had not yet been evolved - see Section 6.4 - Semi-automated Mark II System. Tubes were fabricated from either 1% or 2% Manugel alginate (ISP) in physiological saline. Cross-linkage was performed using

1% calcium chloride also in physiological saline. After formation, the tube forming glass compartment was carefully removed from the rest of the tube forming apparatus with the calcium chloride solution and alginate hydrogel still *in situ*. All the ports were then sealed using either small rubber bungs or machined PTFE stoppers to prevent the calcium chloride solution leaking out. These sealed components were then either stored at 4°C or transported immediately to The Institute of Ophthalmology for OCT visualisation.

With the Kent OCT device it was very easy to visualise the air/glass outer boundary and the glass/calcium chloride solution boundary (the alginate hydrogel tubes are not attached to the glass formation tube but instead there is a thin layer of liquid between the glass tube and the alginate tube). However, it was very difficult to visualise the calcium chloride solution/ hydrogel tube boundaries. Increasing the concentration of alginate from a 1% to a 2% solution made no discernable difference with the Kent OCT device. Other problems included only being able to visualise either the front wall of the tube or the back wall of the tube at one time due to the lack of adjustment range built into the device. Thus to visualise the front part of the tube, the adapter had to be positioned such that the front wall of the tube was correctly placed with respect to the light source and then to view the back wall of the tube, the adaptor had be unscrewed from the optical table and repositioned closer to the light source, so that now the back wall of the tube was then in the correct plane. The tube could in principle be rotated through 180° but this was not compatible with the software to build up the final two-dimensional image. The adjustment built into the device was designed to provide detailed images of the optic retina, a structure in the order of three hundred microns thick and not a glass walled tube of 1.6 mm thick containing a hydrogel tube with a wall of approximately 100 - 300 μm thick *let alone* the fact that the glass tube's diameter was overall 7.2 mm in diameter - i.e. nearly an order of magnitude out of the range of the device. Altering the adjustment was not possible due to the overall design of the Kent device.

Matters were made worse due to the device being designed to be used with the eye. The eye has two focusing structures, the main focusing structure is the cornea with the adjustable lens providing the necessary fine tuning to focus light onto the retina. The refractive index of the human lens and cornea are approximately 1.4 and 1.376 respectively. The device was therefore calibrated for this arrangement. The refractive index of the glass wall of the tube (Duran© glass) was 1.473 (λ = 587.6 nm) (Data sheet - Schott Glass UK, Stafford, UK) . As a result, measurements obtained with the tube forming device had a lens-effect factor due to the circular glass tube wall e.g. for the 4 mm inside diameter glass tube the magnification was approximately 1.6x. This resulted in the reference mirror being required to be move over 2.5 mm just to image the front wall of the tube. Combined with the diameter of the lumen of the glass tube (diameter of 4 mm), this made imaging of anything other than the glass wall

only or the alginate construct alone possible due to limitations of the total amount of gross adjustment possible.

Because the hydrogels could not easily be viewed with the device i.e. the liquid/hydrogel outer boundary and hydrogel/liquid inner boundary could not be easily discerned, a contrast agent was required. Since in practice the alginate tubes would contain mammalian cells which were known to be capable of being visualised by the Kent OCT device - the layer of rods (elongated cells 50 x 3 μm) and cones (elongated cells 60 x 1.5 μm) making up the retina were regularly seen when the device was used to visualise patients' eyes, it was decided to use glass beads of similar overall dimensions (Podoleanu *et al*, 1998). Glass beads of 3 - 10 microns in diameter (Polyscience, Warrington, Pennsylvania, USA) were added to the alginate solutions and then thoroughly mixed for several hours on a roller. Glass beads were added at a concentration initially of 0.1% weight/volume. Due to the large refractive index difference between the beads and the surrounding hydrogel it was possible to easily visualise the bead/hydrogel constructs. A series of range finding experiments were performed with different glass bead concentration. In general 0.01% weight/volume bead:alginate solutions were used, as this was more economic on the glass bead ($1000 per gm) but still provided excellent OCT visualisation. Interestingly it was probable that the lack of substantial refractive index difference between the hydrogel and the liquid which made visualisation difficult was due to its composition - even a 2% alginate hydrogel is approximately 98% water. Glass beads were used as substitute cells in order to allow a large number of preliminary experiments to be performed without worrying about the issues involved in transporting and storing actual cellular material across London. Also the beads gave a high degree of flexibility in terms of working arrangements i.e. allowing experiments to be slotted in between the clinical duties of the Kent OCT device. The device, however, was suitable for living cell work since it used a 843 nm wavelength near infrared light source which is consistent with the exposure limit for permanent intrabeam viewing stipulated by the American National Standard Institute (Washington, USA).

Experiments were carried out using cell culture media (Dulbecco Modified Eagle's Medium, Gibco BRL, Gathersburg, Maryland, USA) to displace the cross-linking agent, the cell culture media made no difference to the device in that it still permitted easy viewing of the bead/hydrogel tube and glass outer tube as discrete entities separated by a thin layer of fluid.

9.2.2 Results and discussion

In order to sample the tube at various positions along its length, the tube had to be physically moved up and down in its adaptor. Scanning a number of glass rods (3) along their length (15 cm - the maximum length the adaptor/OCT device could accommodate) confirmed that

the precision bore tube had an average inside diameter of 4 mm +/- 20 μm (after correction for the lens effect). This agreed well with the data from Glass Precision Engineering (Leighton Buzzard, Bedfordshire, UK) who specify that their manufacturing tolerance is +/- 10 μm. The bead/hydrogel tubes were easily visualised and their wall thickness determined. Overall the results were disappointing in terms of physical consistency. OCT tube imaging often exposed complete absences of wall for short distances (up to a few cm) and a very wide range of thicknesses, up to a maximum of just over 300 μm. The more gross wall discontinuities could be confirmed by visualisation of the same sample under a light microscope but only when OCT had identified them. The wall discontinuities and a lack of consistency were shortcomings in the reliability of the particular tube fabrication device at its particular stage of development and not the OCT device, i.e. they were real and not artefacts. Previous attempts to measure the wall thickness *in situ* using a vernier microscope had suggested this problem but the measurements were difficult since visualisation was poor for two main reasons. Firstly even when using glass beads:alginate solution at 1% weight/volume it was difficult to detect discrete wall edges and secondly the glass acted as a lens which distorted the image.

Measuring the hydrogel tubes out of the glass tubes was complicated, if not impossible, for 3 reasons. Firstly, handling the tubes i.e. removing the tubes from their glass supports is potentially likely to distort the hydrogel's dimensions due to their overall fragility. Likewise, trying to measure the hydrogel once out of the glass tube with a vernier gauge is extremely difficult since the hydrogel is totally transparent (although food colouring can be added to partially overcome this difficulty), but more importantly the fragility of the hydrogel and its permanent deformability also hinders any direct measuring process. Finally, if the tubes are exposed to air on removal from their glass formers, drying out quickly occurs (syneresis) which therefore changes their overall dimensions.

Finally, one preliminary experiment was performed to confirm that alginate constructs containing mammalian cells could be visualised without glass beads as a contrast agent. Tubular constructs were fabricated using immortalised rat smooth muscle cells (A7r5) at a final concentration of 10^5 per ml of 1% alginate solution. No glass beads were added and the calcium chloride solution was displaced with cell culture media (DMEM) after 20 minutes. The constructs were placed on ice for transportation. The construct was then visualised using the Kent OCT device approximately 1 hour later (the fastest possible time for travel between the two sites). The alginate/cell constructs were clearly visible with the Kent OCT device but again wall consistency was extremely poor. In terms of OCT detection, the beads and the cells gave almost identical images on the Kent OCT device. Thus confirming that the beads were a reasonable alternative for experimental studies.

9.2.3 Conclusions

The Kent device experiments demonstrated that OCT was potentially capable of delivering quantitative data with respect to hydrogel tube wall thickness, however, this particular machine was far from ideal being produced solely as a clinical/animal research ophthalmological device. Some of the disadvantages could potentially have been over come e.g. using refractive index fluid (Cargille, Cedar Grove, New Jersey, USA) formulated for the correct specific refractive index for the specific wavelength around the glass tube to try and correct the difference in magnifying effect between glass tube and cornea/eye/lens. However, overall the capability for visualising the posterior chamber of the eye compared with tissue engineered tubular constructs were too deeply designed into the device for any real modifications to be made. Furthermore, the particular device was under an ever increasing clinical work load and therefore gaining time slots was proving more and more difficult. It was therefore decided to look for an alternative, more research orientated OCT source, preferably one which was not specifically designed for a particular application such as the Kent device. Another requirement was to switch to a totally optic fibre based system, since the design and the fabrication of the Kent machine, the optic fibre technology had moved forward at a fast pace due to pressures from the booming telecommunications industry. A totally optic fibre based system is an essential prerequisite if OCT were to be used for the automation of tissue engineering since it is far easier to have an optic fibre connected to each bioreactor rather than moving individual bioreactors to the OCT device each time visualisation is required (this arrangement is still perfect for the clinical setting).

9.3 Cranfield OCT

Through a collaboration with Professor Ricky Wang (Cranfield Biomedical Department, Cranfield University) an alternative OCT device (Cranfield OCT) was made available. The Cranfield OCT was based on a fibre optic implementation of the Michelson interferometric principle (Wang and Elder, 2002). Below is a brief overview of the Cranfield system, a schematic overview is depicted in Figure 9.2. A broad band 1 mW light source (super luminescence diode - $\lambda = 823$ nm with a spectral band width of 25.2 nm (Superlum, Moscow, Russia) was coupled to an optic fibre via a collimating lens. The light then travels in the fibre to a 50/50 optic fibre coupler (the solid state equivalent of a half mirror) where the beam of light is split. One beam of light then travels on via optic fibre to a moving reference mirror i.e. the reference arm of the interferometer. The other beam travels on and via another collimating lens and an objective lens to the specimen i.e. the sample arm. When the light reflected from the reference arm is combined with the light from the sample arm, these two beams of light will interfere if the two paths are different by less than the coherence length of light. A broad band light source is used since the broader the spectral width the greater the axial resolution of the particular OCT system.

Figure 9.2

Schematic overview of the Cranfield OCT.

Key:

C = Collimator lens
D = Detector
DM = Double pass mirror
G = Grating
L = Lens
M = Mirror
ND = Neutral density filter
PC = Polarisation controller

Image courtesy of Professor Ricky Wang - Cranfield University.

The amplitude of the reflected light as a function of depth within the specimen is obtained by scanning the reference mirror at a constant velocity and then digitising the magnitude of the resulting interferometric fringes. Cross-sectional images were obtained by recording sequential axial reflectance profiles whilst the sample is moved transversely across the path of the light beam. This movement was carefully controlled using a precision made stage and stepper motors.

Using the Superlum 823 nm super luminescence diode as the broad band light source results in a 1.2 μm axial resolution in air or 8.8 μm in tissue (assumes that the average refractive index of bulk tissue is 1.37) (Wang and Elder, 2002). The transverse resolution was 16 μm (N.B. axial and transverse resolution are not linked in OCT as they are in conventional confocal light microscopy). Imaging was performed by directing low coherence light at the glass tubes with the alginate hydrogel tubes *in situ* and detecting the reflections from its internal structures by the use of an optic fibre integrated scanning system. Polarisation controllers were used in both the reference and sample arms in order to maximise fringe detection. This OCT system employs a balanced detection scheme to minimise the excess noise arising from the Superlum light source (Above description adapted from the original description in Wang and Elder, 2002). Being a research based instrument and having the advantage of being totally fibre optics based, the device was of a far simpler construction than the Kent OCT system (plus a 75% reduction in overall physical size) thus allowing far easier modification and customisation for a particular application.

Sealed glass tubes with their hydrogel construct *in situ* were placed flat on a purpose made adaptor on a motorised two-dimensional translation stage. Gross focusing was aided by a visible light source passing down the sample arm.

Two types of experiment were performed; static and dynamic. The static experiments were performed on either hydrogel tubes containing glass beads or hydrogel tubes containing mammalian cells. These static experiments were to measure wall thickness and continuity. Dynamic experiments were performed using cell hydrogel constructs to explore the possibility of using OCT to monitor flow characteristics within constructs.

9.3.1 Alginate/glass bead constructs

9.3.1.1 Materials and methods

Initial experiments were performed exactly as per the original Kent OCT experiments, except that the tube forming device will the ball regulator was used through out (Just prior to collaborating with Professor Wang, experiments had shown that the use of a ball compared to the earlier "missile" shaped regulator resulted in highly consistent alginate construct

formation - see Section 6.4 - Semi-automated Mark II System), it was therefore decided to only use the ball devices for Cranfield University experiments in order to maximise effective use of available OCT time). This tube forming device had already demonstrated a linear relationship between the amount of alginate solution added to the device and the length of tube subsequently produced. Furthermore the results were highly reproducible (see Section 6.4.2).

Alginate solutions were prepared using Manugel DMB alginate (ISP, Tadworth, Surrey, UK) dissolved in normal physiological saline (0.9% sodium chloride (Sigma, St. Louis, Missouri, USA)) dissolved in water for injection (BioWhittaker, Walkersville, Maryland, USA). After adding the alginate powder, the solutions were rolled on an SRT2 roller mixer (Stuart Scientific) overnight. Since visualisation with the Institute of Ophthalmology OCT device had been poor when using alginate alone it was decided to again use the glass bead construct agent at 0.01% weight/volume. The beads were 3 - 10 μm in diameter (Polyscience, Warrington, Pennsylvania, USA). After adding the glass beads the mixture was rolled for a further 2 hours to ensure homogeneity. Calcium chloride solution was produced at 1% weight/volume (Sigma, St. Louis, Missouri, USA) also in physiological saline.

Tubes were constructed from 1% solutions using a combination of different precision glass bore tubes (Glass Precision Engineering, Leighton Buzzard, Bedfordshire, UK) and regulator balls (Precision Plastic Ball Company, Ilkley, Yorkshire, UK). Both the ball and tube manufactures claimed a tolerance range of +/-10 μm for their respective products. Three combinations of the glass tube/ball regulator device were used resulting in different wall thicknesses - see Figure 9.3. The 3.65 mm inside diameter glass tube and 3.4 mm diameter ball regulator combination was not used as previous experiments had revealed that the gap between the float and the glass wall of 0.125 mm was considered to be probably inadequate to produce a useful tissue engineered construct. From previous range-finding experiments, the resulting final wall thickness can be estimated to be approximately 45 - 55% of the gap size for this range of sizes. Therefore only combinations of ball/tube sizes appropriate for tissue engineering were used, i.e. the combination with gap sizes of 0.238 mm, 0.3 mm and 0.413 mm.

The ball regulated device was operated as previously described in Chapter 6. The syringe driver (Harvard PHD 2000) was set to deliver the calcium chloride solution at a fixed rate of 20 $mlmin^{-1}$.

Aliquotes of the homogeneous glass bead/alginate solution were drawn up into a precision 1 ml ground glass syringe with care to expel all the air bubbles prior to adding 600 μL to the device. At this stage in the research, there was only a limited number of base units available, therefore in order to prepare a reasonable size batch of tubes for transportation to Cranfield

Tube/regulator combination	A	B					C
Gap between glass tube wall and regulator (μm)	238	300					413
Inside diameter of glass tube (mm)	3.65	4.00					4.00
Diameter of ball regulator (mm)	3.174	3.400					3.174
Tube	1*	2	3	4*	5*	6**	7
Average alginate/ glass bead construct wall thickness (μm)	115.6	157.0	154.0	159.0	144.2	173.0	205.6
No of samples	5	6	6	6	5	6	5
Standard deviation	18.83	5.2	8.49	30.15	21.24	12.03	12.04
Wall thickness/ Gap	49%	52%	51%	53%	48%	58%	50%

* Careful examination of the raw data suggested that these constructs were slightly flawed possible due to the regulator becoming minimally contaminated by gelled alginate shortly after commencing the process (i.e. commencing as a regular walled tube an then suddenly becoming very slightly thinner).

** Larger wall thickness may have been due to this experiment having a 10x concentration of glass beads compared to all the other data in this table. Alternatively, it may have been a problem with the size of the regulator and/the glass tube. (The beads and the glass tubes were both precision manufactured to a tolerance of +/-10 μm. This degree of accuracy could not be checked by UCL micrometers e.g. Mitutoyo PK-0505 has a manufacture's claimed accuracy of +/-20 μm and Swiss Precision digiMax has a manufacture's claimed accuracy of +/-10 μm).

Figure 9.3

Table of results for experiments conducted using different combinations of glass tube/ball regulator sizes to produce alginate/glass bead constructs with walls of different thicknesses.

Data generated in collaboration with Garr Chau (UCL) and Dr. Yonghong He (Cranfield University).

University to undergo OCT evaluation, the glass tubes with the hydrogel constructs *in situ* were carefully removed from the base units and carefully stoppered in order to retain the calcium chloride solution. The individual base unit could then be cleaned and attached to a fresh glass tube to produce another hydrogel construct. The drawback of this approach was that the hydrogel tube had to be disrupted by twisting the base unit through 90 - 180° relative to the glass tube in order to sever the hydrogel plug attaching the hydrogel construct to the base unit. In practise, in a bioreactor this detachment would never be used since the plug is essential to maintain the constructs attachment to the base unit. Tubes were transported in a vertical position since early experiments quickly revealed that if any bubbles were present when carrying the tubes in a horizontal position resulted in the hydrogel tubes being easily damaged.

The glass tubes with their hydrogel *in situ* were mounted vertically on the OCT motorised translation stage. The beam of visable light was focused on the glass tube which grossly focused the beam of near infrared light in the sample arm of the device. The device was set to sample at a frequency of 20,000 samples per second. Because of the drawback to using the bungs (potential damage to the extremes of the hydrogel constructs) it was decided to only measure the centre portions of the 15 cm long tubes. OCT images were therefore produced at the centre of each tube (7.5 cm) plus 2.5 cm in either direction (5 cm + 10 cm). Thus the first 5 cm and the final 5 cm of each tube was not examined.

The data set for each scan was converted to computer image via a Matlab programme (The MathWorks, Natwick, MA, USA) to produce a cross-sectional format with the horizontal axis representing the dimension along the tube and the vertical axis representing depth below the surface. Because of the 1.6 mm thickness of the wall of the glass tube only the glass/liquid interface is present. The air/glass interface was easily detected but due to the design of the machine could not be captured if the hydrogel tube was to be included in the scan. Since the hydrogel tube was the object of interest the position of the air/glass interface was not required. The computer images were exported as high resolution .jpg files for later examination. Using Photoshop 7 (Adobe, San Jose, CA, USA) it was possible to measure the thickness of the tube walls. (Later experiments did not have this intermediate step, instead a MatLab program was written to extract the thickness directly from the data files).

9.3.1.2 Results and discussion

As well as scanning the tubes longitudinally at the 5 cm, 7.5 cm and 10 cm mark, additional data was obtained by axially rotating each tube through 180°. The tubes were also scanned transversely. Figure 9.4 shows a typical longitudinal image and Figure 9.5 shows typical cross-sectional images of an alginate/bead construct in the forming tube. The results for the

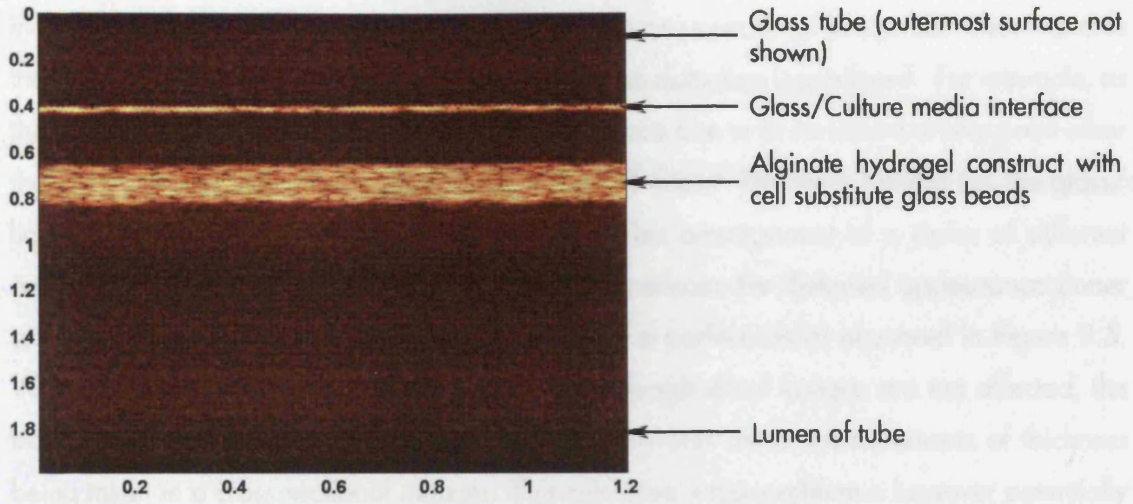

Figure 9.4
A typical computer generated longitudinal image of an alginate/glass bead construct created using the combination of a 4 mm inside diameter glass rod and 3.6 mm diameter ball regulator.

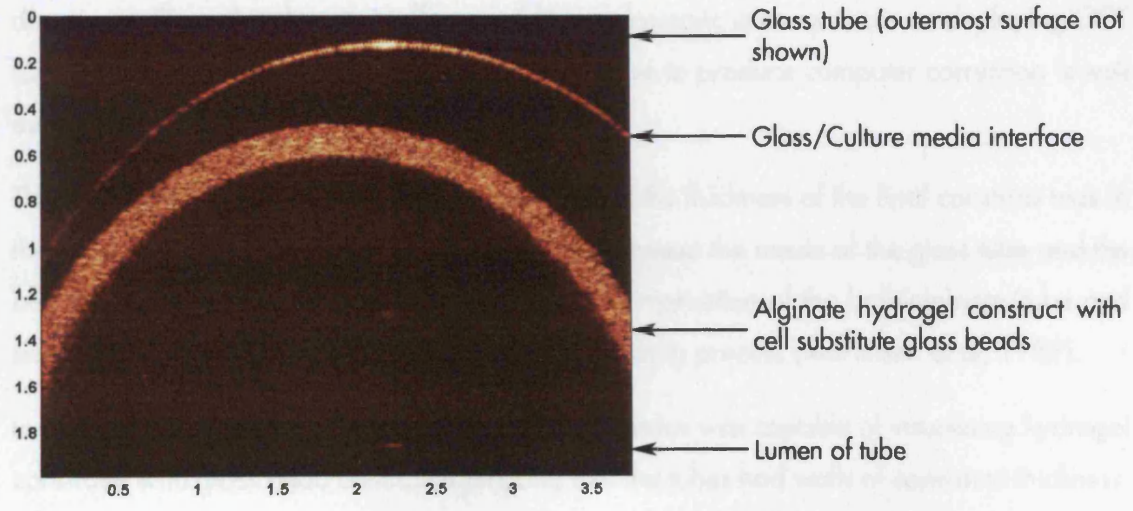

Figure 9.5
A typical computer generated crosssectional image of an alginate/glass bead construct created using the combination of a 4 mm inside diameter glass rod and 3.6 mm diameter ball regulator.

three different tube forming combinations is contained in Figure 9.3.

As with the original Kent OCT experiments, the glass beads provide the contrast agent by appearing as bright yellow dots due to their different refractive index to the surrounding hydrogel. Both cross-sectional and transverse images show the wall of the constructs are independent of the wall of the rigid glass tubes. The cross-sectional image also demonstrates that due to the round geometry of the glass tube and distortion is produced. For example, as the near infrared beam reaches the air/glass interface due to its curvature at any point other than that perpendicular to the beam, refraction will occur. The layer behind i.e. the glass/ liquid interface will therefore appear distorted. This arrangement of a series of different angles as the beam passes through the sample produces the distorted appearance (inner surface of glass tube does not appear as a part of a perfect circle) observed in Figure 9.5. Whilst perpendicular to the long axis of the tube longitudinal images are not affected, the transverse scanning distortion problem currently prevents direct measurements of thickness being taken in a cross-sectional manner. This refractive index problem is however potentially resolvable in a very simple manner. Professors Adrain Podeanu and David Jackson (University of Kent, Canterbury, Kent, UK) have demonstrated that a computer correction can be made if the ratio of curvature, refractive indices and perpendicular specimen thickness are known. From this data, corrected images can be produced (Charalambous *et al*, 2003, Podoleanu *et al*, 2004). Charalambous has demonstrated for the cornea in eyes that a longitudinal scan of 2 mm produces a distortion of greater than 0.2 mm in both the axial and longitudinal directions. Since this distortion effect would have dramatic consequences on deploying OCT for monitoring refractive index eye surgery, the drive to produce computer correction is well established.

The data presented in Figure 9.3 demonstrates that the thickness of the final construct was in the order of 50% of the size of the physical gap between the inside of the glass tube and the ball regulator. This is due to a combination of the interaction of the ball/alginate/tube and also the shrinkage which accompanies the cross-linking process (Martinsen *et al*, 1989).

In conclusion, having demonstrated that the OCT device was capable of visualising hydrogel constructs with glass bead contrast agent and that the tubes had walls of consistent thickness, it was decided to undertake similar experiments with cells instead of the beads (Mason *et al*, 2004a).

9.3.2 Alginate/cell constructs

9.3.2.1 Materials and methods

A 1% alginate solution (weight/volume) was prepared by adding Manugel DMB (ISP,

Tadworth, Surrey, UK) to physiological saline (NaCl - Sigma, St. Louis, Missouri, USA; WFI - BioWhittaker, Walkersville, Maryland, USA). This solution was then agitated by rolling over night. Adult mesenchymal stem cells were harvested as previously described and mixed with homogeneous alginate solution by gentle pipetting. The final density of cells was 3 x 10^6 per ml. Aliquotes of 600 µl were drawn up into 1 ml syringes to load the tube forming device.

The same three glass tube/ball regulator combinations were deployed as for the alginate/ glass bead experiments (see Figure 9.3 for dimensions). Glass tubes of 12 cm in length were used since 600 µm is adequate to produce a 12 cm tube. The syringe driver (Harvard PHD 2000) delivering the calcium chloride was set at the same fixed rate as for production of constructs for all the OCT experiments - 20 $mlmin^{-1}$. The syringe driver was run until long enough to expel the excess cell/alginate mixture together with the float from the glass tube.

A small quantity (<200 µL) of calcium chloride solution was removed from each tube in order to allow a very small air space and thus facilitate the insertion of rubber bungs required for transportation. In order to avoid damaging the tubes by needing to detach the base unit, and because of the success of the earlier experiments deploying glass beads, addition base units were fabricated. The bases could therefore be left connected to the glass/tube and thus not disturb the cell/hydrogel attachment plug. The devices with the constructs *in situ* were transported for scanning at Cranfield University in the vertical position.

9.3.2.2 Results and discussion

As previously, the tube forming device was mounted horizontally on the motorised translation stage for OCT evaluation. Overall the quality of the OCT images was very similar to the alginate/glass bead experiments (a situation witnessed previously with the Kent OCT device) despite the difference in size and refractive indices. Like the glass beads, the mesenchymal stem cells acted as an excellent "contrast agent" due their relatively high refractive index compared to the surrounding hydrogel. Figure 9.6 shows a typical longitudinal image and Figure 9.7 a typical cross sectional image. Figure 9.8 shows a series of longitudinal scans (arranged in order) along the entire length of an alginate/cell construct. The images show the ease with which the flexible tissue-engineered construct is free to move from side-to-side within the glass tube. This is inferred by the changing extralumenal gap between the construct and the glass tube along the length of the construct. Likewise OCT imaging in exactly the same location before and after gentle rotation resulted in images with identical wall thickness but different extralumenal gap widths. The 4 mm inside diameter glass tube/ 3.4 mm float combination had its construct's wall thickness imaged every 15 mm along two aspects - 180° apart - see Figure 9.8. For the other glass tube/float combinations, only the mid point of each tube plus one point 15 mm distal and 15 mm proximal. Again the tube was rotated to

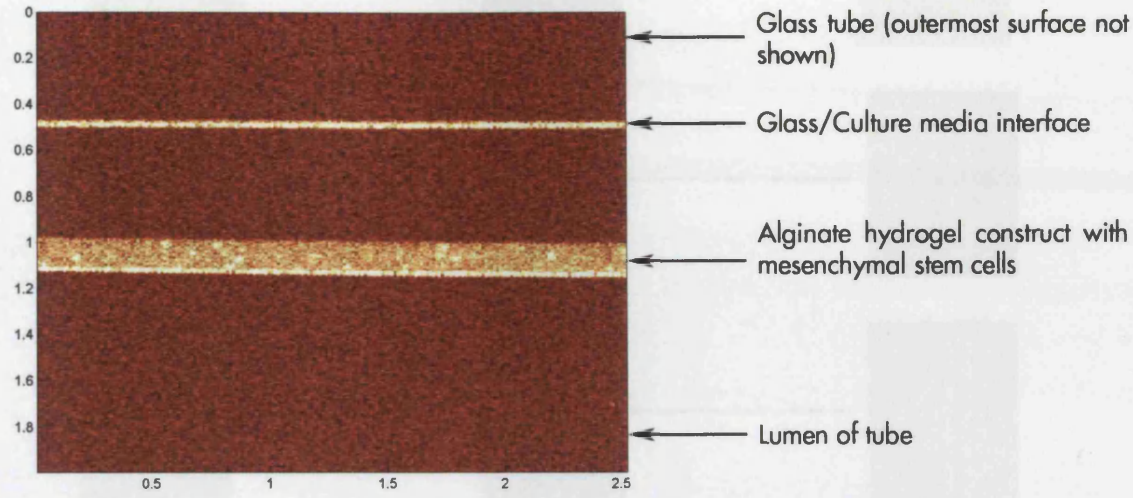

Figure 9.6
A typical computer generated longitudinal image of an alginate/mesenchymal stem cell construct created using the combination of a 4 mm inside diameter glass rod and 3.6 mm diameter ball regulator.

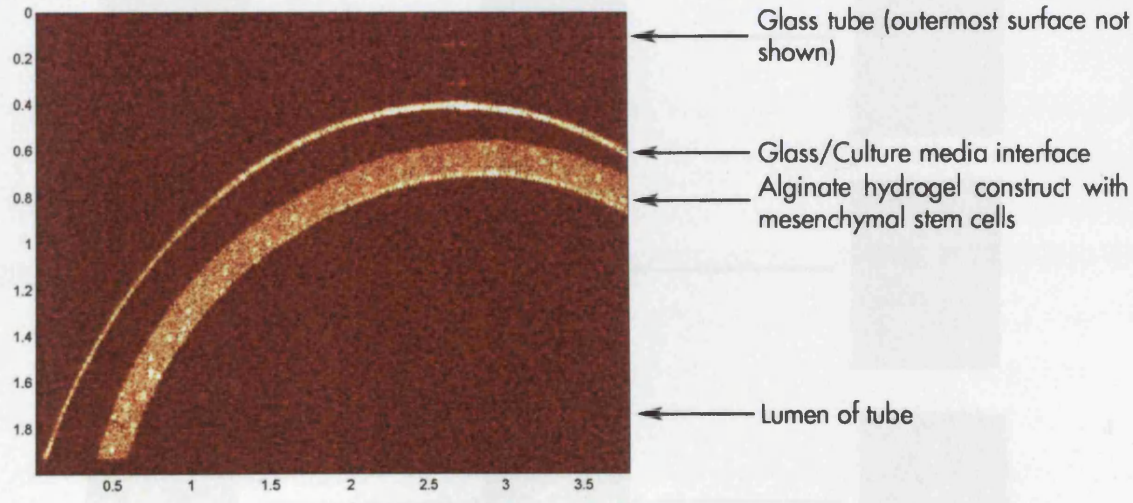

Figure 9.7
A typical computer generated cross-sectional image of an alginate/mesenchymal stem cell construct created using the combination of a 4 mm inside diameter glass rod and 3.6 mm diameter ball regulator.

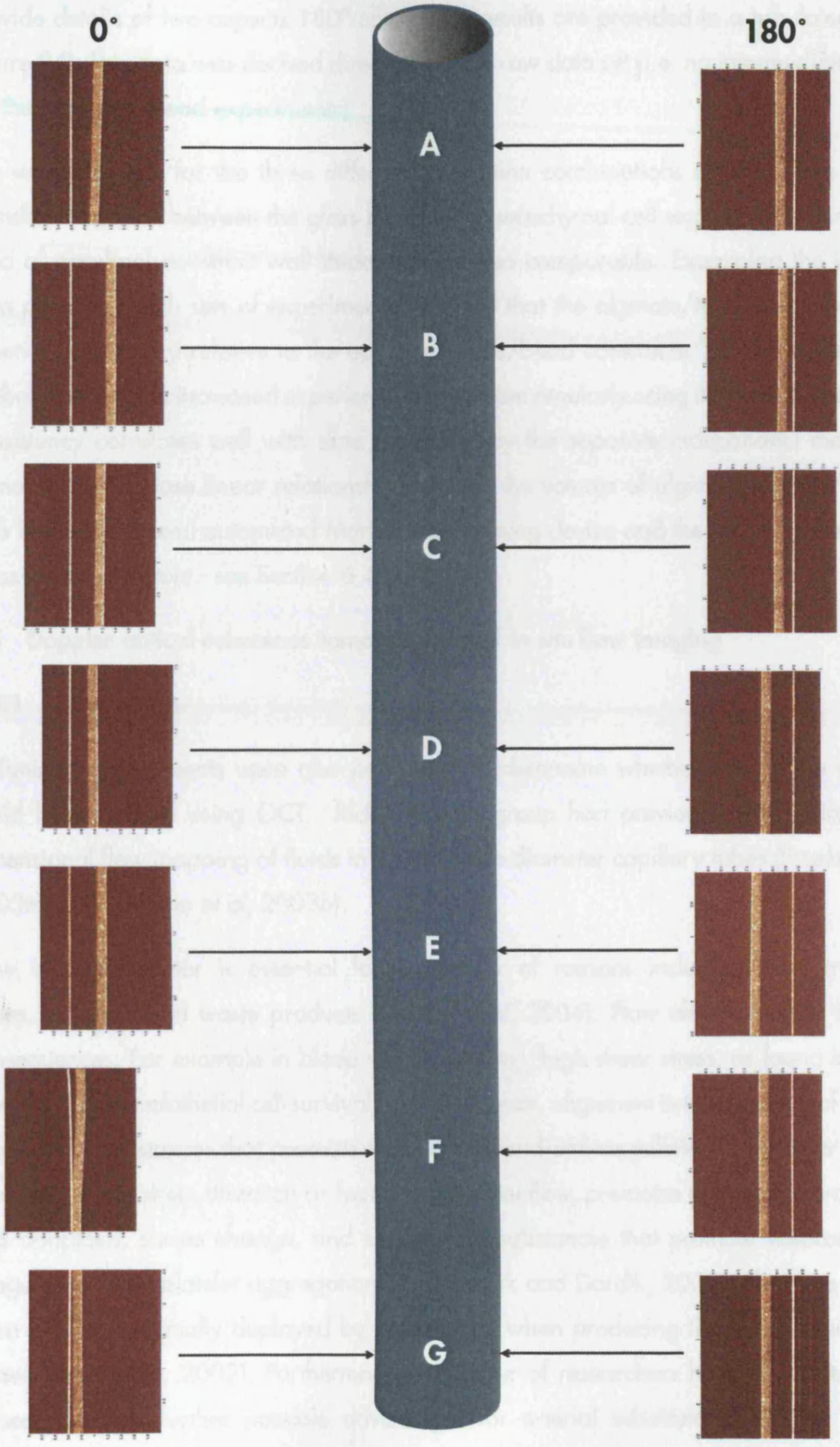

Figure 9.8
OCT computer generated images of an MSC/alginate construct in situ produced using the combination of a 4 mm I/D glass tube/3.4 mm ball regulator. Average wall thickness 0.145 +/-15 µm (n = 14).

Construct imaged at 15 mm intervals at 0° and 180° (Glass wall aligned).

provide details of two aspects 180° apart. The results are provided in a tabulated form in Figure 9.9. This data was derived directly from the raw data set (i.e. no intermediate steps as for the cell/glass bead experiments).

The wall thickness for the three different fabrication combinations of glass tube and ball correlate very well between the glass bead and mesenchymal cell experiments. Likewise, the ratio of gap:final construct wall thickness was also comparable. Examining the individual data points for both sets of experiments, revealed that the alginate/MSC tubes were of far superior consistency relative to the earlier alginate/bead constructs. This improvement was probably due to the increased experience gained from regularly using the device. The physical consistency correlates well with data generated by the separate independent method that demonstrated a close linear relationship between the volume of alginate solution/beads or cells loaded into semi-automated Mark II tube forming device and the length of the resulting cross-linked construct - see Section 6.4.2

9.4 Doppler optical coherence tomography and *in situ* flow imaging

9.4.1 Introduction

Preliminary experiments were also performed to determine whether flow in the constructs could be visualised using OCT. Ricky Wang's group had previously demonstrated two-dimensional flow mapping of fluids in 1 mm inside diameter capillary tubes (Proskurin *et al*, 2003a and Proskurin *et al*, 2003b).

Flow in a bioreactor is essential for a number of reasons including mass transfer of gases, nutrients and waste products (Martin *et al*, 2004). Flow also has other biological consequences. For example in blood vessels *in vivo*, "high shear stress, as found in laminar flow, promotes endothelial cell survival and quiescence, alignment in the direction of flow, and secretion of substances that promote vasodilation and anticoagulation. Low shear stress, or changing shear stress direction as found in turbulent flow, promotes endothelial proliferation and apoptosis, shape change, and secretion of substances that promote vasoconstriction, coagulation, and platelet aggregation" (Paskowiak and Dardik, 2003). Flow has therefore been almost universally deployed by researchers when producing tissue-engineered blood vessels (Tranquillo, 2002). Furthermore, a number of researchers have demonstrated that pulsed flow has further possible advantages for arterial substitute fabrication including enhancing their physical properties possibly by affecting the rate of extracellular matrix deposition and remodelling (Solan *et al*, 2003).

Ricky Wang's group have described a technique that employs laser Doppler optical coherence tomography (DOCT) to estimate accurately two-dimensional flow mapping for a highly light

Combination	A	B*	C
Gap between glass tube wall and regulator (μm)	238	300	413
Inside diameter of glass tube (mm)	3.65	4.00	4.00
Diameter of ball regulator (mm)	3.174	3.400	3.174
Average alginate/ mesenchymal stem cell construct wall thickness (μm)	110	145	195
No of samples	6	14	6
Wall thickness/ Gap	46%	48%	47%

*Published: Mason *et al*, 2004a

Figure 9.9

Table of results for experiments conducted using different combinations of glass tube/ball regulator sizes to produce alginate/adult mesenchymal stem cell constructs with walls of different thicknesses.

Data generated directly from the raw data (error +/-15 μm) in collaboration with Prof Ricky Wang and Dr. Yonghong He (Cranfield University).

scattering fluid flowing in a tube (Proskurin *et al*, 2003b). By combining OCT with Doppler velocimetry a technique Doppler optical coherence tomography is possible (Wang *et al*, 1995, Proskurin *et al*, 2003b and Moger, 2003). DOCT is a non-invasive imaging technique for determining fluid flows in highly light scattering media or biological tissue. This is based on the principle that the Doppler frequency shift in the light that is backscattered from the moving objects within a sample either adds to or subtracts from the fixed Doppler frequency, depending on the flow direction. DOCT is starting to be used in clinical applications, e.g. providing quantitative cross-sectional imaging of flow in retinal blood vessels (Yazdanfar *et al*, 2000). OCT utilises only the amplitude of back-scattered light as a function of depth within the tissue, whereas DOCT additionally employs interferometric phase information to monitor Doppler shifts in the back-scattered spectrum. The phase-sensitive detection of interference of the back-scattered light from the tissue and reflected light from a moving reference mirror enables in-depth localisation of the Doppler shifts arising from flow in the sample. Thus, DOCT is capable of producing simultaneous imaging of both the tissue's architecture and its localised blood flow. To date, DOCT has been used to measure blood flow profiles captured in a few milliseconds in human retina (Yazdanfar *et al*, 2003) and skin (Zhao *et al*, 2000; Nelson *et al*, 2001).

Data are summarised here as a "gold standard" to judge the effectiveness of the near identical DOCT device in a tissue engineering bioreactor setting with an alginate/MSC construct *in situ*. The particular device deployed by Professor Proskurin (member of Professor Wang's group at Cranfield University) used a light source with a wave length of 1298 nm with a band width of 52 nm delivering 0.5 mW of power. The highly light scattering fluid flowing through the target tube was a 0.5% intralipid solution [Intralipid solution is a fat based emulsion which is widely used as a phantom material for the investigation of the optical properties of biological tissues (Driver *et al*, 1989)]. The tube was a cylindrical transparent capillary tube with an outside diameter of 3 mm with a wall thickness of 2 mm. The capillary was mounted on a goniometer that could be set to the desired Doppler angle (perpendicular viewing of flow is not possible with DOCT). Flows with Reynolds numbers in the range 30 - 100 were created to ensure laminar flow. A typical laminar velocity flow profile generated by DOCT is shown in Figure 9.10. The figure shows a typical parabolic flow profile for a Newtonian fluid flowing in a laminar fashion (Proskurin *et al*, 2003a and Proskurin *et al*, 2003b).

9.4.2 Materials and methods

A description for the proof of principle experiments with respect to the potential of deploying DOCT to monitor flow through tissue-engineered constructs *in situ* now follows (Mason *et al*, 2004b). It was decided to use a hydrogel tube constructed using the 4 mm inside diameter glass tube/3.174 mm ball regulator combination. Initial experiments with Professor

Figure 9.10

DOCT proof of concept experiment - Proskurin *et al*, 2003a, 2003b. DOCT computer generated spectroscope image of laminar flow (1.8 ml/min) in a capillary tube with a lumen of 1 mm and wall thickness of 2 mm (top picture). For orientation purposes, the bottom picture has the same image superimposed on a cartoon of the glass capillary tube (walls shown in grey) plus flow direction arrows. The fluid velocity within the lumen was a typical parabolic shape for a Newtonian fluid in a fully developed laminar flow with the highest velocity at the mid-line and zero flow at the edge. These data are presented as a "gold standard" to judge the effectiveness of the near identical DOCT device in a tissue engineering bioreactor setting with an alginate/MSC construct *in situ*. Spectroscopic image courtesy of Prof. Ricky Wang (Cranfield).

Proskurin's 1298 nm device used for his original flow work (Proskurin *et al,* 2003a and Proskurin *et al,* 2003b) resulted in very poor quality OCT images, but switching to the 823 nm wavelength device used for the static experiments described above resulted in near perfect images after some simple optimisation. Thus from these preliminary experiences, it would appear that the 823 nm light source is far superior to the 1298 nm light source for tissue engineering applications in terms of image quality (the reason for this discrepancy requires elucidation). The circuit of the 823 nm device was therefore properly modified to allow the Doppler component from the 1298 nm device to be combined with OCT.

The tube forming device with its construct *in situ* was placed on the goniometer at an angle of 5° from perpendicular to the glass tube. A 0.5% intralipid solution was flowed through the device being careful to prevent air bubbles entering the device. Flow was by gravity feed from an overhead container at a rate of 20 $ml min^{-1}$. After passing through the construct the fluid exited via a tube pushed over the glass and was collected in beaker for recirculation. Once the system was running with no air bubbles, a haemostat clamp was applied to the silastic tube running from the reservoir to the device in order to stop the flow. A series of images were taken to demonstrate static conditions.

9.4.3 Results and discussion

A flat velocity profile was obtained, see Figure 9.11. The haemostat was then removed, once flow had resumed for several seconds (steady state), another series of images were obtained, see Figures 9.12 (Mason *et al,* 2004b). The only limitation of the set up was that because of the thickness of the tube, 4 mm inside diameter with a wall thickness of 1.6 mm (compared with the capillary used to generate the image in figure 9.10 which had a 1 mm inside diameter and 2 mm wall thickness) is was only possible to image half the tube at a time. However, half a parabola can be clearly seen in the partial scan shown in Figure 9.12. This parabolic velocity profile suggests that the flow through the lumen of the construct is laminar in its behaviour. From the Doppler frequency shifts shown in the spectrogram data, the fluid velocity can be estimated. After correcting for the Doppler angle (85°), the estimated maximum flow velocity in the centre of the lumen was 54 $mm sec^{-1}$. Concurrently, there was also a very slow flow in the space (approximately 280 μm) between the construct and the glass wall (i.e. between points a + b).

The "gold standard" (Figure 9.10) and the experimental data (Figure 9.11) derived from the tissue-engineered construct give very similar flow profiles - parabola shape, which for a Newtonian fluid would suggest laminar flow. It is believed that this is the first time that flow has been imaged in a tissue-engineered construct *in situ.*

9.5 Conclusions

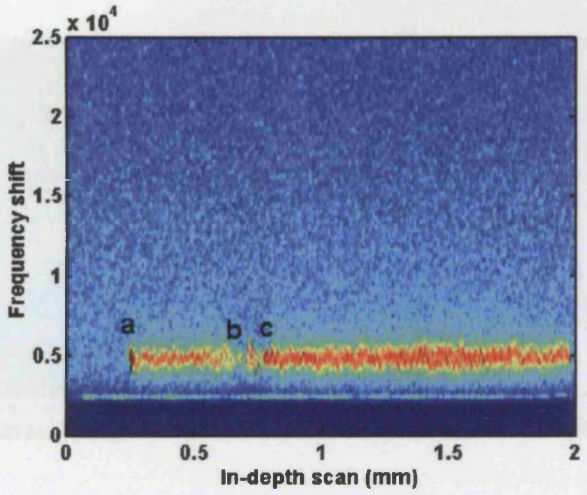

Figure 9.11

DOCT - No flow through *in situ* construct.
DOCT computer generated spectrogram image of conditions of no flow in an alginate/mesenchymal stem cell construct produced using the combination of a 4 mm I/D tube/3.174 mm ball regulator. Only a partial scan is shown (approximately one half of the inside of the glass tube). Point a is at the point of the glass tube/fluid interface, point b is at the fluid/outer edge of the construct interace, point c is at the inner edge of the construct/liquid interface. The distance between points b + c is the thickness of the wall of the construct = 220 +/-9 microns. The image shows a flat velocity profile. The outer surface of glass tube not shown.

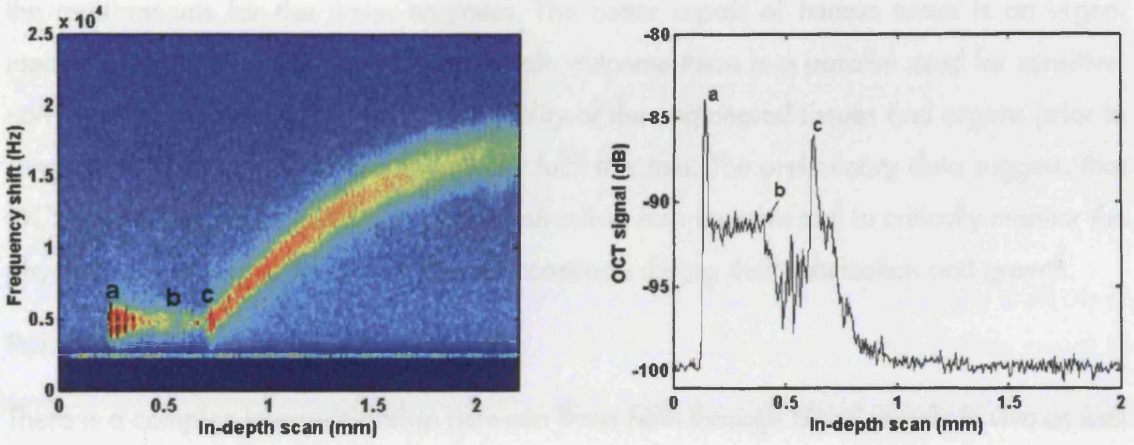

Figure 9.12

DOCT - Laminar flow through *in situ* construct.
A spectrogram image of steady state flow (approximately 20 ml/min) through the same tissue-engineered construct as in Figure 9.11 together with its corresponding OCT structural/depth profile. Only a partial scan is shown (approx. one half of the inside of the glass tube). Points a, b and c are as per Figure 9.11. The parabolic velocity profile suggests that the flow through the lumen of the construct is laminar in its behavior. From the Doppler frequency shifts shown in the spectrogram data, the fluid velocity can be estimated. After correcting for the Doppler angle, the estimated maximum flow velocity in the centre of the lumen was 54 mm/sec. Coexisting, there was also a very slow flow in the space (approximately 280 microns) between the construct and the glass wall (between points a + b). This undefined flow profile in this extralumenal region may be as a result of the combination of flow along the extralumenal path and flow back and forth through the pores of the construct. The outer surface of glass tube not shown.

In proof of principle experiments, OCT and DOCT have each been demonstrated to be capable of both imaging for physical consistency and for quantifying and characterising flow through tissue-engineered constructs *in situ*.

9.5.1 OCT

In summary, the role of OCT for the clinician, the natural scientist including developmental biologist, and the material scientist is rapidly evolving. The same demands that are driving this progress (real time, non-invasive, non-destructive and low operating costs) match exactly the requirements for the tissue engineer. The better repair of human tissue is an urgent medical goal and in order to achieve a safe outcome there is a parallel need for sensitive, non-invasive methods of assessing the quality of the engineered tissues and organs prior to surgical implantation. OCT can potentially fulfil this role. The preliminary data suggests that OCT can be utilised as a real time, non-destructive, non-invasive tool to critically monitor the physical consistency of tissue-engineered constructs during their fabrication and growth.

9.5.2 DOCT

There is a complex interrelationship between flows both through blood vessels *in vivo* as well as engineered vessels *in vitro*. Being able to understand this interrelationship has enormous implications for the tissue engineer. DOCT is a novel optical instrument already starting to be developed to study rheology properties of tissues quickly, easily and safely *in vivo*. Capable of precise non-invasive real-time imaging, it is potentially ideal for the continuous monitoring of engineered tissues *in vitro*. A detailed velocity flow profile generated in real time can directly provide the engineer with a variety of crucial information including the state of flow, i.e. turbulent, transitional or fully developed laminar flow. The latter is likely to prove essential for the engineering of substitute arteries. Indirectly the flow velocity data allow the shear rate to be calculated from the gradient of the derived velocity profiles. For a parabolic profile, the shear rate is greatest at the wall of the tube and lowest at the centre. If the viscosity of the culture medium is known, the shear stress can be calculated, e.g. for the critical interface between the culture medium and the innermost layer of cells forming the lining of the lumen of the living construct. Flow characteristics and shear stresses are essential factors to be able to monitor in order to control and thus maintain the *in vitro* tissue in a healthy state. Furthermore, accurately manipulating these factors may potentially be a means of stimulating growth and maturation of the constructs in a non-pathological manner, thus potentially shortening production times and reducing costs.

In conclusion, OCT and DOCT when combined appear to be a promising solution for on-line quality control monitoring and analysis of flow in sterile, sealed bioreactors.

10.0 Final discussion, conclusions and future research

10.1 Final discussion and conclusions

For thousands of years doctors have treated patients with a variety of medications and surgical interventions. Depending upon the particular presenting pathology, few of these treatments however provide life-long cures. The vast majority of these therapies manage symptoms but at a price e.g. side effects and continual financial expense. Regenerative medicine by deploying living cells alone or in combination with a scaffold (tissue engineering) potentially offers a superior alternative - a permanent cure.

Many challenges lie ahead before regenerative medicine products become first-line routine clinical practice, including the mass production (allogeneic therapies) or mass customisation (autologous therapies) that will eventually be required if these types of therapy are to be produced in adequate quantities to meet clinical demand. Both the discovery phase and scaling of the production requires an interdisciplinary approach of far greater complexity and magnitude than today's biopharmaceutical drugs. Furthermore, production needs to comply with current good tissue practices (CGTP) whilst meeting at an overall price which is acceptable to both healthcare providers and patients.

The necessary bioprocessing for regenerative medicine products is very different from the current biopharmaceutical manufacture where the cells are used as small factories to produce a pharmacologically active substance e.g. a monoclonal antibody or a recombinant protein. The well-being of the cells in these processes is only of issue with respect to their output of the biopharmaceutical. Regenerative medicine bioprocessing is quite different in that instead of deploying cells to make pharmaceutical products, the cells are the final product and their welfare is therefore the number one priority. Furthermore, the bioprocess starts with the collection of living material from a patient (autologous) or donor (allogeneic) and ends at the implantation and integration of the living product into the patient. Taking this whole bioprocessing approach, this thesis has studied a number of the potentially core issues including:

- Suitable scaffold polymers
- Semi-automation of the bioreactor
- Continuous real time non-invasive monitoring

10.2 Suitable scaffold polymers

An extensive review of natural polymers is included in Chapter 2 (Alginate) and in Appendix A1 (Natural Polymers). A similar extensive review of synthetic polymers e.g. polyglycolic acid (PGA) was also conducted (not included in this thesis for the sake of brevity). The purpose was

to examine in depth the polymers currently available to the tissue engineer but with a view to automation since this was perceived from the outset to be key to the consistent production of the many units of tissue required to meet the longer term demands of routine clinical practice. It was concluded that a sterile liquid-based approach was potentially far easier to automate than a pre-formed solid scaffold based methodology. For example, it is potentially easier to produce a homogeneously cell seeded scaffold material when the polymer is liquid than when the polymer is in a pre-formed three-dimensional shape. However, this requires the liquid polymer to be capable of being fabricated into a three-dimensional geometry using mild "cell friendly" conditions. This prerequisite rules out the present generation of synthetic materials which require high temperature or caustic agents (Thomson et al, 2000) hence the focus on natural materials. Animal based products e.g. collagen were ruled out on the basis of poor batch to batch variability and more importantly their potential to transmit zoonoses e.g. prion and retroviruses. (In the future, when recombinant versions are produced in volume, these issues will no longer be a problem.) It was therefore decided to experiment with sodium alginate (a polysaccharide derived from seaweed). Sodium alginate has an excellent record in medication including its use as a topical agent (bandages), oral medication (stomach ulcer therapies) and internally (cell encapsulation). Furthermore it is capable of turning almost instantaneously from a liquid into a hydrogel when exposed to calcium ions. Its main disadvantage for the tissue engineer is its inability to interact with cells. Whilst the cells could survive the process of being harvested, mixed with alginate solution, fabricated into a tube and cross-linked with calcium chloride solution, they failed to thrive (Chapter 7). This situation was remedied by covalently bonding cell friendly peptides e.g. -GRGDY to the alginate resulting in cell attachment, cell elongation and intercellular networking within the construct (Chapter 8). It must be noted that there was no evidence of cell proliferation within the different derivatised alginate hydrogels when using either immortalised rat smooth muscle cells or human mesenchymal stem cells - this also reflects the normal *in vivo* situation. If this is the case, then the implication is that the number of cells required in the finished product would have to be mixed with the derivatised alginate prior to initial fabrication. This approach may well have major benefits since the expansion of cells in culture is potentially easier and less costly than the same expansion in a three-dimensional construct.

10.3 Semi-automation of the bioreactor

Successful tissue engineering bioreactors i.e. ones capable of delivering regenerative medicine therapies to meet clinical demands require certain fundamental characteristics including:

- The ability to retain total sterility through out the entire process
- Low cost of production including sterilisation prior to use
- Ease of disposability

Furthermore, ideally the bioreactor needs to be a multitasking device i.e. one capable of taking a few cells from the patient/donor and containing all the unit operations required to produce a neo-organ without opening the device (Martin *et al*, 2004). The multitasking would include cell isolation, cell expansion and harvesting, seeding to form a homogeneous cell/scaffold construct and maturation. This thesis addresses some of the seeding and fabrication issues plus starts to explore the maturation phase of such a bioreactor.

Initial experiments were conducted using a novel electrostatic spraying methodology using fluidised alginate powder to form three-dimensional structures. The hypothesis was, that if alginate powder and desiccated cells could be homogeneously mixed prior to or during the spray process, then potentially a homogeneous structure could be built up, cross-linked with calcium chloride solution (also sprayed) to maintain the three-dimensional shape and the cells rehydrated (for brevity, details of this research are not included in this thesis). It was during this powder coating study and the insight it gave into alginate as a material, such as its ability to rapidly cross-link, that the first of the tube forming devices described in this thesis was invented (Chapter 4).

The initial tube forming device deployed a piston and rod to be drawn down a glass barrel with a regulator element in tow (Figure 4.3). Whilst this produced alginate hydrogel tubes it was far from ideal with respect to the goal of the semi-automation of the fabrication of tissue-engineered tubular constructs e.g. substitute coronary artery. The main problem was the piston and its drive rod. For example, the overall size of the device needed to be a minimum of twice the length of the tubular construct to be fabricated taking into account the length of the drive rod and its distance of travel during the fabrication process. This would have resulted in the requirement for an overall extremely large container in which to house the bioreactor which would have added to production cost (need for a larger production facility) plus transportation issues. This would have increased both the fixed and variable costs. However the piston driven device both in its manual form (Chapter 5) and its semi-automated form (Appendix 2) did demonstrate proof of concept. The fluid driven tube forming device (Figure 5.1) was established and refined as a direct response to the potential difficulties envisaged with the piston driven device. Furthermore, this alternative design simplified a number of steps including:

- Loading the device with a homogeneous mixture of polymer and cells - an in line static mixer could easily be incorporated into the device's base unit during its manufacture
- Capable of deploying standard syringes and syringe drivers instead of a complex machinery involving pistons, drive rods and drive units
- Overall the design was far more compact lending itself toward full automation

- Without the drive rods and complex loading of the cell/polymer mixture, the design was potentially better for the retention of complete sterility throughout the whole bioprocess

Having established a manual version of the fluid driven device (Chapter 5) a semi-automated version (Chapter 6) soon followed. Reliability and consistence of product were initially both problems (as they also had been with the piston driven versions). Using a number of different techniques including digital high speed video imaging (Section 6.2.1) and dynamic pressure recording studies (Section 6.3) the operating procedure was improved and the design was refined into the semi-automated Mark II system with its ball regulator (Section 6.4). This system was capable of both high reliability with respect to tube forming runs (approaching a 100% tube fabrication success record even between different operators after only a short training period of typically less than half a day) plus capable of the fabrication of cell/alginate tubular constructs of high consistency. This was confirmed by both physical measurements (Section 6.4.2) and by optical coherence tomography (Section 9.3).

10.4 Continuous real time non-invasive monitoring

An important aspect of any tissue engineering automated production system will be monitoring and control. This is especially important when autologous cells are deployed due to a number of factors including interpatient variability, biopsy size and site, and storage conditions (Mayhew *et al*, 1998). Monitoring must both allow the process to be controlled as well as integrate with standard hospital information systems (HISs) in order to keep the clinicians aware of overall progress and predicted availability in order to allow seamless and efficient scheduling of the patient's admission, work-up and procedure.

This thesis demonstrates the potential for optical coherence tomography (OCT) as a monitoring technology in the tissue engineering manufacturing process. Whilst already successfully deployed in the clinic (over 1600 machines already installed in ophthalmology departments throughout North America (Fujimoto, 2003a), its role as a low cost monitoring device for tissue fabrication is novel (Section 9.3). Furthermore by coupling a laser to create a Doppler laser optical coherence tomography (DOCT) system, the same OCT device doubles up as an instrument capable of monitoring flow through and around the tissue-engineered construct (Section 9.4). To scale OCT and DOCT to a production facility, and in the process enjoy some economies of scale, would require the linkage of a large number of bioreactors to a central OCT/DOCT device via optical fibres and using the system in a time-share mode. Since all these components are already mass produced for the highly competitive global communications industry, the cost of OCT/DOCT and the optical connections required to couple to the individual bioreactors continue to rapidly fall in price. For example, the Cranfield

OCT device costs in the order of £30,000 to assemble and could potentially service a large number of bioreactors whilst the Kent OCT which was the "state of the art" approximately five years earlier was approximately an order of magnitude more expensive to build, required a dedicated full-time technician and a large space but could only handle a single bioreactor.

10.5 Current and future research

At the end of a number of chapters are suggestions for future research, In addition, a number of the topics within this thesis are continuing to be progressed in the new Regenerative Medicine Bioprocessing Facility in the Department of Biochemical Engineering at UCL under the guidance of Professor Peter Dunnill, Professor Mike Hoare and myself. They include:

10.5.1 Derivatised alginate polymer

In collaboration with Dr. Alethea Tabor (Reader, Department of Chemistry, UCL) the research on the derivatised alginate has progressed via two chemistry undergraduate students and now a masters student. The research into the effects of derivatised alginate on human mesenchymal stem cells was continued by Julia Markusen (Merck Research Fellow who undertook a PhD at UCL) until her return to Merck, Rahway, NJ, USA in late 2004) - Paper submitted to Tissue Engineering journal "Characterisation of Adult Human Mesenchymal Stem Cells Entrapped in Alginate–GRGDY". This relationship between the derivatised alginate polymer and the cells after being cross-linked into a specific three-dimensional shape is being continued by Leda Pittarello (PhD student at UCL), Carol Chu (PhD student at UCL) and Charo Scott (Merck Research Fellow undertaking a PhD at UCL). In particular, Charo Scott's proposed research will expand further the work with the cell/alginate-GRGDY beads but will deploy the ultrascale down methodology development by Professor Gary Lye's team at UCL.

10.5.2 Automated tissue engineering bioreactors

This topic has now been sub-divided into a number of sectors which are, however, run as one integrated project. The semi-automated fluid driven bioreactor described in Section 6.4 is currently being progressed towards a fully integrated and automated system by Alfred Ding (PhD student at UCL) in collaboration with Martin Town (UCL) and Dr. Julian Mason (Kingston University). The essential parameters within the bioreactor e.g. media flow rate, dissolved oxygen tension (DOT), nutrient requirements and metabolite removal are being modelled by Spyros Gerontas (PhD student at UCL) under the guidance of Professor Mike Hoare (UCL) based on experimental data from a number of researchers within the Regenerative Medicine Bioprocessing Group. The models generated will feed directly into the design work for the automated bioreactor and its standard operating instructions. Finally the control aspects e.g. linking the data generated by the various monitoring modalities associated with the bioreactor

e.g. pH. temperature, DOT, OCT and DOCT into the control process are being researched by Matt Scutcher (PhD student at UCL) under the guidance of Dr. Yuhong Zu (UCL). A tracking system is also being devised which will integrate with both the bioreactor work and with standard HISs in order to fulfil the requirement to accurately track cells plus communicate with the hospital information systems. The research centres around radio frequency identification devices (RFID) and is in collaboration with Dr Paul Schmidt (Consultant at Portsmouth NHS Trust and CEO of Proxximity Ltd, Portsmouth, UK).

10.5.3 Optical coherence tomography

Garr Chau (PhD student at UCL) under the supervision of Dr. Susana Levy (UCL) has continued the OCT and DOCT collaboration with Professor Ricky Wang's group at Cranfield University, including beginning to study the actual moment in time and location with respect the regulator when the alginate solution becomes a gel and its effect on the final thickness of the wall of the newly formed construct. This follows on from a collaboration with Dr. Ian Eames (Department of Mechanical Engineering, UCL) and Dr. Mark Landeryou (Department of Medical Physics, UCL) to mathematically model the fluid dynamic theory underlying the Mark II semi-automated fluid driven tube forming device (paper in preparation for submission to Biotechnology and Bioengineering). Garr Chau is also developing the idea of deploying a static mixer for combining cells with polymer in order to create a totally homogeneous mixture for loading into the tube forming device whilst not effecting cell viability. The data from these mixing experiments will be analysed and mathematically modelled by Ju Wei Wong (PhD student at UCL) to help produce part of a suite of generic optimisation tools.

10.6 Summary

Overall this MRC funded PhD project has now evolved into an integrated programme of research which is continuing to expand in terms of facilities, number of in-house researchers, staff involvement and number of external collaborators. During this progression, the bioreactor methodology and design received the Overall Winner Award in the Medical Futures Innovation Awards in 2002, sponsored by the National Endowment for Science, Technology and the Arts (NESTA) and was highlighted in evidence given to the House of Commons Select Committee on Science and Technology (House of Commons Select Committee on Science and Technology, 2002) as well as receiving both national and international media attention.

APPENDIX 1

A1.0 Supplementary introductory material

This appendix contains supplementary material on two key topics:

- Scaffold concepts and physical formats
- Natural polymers

A1.1 Scaffold concepts and physical formats

This section collects together the various scaffold concepts currently available to the tissue engineer when considering the most appropriate option for a particular application. The chosen route potentially has great bearing on subsequent scale-out and manufacture for the particular tissue-engineered product to enter routine clinical practise.

1.1.1 Classification of scaffold concepts

A potential biomaterial must be compatible with the desired tissue response. Hubbell classified approaches to selecting biomaterials for various tissue engineering applications according to the type of tissue response required (Hubbell, 1995):

- Conducting or guiding an otherwise normal biological response
- Inducing a "super normal" biological response
- Blocking a naturally occurring but undesirable biological phenomenon

Scaffolds formats therefore require one or more of the above criteria in various combinations to meet different tissue engineering requirements.

A1.1.2 Scaffold formats

The various potential formats for tissue engineering have been subdivided by Pachence and Kohn of VectraMed (Plainsboro, NJ, USA) into three well defined categories; barriers, gels and matrices (Pachence and Kohn, 2000). These subdivisions have been used as a guide for the following brief review of scaffold design concepts.

A1.1.2.1 Barriers

Often in surgical procedures it is desirable to have a barrier so that the desired healing cell activity on one surface, is not disrupted by unwanted cells and their extracellular matrix migrating into the repairing zone. Good examples are; nerve repair, periodontal surgery and abdominal adhesion prevention. Barrier layers can either be flat sheets (e.g. prevention of intra-abdominal adhesions) or tubes (e.g. guiding peripheral nerve repair).

Successful peripheral nerve regeneration requires proximal to distal axonal growth whilst at the same time precluding fibroblast invasion into the gap, which would physically inhibit

the growing axon from reaching its target. Various tubular structures have been tried experimentally as suitable conduits in this situation including PGA (Strauch, 2000), poly-hydroxybutyrate (Mohanna *et al*, 2003) and collagen (Kitahara *et al*, 2000). Poly(vinyl alcohol) (PVA) is already commercially available for nerve regeneration. PVA can be formed into strong flexible hydrogels that can be easily moulded into a variety of three-dimensional shapes. This technology was created by Ku at Georgia Tech (Atlanta, USA) (Ku *et al*, 1999) and subsequently developed by SaluMedica (Atlanta, USA) as Salubria (McKenna, 2001). SaluMedica are currently investigating Salubria's properties in the field of tissue engineering especially in relationship to nerve repair using a cuff of the material to guide nerve regeneration (SaluBridge Nerve Cuff). [Peripheral nerves have been demonstrated to successfully regenerate across a gap when an entubulation technique is utilized. Thus a nerve cuff eliminates the need for a conventional nerve graft, thereby removing the need for a donor operation site with its associated potential morbidity (Lundborg *et al*, 1997).]

Periodontal regeneration means healing after periodontal surgery (e.g. treatment for advanced adult periodontitis) that results in the restoration of the tooth supporting tissue i.e. cementum, alveolar bone and periodontal ligament attachments whilst preventing epithelial ingrowth into the healing site. This can be successfully achieved using Epi-Guide bioresorbable barrier matrix (Sulzer Dental, Carlsbad, CA, USA) which organises fibroblasts and epithelial cells to help arrest unwanted epithelial migration whilst maintaining space around the teeth for development of bone and periodontal support tissues (Vernino *et al*, 1999). Epi-Guide is an 18 by 30 mm membrane made of poly(lactic acid).

Post surgical adhesions can occur following virtually all types of surgical procedure. Adhesions may cause intestinal obstruction, pain or infertility following abdominal/pelvic surgery. Such complications may require subsequent surgical intervention. The avoidance of adhesions is highly desirable. Part of the pathological formation of adhesions is due to the unwanted migration of inflammatory cells and fibroblasts and their formation of excessive extracellular matrix. Hyaluronic acid based sheets are available to combat this problem by acting as a physical barrier e.g. Seprafilm bioresorbable membrane (Genzyme Corporation, Cambridge, USA). Seprafilm turns to gel in a few days but remains *in situ* for about a week before being fully degraded. Randomised clinical trials have demonstrated that Seprafilm effectively and safely reduces the formation of post surgical adhesions for patients undergoing abdominal surgery (Becker *et al*, 1996) and pelvic surgery (Diamond, 1996).

Post implantation, barriers can undergo one of two routes; degrade (totally or partially) or become seeded with migrating cells. Any seeding of the material which eventually may happen can only occur *in vivo*, this is a contrast to the gels and three-dimensional scaffolds described below.

A1.1.2.2 Hydrogels

Hydrogels are used to encapsulate and isolate cells from surrounding tissues e.g. to preclude a host antibody response to transplanted allograft and xenograft cells. The gel approach, involves premixing cells and the liquid polymer prior to forming a three-dimensional shape which is then allowed to set to form a cell-gel construct. The most commonly used materials for hydrogel production are collagen and alginate (Wallace *et al*, 2003 and Drury and Mooney, 2003). There are, however, many potential alternative gels including sol-gels and fibrin (Mann, 2003, Boninsegna *et al*, 2003, Peterson *et al*, 1998, Ye *et al*, 2000 and Hench and Polak, 2002).

An early example of the use of gels for tissue engineering was by Bell who successfully used collagen gels as a scaffold to maintain and grow fibroblasts as the basis of a living skin equivalent (LSE) (Bell *et al*, 1981, Bell *et al*, 1983 and Bell *et al*, 1991). Bell used this technology to establish Organogenesis (Canton, USA) in 1985, and by December 1986, over 700 LSEs had been successfully grafted onto laboratory rats. This methodology was developed and refined to eventually create the commercial skin substitute product Apligraf which obtained FDA approval in May 1998 for the treatment of chronic leg ulcers.

Hydrogels have also been used for the maintenance and immunoprotection of xenograft and homograft cells e.g. hepatocytes (Balladur *et al*, 1995) and islets of Langerhans (Lanza *et al*, 1999) used for transplantation. Maintenance of the integrity of these hydrogels for long-term implants is a problem due to *in vivo* degradation, however, for tissue engineering where scaffold degradation is desirable this is an advantage. [Non-biodegradable porous materials are better suited to situations where long term integrity is required e.g. implanting immunologically non compatible cells e.g. AN69 (acrylonitrile and sodium methyl sulfonate coploymer) (Hospa, Lyon, France) (Pakhomov *et al*, 2002).]

Another application of gels for tissue engineering is organ printing. Several research centres are exploring the use of specially adapted of matrix printers to lay down human cells and bonding agents in precise three-dimension geometries, described as organ printing. Using this methodology, organ printing is automated and fully computer controlled, thus potentially capable of the high speed fabrication of tissues (Wilson and Boland, 2003). This platform technology is broadly based on personal computers that are bespoke programmed to drive highly modified inkjet type printers, plotters or "cell dispensers". The "inks" are cells and biodegradable gels (Markwald, 2003). [A recent review of organ printing can be found in Mason, 2005.]

A1.1.2.3 Preformed three-dimensional scaffolds

Preformed three-dimensional scaffolds are currently a key component for the tissue engineer for most applications. It is possible to construct an organ without using a scaffold (L'Heureux *et al*, 1998), but the mainstream approach is presently to deploy a scaffold as a temporary artificial extracellular matrix. The fundamental difference between gels and preformed scaffolds lies in the time of cell seeding with respect to the formation of the desired three-dimensional living construct. Cell seeding methodology also differs e.g. cells and solutions can be potentially mixed to homogeneity prior to gelling whilst preformed scaffolds are a much greater challenge (Radisis *et al*, 2003).

Professor Ioannis Yannas at the Brigham and Women's Hospital (Boston, USA) working with collagen sponges was one of the first to show that an important property of a successful scaffold was pore size (Dagalakis *et al*, 1980). Pore orientation, and fibre structure are also important characteristics in the design of "cell friendly" preformed scaffolds (Yannas *et al*, 1980, Yannas and Burke,1980).

Many techniques have been developed in order to form three-dimensional scaffolds from both synthetic and biologically derived resorbable polymers with or without additional "cell friendly" features e.g. treating PGA with sodium hydroxide in order to increase cell attachment (Nam *et al*, 1999). Biomaterials such as type I collagen and PGA have been used in combination with other extracellular matrix components, attachment factors, and growth factors to induce new tissue generation or damaged tissue regeneration.

Because of the rapid growth of tissue engineering over the past decade, several commercial companies are now starting to supply commercially ready-made scaffolds e.g. Cellon S.A. (Luxenburg) supply sterile PLA sheets and conduits ready for cell implantation.

A1.2 Natural polymers

This section reviews the potential natural polymers currently available to create tissue-engineering scaffolds and is supplementary to the overview of alginate and the reasons why it was specifically chosen as the scaffold material for this thesis - see Chapter 2. (An equivalent review of biodegradable synthetic polymers was also undertaken, but has not be included in this thesis)

A1.2.1 Background

Historically biomaterials were selected on the presumption that implantable medical devices should be constructed of inert materials which would not interact with the patient's tissues. Thus, their functional performance was restricted to simple mechanical or physical gaols with no true integration into the body e.g. the Charnley total hip replacement invented in 1962 by Sir John Charnley made of a metal ball and a plastic cup. However, these so

called inert materials are never totally inert *in vivo*, for example degradation and wear debris are common problems (Weightman *et al*, 1991 and Isaac *et al*, 1996). Recently, the conceptual approach to biomedical device materials is changing and biointeractivity is now the major requirement rather than inertness. For example, biomimetic synthetic polymers have been created to elicit specific cellular functions and to specifically direct cell-cell interaction (Hubbell, 1995). Today the major focus of biomaterials for tissue engineering applications centres around their biointeractivity. Often attempts to direct the cellular response with the specific biomaterial is a key design consideration e.g. the arginine-glycine-aspartate (RGD) peptide sequence has been incorporated into biomaterials in order to stimulate cell adhesion to the biomaterial (Massia and Hubbell, 1990) and subsequent cellular migration through the material (Massia and Hubbell, 1991b). Massia demonstrated that when cell-non-adhesive glass was covalently coated with the synthetic peptide glycine-argine-glycine-aspartate-tyrosine (GRGDY) human foreskin fibroblasts attached and spread by migration over the surface. Furthermore, the process of incorporating the RGD peptide into a biomaterial has been commercialised e.g. PepTide adhesive coating by Telios Pharmaceuticals (San Diego, CA, USA) consists of polytetrafluoroethylene or polyethylene terephthalate coated with RGD peptide (Olivieri and Tweden, 1999).

Due to the diversity of biological responses to different biomaterials, it is important for the tissue engineer to have multiple well characterised biomaterials options available, since each tissue application will probably call for a unique environment for its specific cell population. Unfortunately as yet there are only a few biodegradable biomaterials suitable for tissue engineering which have sufficient data e.g. *in vivo* toxicology studies, detailed knowledge of degradation mechanism and its rate.

Present day biomaterial research applications include:

- Support for new tissue growth and maturation with maximal cell-cell communication and ease of availability to nutrients and bioactive agents e.g. a tissue engineering scaffold
- Prevention of undesirable *in vivo* cellular activity i.e. as a physical barrier to unwanted tissue growth, e.g. surgically induced adhesions which are highly undesirable.
- Guided tissue response e.g. enhancing a particular cellular response while inhibiting others e.g. tubular conduits for peripheral nerve repair
- Enhancement of cell attachment and subsequent cellular activation e.g. enhancing fibroblast attachment, proliferation, and production of extracellular matrix for dermis repair
- Inhibition of cellular attachment and/or activation e.g. prevention of platelet attachment to a synthetic vascular conduit

- Prevention of a biological response e.g. blocking antibodies against homograft or xenograft cells used after transplant surgery to prevent host versus graft rejection.

(Source: a modified version from Pachence and Kohn, 2000)

Commercial biodegradable polymers suitable for tissue engineering must ideally possess:

- Robust manufacturing feasibility using validated current good manufacturing processes (cGMP), including the availability of sufficient commercial quantities of the bulk polymer and the capability to form the polymer into the final product design at a realistic cost
- Mechanical properties that adequately address short term scaffold function but do not interfere with the long term function of the construct *in vivo*
- Low or negligible toxicity of degradation products, in terms of both local tissue and systemic inflammatory and immunological responses
- Ability to deliver bioactive agents e.g. the manufacturing process is not so harsh as to render the bioactive agent inactive
- Easy to sterilise
- Possess acceptable shelf life

(Source: a much modified version from Pachence and Kohn, 2000)

A1.2.2 Collagen

Collagen consists of a family of proteins which combined constitute about one third of the body's protein (Walter and Talbot, 1996). Its major role is as an important structural protein which is found in every major tissue that requires strength and flexibility e.g. skin, cornea, bone and tendon (collagen comprises approximately 90% of the organic matrix of bone (Walter and Talbot, 1996)). Collagens are a major constituent of connective tissue and are synthesised by fibroblasts and "fibroblast-like cells" (extracellular matrix) and epithelial cells (basement membrane). Collagens are extracellular protein containing three helical polypeptide chains each approximately 1050 amino acid residues long. The three strands wind around each other to form a superhelical cable, which is held together by hydrogen bonds. The amino acid sequence of collagen is highly regular with nearly every third residue being glycine. With respect to the hydrogen bonds, the hydrogen donors are the peptide -NH groups of the glycine residues and the hydrogen acceptors are the peptide -CO groups of residues on other chains. Collagen overall is a rod shaped molecule about 300 nm long and 1.5 nm in diameter (Stryer, 1988). Although collagens are metabolically very stable, they can be easily degraded *in vivo* and removed or remodelled e.g. during growth (once the adult stature is attained, the turnover of collagen is slow). The underlying catabolic processes can be either by collagenases or non-specific proteases (Walter and Talbot, 1996).

A1.2.2.1 Type I collagen

Currently there at least 14 different types of human collagen described, most of which are fibrillar in nature, the most abundant is type I collagen (van der Rest *et al*, 1990). Due to its ease of purification from animal and human tissues (van der Rest and Garrone, 1991), abundance, (it makes up more than 90% of all fibrous proteins) and its unique physical and biological properties, type I collagen has been used extensively in the formulation of biomedical materials e.g. gels, matrices and films for soft tissue repair (Pachence, 1996). Since type I collagen is found in high concentrations in mammalian tendon, skin, bone and fascia, these are currently harvesting sources for its isolation prior to downstream processing.

Collagen has a long and successful history as an absorbable suture material e.g. catgut sutures were in use from as early as 175 AD when they were referred to by the outstanding physician, Galen of Pergamon. Galen, who built his reputation by treating wounded gladiators, used cat gut sutures in his clinical practice.

Today surgical "catgut"/gut is harvested from sheep intestinal mucosa or serosa of bovine intestine. Ethicon gut sutures (Ethicon, Somerville, USA) for example, contain a minimum of 97% pure ribbons of collagen (Ethicon Inc., 1994). In order to meet USP specifications, Ethicon processed ribbons of intestinal mucosa are electronically spun and polished into monofilament strands of the desired diameter with a tolerance of within 5 microns along the entire length of the strand using Ethicon's Tru-Gauging process (Ethicon Inc., 1994). Such accuracy is required in order to avoid thin and thick spots which if present lead to early suture failure due to fraying, which is an inherent problem with collagen. *In vivo*, plain, i.e. uncoated gut, tensile strength is rapidly lost within 7 - 10 days and is totally digested by body enzymes and macrophages within 70 days (Ethicon Inc., 1994). Since this is a xenograft there is a moderate tissue reaction as the catgut is absorbed. Plain gut is indicated for suturing tissues, which heal rapidly and require very little strength e.g. suturing subcutaneous fatty tissue. Gut suture life can be increased by exposing the collagen ribbons to chromium salt tanning solution prior to spinning into strands to form chromic gut sutures. These sutures resist *in vivo* enzymatic degradation and therefore retain their tensile strength for about double the time i.e. 10 - 14 days (Ethicon Inc., 1994).

Other medical applications of collagen based biomaterials include; processed porcine heart valves (Strawich *et al*, 1975), tendons and ligaments. Commercially available porcine valves include the St Jude Medical (St Paul, USA) Biocor porcine valve. In order to increase its resistance to wear and tear, the Biocor porcine valve is treated with glutaraldehyde. This valve has an excellent reputation spanning over 15 years (Myken *et al*, 2000).

The primary structure of collagen has a high content of proline and hydroxyproline, with every

third amino acid being glycine and shows a strong sequence homology across genera (Stryer, 1988). Due to of its phylogenetically well-conserved primary sequence, collagen is only mildly immunoreactive (Anselme *et al*, 1990). Anselme implanted bovine type 1 collagen sponge into rats and found that after 8 hours the collagen implant was filled with polymorphonuclear leucocytes, after 8 days fibroblasts had secreted a granulation tissue within the sponge and the polymorphonuclear leucocytes had almost gone. The small amount of sponge left after one month consisted of densely packed fibrils. Antibodies to type 1 collagen were not detected in the rats' blood.

The characteristics of collagen can be altered by changing the degree of intermolecular cross-linking. Collagen cross-linking can be increased through a number of physical or chemical techniques. Physical methods include: drying, ageing, anhydrous heating and irradiation (UV or gamma irradiation). Chemical modification is by adding various agents including either formaldehyde or glutaraldehyde (Pachence *et al*, 1987). Increasing the intermolecular cross-links:

- Increases biodegradation time by making collagen less susceptible to enzymatic degradation
- Decreases the capacity of collagen to absorb water.
- Decreases its solubility
- Increases the tensile strength of collagen fibres

(Source: Pachence and Kohn, 2000)

Thus by varying the amount of cross-linking, different properties can be achieved that may be suitable for different tissue engineering applications.

Substrate attachment sites are necessary for growth, differentiation, replication, and metabolic activity of most cell types in tissue culture (Pachence and Kohn, 2000). Collagen and its integrin binding domains (e.g. arginine-glycine-aspartate-threonine [RGDT] and aspartate-glycine-glutamate-alanine [DGEA] peptide sequences) allow cells to "dock" on a surface, a vital step in maintaining viable anchorage dependant cell types in culture (Yamada *et al*, 1992).

Collagen's natural cell "friendliness" lead to it being tried very early on as a scaffold material e.g. for the production of a dermal equivalent (Yannis *et al*, 1980). Yannis and Burke were early pioneers in the field of tissue engineering. After promising work with animal models e.g. experimental full thickness wounds on guinea pigs (Yannis and Burke, 1980), they successfully applied their knowledge to human patients (Burke *et al*, 1981). Ten patients with extensive burns (greater than 50% of the total body surface), had their burns surgically debrided and then treated with a skin equivalent constructed of a temporary Silastic epidermis and a

porous collagen-chondroitin-6-sulphate fibrillar dermis. Following grafting with the bilayer, fibroblasts from the wound bed quickly populated the structure. Likewise angiogenesis from the wound bed into the graft was seen, thus a "neodermis" was formed. After a further period of up to 6 weeks, the Silastic top layer was removed leaving a vascularised "neodermis" which was then covered with a conventional autologous epidermal mesh skin graft. Patients were followed up for over a year and reasonably promising functional and cosmetic results were observed. The authors stated that the benefits of this bilayered artificial skin was its ease of sterilisation, its ability to be stored at room temperature, the manufacturing process could potentially be scaled-up for mass production, and its immediate availability to surgeons.

Another pioneer in the field was Bell, who also worked with collagen based skin equivalents but was more concerned with growing the organ *in vitro* (Bell *et al*, 1981). His laboratory produced living constructs consisting of a dermal equivalent made from fibroblasts cast in a collagen matrix and then seeded with epidermal cells to provide an epidermis, thus a bilayered structured was formed ready for implantation (Bell *et al*, 1983).

One of Bell's first living skin equivalents was constructed from human fibroblasts, in soluble rat tail collagen in the form of a contracted gel (Bell *et al*, 1981). Bell, armed with a series of successful attempts at using these living constructs formed Organogenesis Inc (Canton, USA) in order to further this work, resulting eventually in the FDA approved skin product Apligraf. Organogenesis use bovine tendon as the source of their type I collagen. Apligraf has demonstrated its clinical advantage over conventional wound healing approaches and has gained FDA approval for both venous leg ulcer treatment (May 1998) and diabetic foot ulcer treatment (June 2000) (Falanga *et al*, 1998). An alternative source of collagen is deployed by Smith and Nephew (formerly Advanced Tissue Sciences (La Jolla, USA)) who initially grew well charachterised human fibroblasts and specifically cultured these cells to produce a human collagen scaffold prior to epidermal cell seeding. The resulting product Dermograft is also FDA approved for chronic leg ulcers (September, 2001).

Although there are many suggested uses for collagen in medicine, there are presently only a few commercially available collagen devices. Possible reasons include:

- High cost of preparing pure type I collagen versus producing synthetic biomaterials
- Variability of isolated collagen e.g. cross-linking density, fibre size trace impurities
- Difficulties in handling and storage of collagen c.f. synthetic polymers
- Potential transmission of pathogens e.g. prions

(Source: a modified version from Pachence *et al*, 1987)

Mainly due to the concern over the issue of prion transmission, recombinant human collagen types I and III have been manufactured (FibroGen Incorporated, San Francisco, CA, USA).

FibroGen presently produce commercial human collagen using yeast fermentation through the insertion of a human collagen gene. However, in collaboration with PPL Therapeutics (Edinburgh, Scotland) FibroGen also created human collagen in "safe" (i.e. believed to be pathogen free) transgenic animals which secrete human collagen in their milk. Finally in order to reduce costs, FibroGen has also demonstrated that human collagen can be produced as a transgenic plant product. This last development could have the ability to produce sizeable quantities of quality collagen at significantly reduced cost compared to the present yeast based process, thus overcoming the present problems of using animal derived collagen. Fibrogen currently has an NIH funded program to evaluate its recombinant collagen technology in the field of tissue engineering.

A1.2.2.2 Small intestinal submucosa

Small intestinal submucosa (SIS) is a naturally occurring complex extracellular matrix derived from xenograft sources, most commonly porcine. The submucosa is found between the inner mucosa and outer muscular layers of the intestine. After being harvested, small intestine is mechanical stripped of its mucosal layer leaving an acellular tube or if cut open a flat sheet. SIS is thus a naturally derived matrix. The *in vivo* function of the submucosa is to provide strength to the intestine and is predominantly a complex of matrix collagens type I, II and V. It is also a reservoir for cytokines that guide repair and replacement of the high turnover intestinal epithelial cells. SIS is extracted from the intestine in a manner which retains the natural composition of the matrix collagen molecules, growth factors (e.g. TGF-β, FGF-2, VEGF), glycosaminoglycans (hyaluronic acid, chondroitin sulphate, heparin and heparin sulphate), proteoglycans and glycoproteins (e.g. fibronectin). These retained bioactive substances signal cells to repopulate the SIS and form new tissue, i.e. the SIS acts as an interactive scaffold for cell incorporation and tissue remodelling (Voytik-Harbin *et al*, 1997). The manufacturing process used by one of the main commercial proponents of SIS, namely Cook Biotech Incorporated (West Lafayette, USA) has been FDA validated to ensure that any retained animal viruses are completely inactivated. Other steps have been taken to ensure that SIS is safe including:

- Strict control of porcine production facilities
- Use of a validated disinfection process in addition to terminal sterilisation
- Independent laboratory testing to verify biocompatibility of the material
- Extensive multicentre preclinical testing
- No harmful immunological responses observed in either animal or human studies e.g. SIS has not been shown to activate the complement cascade *in vitro* unlike the complement involved hyperacute rejection observed in porcine whole organ xenografts into primates (McPherson *et al*, 2000)

(Source: Cook Biotech Inc. SIS Sales Literature, 2000)

SIS can be cut, rolled or folded in order to produce a specific three-dimensional shape. It can then be sutured or stapled in order to retain this desired shape. The shelf life of SIS is in the order of 1 year.

Cook Biotech have produced a variety of SIS based products including Oasis (a sheet of SIS for skin regeneration), Stratasis (aimed a providing pubourethral support as a sling of SIS for use in the treatment of female urinary incontinence), Surgisis (soft tissue bulking implantation material), Vivosis (tissue culture disks, sheets and inserts) and VetBiosist for veterinary applications.

A1.2.3 Proteoglycans and glycosaminoglycans

Proteoglycans are proteins containing one or more covalently linked glycosaminoglycan chains. Human connective tissues are rich in proteoglycans, which consist of units made of polysaccharide (approximately 95%) and protein. These very large polyanions bind water and cations and thereby form the extracellular matrix (ECM) of tissues. Proteoglycans are important in joints and other structures that are subject to mechanical deformation. Glycosaminoglycans (GAGs), the polysaccharide chains in proteoglycans, are made up of disaccharide repeating units containing a derivative of an amino sugar, either glucosamine or galactosamine. At least one of the sugars in the disaccharide has a negatively charged carboxylate (e.g. carboxyl group of glucuronic acid in hyaluronic acid) or sulphate group (e.g. dermatan sulphate) (Walter and Talbot, 1996). Hyaluronate, chondroitin sulphate, keratan sulphate, heparan sulphate, and heparin are the major glycosaminoglycans. In the proteoglycan from cartilage, keratan sulphate and chondroitin sulphate chains are covalently attached to a polypeptide backbone called the core protein. About 140 of these proteins are noncovalently bound at intervals of 30 nm to a very long filament of hyaluronate. GAG polymers are present in both the ECM as well as on cell surfaces. GAG's on cell surfaces act as docking sites for fibroblast growth factor and other proteins that stimulate cell proliferation (Stryer 1988).

A1.2.3.1 Hyaluronic acid

The largest GAG, hyaluronic acid (HA), is a naturally occurring glycosaminoglycan, consisting of a repeating dimer of glucuronic acid and N-acetyl-glucosamine with unbranched units containing 5,000 carbohydrate residues (McGilvery and Goldstein, 1983). Hyaluronic acid functions *in vivo* as both a lubricant and a resilient buffer against mechanical damage as well as being important for the regulation of water balance in tissue. Its name is derived from the Greek word for glass, hyalos, which describes HA's transparent glassy appearance.

Hyaluronic acid can be isolated from natural sources (e.g. rooster combs) and via microbial fermentation (Brache *et al*, 1985). Unfortunately, the animal source is limited and the microbial one currently expensive.

Hyaluronic acid is a widely distributed and highly evolutionarily conserved polysaccharide which plays an important role in a variety of vertebrate soft tissues. No species variation has been found and hence it is a highly desirable biomaterial since it is not antigenic and therefore does not illicit an inflammatory response when use as a xenograft (Pachence *et al*, 2000). By nature of its ability to form highly hydrated and viscous matrices, HA provides stiffness, resilience and lubrication to various tissues e.g. synovial fluid of joints, the vitreous humor of the eye, arterial walls, umbilical cord and the ability of connective tissues to resist compressive forces. HA is a major constituent of the extracellular matrix where it has a large influence on a variety of cellular events e.g. cell migration and proliferation.

Its main disadvantage is a limited range of mechanical properties. In order to change these, HA can be chemically modified, e.g. by esterification of the carboxyl moieties (Kvam *et al*, 1992) which reduces its water solubility and increases its viscosity. Hyaluronic acid can be cross-linked to form molecular weight complexes of the order of 10^7 Dalton or to form gels (Balazs *et al*, 1987). In Balazs's method, hyaluronic acid is cross-linked using aldehydes to form bonds between the C-OH groups of the polysaccharide and the amino groups of the protein, thus yielding high molecular weight complexes. The resultant gels can be formed into sheets, tubes and other three-dimensional shapes. Extensive esterification produces materials which are highly resistant to *in vivo* degradation by hydrolysis (Hubbell *et al*, 1995).

The major proponent of HA technology is FAB (Fidia Advanced Polymers, Italy) which has dedicated much attention to the chemical preparation of hyaluronic acid, with the aim of developing biopolymers which retain the biocompatibility of the parent molecule but have a range of different physical properties e.g. elasticity, viscosity and plasticity.

Hyaluronic acid's biological properties make it an ideal candidate for the development of innovative biomaterials for various clinical indications. Purified medical grade HA is currently employed in a very wide range of medical uses including; reducing the incidence of post operative adhesions (Epifilm Otologic lamina discs, Medtronics Xomed, Minneapolis, USA), as a component of wound healing formulations (Cystistat, Bioniche Life Sciences Inc, London, Canada) and in various cosmetic preparations (Cellex-C Advanced C Skin Hydration Complex, Cellex, Toronto, Canada).

FAB has optimised a number of well defined patented chemical modifications to HA that have been successfully employed to produce a novel range of viscoelastic biopolymers (e.g. Soranzo *et al*, 2000). These HA derivatives can range from soluble to solid hydrogel. Moreover, these

derivatives have prolonged and controllable degradation rates compared to the natural HA.

A1.2.4 Fibronectin, fibrinogen and fibrin

The fibronectins are a family of glycoproteins which function as "molecular glues" since they are essential for many cell-to-cell interactions and cell-to-surface interactions (Walter and Talbot, 1996). Whilst synthesised by a variety of different cells, the main source is vascular epithelial cells. Fibronectin consists of two identical 250 Kd polypeptide chains that are linked by a disulphide bond (Stryer, 1988). Possessing receptors for both cells and extracellular matrix e.g. collagen, heparin, fibronectin and fibrin, fibronectins are present in plasma, on cell surfaces, on collagen fibres and in basement membrane. Their functions include; connective tissue organisation and anchorage, cell-to-cell binding, cell cytoskeleton structure and motility, wound healing and coagulation (Walter and Talbot, 1996). Interestingly the glycine-arginine-aspartate (RGD) peptide was first discovered in fibronectin (Piersbacher and Ruoslahti, 1984).

Fibrinogen is a glycoprotein synthesised by the liver and plays an essential part in the blood clotting process. Present in plasma (200 - 400 mgl^{-1}), fibrinogen has a molecular weight of approximately 340 KDa. It consists of six polypeptide chains of three different types (α, β and γ) arranged in a symmetrical structure and linked by disulphide bridges. During the physiological clotting cascade, thrombin cleaves the α and β chains resulting in the formation of fibrin, an important structural component of a blood clot. Fibrin has a long history of use in modern medicine e.g. during World War I, Harvey described the deployment of fibrin sheets to stop bleeding during surgery (Harvey, 1916). Today, tissue sealants with a fibrinogen and/or fibrin component are routinely used in surgery e.g. CoStasis (Angiotech Pharmaceutical, Vancouver, Canada) which uses autologous fibrinogen and Tisseel (Baxter, Deerfield, IL, USA) which uses fibrinogen derived from human pooled plasma. A similar allogeneic product is under development by the Scottish National Blood Transfusion Service (Edinburgh, Scotland).

The deployment of fibronectin in tissue culture has a long history e.g. coating tissue culture plates to assist cell attachment. However, the use of fibronectin in tissue engineering is less advanced. Mats and cables made from fibronectin have been suggested as suitable materials for nerve guides to assist nerve regeneration (Ahmed *et al*, 2003). Liquid fibronectin when mixed with alginate has also shown potential in nerve repair in rats (Mosahebi *et al*, 2003).

Combining fibronectin and fibrinogen has also demonstrated potential for tissue-engineering scaffolds. Dr. Sarah Underwood at University College London has described a potentially appropriate method for the wet extrusion of human plasma derived fibronectin-fibrinogen cables (Underwood *et al*, 2001). This same material has also been demonstrated to be

potentially superior to fibronectin alone with respect to cell (Schwann cells) migration on a scaffold at low fibrinogen concentrations. However, at higher concentrations of fibrinogen, cell migration is inhibited (Ahmed *et al*, 2000).

Finally, with respect to processing of allogeneic pooled blood donations, Baxter who manufacture Tisseel surgical sealant, process the pooled material using a "patented double vapour heat deactivated" procedure which destroys hepatitis B, hepatitis C and HIV (polymerase chain reaction tested). However, parvovirus B19, which can easily infect immunocompromised or pregnant patients remains active when present (Baxter product information leaflet). This deficiency reflects the difficulties experienced when handling allogeneic material especially when pooled. Alternative source e.g. bovine and autologous are also not without difficulties, namely risk of prion transmission and blood fibrinogen concentration variability between patients respectively.

A1.2.5 Chitin and chitosan

The amino polysaccharide chitosan (poly 1,4 D-glucosamine) is a biosynthetic partially deacetylated derivative of chitin (Sundararajan and Matthew, 1999). Chitin is a naturally occurring polysaccharide which is the primary structural polymer in arthropod (crabs, spiders, insects) exoskeletons and fungal cell walls/structural membranes of mycelia, stalks and pores (Hamlyn and Schmidt, 1994). Chitin is commercially produced from both crustacean exoskeletons and fermented from fungi e.g. Lentinus edodes and Absidea coerula (Peter, 2002). Commercially available preparations of chitosan have degrees of deacetylation ranging from 50 - 90% and depending upon the source and processing method, chitosan may have a molecular weight in the order of 300 - 1000 KDa (Sundararajan and Matthew, 1999).

Chitosan is a β-1,4-linked polymer of 2-amino-2-deoxy-d-glucose. It is thought that the degradation of both chitin and chitosan *in vivo* is due to the enzyme lysozyme which slowly depolymerises these polysaccharides, the end products being simple carbohydrates, CO_2 and water. (Muzzarelli *et al*, 1988).

Chitosan has been fabricated into three-dimensional scaffolds which could be potentially deployed in tissue engineering (Sundararajan and Matthew, 1999). Sundararajan and Matthew produced a variety of potential scaffolds including membranes, beads and tubes and demonstrated that porous three-dimensional chitosan structures could be easily fabricated with good control over pore morphology. These scaffolds were prepared by controlled freezing and lyophilisation of chitosan solutions and gels. Mean pore diameters were controlled in the range 1 - 250 μm by varying the freezing conditions.

Chitosan has been demonstrated to possess biocompatibility features favourable for its use in constructing a tissue engineering scaffold e.g. it can support the growth and phenotypic expression (confirmed by reverse transcriptase polymerase chain reaction) of human osteoblasts and chondrocytes (Lahiji *et al*, 2000).

In May 2001, the American Society for the Testing of Materials (ASTM) (West Conshohocken, PA, USA) produced a guide (F 2103-00) titled "Standard guide for characterisation and testing of chitosan salts as starting materials intended for use in biomedical and tissue-engineered medical product applications" in response to the growing interest of chitosan for tissue engineering. The regulatory issues dealt with included; documentation, impurity levels, safety and toxicology, good manufacturing practice (GMP)/ISO 9000 guidelines and regulatory standards. This guide coincided with a similar guide for alginate and represents some of the drive ASTM is making to ensure quality and standardisation of tissue-engineered medical products (TEMPS) (Dornish *et al*, 2001).

A1.2.6 Amino acid and peptide repeats

A1.2.6.1 Peptide repeats

Novel synthetic protein structures based on a repeating pentapeptide (valine-proline-glycine-valine glycine) (VPGVG) found in elastin have been produced (McPherson *et al*, 1992). The VPGVG repeat is expressed as a recombinant polypeptide using bacteria, isolated, purified and then gamma irradiated in order to cross-link the polymer to form an elastic hydrogel. To make this polymer cell friendly the RGD peptide has been covalently bonded to the polymer (Nicol *et al*, 1992). Using bovine aortic endothelial cells, Urry's group demonstrated that these modified polymers were able to support cell adhesion and growth provided the ratio of VPGVG :RGD in the polymer was no greater than 60:1 (Nicol *et al*, 1992).

A range of novel elastin based polymers is produced by Protein Polymer Technologies Inc (PPTI) (San Diego, USA). Their technology has enabled the creation of polymers that combine the repeating blocks of amino acids responsible for the elasticity of elastin with the repeating blocks of amino acids responsible for the strength of silk (Ferrari *et al*, 2001). These high molecular weight polymers can be processed into a variety of forms including gels, sponges, films and fibres. PPTI's initial targeted products for this range of "silk-elastin" polymers includes, urethral bulking agents for female urinary stress incontinence (clinical phase II trial stage), dermal products for cosmetic and reconstructive surgery (clinical phase II trial stage), tissue adhesives, localised controlled drug delivery systems and tissue engineering scaffolds (McKenna, 2001).

A1.2.6.2 Amino acid repeats

The deployment of amino acid repeats in tissue engineering is yet to be demonstrated, however, there are a number of researchers who have suggested that because of their unique advantages, they may have a role to play in tissue engineering (Chiang and Yeh, 2003, Deming, 1997 and Pachence and Kohn, 2000).

A1.2.6.3 Poly(amino acids)

One option for the creation of new tissue-engineering scaffold materials is to synthesise new polymers derived from novel amino acids sequences. Many different types of poly(amino acids) have been investigated for use in biomedical applications. Poly(amino acids) have several potential advantages as biomaterials (Palapura and Kohn, 1992):

- A very large number of novel peptide-based polymers and copolymers can be prepared from a variety of amino acids
- The side chains offer sites for the attachment of small peptides, bioactive agents, cross-linking agents, or other groups that can be used to modify the physicomechanical properties of the polymer
- Since these polymers release naturally occurring amino acids as the primary products of polymer backbone cleavage, their degradation products theoretically have minimal levels of systemic toxicity and immunogenicity

Poly(amino acids) have already been used as artificial skin substitutes for covering burns (Aiba *et al*, 1985) and as drug delivery systems (Negishi *et al*, 1987). Poly(L-lysine) has for a long time been involved in the development of gene therapy delivery vehicles e.g. work at Genzyme Corporation (Framingham, USA) has demonstrated that complexing recombinant adenoviral vectors with polycations such as poly(L-lysine) improves the transgene's expression (Kaplan *et al*, 1998).

Poly(amino acids) despite their potential have yet to find a biomaterial market niche. Their main drawbacks include high cost, processing problems and unpredictable *in vivo* degradation. The starting materials for the synthesis of poly(amino acids) are N-carboxy anhydrides. These anhydrides are expensive to produce and difficult to handle because they are extremely reactive and are very sensitive to moisture (Palapura and Kohn, 1992). In general, most poly(amino acids) are highly insoluble and therefore at present they are virtually impossible to process in to three-dimension structures. *In vivo*, poly(amino acids) degrade via enzymatic hydrolysis of their amide bonds, it is therefore difficult to control their *in vivo* degradation because levels of enzymes and their activity vary between patients. Because of these difficulties, only a few poly(amino acids), usually derivatives of poly(glutamic acid) are currently being investigated as biomaterials (Palapura and Kohn, 1992).

A1.2.7 Silk

Silk is made up of long repeats sequences of alanine-glycine (-AG-$_n$). Using recombinant technology the exact length of the AG repeat can be controlled in order to vary the mechanical properties of the recombinant silk. In order to create a cell friendly environment the RGD or tyrosine-serine-glycine-serine-arginine (YIGSR) peptide sequences can be added, this approach has been undertaken by Protein Polymer Technologies Inc (PPTI) (San Diego, USA) (Ferrari and Cappello, 2001). This modified recombinant silk can then be spun into fibres in order to form three-dimensional shapes.

Silk enhanced with an RGD peptide sequence and parathyroid hormone has been demonstrated *in vitro* to stimulate osteoblast activity (Sofia *et al*, 2001). Sofia took silkworm cocoons and boiled them for an hour in a soap solution to remove sericin (a protein known to cause an immunological reaction *in vivo*). The boiled silk was processed into flat sheets which were then coated with the bioactive agents prior to adding bone cells. After four weeks the osteoblasts were shown to be producing mRNA coding for procollagen as well as depositing extracellular calcium.

A1.2.8 Coral

Coral has a successful history in orthopaedic surgery as a replacement for bone. It has FDA approval for jaw reconstruction. Coral used in medicine is commonly harvested from reefs in the Indian Ocean. After harvesting, it requires antimicrobial treatment and cutting into the required shape prior to implantation. It is highly porous and is composed of hydroxyapatite i.e. it has a similar chemical composition to the inorganic component of natural bone. Processed coral is biocompatible and degrades minimally *in vivo*.

An example of its potential in tissue engineering has been demonstrated in restoring part of a human thumb (Vacanti *et al*, 2001). In 1998, the patient, Raul Mercia, was a 36 year old male landscaper who suffered an avulsion injury to the distal phalanx of his non dominant hand. The wound was initially covered with a pedicle skin graft from the abdomen which was divided from its abdominal blood supply by day 19. A block of processed natural coral (500 pore ProOsteon, Interpore International, Irvine, USA) was carved using a motorised burr into the size and shape of the missing distal phalanx. At 12 weeks, the coral phalanx was placed under the skin flap created by the skin graft by the surgeon (John Shufflebarger). Twenty million autologous periosteal cells were suspended in 1.5 ml of 1% alginate in saline. This solution was then injected into the coral. Cells were fixed in position by cross-linking the alginate with calcium chloride solution (0.5 mmolL^{-1}).

The results of the above procedure were periodically reviewed for approximately 3 years

after the procedure (Hentz and Chang, 2001). At 3 months after the procedure, Raul Mercia was able to resume his work as a landscape gardener. Ten months after the procedure a biopsy showed that 5% was new bone, 30% was coral and the remainder was soft tissue. At 28 months, whilst being cosmetically reasonable, the mechanical result was an unstable weak thumb with minimal pinching ability (approximately 25% of normal power). Many surgeons would argue that this result was poor compared to either a toe to thumb transfer or using autologous bone instead of coral to treat this particular injury. However, the procedure did demonstrate proof of principle for using a permeable biocompatible support structure seeded with cells suspended in hydrogel (Vacanti *et al*, 2000).

APPENDIX 2

A2.0 Piston Driven Devices

Following the earlier experiments with the manual powered and coordinated piston driven prototype (Chapter 4), it was decided that a new system built on the same underlying principle but semi-automated, would be fabricated. The new system would include a degree of semi-automation in order to achieve two major goals believed necessary to obtain reproducible tubular constructs:

- Precise coordination of the piston movement with the delivery of the calcium chloride solution
- Controllable piston acceleration, "cruise" and deceleration at reproducible rates

The crucial moment in time for the process is that at which the piston first starts to move. At this precise moment the calcium chloride solution needs to be injected into the barrel to fix the newly formed layer of alginate on its wall. If the calcium chloride mixes with the alginate before the piston starts to move, cross-linking occurs with the alginate gelling, thus trapping the regulator and corrupting that particular run of the experiment. If insufficient or injected too late, a tube is formed but is substandard with highly variable wall thickness and trapped air bubbles. Thus, the key is to synchronise the start of the movement exactly with the start of the injection of the calcium chloride solution. Furthermore, both the rate and the volume of calcium chloride injected must be near identical to the rate and the volume displaced by the piston. To achieve this, two identical barrels and pistons were employed i.e. both in terms of length and internal diameter. Since the barrel with an 8 mm inside diameter had proven experimentally most robust during initial testing - see Chapter 4, (i.e. in terms of successful manual tube production runs), this diameter glass barrel was selected for the prototyping of the semi-automated system.

A2.1 Pneumatic drive

The complete pneumatic drive tube-forming device can be seen in Figure A2.1. The barrels were quartz glass tubes of approximately 22 cm in length with an 8 cm internal diameter. The pistons were machined from polytetrafluoroethylene (PTFE) to be a 0.05 mm interference fit (i.e. the outer diameter of the PTFE piston was 0.05 mm greater than the inside diameter of the glass barrel) and mounted on threaded studding to allow for fine adjustment. The barrels were mounted in a vertical position one above the other with a gap in between to allow the positioning of a rigid piston linking device such that the two pistons moved down in an identical manner i.e. start, accelerate, "cruise", decelerate and stop identically, see Figure A2.2. The rigid piston linking device was attached via a simple fixed arm to the carriage on a slot-type pneumatic ram. The actuator ram selected was a pneumatic double acting slot-

Figure A2.1

Piston driven tube forming device complete with pneumatic ram.
(Photographer: Dave Sayer - © The Wellcome Trust Medical Photographic Library - 2003)

Figure A2.2

Range of travel - Pneumatic tube-forming device.
(Photographer: Dave Sayer - © The Wellcome Trust Medical Photographic Library - 2003)

type rodless linear drive (Hoerbiger-Origa Systems GmbH, Altenstadt, Germany. Part No: 120S2040) kindly loaned by the Department of Chemical Engineering, UCL. The double acting linear actuator consisted of a cylindrical barrel and a rodless piston. The piston in the cylinder is freely movable and being double acting it is under the control of the supply air in both directions of travel. This particular unit has an operating pressure range of 0.5 – 8 bar and an operating speed range of 1 $cmsec^{-1}$ to 6 $msec^{-1}$. The unit has a cylinder bore of 40 mm. Using the equation:

$$\text{Force (N)} = \text{Pressure (N/m}^2\text{)} \times \text{Surface area of piston (m}^2\text{)}$$

The theoretical maximum force that can be generated by this ram is 1006 N at 8 bar (1 bar = 100,000 N/m^2). However up to 30% losses are to be expected in real applications (Stacey, 1998).

The ram was powered by compressed air either from the main laboratory supply or from a freestanding cylinder. The control system was an open-loop system i.e. it possessed no feedback unlike a closed-loop control system. This setup had the advantage of being simple but potentially slightly less accurate. The acceleration and velocity of the pneumatic actuator depended upon the rate compressed air entered and exited the unit. Since air is a compressible fluid, the volume of a given mass of air depends upon its pressure (Boyle's law) and temperature (Charles' law). The change of temperature of the air across an actuators is typically negligible and thus can be neglected (Pinches and Callear, 1997), however the pressure can vary greatly as the load and flow rates change. Pneumatic actuator speed control in general is either achieved by either metering the quantity of air entering (meter-in flow control) or leaving (meter-out flow control). The system used had meter-out flow speed control, whereby the exhaust air is metered which sets up a back pressure which compensates for variations in system loads thus theoretically helping to smooth the operation movement. The method used to meter-out the exhaust air was by using an adjustable restricter (bleed screw) in the exhaust port. Movement of the ram was therefore controlled via electronically synchronised inlet valve and outlet port i.e. compressed air accessed (via one of a pair of SMC ASS500 solenoid valves – non adjustable: open/close only with no in-between positions) one end of the double acting drive whilst air was bleed in a controlled manor (via a pair of solenoid controlled CompAir Series bleed screw valves - adjustable) at the opposite (exhaust) end. Only when air was allowed to bleed from the system could the ram move. By varying the pressure of compressed air entering the system via a Norgren gauge and altering the exhaust bleed rate it was possible to modify the velocity of the ram. In practise, the device only worked (i.e. produced hydrogel tubes) over a very narrow range of settings. If the speed was too low then the run would become flawed by the linking agent becoming associated with the alginate solution between the regulator and the barrel wall. Too fast a speed resulted

in visually very erratic regulator movement. In practise, the optimal setting were 1-2 bar inlet pressure coupled to a single 360° +/- 90° outward turn on the exhaust bleed screw from the fully screwed-in (closed) position. This pressure range equates to a theoretical force in the order of 1250 - 2500 N (ignoring inefficiencies in the system e.g. seal stiction). These settings resulted in average piston velocities of 7.5 - 10 cm per second calculated by electronically timing a series of tube producing runs of known length. Customised physical stops prevented excessive ram movement. The advantage of physical stops was that they gave very precise end points with extremely short deceleration times compared to the more conventional cushioned stops which block off the exhaust port just prior to the final part of the piston stroke, thus controllably slowing its velocity prior to coming to a complete halt. Reduced deceleration times were thought essential if run corruption was to be avoided i.e. the premature mixing of alginate solution and calcium chloride solution in the last part of the tube-forming run.

The top barrel was for tube fabrication, whilst the bottom barrel was to hold the calcium chloride charge. The top barrel and regulator element were an identical set up to the original manual device. The bottom barrel had no regulator but was capable of being filled from a calcium chloride reservoir via a three-way tap. The three-way tap controlled whether the bottom barrel was linked to the reservoir or to an injector nozzle directly above the top of the tube fabrication barrel.

A2.1.1 Operation cycle

A basic operation cycle (after presetting all the pneumatic valves) of the semi-automated pneumatic driven device consisted of:

1. Filling the calcium chloride reservoir (initially 2% in water was used)
2. Pneumatically lowering the pistons to their lower-most point
3. Turning the three-way tap to connect the calcium chloride reservoir to bottom barrel
4. Pneumatically raising the pistons to their uppermost position, see Figure A2.3, this creates a vacuum in the lower barrel which sucks the calcium chloride solution in from the reservoir, thus charging the lower barrel. The uppermost piston position was adjusted such as to leave a space above the upper piston sufficient to add the alginate solution and regulator
5. Adding 2 ml of alginate solution (initially 4% Kelco Manugel was used) directly to the space above the upper piston
6. Adding the regulator to the alginate solution
7. Finely adjusting the position of the top of the regulator (and therefore the alginate-air interface around its perimeter) so as to be flush with the top of the glass barrel

Figure A2.3

Piston driven device - Hydrogel tube-forming barrel (Upper glass barrel).
(Photographer: Dave Sayer - © The Wellcome Trust Medical Photographic Library - 2003)

8. Turning the three-way tap such that the injector nozzle and lower barrel are connected
9. Pneumatically lowering the pistons. This causes the top barrel wall to be coated in alginate at exactly the same time as calcium chloride is transferred via the injector nozzle to the top barrel thus cross-linking the polymer
10. Waiting for a period of 5 - 10 minutes before detaching the uppermost barrel in order to remove the piston which in turn delivered the hydrogel tube complete with embedded regulator

A2.1.2 Trouble shooting

A range of glass quartz barrel sizes were tried including 8 mm (i.e. approximately the same dimension as synthetic graft used for peripheral vascular disease bypasses e.g. GORE-TEX Vascular Graft) and 4 mm inside diameter (i.e. approximately the same dimension as human saphenous vein which is currently used as conduit for coronary artery bypass graft surgery). Once again, the device produced hydrogel tubes, however, reproducibility was a major issue. One run would produce a full length tube with good consistency of wall thickness (e.g. using 8 mm inside diameter glass and a 7.5 mm outside diameter PTFE regulator, 4% Manugel alginate solution, 2% calcium chloride solution gave wall thicknesses in the order of 250 +/- 100 μm – Mitutoyo electronic micrometer gauge), and then the next few runs would either "corrupt" i.e. the regulator would travel a short distance down the barrel before prematurely becoming entrapped in cross-linked gel and/or the wall thickness would vary widely or be total absent. Frequently the resulting tube would be discontinuous for a proportion of its length.

A problem identified early on was the quality of manufacture of the glass barrel. Measurement of the tolerance range for standard quartz glass tubing showed it varied widely along its length e.g. the 8 mm diameter tube varied by up to +/- 0.5 mm (micrometer gauge on different parts of two 1 m lengths cut up into 15 - 20 cm length pieces. Since the gap between the barrel and the regulator determines the wall thickness, precision bore tubing was required. A manufacturer was identified (Precision Glass engineering, Hemel Hempstead, Herts., UK) who using a precision machined mandrels produced 8 mm inside diameter tubing +/- 0.01 mm over a one metre length and also 4 mm +/- 0.01 mm over a one metre length. The glass selected was borosilicate (U.S. Pharmacopoeia Specification: 1A) as opposed to regular quartz. Using this specification tube did unfortunately not have the desired improvement on the success rate, however, this precision bore tubing has been continued with because of its potential crucial relationship to wall thickness.

Rigid plastic tubing e.g. Perspex for the barrel was also successfully tried. Interestingly cut-

down medical syringes (Becton Dickinson Plastipak: 10, 20 and 50/60 ml) when tried failed due to an inability of the alginate solution to coat the wall of the barrel, probably due to prior treatment of the plastic inner wall by the manufacturer in order to reduce piston stiction forces which might otherwise interfere with the smooth operation of the syringe. Stiction (static friction) is friction that prevents relative movement between two movable components in their stationary position immediately prior to slipping occurring i.e. initial movement of one component relative to the other. Other non-coated plastics were also employed with similar results to the Perspex and precision bore glass, thus the process was not just limited to barrels made of glass.

A range of different diameter, length and shaped regulators was also tried. Two types of regulator (both of which work excellently using the original manual technique) were tried:

- Pure bullet shaped – i.e. no contact with the barrel
- Finned bullet - Bullet shaped but with the addition of little pegs at 90° intervals around the circumference at the two ends of the regulator to act as guides in order to centralise the regulator. The gaps between the pegs and the barrel were a loose fit, in the order of 10 μm. This gap was just sufficient to allow the finned regulator to travel smoothly down an empty glass barrel solely under the influence of gravity.

The finned bullet with certain types of alginates (high G content) left continuous grooves running the length of the tube (visualised by Leica TCS SP confocal microscopy system in the Department of Anatomy, UCL), however, the grooves did not break through the tube wall. The big advantage of the simple bullet shape is ease of manufacture and therefore numerous different lengths, diameters and shapes could be tried.

One factor which did make a difference was the relative density of the regulator to the different alginate solutions. The density of alginate solutions were of the order of just over 1000 Kgm^{-3} depending upon the alginate concentration i.e. just greater than water. A range of different substances (including Dural (alloy of 95% aluminium, 4% copper and 1% magnesium with a density of 2800 Kgm^{-3}) and PTFE (density 2200 Kgm^{-3}) and polypropylene (density 910 Kgm^{-3})) were machined up with identical dimensions. The lower relative density plastic polypropylene (density of 910 Kgm^{-3}) worked best, however, all the materials could function as regulators. The only proviso being that the higher density regulators completely submerged (and thus aborted the run) if left for any length of time between being added to the alginate and drawing down the piston, whereas the polypropylene regulators could be left indefinitely. The Dural regulators whilst being relatively strong and more robust than the plastic regulators suffered from poor corrosion resistance. The bulk of the experiments were therefore carried out with the plastic regulators.

However, despite trying to optimise the barrel and the regulator components, the consistency and reproducibility remained poor. The same barrel, regulator and piston when removed from the semi-automation platform and used manually performed substantially more reproducibly i.e. virtually always producing a continuous tube with no regulator fouling, albeit less scientifically in terms of the timing and force used. Focus therefore shifted towards the pneumatic drive mechanism and the pistons themselves.

One weakness in the system is the 1 cm long pistons which were manufactured from PTFE to give a 0.05 mm interference fit. PTFE being compressible gives an excellent seal along their length when first machined, however, after repeated use the PTFE becomes permanently deformed and the seal is eventually lost necessitating frequent replacement. Also as the interference fit reduces so too does the force required to overcome the stiction between piston and barrel.

Another weakness is the use of pneumatic ram. Using a number of different digital imaging devices including a NAC HSV 500 Digital High Speed Video system (NAC Image Technology, Inc. Tokyo, Japan) it was possible to view the progress of the regulator and piston during a tube forming run. The NAC HSV 500 stores its individual images in digital form in its memory. It records at 500 frames per second (fps) as .tiff files (Tag Image file Format – Adobe Systems) with a maximum recording time of 5 seconds. (Kindly loaned by the Engineering and Physical Science Research Council (EPSRC)). Using a PC running Windows operating system, the individual .tiff files were converted to .jpg files (Joint Photographic User Group) using PicaView (ACD Systems – www.acdsystems.com) before they could be strung together using AVI Constructor (www.aviconstructor.com) to create a continuous AVI (Audio Video Interleave - Microsoft) "movie". By having a precise scale directly behind the glass barrel and knowing that the time difference between two consecutive .tiff files is exactly 0.002 seconds, it was possible to calculate the velocity of the regulator and piston. The average velocity of the piston was slower than the average velocity of the regulator during a tube-forming run. Furthermore, instead of observing the desirable smooth movement down the barrel, an erratic staccato movement of the piston and regulator was exhibited on the vast majority of runs. On closer examination, there appeared to be two distinct components, an initial judder on "dive" (i.e. the moment that the regulator first commenced its downward journey) and a random variation down the tube. The "dive" problem was the most significant factor since it appeared to correlate well with the success or failure of a particular run. In short, if the dive was jerky then the tube was almost certain to be flawed. Simple experimentation revealed that the ram with either no resistive force or with high downward force (50 Kg weight hung from the fixed linkage between the pistons producing approximately 500 N of additional downward force i.e. in the direction of tube production) ran smoothly but with low resistive

forces ran jerkily and unpredictably. For comparison, the maximum force required to produce a tube using the device was < 20 N, which is negligible compared to the theoretical maximum force of the ram (>1000 N). This was measured using a simple strain gauge attached to the fixed linkage, which was temporarily detached from the ram. After priming and loading the system, the strain gauge was manually pulled down to produce a tube in the same manner as the pneumatic ram and the maximum value recorded. This value was just prior to "dive" i.e. to overcome stiction forces.

The pneumatic ram was therefore stripped and rebuilt to the manufacturer's exact specifications just in case it was a fault. Likewise the switching equipment was examined and reassembled. After the rebuild, once again with zero load or high downward force the ram ran smoothly but connected to the tube-forming device it was once again jerky.

The "ideal movement" of the piston for the tube-forming device is probably one where:

- The piston is stationary in the cylinder loaded with alginate solution and regulator. Extremely rapid acceleration occurs to the ideal velocity of 0.1 - 0.2 $msec^{-1}$ i.e. the regulator's dive starts smoothly and continues in the same manner until the tube is completed and the regulator is once again at rest
- Velocity is constant during tube production
- Extremely rapid deceleration to a final halt at the end of tube production.

A simple graphical representation of the above would be a perfect square wave if velocity (y axis) were plotted against time (x axis), see Figure A2.4. Instead of this ideal movement a more erratic movement was observed which could have be due to a number of factors which include:

- Variability of the compressed air delivery source
- Deformability due to pressure changes of tubing and ancillary components connecting the compressed air source to the pneumatic ram
- The volume of air above the bidirectional ram piston
- The volume of air displaced from below the bidirectional ram piston
- Stiction between:
  - The bidirectional ram piston seals (2) and its cylinder
  - The pistons and cylinders of the actual tube forming device (2)
- Backlash in the system due to deformable seals in:
  - Pneumatic ram assembly
  - Tube forming device (2)

Each of the above factors was considered in relation to this "ideal movement".

The compressed air source made little if any difference, neither mains supply nor cylinder

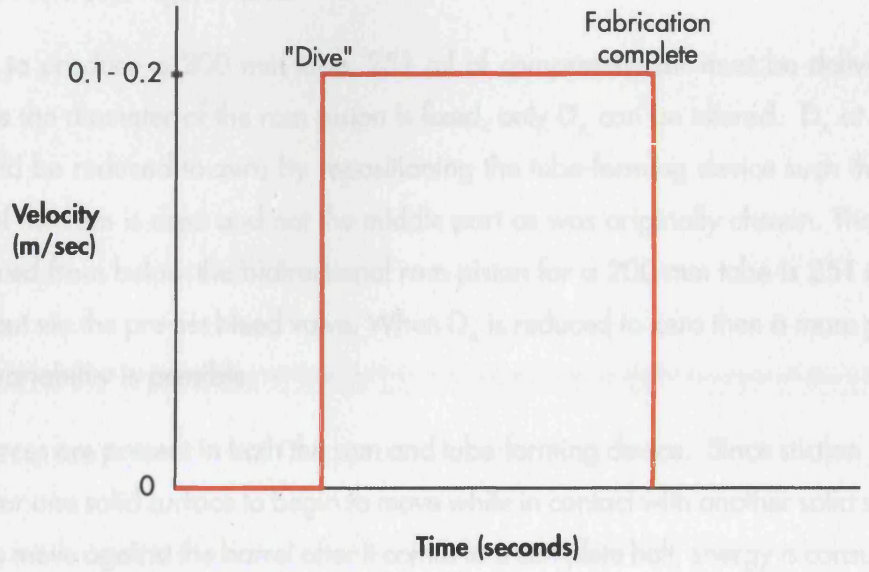

Figure A2.4

Graphical representation of the "ideal" movement of the piston.

The regulator ideally would have a similar square wave shape except its velocity would be higher since it travels further during the same time period i.e. the gap filled with alginate solution between the regulator and piston crown is greater at the top than at the bottom when the tube has been formed.

supply appeared to change the movement characteristics.

Approximately one metre of 4 mm inside diameter purpose made compressed air hose was used to connect the regulated supply to the valves and to the ram, thus creating a "dead space" (V_H) in the order of 12.5 ml. Redesigning the rig in order to reduce this dead space was an option e.g. mounting the regulator and valves directly adjacent to the ram uppermost compressed air input. This would effectively reduce V_H to almost zero.

The volume of air above the bidirectional ram piston (V_A) is dictated by the diameter of the bidirectional piston (40 mm) and its position relative to its overall stroke length (1200 mm) see Figure A2.5 and Figure A2.6.

Therefore to produce a 200 mm tube, 251 ml of compressed air must be delivered to the ram. Since the diameter of the ram piston is fixed, only D_A can be altered. D_A at the start of a run could be reduced to zero by repositioning the tube-forming device such that only the top part of the ram is used and not the middle part as was originally chosen. The volume of air displaced from below the bidirectional ram piston for a 200 mm tube is 251 ml. This air is forced out via the pre-set bleed valve. When D_A is reduced to zero then a more predictable pressure variability is possible.

Stiction forces are present in both the ram and tube-forming device. Since stiction is the force required for one solid surface to begin to move while in contact with another solid surface, for a piston to move against the barrel after it comes to a complete halt, energy is consumed to get initial movement. In general the bigger the piston (i.e. the larger the circumference) and the lower the velocity the more pronounced the stiction effects – these are well known challenges to the semi-automobile engine manufactures. Since both the ram piston and the tube forming piston and calcium chloride delivery piston are all moving at the same speed due to rigid coupling only the diameter of the pistons is an indicator of which component has the most significant impact on the overall system. Since the ram piston is 40 mm in diameter (125.7 mm circumference) it is much larger than the 8 mm and 4 mm pistons (28.0 and 12.6 mm in circumference respectively) used in the tube forming part of the system. Therefore stiction forces in the ram are probably the more significant although their respective components will also further influence this. Stiction in the ram is produced by the barrel of the pneumatic ram (anodised aluminium) and its two deformable piston seals (nitrile (NBR) O-rings) at each end of the bidirectional piston, whereas stiction in the device is due to PTFE interference fit pistons interacting with the glass barrels (2).

The volume above the ram (V_A) compounds the stiction problem. The cycle of events includes:

1. System is at rest in the loaded position

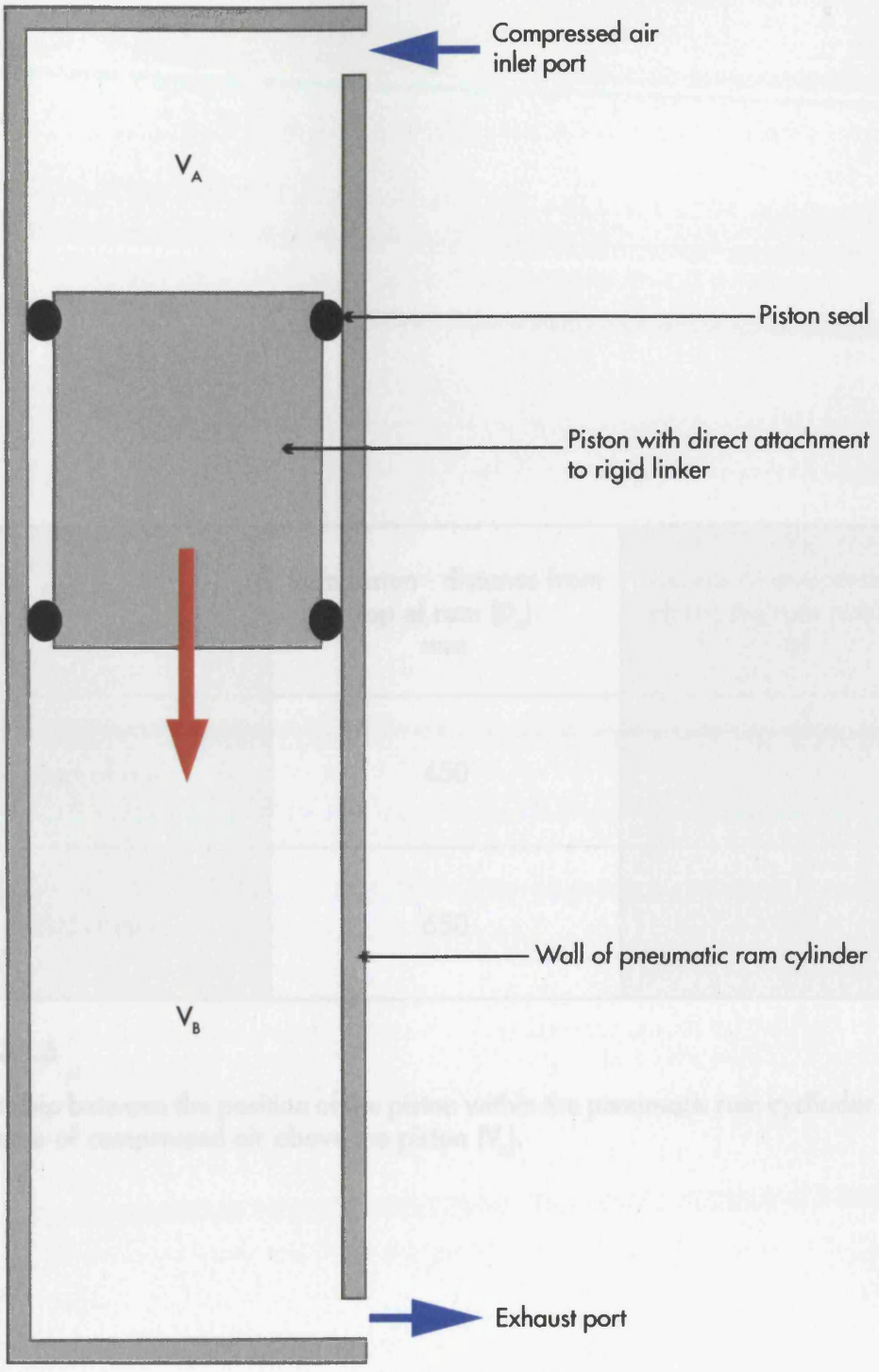

Figure A2.5

Schematic of the pneumatic double acting rodless linear drive.

The red arrow indicates the direction of piston movement during the tube forming process. V_A and V_B are the total volume above and below the piston respectively.

Tube forming event (200 mm length tube)	Ram piston - distance from top of ram (D_A) mm	Volume of compressed air above the ram piston (V_A) ml
Start of run	450	565
End of run	650	817

Figure A2.6

Relationship between the position of the piston within the pneumatic ram cyclinder (D_A) and the volume of compressed air above the piston (V_A).

2. The inlet solenoid and outlet bleed hole simultaneously open
3. Compressed air enters the space above the ram piston, initially V_A is unchanged as the pressure above the ram piston rises (P_A) rises
4. P_A rises until is able to overcome all the resistive forces in the system i.e. stiction and all the pistons initially move. Air is displaced under the ram piston through the bleed hole
5. Once the stiction forces are overcome, less force is required to keep the system in motion and therefore due to the now excessive P_A the pistons jerk forward, however since the compressed air rate of delivery is unchanged, the ram piston slows or stops
6. P_A again rises until sufficient to restart and/or reaccelerate the ram piston
7. The above jerky cycle continues until the physical end stop is reached and the system is once again at rest
8. This jerkiness in the ram piston is directly transmitted to the pistons in the tube forming part of the system resulting in erratic exposure of alginate solution to calcium chloride solution and hence irregularly walled hydrogel tubes or a totally corrupted run with the regulator becoming trapped in alginate hydrogel part way down the glass barrel. Once trapped, calcium chloride solution rushes past the regulator and the latter part of the run is ruined.

In contrast to the above cycle, the tube-forming device when powered manually does not have this jerkiness of movement and therefore better tubes are manufactured. The pneumatic ram has a number of dynamic cylinder forces that influence the movement of the piston. In its simplest form, the linear actuator converts pneumatic energy into mechanical linear movement. Thus the energy supplied is determined by:

- Pressure
- Flow rate

Both these variables were adjusted in attempts to optimise tube production runs. The total load is determined by:

- Magnitude of the out required to drive the tube-forming device e.g. stiction in the glass barrels between PTFE piston and glass wall due to the required interference fit
- Seal friction (Stiction)
- Rate of acceleration required
- Air-flow resistances
- Back-pressure

As before, the above variables were experimented with in order to improve production runs.

Examining a tube-forming cycle from the pneumatic ram prospective illustrates the potential difficulties experienced with the system, see Figure A2.7:

1. At the start of the cycle, both the inlet valve and exhaust port are simultaneously opened
2. Pressure (P_A) builds up in the volume above the piston (V_A) whilst the volume below the piston (V_B) falls to atmospheric pressure since the exhaust port is open to atmosphere (open-loop system)
3. P_A continues to rise, but there is no piston movement until the force to initiate movement is greater than the forces resisting movement
4. As the piston accelerates from rest, air is forced out of the exhaust port which increases the back-pressure under the piston, which in turn reduces the piston's acceleration rate
5. Only when the driving and resistive forces are equal will the piston have zero acceleration i.e. constant velocity
6. The run ends when the rigid linking piece hits the end stop, resulting in rapid deceleration of the piston and rapid rise in P_A

The final factor considered was backlash. This was reduced in two distinct ways:

1. All the couplings were rigid
2. All the pistons after travelling in the direction for loading were always moved a short distance in the opposite direction (i.e. the same direction as for a tube production run) in order to align the deformable seals in the correct orientation prior to a run. Any positioning problems caused by this manoeuvre were then corrected by adjusting the threaded portion of the PTFE pistons.

Overall the pneumatic drive under conditions of light load very frequently produced a very erratic staccato linear movement and not the smooth movement that was originally envisaged for this drive. However a number of tubes have been constructed in this manner with a variety of different alginates, alginate concentrations (0 - 6%) and calcium chloride solutions (0.1 - 4%), which had no discontinuities in their walls. Furthermore, tubes consisting of alginate hydrogel with embedded glass beads or live cells and also discs cut from their walls using a 7 mm in diameter "cookie cutter" have been the basis of all the initial cell development work - described below and in the main body of the Thesis e.g. Chapter 7 and Chapter 8.

Wall thicknesses were measured from tubes produced using different diameter regulators, since the difference in diameters between the inside of the barrel and the outside of the regulator directly govern the thickness of the wall of the tube. Only tubes which possessed a totally intact wall after expulsion from the glass barrel were used. Regulators were constructed which produced wall thicknesses that would potentially allow good mass transfer. In humans

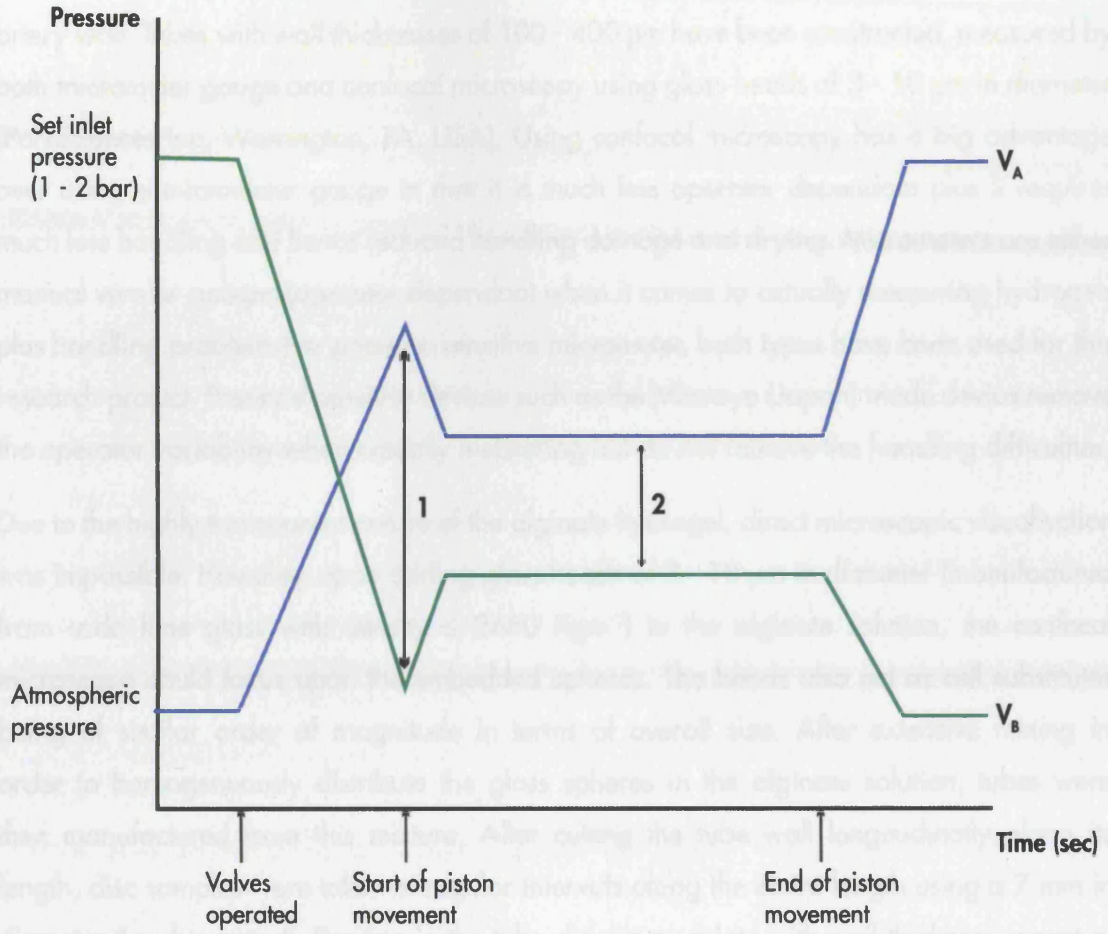

KEY

V_A = Pressure above double acting piston (Inlet side)
V_B = Pressure below double acting piston (Exhaust side)

1 = Pressure difference required to start piston movement
2 = Pressure difference required to maintain piston movement

Figure A2.7

Theoretical pressure variation in pneumatic ram during tube-forming cycle.

[Modified from Pinches and Callear, 1977]

the maximum distance of cells from a blood vessel capable of O_2/CO_2 gaseous exchange (i.e. a capillary) is in the order of 100-200 μm, it was therefore decided to produce tubes with a wall thickness of no greater than 400 μm but preferably in the order of 200 μm. This dimension also correlates well with the wall thickness of a normal healthy human coronary artery wall. Tubes with wall thicknesses of 100 - 400 μm have been constructed, measured by both micrometer gauge and confocal microscopy using glass beads of 3 - 10 μm in diameter (PolySciences Inc, Warrington, PA, USA). Using confocal microscopy has a big advantage over using a micrometer gauge in that it is much less operator dependant plus it requires much less handling and hence reduced handling damage and drying. Micrometers are either manual vernier gauges (operator dependant when it comes to actually measuring hydrogels plus handling problems) or pressure sensitive micrometer, both types have been used for this research project. Pressure sensitive devices such as the Mitutoyo (Japan) made device remove the operator variability when actually measuring but do not remove the handling difficulties.

Due to the highly transparent nature of the alginate hydrogel, direct microscopic visualisation was impossible. However, upon adding glass beads of 3 - 10 μm in diameter (manufactured from soda lime glass with density $\leq$ 2480 Kgm^{-3}) to the alginate solution, the confocal microscope could focus upon the embedded spheres. The beads also act as cell substitutes being of similar order of magnitude in terms of overall size. After extensive mixing in order to homogeneously distribute the glass spheres in the alginate solution, tubes were then manufactured from this mixture. After cutting the tube wall longitudinally along its length, disc samples were taken at regular intervals along the entire length using a 7 mm in diameter "cookie cutter". Position in the tube did not correlate with wall thickness except at the extremes, therefore, the first and last 2 - 3 cm of tube were not measured e.g. the last portion of the tube contained the trapped regulator. Furthermore, great care was taken to avoid deforming the delicate hydrogel during handling, if there was any doubt, then that tube or disc was discarded. At all times the alginate gels were kept in calcium chloride solution (to prevent drying and therefore unwanted shrinkage) including under the confocal microscope using Sigma Coverwell press-seal imaging chambers. These chambers are made from optical grade polycarbonate bonded to a silicone spacer gasket. When pressed against a glass microscope slide they form a sealed chamber (20 mm diameter) for an up to 1 mm thick free-floating specimens, thus avoiding compression artefacts. The hydrogel discs were scanned visually to check for homogeneity of the beads. Selecting the approximate centre of each disc (i.e. trying to avoid possible distortion at the edges due to the "cookie cutter" and by focusing the confocal microscope on the nearest bead in the microscope field (i.e. the bead at the top of the alginate disc) and then focusing through the alginate on the bead furthest away (i.e. the bead at the base of the alginate disc) and then using the computational power of the

microscope's central processor unit to "subtract" the two vertical positions in space gives an indirect measurement of the thickness of the disc and hence of the tube wall thickness. Due to handling difficulties it was not possible to measure the same disc using both a micrometer and the indirect confocal microscopy method.

The data collected using the indirect confocal microscopy method confirmed that the pneumatic device formed tubes were highly variable along their length (much more so than the manually produced tubes). However, trends suggested that average wall thickness depended upon a range of different variables including:

- Barrel/regulator gap (see Figure A2.8)
- Percentage alginate in solution (see Figure A2.9)

Increasing either the barrel/regulator gap or the alginate concentration lead to an average increase in wall thickness. However, some factors appeared to make no difference to wall thickness including the cross-linking time (see Figure A2.10).

Because cross-linking time appeared to have no effect on wall thicknesses, it was possible to prepare hydrogel tubes in advance of confocal microscopy sessions.

Other parameters which require further investigation include:

- Alginate type
- Calcium chloride concentration
- Presence/absence of competing ions in the calcium chloride solution e.g. sodium ions

Preliminary investigations (small sample numbers) suggested that these parameters do play a role in hydrogel wall thickness especially alginate type.

Weighing the discs with their known diameters was also attempted but it was difficult to get reproducible results due to inability to consistently remove excess moisture from the hydrogels which are >96% water. Handling is a particular challenge as it can result in gel deformation with water being permanently squeezed out. Prolonged freeze drying (48 hours in an Edwards freeze drier) of the discs and weighing also failed to determine the volume and hence disc thickness due to the minuscule quantity of solid material left after extended lyophilisation, to remove all the moisture for consistence between samples. For example a disc made of 4% alginate with a wall thickness of 250 μm and 7 mm diameter has a theoretical volume of 9.6 x 10^{-9} ml. If a 4% solution is used then approximately 3.6 x 10^{-10} ml of alginate solid will be present, after extensive lyophilisation.

Optical coherence microscopy has also been used to measure wall thickness. This non-invasive method of imaging is covered in Chapter 9.

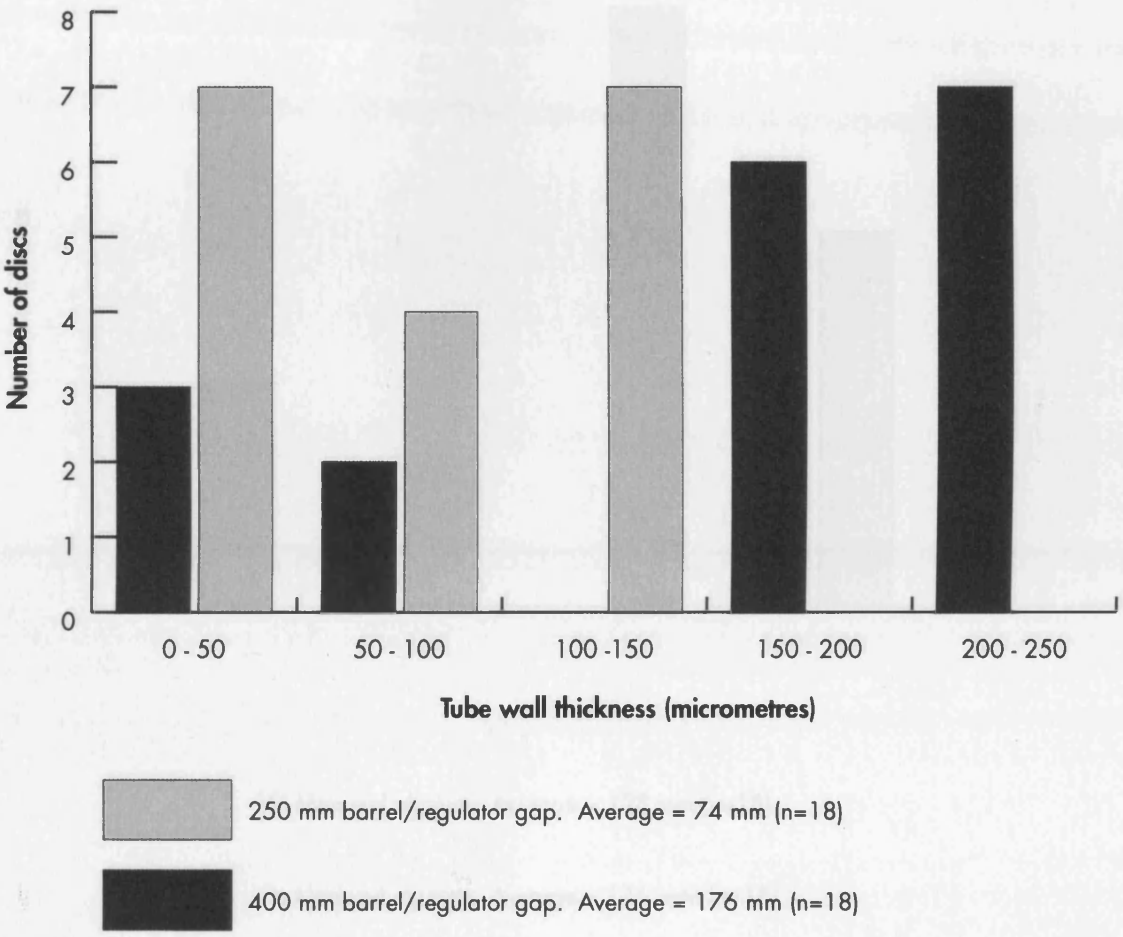

Figure A2.8

Effect of barrel regulator gap on final tube wall thickness for a 4% solution of Manugel alginate cross-linked with 2% calcium chloride solution for 24 - 30 hours.

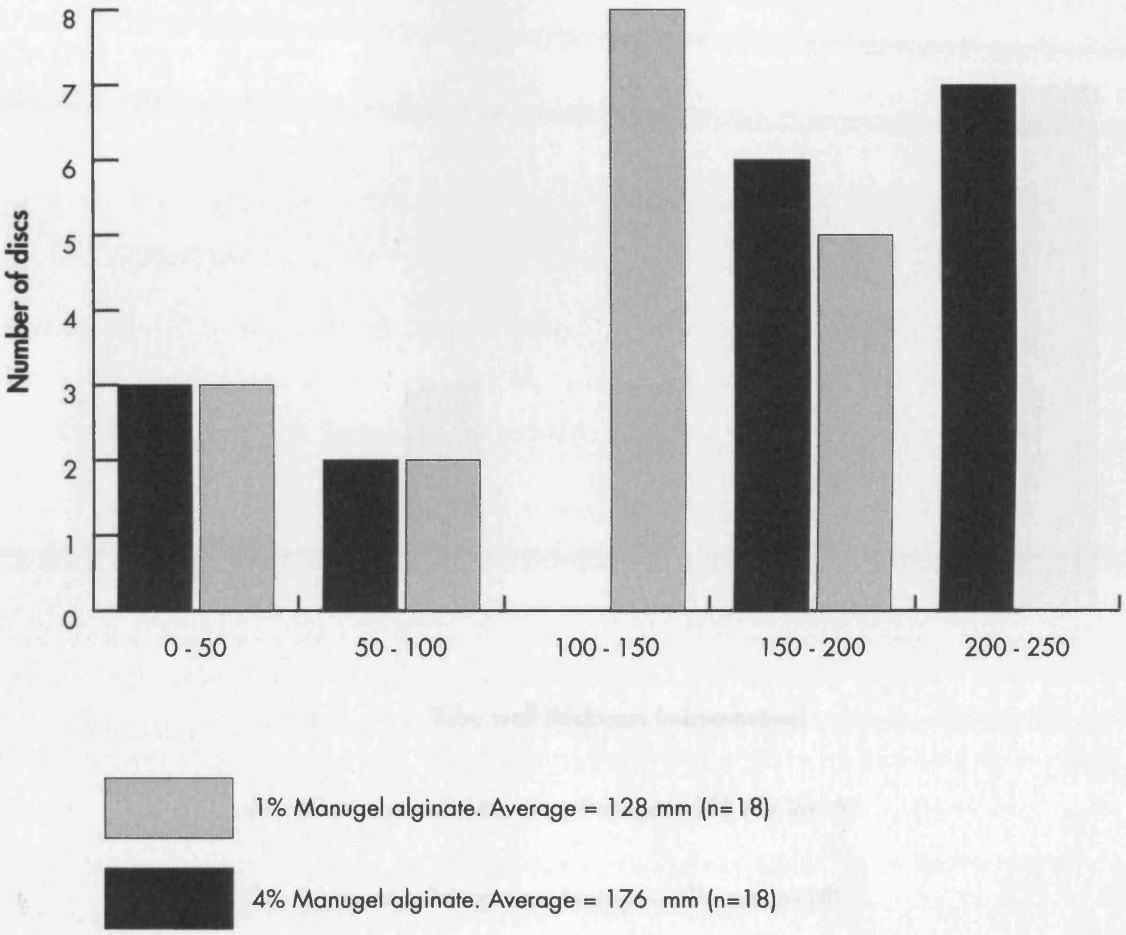

Figure A2.9

Effect of alginate solution concentration on final tube wall thickness using a barrel/regulator gap of 400 µm and cross-linked with 2% calcium chloride solution for 24 - 30 hours.

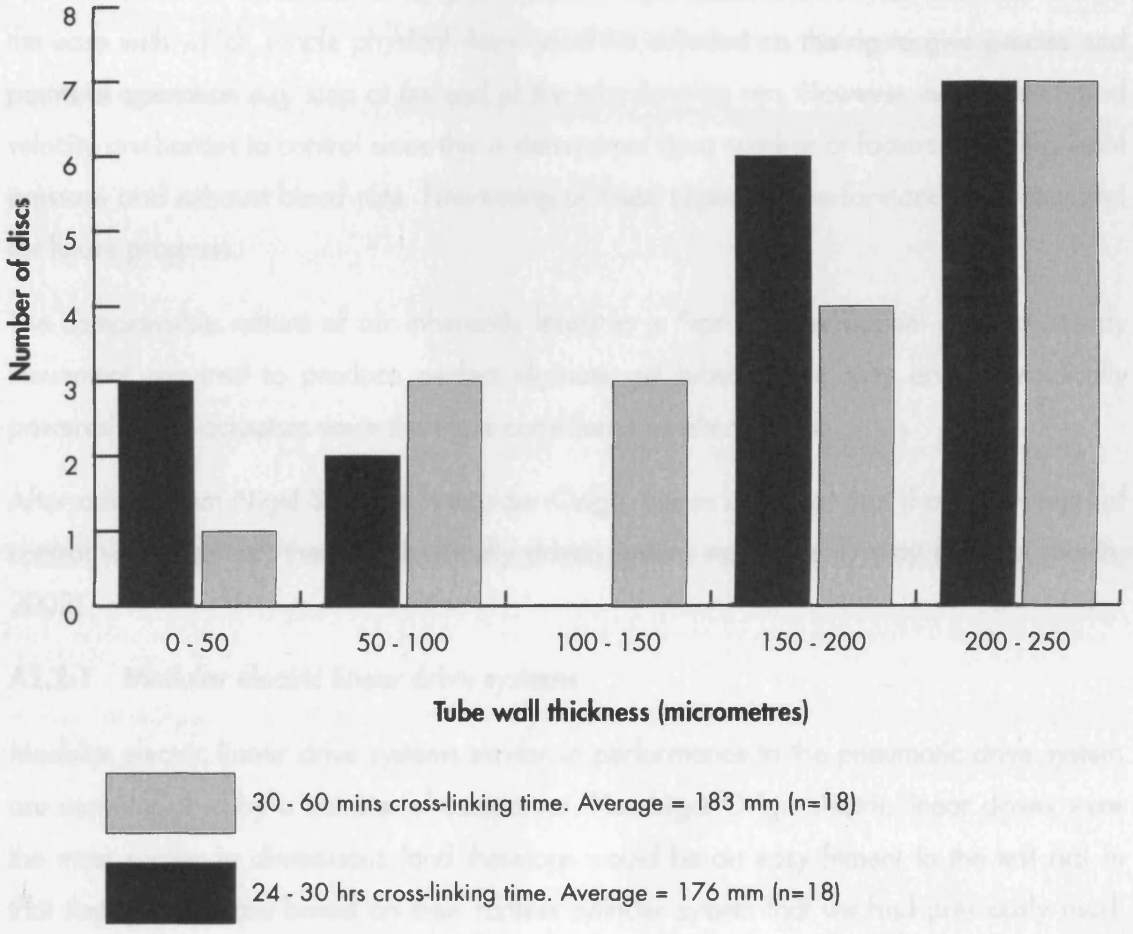

Figure A2.10

Effect of cross-linking time on final tube wall thickness for a 4% solution of Manugel alginate cross-linked with 2% calcium chloride solution.

A2.2 Alternative linear actuators

Even if the initial "dead space" above the ram piston was reduced significantly by redesigning the experimental rig the "dead space" produced as the device operates is still significant at 251 ml for a 20 ml tube. Whilst the pneumatic drive had helped develop the piston driven device, pneumatic power for this application has a further drawback, lack of precise control. Pneumatic drive is ideally suited to "point to point" operations and this was demonstrated by the ease with which simple physical stops could be adjusted on the rig to give precise end points of operation e.g. stop at the end of the tube-forming run. However, acceleration and velocity are harder to control since this is determined by a number of factors including input pressure and exhaust bleed rate. Fine-tuning of these aspects of performance was required for future progress.

The compressible nature of air inherently leads to a "springy" movement and not steady movement required to produce perfect alginate gel tubes. Electrically and hydraulically powered linear actuators were therefore considered as alternatives.

After advice from Nigel Smith at Hoerbiger-Origa, it was apparent that if a higher level of control was required, then an electrically driven system was the only way forward (Smith, 2002).

A2.2.1 Modular electric linear drive systems

Modular electric linear drive systems similar in performance to the pneumatic drive system are manufactured by a number of companies. Hoerbiger-Origa electric linear drives were the most similar in dimensions (and therefore would be an easy fitment to the test rig) in that their product are based on their rodless cylinder system that we had previously used. Options included electric screw drive which is suitable for high force applications and low speed work (our requirement of approximately 1 $cmsec^{-1}$ is considered slow by linear drive manufacturers) and electric toothed belt drive which is suitable for applications requiring accurate positioning and high speed. Thus the screw drive version was potentially the best option for the application. However, the whole area of drives is considered at length in Chapter 5 and Chapter 6 as it was also a major influence on the reproducibility of the subsequent fluid driven versions of the tube forming device.

A2.3 Conclusions

Whilst the piston driven device was very capable of producing tubes of alginate, alginate plus live cells or alginate plus glass beads, it had certain fundamental drawbacks if this technique of creating a tube within a barrel was to be used in a commercial setting where for example, hundreds of thousands of metres of tube for blood vessel creation would be required *per*

annum. These include:

- Sterility issues
- Handling
- Overall size
- Cost

Sterility issue are mainly due to the mode of filling the device with a shot of alginate solution and then having to add the regulator element. During these steps the device is "open" to the environment and thus would need to be carried out in a sterile environment e.g. a biosafety cabinet. The length of the barrel (an absolute minimum of 25 cm for a vessel suitable for CABG surgery) and the fact that the barrel must be upright during these steps makes these operations very challenging. This is further complicated in that most patients will require at least three vessels of 25 cm in length (allowing for a small amount of unavoidable wastage). If vessel for peripheral vascular disease bypass is contemplated, individual vessels of the order of 1 meter will be required (i.e. capable of running the entire length of the leg). Peripheral vascular disease (PVD) is a common medical condition in which the arteries that carry blood to the legs or arms become narrowed or blocked due to atherosclerotic plaques. PVD affects approximately 5% of the population aged over 50 years. The most common symptom is extremely painful cramping in the leg and/or thigh especially on walking (claudication). For example, the US estimates that it has 8 million people with PVD, 62% are symptomatic and require medical management (Society of Cardiovascular and Interventional Radiologists, USA). Medical management includes life style advice, medication for symptomatic relief (e.g. Praxilene – Merck), bypass graft surgery and amputation. Thus the blood vessel lengths required for PVD grafting would require extremely large custom-made sterile hoods for loading the piston driven device.

Handling of the hydrogel tubes is also difficult. Since the drive required to fabricate the tubes is expensive, each drive would be required to produce many tubes per unit time. This would require the glass barrel containing the hydrogel tube to be uncoupled from the drive and transferred into a suitable bioreactor circuit, which in turn would necessitate couplings at each end of the barrel if the barrel was to be retained as part of the flow circuit. This presents three major obstacles:

- The upper most part of the tube is not attached in any way to the barrel
- The lower most part contains the parked regulator embedded in gelled alginate
- Sterility issues involved in making couplings

Alternatively, removing the tube from the barrel prior to inserting it in a bioreactors also has major obstacles:

- Sterility issues involved in removing, handling and coupling the tube

- High risk of damaging the fragile hydrogel tube either due to deforming the tube by external force or merely the weight of the tube itself
- Coupling difficulties associated with attaching a hydrogel to a fixed input and output connectors
- Removal of the regulator and detachment of the piston (cut off) – this adds another unit operation and thus increases costs.

In brief, economically handling a one metre long "free-standing" tube with a 200 μm thick wall composed of 99% water in sterile conditions represents a significant challenge!

The overall size of the device is also an issue, for example if a continuous 1 metre length of tube was required to produce a bypass graft suitable for peripheral vascular disease surgery, the minimum height of the overall device is over 2 m (1 m cylinder plus 1 m piston stroke). Even the minimum device height for a single coronary artery bypass graft (CABG) would be in the order of 50 cm. The above dimensions assumes that the device is reconfigured so that the tube forming barrel and the calcium chloride tube are arranged parallel to open another, both at the same height thus minimising the overall height, i.e. not one above the other as per the prototype rig.

Sterility issues aside, the dimensions of the device and the size of the "hoods" required to service them would require a factory of enormous proportion just to serve a small geographical area. For example, today over 200 CABG operations are carried out in London each week, assuming that each vessel takes 10 weeks to grow and that each patient requires three 25 cm lengths, then 6000 cylinder devices of 50 cm in height would be required.

In summary, the approach to producing a tube within a cylinder is highly feasible; however driving the process with a piston is not a commercial option unless very short lengths of vessel are required e.g. arterio-venous shunts for long-term kidney dialysis patients (approximately 10 cm in length). This issue and other disadvantages of using a piston within the tube forming barrel are discussed in Section 10.3, however, by recognising these shortfalls, it was possible to design and incorporate a far better drive methodology - fluid drive, into the next version of the device (see Chapter 5).

REFERENCES

Abramowitz J, Dai C, Hirschi K.K, Dmitrieva R.I, Doris P, Liu L, Allen J.C. Ouabain- and marinobufagenin-induced proliferation of human umbilical vein smooth muscle cells and a rat vascular smooth muscle cell line, A7r5. Circulation 2003;108:3048-3053.

Ahmed Z, Idowu B.D, Brown R.A. Stabilisation of fibronectin mats with micromolar concentrations of copper. Biomaterials 1999;20(3):201-209.

Ahmed Z, Underwood S, Brown R.A. Low concentrations of fibrinogen increase cell migration seen on fibronectin/fibrinogen composite cables. Cell Motility and the Cytoskeleton 2000;46(1):6-16.

Ahmed Z, Underwood S, Brown R.A. Nerve guide material made from fibronectin: assessment of in vitro properties. Tissue Engineering 2003;9(2):219-231.

Aiba S, Minoura N, Fujiwari Y, Yamada S, Nakagawa. Laminates composed of polypeptides and elastomers as a burn wound covering. Physicochemical properties. Biomaterials 1985;6:290-296.

Albert B, Bray D, Lewis J, Raff M, Roberts K, Watson J. The Cell. 2nd Edition. Published by Garland Publishing 1989:54-55.

Alsberg E, Anderson K.W, Albeiruti A, Rowley J.A, Mooney D.J. Engineering growing tissues. Proceedings of the National Academy of Sciences of the United States of America 2002;99:12025-12030.

Al-Shamkhani A, Duncan R. Radioiodination of alginate via covalently-bound tyrosinamide allows monitoring of its fate in vivo. Journal of Bioactive and Compatible Polymers 1995;10:4-13.

Alvarez-Macarie E, Augier-Magro V, Baratti J. Characterization of a thermostable esterase activity from the moderate thermophile Bacillus licheniformis. Bioscience, Biotechnology and Biochemistry 1999;63:1865-1870.

Anselme K, Bacques C, Charriere G, Hartmann D.J, Herbage D, Garrone R. Tissue reaction to subcutaneous implant of a collagen sponge. A histological, ultrastructural and immunological study. Journal of Biomedical Materials Research 1990;24:689-703.

Armstrong R.D, Ogier W.C, Maluta J. Clinical systems for the production of human cells and tissues. Biotechnology 1995;13:449-453.

Atala A, Cima L.G, Kim W, Piage K.T, Vacanti J.P, Retik A.B, Vacanti C.A. Injectable alginate seeded with chondrocytes as a potential treatment for vesicoureteral reflux. Journal of Urology 1993;150:745-747.

Atala A, Kim W, Paige K.T, Vacanti C.A, Retik A.B. Endoscopic treatment of vesicoureteric reflux with a chondrocyte-alginate suspension. Journal of Urology 1994;152: 641-643.

Atkins E.D.T, Niedusynski I.A, Mackie W, Parker K.D, Smolko E.E. Structural components of alginic acid. Crystalline structure of poly-alpha-L-guluronic acid. Results of X-ray diffraction and polarised infrared studies. Biopolymers 1973;12:1879-1887.

Balazs E.A, Leshchiner A. Cross linked gels of hyaluronic acid and products containing such gels. Biomatrix Inc, Ridgefield, USA 1987. US Patent No: 4636524.

Balladur P, Crema E, Honiger J, Calmus Y, Baudrimont M, Delelo R, Capeau J, Nordlinger B. Transplantation of allogeneic hepatocytes without immunosuppression: long term survival. Surgery 1995;117:189-194.

Barnes K.E. Human tissue in drug discovery: promise and pitfalls. Drug Discovery Today 2004;9(2):55.

Barton J.K, Rollins A, Yazdanfar S, Pfefer T.J, Izatt J.A. Photothermal coagulation of blood vessels: a comparison of high-speed optical coherence tomography and numerical modelling. Physics in Medicine and Biology 200146(6):1665-1678.

Barton J.K, Hoying J.B, Sullivan C.J. Use of microbubbles as an optical coherence tomography contrast agent. Academic Radiology 2002;9(Supp 1):52-55.

Beck S. Histology Kits: Avidin and biotin team up to tackle the tissue. The Scientist 1998;12:16-25.

Becker J.M, Dayton M.T, Fazio V.W, Beck D.E, Strkker K.C, Wexner S.D, Wolff B.G, Roberts P.L, Smith L.E, Sweeney S.A, Moore M. Prevention of postoperative abdominal adhesions by a sodium hyaluronate based bioresorbable membrane: a prospective randomised double blinded multicenter study. Journal of the American College of Surgeons 1996;183:297-306.

Bell E, Ehrlich H.P, Buttle D.J, Nakatsuji T. Living tissue formed in vitro and accepted as skin equivalent tissue of full thickness. Science 1981;211:1052-1054.

Bell E, Sher S, Hull B, Merrill C, Rosen S, Chamson A, Asselineau D, Dubertret L, Coulomb B, Lapiere C, Nusgens B. Neveux Y. The reconstitution of living skin. Journal of Investigative Dermatology 1983;81(Suppl 1):,2-10.

Bell E, Rosenberg M, Kemp P, Gay R, Green G.D, Muthukumaran N, Nolte C. Recipes for reconstituting skin. Journal of Biomechanical Engineering 1991;113:113-119.

Bent A.E, Tutrone R.T, Lloyd L.K, Badlani G, Kennelly M.J. Treatment of intrinsic sphincter deficiency using autologous ear cartilage as a periurethral bulking agent. Neurourology and Urodynamics 1999;18(4):296-297.

Bent A.E, Tutrone R.T, McLennan M.T, Lloyd L.K, Kennelly J.K, Badlani G. Treatment of intrinsic sphincter deficiency using autologous ear chondrocytes as a bulking agent. Neurourology and Urodynamics 2001;20:157-165.

Bierman E.L. The effect of donor age on the in vitro life span of cultured human arterial smooth-muscle cells. In Vitro 1978;14(11):951-955.

Bjorkerud S, Bjorkerud B, Joelsson M. Structural organization of reconstituted human arterial smooth muscle tissue. Arteriosclerosis and Thrombosis 1994;14:644-651.

Blaine G. The uses of plastics in surgery. Lancet 1946 October 12th 525-528.

Blaine G. Experimental observations on absorbable alginate products in surgery. Annals of Surgery 1947;125(1):102-114

Blaine G. A comparative evaluation of absorbable haemostatics. Postgraduate Medical Journal 1951;27:613-620.

Blondel B, Roijen I, Cheneval J.P. Heart cells in culture: a simple method for increasing the proportion of myoblasts. Experientia 1971;27:356-358.

Blue S.R, Singh V.R, Saubolle M.A. Bacillus licheniformis bacteremia: five cases associated with indwelling central venous catheters. Clinical Infectious Diseases 1995;20:629-633.

Bodnar A.G, Ouellette M, Frolkis M, Holt S.E, Chiu C.P, Morin G.B, Harley C.B, Shay J.W, Lichtsteiner S, Wright W.E. Extension of life-span by introduction of telomerase into normal human cells. Science 1998;279(5349):349-352.

Bonin L.R, Madden K, Shera K, Ihle J, Matthews C, Aziz S, Perez-Reyes N, McDougall J.K, Conroy S.C. Generation and characterization of human smooth muscle cell lines derived from atherosclerotic plaque. Arteriosclerosis, Thrombosis and Vascular Biology 1999;19(3):575-587.

Boninsegna S, Bosetti P, Carturan G, Dellagiacoma G, Dal Monte R, Rossi M. Encapsulation of individual pancreatic islets by sol-gel SiO2: a novel procedure for perspective cellular grafts. Journal of Biotechnology 2003;100(3):277-286.

Boppart S.A, Tearney G.J, Bouma M.E, Southern J.F, Brezinski M.E, Fujimoto J.G. Noninvasive assessment of the developing Xenopus cardiovascular system using optical coherence tomography. Proceedings of the National Academy of Sciences of the United States of America 1997;94:4256-4261.

Boppart S.A, Bouma B.E, Pitris C, Southern J, Brezinski M.E, Fujimoto J.G. In vivo optical coherence tomography imaging. Nature Medicine 1998(a);4:861-865.

Boppart S.A, Bouma B.E, Pitris C, Southern J.F, Brezinski M.E, Fujimoto J.G. In vivo cellular optical coherence tomography imaging. Nature Medicine 1998(b);4:861-865.

Boppart S.A, Bouma B.E, Pitris C, Southern J.F, Brezinski M.E, Fujimoto J.G. Intraoperative assessment of microsurgery with three-dimensional optical coherence tomography. Radiology 1998(c);208:81-86.

Bornstein P, McPherson J, Sage H Synthesis and secretion of structural macromolecules by endothelial cells in culture. In: Pathobiology of the Endothelial Cell, P & S Biomedical Sciences Symposia, Vol. 6. Eds: H.J. Vogel and H.L. Nossel. Academic Press, New York, USA 1982;215-228.

Boshoff C. Personal Communication 2003. Wolfson Institute for Biomedical Research, The Cruciform Building, Gower Street, London.

Bouma B.E, Tearney G.J, Boppart S.A, Hee M.R, Brezinski M.E, Fujimoto J.G. High-resolution optical coherence tomography imaging using a mode-locked Ti: Al2O3 laser source. Optical Letter 1995;20:1486-1488.

Brache J.W, Thacker K. Hyaluronic acid from bacterial culture. Diagnostics Inc, Minneapolis, USA 1985. US Patent No: 4517295.

Brand S, Poneros J.M, Bouma B.E, Tearney G.J, Compton C.C, Nishioka N.S. Optical coherence tomography in the gastrointestinal tract Endoscopy 2000;32:796–803.

Bray C, Blaine G, Hudson P. New treatment for burns, wounds and haemorrhage. Nursing Mirror 1948:86:239-242.

Brezinski M.E, Tearney G.J, Bouma B.E, Izatt J.A, Hee M.R, Swanson E.A, Southern J.F, Fujimoto J.G. Optical coherence tomography for optical biopsy: properties and demonstration of vascular pathology. Circulation 1996;96:1206-1213.

Brezinski M.E, Tearney G.J, Boppart S.A, Swanson E.A, Southern J.F, Fujimoto J.G. Optical biopsy with optical coherence tomography: feasibility for surgical diagnostics. Journal of Surgical Research 1997;71(1):32-40.

Brezinski M. Characterizing arterial plaque with optical coherence tomography. Current Opinions in Cardiology 2002;17:648-655.

Bromley A. Tissue engineering technologies and markets - Clinica Report 2001. PJB Publications.

Bromley A. Tissue engineering - Ready for mass production? Clinica Market Briefing 2003. PJB Publications.

Brown S.L, Lundgren C.H, Nordt T, Fujii S. Stimulation of migration of human aortic smooth muscle cells by vibronectin: implications for atherosclerosis. Carciovascular Reseach 1994;28:1815-1820.

Burke J.F, Yannas I.V, Quinby Jr. W.C, Bondoc C.C, Jung W.K. Successful use of physiological acceptable artificial skin in the treatment of extensive burn injuries. Annals of Surgery 1981;194(4):413-428.

Burnand K.G.B, Young A.E. The New Aird's Companion in Surgical Studies 1998:1-25.

Butler C.E, Yannas I.V, Compton C.C, Correia C.A, Orgill D.P. Comparison of cultured and uncultured keratinocytes seeded into a collagen-GAG matrix for skin replacements. British Journal of Plastic Surgery 1999; 52:127-132.

Cahill K.S, Toma C, Pittenger M.F, Kessler P.D, Byrne B.J. Cell therapy in the heart: cell production, transplantation, and applications. Methods in Molecular Biology 2003;219:73-81.

Caldamone A.A, Diamond D.A. Long-term results of the endoscopic correction of vesicoureteric reflux in children using autologous chondrocytes. The Journal of Urology 2001;165(6):2224-2227.

Califiore R. Personal communication July 2004.

Carbonetto S.T, Gruver M.M, Turner D.C. Nerve fiber growth on defined hydrogel substrates. Science 1982;216:897-899.

Chaoyuan W. Zhanjiang Fisheries College (People's Republic of China) and Regional Sea farming Development and Demonstration Project (RAS/90/002). Training Manual on Gracilaria Culture and Seaweed Processing in China. August 1990.

Charalambous I, Podoleanu A G, Cucu R, Dobre G, Jackson D. Correction of distortions in en-face and longitudinal OCT images of the eye. The International Conference on Advanced Laser Technology. Cranfield, UK. September 2003.

Charo I.F, Nannizzi L, Smith J.W, Cheresh D.A. The vitronectin receptor alpha v beta 3 binds fibronectin and acts in concert with alpha 5 beta 1 in promoting cellular attachment and spreading on fibronectin. Jounal of Cell Biology 1990;111:2795-2800.

Cheng T.C.E, Podolsky S. Just-in-Time Manufacturing. Published by Kluwer Academic Press 1996.

Chiang C.H, Yeh M.K. Contribution of poly(amino acids) to advances in pharmaceutical biotechnology. Current Pharmaceutical Biotechnology 2003;4(5):323-330.

Chopra A.K, Mathur D.K. Isolation, screening and characterization of thermophilic Bacillus species isolated from dairy products. Journal of Applied Bacteriology 1984;57(2):263-271.

Christen T, Bachaton-Piallat M.L, Neuville P, Rensen S, Redard M, van Eys G, Gabbiani G. Cultured porcine conronary artery smooth muscle cells: a new model with advanced differentiation. Circulation Researach 1999;84:99-107.

Chung T.W, Yang J, Akaike T, Cho K.Y, Nah J.W, Kim S.I, Cho C.S. Preparation of alginate/galactosylated chitosan scaffold for hepatocyte attachment. Biomaterials 2002;23:2827-2834.

Civerchia-Perez L, Faris B, LaPointe G, Beldekas J, Leibowitz H, Franzblau C. Use of collagen-hyroxyethylmethacrylate hydrogels from cell growth. Proceedings fro the National Academy of Sciences of the United States of America 1980;77:2064-2068.

Collins K, Mitchell J.R. Telomerase in the human organism. Oncogene 2002;21(4):564-579.

Correas J.M, Bridal L, Lesavre A, Mejean A, Claudon M, Helenon O. Ultrasound contrast agents: properties of action, tolerance and artifacts. European Radiology 2001;11(8):1316-1328.

Coulomb B, Dubertet L, Merrill C, Touraine R, Bell E. The collagen lattice: a model for studying the physiology, biosynthetic function and pharmacology of the skin. British Journal of Dermatology 1984;111(Supp 27):83-87.

Couzin J. Wanted: Pig transplants that work. Science 2002;295:1008.

Cruttenden N. Personal communication 2001. Technical Services, ISP Alginates (UK) Ltd, Surrey, UK.

Culberton J.H, Rand R.P, Jurkiewicz M.J. Advances in microsurgery. Advances in Surgery 1990;23:57-88.

daCosta A.O, deAssis M.C, Marques E.D., Plotkawski M.C. Compariative analysis of three methods to assess viability of mammalian cells in culture. Biocell 1999;23:65-72.

Dagalakis N, Flink J, Stasikelis J.F, Yannis I.V. Design of an artificial skin III. Control of Pore Structure. Journal of Biomedical Materials Research 1980;14:511-528.

Davenpeck K.L, Marcinkiewicz C, Wany D, Niculescu R, Shi Y, Martin J.L, Zalewski A. Regional differences in integrin expression. Role of alpha(5)beta(1) in regulating smooth muscle cell functions. Circulation Research 2001;88:352-358.

De Bartolomeo A, Trotta F, La Rosa F, Saltalamacchia G, Mastrandrea V. Numerical analysis and DNA base compositions of some thermophilic Bacillus species. International Journal of Systematic Bacteriology 1991;41:502-509.

Deming T.I. Facile synthesis of block copolypeptides of defined architecture. Nature 1997;390:386-389.

Denning C, Priddle H. New frontiers in gene targeting and cloning: success, application and challenges in domestic animals and human embryonic stem cells. Reproduction 2003;126(1):1-11.

Diamond M.P. Reduction in adhesions after uterine myomectomy by Seprafilm membrane (HAL-F) a blinded prospective randomised multicenter clinical trial. Seprafilm Adhesion Study Group. Fertility and Sterility 1996;66:904-910.

Diamond D.A, Caldamone A.A. Endoscopic treatment of vesicoureteric reflux in children using autologous chondrocytes - Preliminary results. Pediatrics 1998;102 Supplement:868.

Ding S, Wu T.Y.H, Brinker A, Peters E.C, Hur W, Gray N.S. Synthetic small molecules that control stem cell fate. Proceedings of the National Academy of Science 2003;100(13):7632-7637.

Dornish M, Kaplan D, Skaugrud O. Standards and guidelines for biopolymers in tissue-engineered medical products: ASTM alginate and chitosan standard guides. Annals of the New York Academy of Sciences 2001;944:388-397.

Draget K.I, Skjåk-Braek G, Smidsrod O. Alginate based new materials. International Journal of Biological Macromolecules. 1997;21:47-55.

Draget K.I, Smidsrod O, Skjåk-Break G. Alginates from algae. In: Steinbuchel A, Yoshiharu D. Biotechnology of Biopolymers - From Synthesis to Patents Biopolymers. Wiley VCH, Verlag, Germany 2004;215-244. (Originally published in Biopolymers Vol 6,

Polysaccharides II: Polysaccharides from Eukaryotes 2002).

Drexler W, Morgner U, Kaetner F.X, Pitris C, Boppart S.A, Li X.D, Ippen E.P, Fujimoto J.G. In vivo ultrahigh resolution optical coherence tomography. Optics Letters 1999;24:1221-1223.

Drexler W, Sattmann H, Hermann B, Ko T.H, Stur M, Unterhuber A, Scholda C, Findl O, Wirtitsch M, Fujimoto J.G, Fercher A.F. Enhanced visualization of macular pathology with the use of ultrahigh-resolution optical coherence tomography. Archives of Ophthalmology 2003;121:695–706.

Driver I, Feather J.W, King P.R, Dawson J.B. The optical properties of aqueous suspensions of Intralipid, a fat emulsion. Physics in Medicine and Biology 1989;34:1927-1930.

Drumheller P.D, Hubbell J.A. Polymer networks with grafted cell adhesion peptides for highly biospecific cell adhesion surfaces. Annals of Biochemisty 1994;222:380-388.

Drury J.L, Mooney D.J. Hydrogels for tissue engineering: scaffold design variables and applications. Biomaterials 2003;24(24):4337-4351.

Dvir-Ginzberg M, Gamlieli-Bonshtein I, Agbaria R, Cohen S. Liver tissue engineering within alginate scaffolds: Effects of cell-seeding density on hepatocyte viability, morphology and function. Tissue Engineering 2003;9:757-767.

Eiselt P, Lee K, Mooney D.J. Rigidity of two-component hydrogels prepared from alginate and poly(ethylene glycol) - diamines. Macromolecules 1999;32:5561-5566.

Elliot R.B, Escobar L, Garkavenko O, Croxson M.C, Schroeder B.A, McGregor M, Ferguson G, Beckman N, Ferguson S. No evidence of infection with porcine endogenous retrovirus in recipients of encapsulated porcine islet xenografts. Cell Transplantation 2000;9:895-901.

Ethicon Inc. Surgical Closure Manual - Ethicon Publications, Summerville, USA 1994.

European Commission 2001. Opinion on the state of the art concerning tissue engineering. The Scientific Committee on Medical Products and Medical Devices DOC. SANCO/SCMPMD/2001/0006 Final.

European Commission 2003. Human tissue-engineered products - Today's markets and future prospects. European Commission Joint Research Centre/Institute for Prospective Technological Studies.

Falanga V, Margolis D, Alvarez O, Auletta M, Maggiacomo F, Altman M, Jensen J, Sabolinski M, Hardin-Young J. Rapid healing of venous ulcers and lack of clinical rejection with an allogeneic cultured human skin equivalent. Human Skin Equivalent Investigators Group. Archives of Dermatology 1998;134(3):293-300.

FDA News. FDA improves the safety of human cells and tissues by finalising new rules for "good tissue practice" P04-104, November 18th 2004.

Federal Register. Current good tissue practice for human cell, tissue, and cellular and tissue-based product establishments; Inspection and enforcement; Final Rule. Federal Register 2004;69(226):68612-68688.

Fercher A.F, Hitzenberger C.K, Drexier W, Kamp G, Sattmann H. In vivo optical coherence tomography. American Journal of Ophthalmology 1993;166:113-114.

Ferrari F.A, Cappello J, (PPTI). Functional recombinantly prepared synthetic protein polymer. 2001. US Patent No: 6184348.

Fox J.L. New US committee considers xenotransplants. Nature Biotechnology 2001;19:290-291.

Freed L.E, Vunjak-Novakovic G Tissue engineering bioreatcors. In: Lanza R.P, Langer R, Vacanti J. Principles of Tissue Engineering, Academic Press, San Diego, USA 2000: Chapter 13.

Freshney R.I. Culture of animal cells: A manual of basic technique. John Wiley and Sons 2000.

Fujimoto J.G, Brezinski M.E, Tearney G.J, Boppart S.A, Bouma B, Hee H.R, Southern J.F, Swanson E.A. Optical biopsy and imaging using optical coherence tomography. Nature Medicine 1995;1(9):970-972.

Fujimoto J.G, Bouma B, Tearney G.J, Boppart S.A, Pitris C, Southern J.F, Brezinski M.E. New technology for high-speed and high-resolution optical coherence tomography. Annals of the New York Academy of Sciences 1998;838:95-107.

Fujimoto J.G, Pitris C, Boppart S, Brezinski M.E. Optical coherence tomography. An emerging technology for biomedical imaging and optical biopsy. Neoplasia 2000;2(1-2):9-25.

Fujimoto J.G. www.lightlabimaging.com 2003a.

Fujimoto J.G. Optical coherence tomography imaging for ultrahigh resolution of in vivo imaging. The International Conference on Advanced Laser Technology. Cranfield, UK. September 2003b.

Fultz M.E, Li C, Geng W, Wright G.L. Remodeling of the actin cytoskeleton in the contracting A7r5 smooth muscle cell. Journal of Muscle Research & Cell Motility 2000;21:775-87.

Fultz M.E, Wright G.L. Myosin remodelling in the contracting A7r5 smooth muscle cell. Acta Physiologica Scandinavica 2003;177:197-205.

Funderburgh J.L, Funderburgh M.L, Mann M.M, Corpuz L, Roth M.R. Proteoglycan expression during transforming growth factor beta-induced keratocyte-myofibroblast trans-differentiation. Journal of Biological Chemistry 2001;276:44173-44178.

Gaspar H.B, Howe S, Thrasher A.J. Gene therapy progress and prospects: gene therapy for severe combined immunodeficiency. Gene Therapy 2003;10(24):1999-2004.

Gensheimer D. A review of calcium alginates. Ostomy/Wound Management 1993;39(1):34-43.

Gombotz W.R, Wee S.F. Protein release from alginate matrices. Advanced Drug Delivery Reviews 1998;31:267-285.

Gordon D, Reidy M.A, Benditt E.P, Schwartz S.M. Cell proliferation in human coronary arteries Proceedings of the National Academy of Science USA 1990;87:4600-4604.

Grant G.T, Morris E.R, Rees D.A, Smith P.J.C, Thom D. Biological interactions between polysaccharides and divalent cations: the egg box model. FEBS 1973;32:195-198.

Grasdalen H. High-field 1H-N.M.R Spectroscopy of Alginate: Sequential Structure and Linkage Conformations. Carbohydrate Research. 1983;118,255-260.

Greatorex R.A. Thyroidectomy. In: Calne R, Pollard S.G. Operative Surgery, Gower Medical Publishing, London, UK 2001:1.13-1.20.

Griffith L.G, Naughton G. Tissue engineering - Current challenges and expanding opportunities. Science 2002;295:1009-1016.

Griffith L.G. Nanoscale to microscale materials and devices for tissue engineering. Society of Chemical Engineering (Process Engineering Group)/Institute of Chemical Engineering

Cambridge University, January 2003.

Grunwald J, Mey J, Schonleben W, Hauss J, Hauss W.H. Cultivated human arterial smooth muscle cells. The effect of donor age, blood pressure, diabetes and smoking on in vitro cell growth. Pathologie et Biologie 1983;31(10):819-23.

Guilak F. Functional tissue engineering: The role of biomechanics in reparative medicine. Annals of the New York Academy of Sciences 2002;961:193-195.

Guyton A.C. Partition of the body fluids: Osmotic equilibria between extracellular and intracellular fluids. In: Textbook of Medical Physiology. W.B. Saunders Company. 1986;382-392.

Guyton A.C, Hall J.E. Textbook of Medical Physiology. Publisher: W.B. Saunders, 2000.

Hackel V, Klein J, Megnet R, Wagner F. Immobilisation of microbial cells in polymeric matrices. European Journal of Applied Microbiology 1975;1:291-293.

Hagen A, Skjåk-Braek G, Dornish M. Pharmacokinetics of sodium alginate in mice. European Journal of Pharmaceutical Sciences. 1996;4:S100.

Halstenberg S, Panitch A, Rizzi S, Hall H, Hubbell J.A. Biological engineered protein-graft-poly(ethylene glycol) hydrogels: A cell adhesion and plasmin-degradable biosynthetic material for tissue repair. Biomacromolecules 2002;3:710-723.

Hamlyn P.K, Schmidt R.J. Potential therapeutic application of fungal filaments in wound management. Mycologist 1994;8(4):147-152.

Hannah W.N. Jr., Ender P.T. Persistent Bacillus licheniformis bacteremia associated with an intentional injection of organic drain cleaner. Clinical Infectious Diseases1999;29:659-661.

Hansbrough J.F, Herndon D.N, Heimbach D.M, Solem L.D, Gamelli R.L, Tompkins R.G. Accelerated healing and reduced need for grafting in paediatric patients treated with arginine-glycine-aspartic acid peptide matrix. Journal of Burn Care and Rehabilitation 1995;16(4):377-387.

Harvey S.C. The use of fibrin paper and forms in surgery. Boston medical and Surgical Journal 1916;174:658-659.

Hasse C, Klock G, Schlosser A, Zimmermann U, Rothmund M. Parathyroid allotransplantation without immunosuppression. Lancet 1997;350:1296-1297.

He J.Q, Ma Y, Lee Y, Thomson J.A, Kamp T.J. Human embryonic stem cells develop into multiple types of cardiac myocytes: action potential characterization. Circulation Research 2003;93(1):32-39.

Hedin U, Thyber J. Plasma fibronectin promotes modulation of arterial smooth-muscle cells from contractile to synthetic phenotype. Differentiation 1987;33:239-246.

Helmuth L. Fetal cells help Parkinson's patients. Science 1999;286(5441):886-887.

Hench L.L, Polak J.M. Third-generation biomedical materials. Science 2002;295(5557):1014-1017.

Hentz V.R, Chang J. Tissue engineering for reconstruction of the thumb. Editorial. New England Journal of Medicine 2001;344:1547-1548.

Hirschi K.K. Vascular Repair Break out Session - Tissue Engineering and Regenerative Medicine Symposium, Texas/UK Bioscience Initiative, Imperial College, London, March 2004.

Houseman B.T, Marksich M. The microenvironment of immobilised Arg-Gly-Asp peptides is an important determinant of cell adhesion. Biomaterials 2001;22:943-955.

House of Commons Select Committee on Science and Technology, Memorandum submitted by the National Endowment for Science, Technology and the Arts (NESTA). The United Kingdom Parliament Publications. Appendices to the Minutes of Evidence - Appendix 1, 2002.

Huang D, Swanson E.A, Lin C.P, Schuman J.S, Stinson W.G, Chang W, Hee M.R, Flotte T, Gregory K, Puliafito C.A, Fujimoto J.G. Optical coherence tomography. Science 1991;254:1178-1181.

Hubel K, Engert A. Clinical applications of granulocyte colony-stimulating factor: an update and summary. Annals of Hematology 2003;82(4):207-13.

Hubbell J.A. Biomaterials in tissue engineering. Biotechnology 1995;13:565-576.

Hunt B.J, Poston L, Schachter M, Halliday A. An introduction to vascular biology. Cambridge University Press 2002:3-33.

Hutmacher D.W, Teoh S.H, Zein I, Ranawake M, Lau S. Tissue engineering research: The engineer's role. Medical Device Technology 2000;January/February:33-36.

Hynes R.O. Integrins; versatility, modulation, and signalling in cell adhesion. Cell 1992;69:11-25.

Hynes R.O, Madlambayan G, Mooney D.J. Alginate hydrogels as synthetic extracellular materials. Biomaterials 1999;20:45-53.

Isaac G.H, Dowson D, Wroblewski B.M. An investigation into the origins of time-dependent variation in penetration rates with Charnley acetabular cups - wear, creep or degradation? Proceedings of the Institution of Mechanical Engineers. Part H - Journal of Engineering in Medicine 1996;210(3):209-216.

Janstova B, Luasova J. Heat resistance of Bacillus spp. spores isolated from cow's milk and farm environment. Acta Veterinaria Brno 2001;70:179-184.

Johnson J.L, Jaworowicz W, Cleland J.L, Bailey L, Charnis M, Duenas E, Wu C, Shepard D, Magil S, Magil S, Last T, Jones A.J, Putney S.D. The stabilisation and encapsulation of human growth hormone into biodegradable microspheres. Pharmaceutical Research 1997;14(6):730-735.

Johnson K.A, Rogers G.J, Roe S.C, Howlett C.R, Clayton M.K, Milthorpe B.K. Schindhelm K. Nitrous acid pre-treatment of tendon xenografts cross-linked with glutaraldehyde and sterilized with gamma irradiation. Biomaterials 1999; 20:1003-1015.

Joki T, Machluf M, Atala A, Zhu J, Seyfried N.T, Dunn I.F, Abe T, Carroll R.S, Black P.M. Continuous release of endostatin from microencapsulated engineered cells for tumor therapy. Nature Biotechnology 2001;19:35—39.

Jork A, Thurmer F, Cramer H, Zimmermann G, Gessner P, Hamel K, Hofmann G, Kuttler B, Hahn H.J, Josimovic-Alasevic O, Fritsch K.G, Zimmermann U. Biocompatible alginate from freshly collected Laminaria pallida for implantation. Applied Microbiology and Biotechnology 2000;53:224-229.

Junqueira L.C, Carneiro J, Long J. Muscle Tissue. A Basic Histology. Prentice-Hall 1986 Chapter 11.

Kaplan J.M, Pennington S.E, St.George J.A, Woodworth L.A, Fasbender A, Marshall J, Cheng S.H, Wadsworth S.C, Gregory R.J, Smith A.E. Potentiation of gene transfer to the mouse lung by complexes of adenovirus vector and polycations improves therapeutic potential. Human

Gene Therapy 1998;9;1469-1479.

Kavalkovich KW, Boynton RE, Murphy JM, Barry F. Chondrogenic differentiation of human mesenchymal stem cells within an alginate layer culture system. Society for In Vitro Biology Journal 2004;38:457-466.

Kehlet Barton J, Izatt J.A, Kulkarni M.D, Yazdanfar S, Welch A.J. Three-dimensional reconstruction of blood vessels from in vivo color Doppler optical coherence tomography images. Dermatology 1999;198(4):355-361.

Kelm J.M, Fussenegger M. Microscale tissue engineering using gravity-enforced cell assembly. Trends in Biotechnology 2004;22(4):195-202.

Kemp P.D. Tissue engineering: The company perspective. Tissue Engineering Sector Networking Meeting - Department of Trade and Industry, November 2003a.

Kemp P.D. Personal communication 2003b. Ex-Organogenesis, Canton, Massachucetts, USA - currently Intercytex Ltd, Wythenshawe, Manchester, UK.

Khalil M, Shariat-Panahi A, Tootle R, Ryder T, McCloskey P, Roberts E, Hodgson H, Seldon C. Human hepatocyte cell lines proliferating as cohesive spheroid colonies in alginate markedly upregulate both synthetic and detoxifying liver function. Journal of Hepatology 2001;34:69-77.

Kierstan M, Bucke C. The immobilization of microbial cells, subcellular organelles, and enzymes in calcium alginate gels. Biotechnology and Bioengineering 1997;19(3):387-397.

Kimes B.W, Brandt B.L. Characterization of two putative smooth muscle cell lines from rat thoracic aorta. Experimental Cell Research 1976;98:349-366.

King S.M. Can Dr Soon-Shiong perform miracles? Diabetes World May 1998 Interview with Dr. Soon-Shiong.

Kitahara A.K, Nishimura Y, Shimizu Y, Endo K. Facial nerve repair accomplished by the interposition of a collagen nerve guide. Journal of Neurosurgery 2000;93:113-120.

Klock G, Frank H, Houben R, Zekorn T, Horcher A, Siebers U, Wohrle M, Federlin K, Zimmermann U. Production of purified alginates suitable for use in immunoisolated transplantation. Applied Microbiology and Biotechnology. 1994;40:638-643.

Klock G, Pfeffermann A, Ryser C, Grohn P, Kuttler B, Hahn H.J, Zimmermann U. Biocompatibility of mannuronic acid rich alginates. Biomaterials 1997;18:707-713.

Klug M.G, Soonpaa M.H, Koh G.Y, Field L.J. Genetically selected cardiomyocytes from differentiating embryonic stem cells form intracardiac grafts. Journal of Clinical Investigation 1996;98(1):216-224.

Kobune M, Kawano Y Ito Y, Chiba H, Nakamura K, Tsuda H, Sasaki K, Dehari H, Uchida H, Honmou O, Takahashi S, Bizen A, Takimoto R, Matsunaga T, Kato J, Kato K, Houkin K, Niitsu Y, Hamada H. Telomerized human multipotent mesenchymal cells can differentiate into hematopoietic and cobblestone area-supporting cells. Experimental Hematology 2003;31(8):715-722.

Koivunen E, Wang B, Ruoslahti J. Isolation of a highly specific ligand for $\alpha 5\beta 1$ integrin from a phage display library. Jounal of Cell Biology 1994;124:373.

Ku D.N, Braddon L.G, Wootton D.M. Poly(vinyl alcohol) cryogel. Georgia Institute of Technology, Atlanta, Georgia, USA 1999. US Patent No: 5981826.

Kuo C.K, Ma P.X. Ionically cross linked alginate hydrogels as scaffolds for tissue

engineering: part 1. Structure, gelation rate and mechanical properties. Biomaterials 2001;22:511-521.

Kvam B.J, Atzori M, Toffanin R, Paoletti S, Biviano F. 1H and 13C NMR studies of solutions of hyaluronic acid esters and salts in methyl sulphoxide: comparison of hydrogen bond patterns and conformational behaviour. Carbohydrate Research 1992;230:1-13.

Kyle R.A, Shampo M.A. Albert Michelson JAMA 1981;246(8):880.

Lahiji A, Sohrabi A, Hungerford D.S, Frondoza C.G. Chitosan supports the expression of extracellular matrix proteins in human osteoblasts and chondrocytes. Journal of Biomedical Materials Research 2000;51:586-595.

Lanza R.P, Jackson R, Sullivan A, Ringeling J, McGrath C, Kuhtreiber W, Chick W.L. Xenotransplantation of cells using biodegradable microcapsules. Transplantation 1999;67:1105-1111.

Leinfelder U, Brunnenmeier F, Cramer H, Schiller J, Arnold K, Vasquez J.A, Zimmermann U. A highly sensitive cell assay for validation of purification regimes of alginates. Biomaterials. 2003;24(23):4161-4172.

Leo W.J, McLoughlin A.J, Malone D.M. Effects of sterilization treatments on some properties of alginate solutions and gels. Biotechnology Progress 1990;6:51-53.

Levenberg S, Huang N.F, Lavik E, Rogers A.B, Itskovitz-Eldor J, Langer R. Differentiation of human embryonic stem cells on three-dimensional polymer scaffolds. Proceedings of the National Academy of Sciences of the United States of America 2003;100:12741-12746.

Levin M.P, Tsaknis P.J, Cutright D.E. Healing of the oral mucosa with the use of collagen artificial skin. Journal of Periodontology 1979;50(5):250-253.

L'Heureux N, Paquet S, Labbe R, Germain L, Auger FA. A completely biological tissue-engineered human blood vessel. FASEB Journal 1998;12(1):47-56.

L'Heureux N, Stoclet J-C, Auger F.A, Lagaud G.J-L, Germain L, Adriantsitohaina R. A human tissue-engineered vascular media: a new model for pharmacological studies of contractile response. FASEB 2001;15:515-524.

Lin H.B, Sun W, Mosher D.F, Garcia-Echeverria C, Schaufelberger K, Lelkes P.I, Cooper S.L. Synthesis, surface, and cell-adhesion properties of polyurethanes containing covalently grafted RGD-peptides. Journal of Biomedical Materials Research 1994;28:329-342.

Lindow S.W, Regnell P, Sykes J, Little S. An open-label, multicentre study to assess the safety and efficacy of a novel reflux suppressant (Gaviscon Advance) in the treatment of heartburn during pregnancy. International Journal of Clinical Practice 2003;57(3):175-179.

Linker A, Jones R.S. A polysaccharide resembling alginic acid from a Pseudomonas microorganism. Nature 1964;204:187-188.

Lowel M. Manufacturing of autologous cell transplants. Screening 2003;1:34-36.

Lundborg G, Rosen B, Dahlin L, Danielsen N, Holmberg J. Tubular versus conventional repair of median and ulnar nerves in the human forearm: Early results from a prospective, randomized, clinical study. The Journal of Hand Surgery 1997;22A: 99-106.

Luscinskas F.W, Lawler J. Integrins as dynamic regulators of vascular function. FASEB Journal1994;8:929-938.

Lysaght M.J. Product development in tissue engineering. Tissue Engineering 1995;1(2):221-228

Lysaght M.J, Nguy N.A.P, Sullivan K. An economic survey of the emerging tissue engineering industry. Tissue Engineering 1998;4(3):231-238.

Lysaght M.J, Reyes J. The growth of tissue engineering. Tissue Engineering 2001;7(5):485-493.

Lysaght M.J. Tissue engineering: Great expectations. Engineering Tissue Growth International Conference, Pittsburgh, PA, USA March 2003.

Lysaght M.J, Hazlehurst A.L. Tissue engineering: The end of the beginning. Tissue Engineering 2004;10(1/2):309-320.

Mandel K.G, Daggy B.P, Brodie D.A, Jacoby H.I. Review article: alginate-raft formulations in the treatment of heartburn and acid reflux. Alimentary Pharmacology and Therapeutics 2000;14:669-690.

Mann B.K, West J.L. Cell adhesion peptides alter smooth muscle cell adhesion, proliferation, migration, and matrix protein synthesis on modified surfaces and in polymer scaffolds. Journal of Biomedical Materials Research 2002;60:86-93.

Mann B.K. Biologic gels in tissue engineering. Clinics in Plastic Surgery 2003;30(4):601-609.

Markwald R. Desktop organ printing. Anatomical Record 2003;273B:120-121.

Martin I, Wendt D, Heberer M. The role of bioreactors in tissue engineering. Trends in Biotechnology 2004;22(2):80-86.

Martinsen A, Skjåk-Braek G, Smidsrod O. Alginate an immobilisation material: I. Correlation between chemical and physical properties of alginate gel beads. Biotechnology and Bioengineering 1989;33:79-89.

Martinsen A, Storro I, Skjale-Braek G. Alginate as immobilization material III. Biotechnology and Bioengineering 1992;39:186-194.

Mason C. A method for producing tissue structures. 2000 GB 2360789.

Mason C, Town M.A. Methods for forming hardened sheets and tubes. 2002a; PCT/GB02/0118.

Mason C, Town M.A. Methods for forming matrices of hardened materials. 2002b; PCT/GB02/00547.

Mason C. Automated tissue engineering: A major paradigm shift in health care. Medical Device Technology 2003;14(1):16-18.

Mason C, Town M.A. Devices for use in medicine. 2003a; PCT/GB03/01334.

Mason C, Town M.A. Delivery assembly for use in surgery. 2003b; PCT/GB03/01368.

Mason C, Markusen J.F, Boshoff C.H. Methods employing cells derived from adult bone marrow. 2003; GB 0301834.8.

Mason C, Markusen J.F, Town M.A, Dunnill P.D, Wang R.K. The potential of optical coherence tomography in the engineering of living tissue. Physics in Medicine and Biology 2004a;49:1097-1116.

Mason C, Markusen J.F, Town M.A, Dunnill P.D, Wang R.K. Doppler optical coherence tomography for measuring flow in engineered tissue. Biosensors and Bioelectronics 2004b;20:414-423.

Mason C. Controlled cell deposition techniques. In: Surfaces and Interfaces. Editor:

Vadgama P. Publisher: Woodhead Publishing, Cambridge, UK, 2005. Chapter 17.

Massia S.P, Hubbell J.A. Covalently grafted Arg-Gly-Asp and Tyr-Ile-Gly-Ser-Arg containing synthetic peptides support receptor mediated adhesion of cultured fibroblasts. Analytical Biochemistry 1990;187:292-301.

Massia S.P, Hubbell J.A. Human endothelial cell interactions with surface-coupled adhesion peptides on a nonadhesive glass substrate and two polymeric biomaterials. Journal of Biomedical Materials Research 1991a;25:223-242.

Massia S.P, Hubbell J.A. An RGD spacing of 440 nm is sufficient for integrin alpha V beta 3 mediated fibroblast spreading and 140 nm for focal contact and stress fibre formation. Journal of Cell Biology 1991b;114:1089-1100.

Matsuda T, Kondo A, Makina K, Akutsu T. Development of a novel artificial matrix with cell adhesion peptides for cell culture and artificial and hybrid organs. ASAIO Transactions 1989;35:677-679.

Matsumura G, Hibino N, Ikada Y, Kurosawa H, Shin'oka T. Successful application of tissue engineered vascular autografts: clinical experience. Biomaterials 2003;24(13):2303-2308.

Mayhew T.A, Williams G.R, Senica M.A, Kuniholm G, Du Moulin G.C. Validation of a quality assurance program for autologous cultured chondrocyte implants. Tissue Engineering 1998;4(3):325-334.

McGilvery R.W, Goldstein G.W. Carbohydrates as structural elements. In: McGilvery R.W, Goldstein G.W. Biochemistry, a functional approach. W.B. Saunders, Philadelphia, PA. 1983;178-202.

McKee J.A, Banik S.S.R, Boyer M.J, Hamad N.M, Lawson J.H, Niklason L.E, Counter C.M. Human arteries engineered in vitro. EMBO Reports 2003;4(6):633–638.

McKenna N. Biomaterials firms exploit range of techniques. Genetic Engineering News 2001;21:8,9-51.

McPherson D.T, Morrow C, Minehan D.S, Wu J, Hunter E, Urry D.W . Production and purification of a recombinant elastomeric polypeptide, G-(VPGVG)19-VPGV from Escherichia coli. Biotechnology Progress 1992;8:347-52.

McPherson T.B, Liang H, Record R.D, Badylak S.F. Gal-alpha(1,3)Gal epitope in porcine small intestinal submucosa. Tissue Engineering 2000;6:233-239.

Medical Research Council, Research in Focus: Stem Cell Cloning September 2000.

Menasche P. Myoblast transfer in heart failure. Surgical Clinics of North America 2004;84(1):125-139.

Mercurius K.O, Morla A.O. Inhibition of vascular smooth muscle cell growth by inhibition of fibronectin matrix assembly. Circulation 1998;82:548-556.

Mikkola R, Kolari M, Andersson M.A, Helin J, Salkinoja-Salonen M.S. Toxic lactonic lipopeptide from food poisoning isolates of Bacillus licheniformis. European Journal of Biochemistry 2000;267:4068-4074.

Miura Y, Akimotot T, Kanazawa H, Yagi K. Synthesis and secretion of protein by hepatocytes entrapped within calcium alginate. Artificial Organs 1986;10:460-465.

Moger J, Matcher S.J, Winlove C.P. Measuring red blood cell flow dynamics in a glass capillary using Doppler OCT and Doppler amplitude OCT. The International Conference on Advanced Laser Technology, Cranfield, UK. September 2003.

Mohanna P.N, Young R.C, Wiberg M, Terenghi G. A composite poly-hydroxybutyrate-glial growth factor conduit for long nerve gap repairs. Journal of Anatomy 2003;203(6):553-565.

Morris E.R, Rees D.A, Thom D, Boyd J . Chiroptical and stoichiometric evidence of a specific primary dimerisation process in alginate gelation. Carbohydrate Research 1978;66:145-54.

Mosahebi A, Miberg M, Terenghi G. Addition of fibronectin to alginate matrix improves peripheral nerve regeneration in tissue-engineered conduits. Tissue Engineering 2003;9(2):209-218.

Moses M.A, Klagsbrun M, Shing Y. The role of growth factors in vascular development and differentiation. International Review of Cytology 1995;161:1-48.

Muzzarelli R, Balddassara V, Conti F, Ferrara P, Biagini G, Gazzerelli G, Vasi V. Biological activity of chitosan: Ultrastructural study. Biomaterials 1988;9: 247-252.

Myken P, Bech-Hanssen O, Phipps B, Caidahl K. Fifteen year follow up with the St Jude Medical Biocor bioprosthesis. Journal of Heart Valve Disease 2000;9: 415-422.

Nakamura T.M, Cech T.R. Reversing time: Origin of telomerase. Cell 1998;92(5):587-590.

Nam Y.S, Yoon J.J, Lee J.G, Park T.G. Adhesion behaviour of hepatocytes cultured onto biodegradable polymer surface modified by alkali hydrolysis process. Journal of Biomaterials Science (Polymer Edition) 1999;10: 1145-1158.

National Institutes of Health Bioengineering Consortium. Reparative medicine: Growing tissues and organs. National Institutes of Health, June 2001.

Naughton G. Skin, The first tissue engineered products: The Advanced Tissue Sciences Story. Scientific American 1999;280(4):84-85.

Negishi N, Bennett D.B, Cho C.S, Jeong S.Y, van Heeswijk W.A, Feijen J, Kim S.W. Coupling of naltrexone to biodegradable poly(alpha-amino acids). Pharmaceutical Research 1987;4:305-310.

Nelson J.S, Kelly K.M, Zhao Y, Chen Z. Imaging blood flow in human port-wine stain in situ and in real time using optical Doppler tomography. Archives of Dermatology 2001;137(6):741-744.

Nicol A, Gowda D.C, Urry D.W. Cell adhesion and growth on synthetic elastomeric matrices containing Arg-Gly-Asp-Ser3. Journal of Biomedical Materials Research 1992;26:393-413.

Nielsen J.N. Missile Aerodynamics. Publisher: McGraw-Hill, New York, USA, 1960.

Niklason L.E, Gao J, Abbott W.M, Hirschi K.K, Houser S, Marini R, Langer R. Functional arteries grown in vitro. Science 1999; 284:489-493.

Niklason L.E, Abbott W, Gao J, Klagges B, Hirschi K.K, Ulubayram K, Conroy N, Jones R, Vasanawala A, Sanzgiri S, Langer R. Morphologic and mechanical characteristics of engineered bovine arteries. Journal of Vascular Surgery 2001;33:628-638.

Oerther S, Gall H.L, Payan E, Lapicque F, Presle N, Hubert P, Dexheimer J, Netter P, Lapicque E. Hyaluronate-alginate gel as a novel biomaterial: Mechanical properties and formation mechanism. Biotechnology and Bioengineering 1999(a);63:206-215.

Oerther S, Payan E, Lapique F, Presle N, Hubert P, Muller S, Netter P, Lapique E. Hyaluronate-alginate combination for the preparation of new biomaterials: Investigation of the behaviour

in aquous solutions. Biochimica et Biophysica acta 1999(b);1426:185-194.

Office of Science and Technology Annual Report - Fiscal Year 1999. Food and Drug Administration and Center for Devices and Radiological Health, May 2000.

Okamoto T, Aoyama T, Nakayama T, Nakamata T, Hosaka T, Nishijo K, Nakamura T, Kiyono T, Toguchida J. Clonal heterogeneity in differentiation potential of immortalized human mesenchymal stem cells. Biochemical and Biophysical Research Communications 2002;295(2):354-361.

Oliver L.C, Blaine G. Heamostasis with absorbable alginates in neurosurgical practice. The British Journal of Surgery 1950;37:307-310.

Olivieri M.P, Tweden K.S. Human serum albumin and fibrinogen interactions with an adsorbed RGD containing peptide. Journal of Biomedical Materials Research 1999;46:355-359.

Omstead D.R, Baird L.G, Christenson L, Du Moulin G, Tubo R, Maxted D.D, Davis J, Gentile F.T. Voluntary guidance for the development of tissue-engineered products. Tissue Engineering 1998;4(3):239-265.

Otis L.L, Everett M.J, Sathyam U.S, Colston B.W. Jr. Optical coherence tomography: a new imaging technology for dentistry. Journal of the American Dental Association 2000;131:511-114.

Otterlei M, Ostgaard K, Skjåk-Braek G, Smidsrod O, Soon Shiong P, Espevik T. Induction of cytokine production from human monocytes stimulated with alginate. Journal of Immunotherapy 1991;10:286-291.

Owens G.K. Regulation of differentiation of vascular smooth muscle cells. Physiological Reviews 1995;75:487-517.

Pachence J.M, Berg R.A, Silver F.H. Collagen: Its place in the medical device industry. Medical Device and Diagnostic Industry 1987;9:49-55.

Pachence J.M. Collagen-based devices for soft tissue repair. Journal of Biomedical Materials Research 1996;33:35-40.

Pachence J.M, Kohn J. Biodegradable Polymers. In: Lanza R.P, Langer R, Vacanti J. Principles of Tissue Engineering. Academic Press, San Diego, USA 2000:Chapter 22.

Pakhomov O, Honiger J, Gouin E, Cariolet R, Reach G, Darquy S. Insulin treatment of mice recipients preserves beta-cell function in porcine islet transplantation. Cell Transplantation 2002;11(7):721-728.

Palapura S, Kohn J. Trends in the development of bioresorbable polymers for medical applications. Journal of Biomaterial Applications 1992;6:216-250.

Palop A, Raso J, Pagan R, Condon S, Sala F.J. Influence of pH on heat resistance of Bacillus licheniformis in buffer and homogenised foods. International Journal of Food Microbiology 1996;29:1-10.

Parenteau N. Skin, The first tissue engineered products: The Organogenesis story. Scientific American 1999;280(4):83-84.

Passe E.R.G, Blaine G. Alginates in endaural wound dressing. Lancet 1948 October 23rd 651.

Paszkowiak J.J, Dardik A. Arterial wall shear stress: observations from the bench to the bedside. Vascular & Endovascular Surgery 2003;37(1):47-57.

Patrick Jr. C.W, McIntre L.V. Shear stress and cyclical strain modulation in vascular endothelial cells. Blood Purification 1995;13:112-124.

Patrick Jr. C.W, Mikos A.G, McIntire L.V. Frontiers in Tissue Engineering 1998(a):3-11.

Patrick Jr. C.W, Mikos A.G, McIntire L.V. Frontiers in Tissue Engineering 1998(b):61-82.

Perin E.C, Dohmann H.F, Borojevic R, Silva S.A, Sousa A.L, Mesquita C.T, Rossi M.I, Carvalho A.C, Dutra H.S, Dohmann H.J, Silva G.V, Belem L, Vivacqua R, Rangel F.O, Esporcatte R.,Geng Y.J, Vaughn W.K, Assad J.A, Mesquita E.T, Willerson J.T. Transendocardial, autologous bone marrow cell transplantation for severe, chronic ischemic heart failure. Circulation 2003;107(18):2294-2302.

Persidis A. Tissue Engineering. Nature Biotechnology 1999;17(5):508-510.

Peters M.C, Isenberg B.C, Rowley J.A, Mooney D.J. Release from alginate enhances the biological activity of vascular endothelial growth factor. Journal of Biomaterials Science (Polymer Edition) 1998;9:1267-1278.

Peter M.G. Chitin and chitosan from fungi. In: Steinbuchel A. Biopolymers Volume 6: Polysaccharides II. Wiley VCH, Verlag, Germany 2002;123-157.

Peterson K.P, Peterson C.M, Pope E.J. Silica sol-gel encapsulation of pancreatic islets. Proceedings of the Society for Experimental Biology & Medicine 1998;218(4):365-369.

Piersbacher M.D, Ruoslahti E. Cell attachment activity of fibronectin can be duplicated by small synthetic fragments of the molecule. Nature 1984;309:30-33.

Pinches M.J, Callear B.J. Power Pneumatics. Published by Prentice Hall Europe 1997

Podoleanu A.G, Seeger M, Dobre G.M, Webb D.J, Jasckson D.A, Fitzke F.W. Transversal and longitudinal images from the retina of the living eye using low coherence reflectometry. Journal of Biomedical Optics 1998;3(1),12-20.

Podoleanu A, Charalambous I, Plesea L, Dogariu A, Rosen R. Correction of distortions in optical coherence tomography imaging of the eye. Physics in Medicine and Biology 2004;49:1277-1294.

Preston S.L, Alison M.R, Forbes S.J, Direkze N.C, Poulsom R, Wright N.A. The new stem cell biology: something for everyone. Molecular Pathology 2003;56:86-96.

Price L.S. Morphological control of cell growth and viability. Bioessays 1997;19:941-943.

Proskurin S.G, Sokolova I.A, Wang R.K. Imaging of non-parabolic velocity profiles in coverging flow with optical coherence tomography. Physics in Medicine and Biology 2003(a);48:2907-2918.

Proskurin S.G, He Y, Wang R.K. Determination of flow velocity vector based on Doppler shift and spectrum broadening with optical coherence tomography. Optics Letters 2003(b);28:1227-1229.

Radisic M, Euloth M, Yang L. Langer R, Freed L.E, Vunjak-Novakovic G. High-density seeding of myocyte cells for cardiac tissue engineering. Biotechnology and Bioengineering 2003;82(4):403-414.

Read T.A, Sorensen D.R, Mahesparan R, Enger P.O, Timpl R, Olsen B.R, Hjelstuen M.H.B, Haraldseth O, Bjerkvig R. Local endostatin treatment of gliomas administered by microencapsulated producer cells. Nature Biotechnology 2001;19:29-34.

Redekop W.K, McDonnell J, Verboom P, Lovas K, Kalo Z. The cost effectiveness of Apligraf treatment of diabetic foot ulcers. Pharmacoeconomics 2003;21(16):1171-1183.

Rehm B.H.A, Valla S. Bacterial alginates: biosynthesis and applications. Applied Microbiology and Biotechnology 1997;48:281-288.

Roe S.C, Milthorpe B.K, True K, Rogers G.J, Schindhelm K. The effect of gamma irradiation on a xenograft tendon bioprosthesis. Clinical Materials 1992;9:149-154.

Ronan J.M, Thompson S.A. (Boston Scientific Corporation, Natick, MA, USA). Medical devices comprising ionically and non-ionically crosslinked polymer hydrogels having improved mechanical properties. United States Patent: 6,387,978 January 2001.

Rowley J.A, Madlambayan G, Mooney D.J. Alginate hydrogels as synthetic extra cellular matrix materials. Biomaterials 1999;20:45-53.

Rowley J.A, Mooney D.J. Alginate type and RGD density control myoblast phenotype. Journal of Biomedical Material Research 2002;60:217-223.

Ruoslahti E, Pierschbacher M.D. New perspectives in cell adhesion: RGD and integrins. Science 1987;238:491-497.

Ruoslahti E. RGD and other recognition sequences for integrins. Annual review of cell and developmental biology 1996;12:69-715.

Sabra W, Zeng A-P, Deckwer W-D. Bacterial alginate: physiology, product quality and process aspects. Applied Microbiology and Biotechnology 2001;56:315-325.

Salkinoja-Salonen M.S, Vuorio R, Andersson M.A, Kampfer P, Andersson M.C, Honkanen-Buzalski T, Scoging A.C. Toxigenic strains of Bacillus licheniformis related to food poisoning. Applied & Environmental Microbiology 1999;65:4637-4645.

Saltzman W.M. Cell interactions with polymers. In: Lanza R.P, Langer R, Vacanti J. Principles of Tissue Engineering. Academic Press, San Diego, USA 2000:Chapter 19.

Sambanis A. Encapsulated islets in diabetic treatment. Diabetes Technology and Therapeutics 2003;5(4):665-668.

Sanders M. Molecular and cellular concepts in atherosclerosis. Pharmacology and Therapeutics 1994;61:109-153.

Santini F, Borghetti V, Amalfitano G, Mazzucco A. Bacillus licheniformis prosthetic aortic valve endocarditis. Journal of Clinical Microbiology 1995;33:3070-3073.

Saraswathi S.J, Babu B, Rengasam R. Seasonal studies on the alginate and its biochemical composition I: Sargassum polycystum (Fucales), Phaeophyceae. Phycological Research 2003;51(4) 240-243.

Sauter G, Simon R, Hillan K. Tissue microarrays in drug discovery. Nature Reviews - Drug Discovery 2003;2:962-972.

Scharp D.W, Swanson C.J, Olack B.J, Latta P.P, Hegre O.D, Doherty E.J, Gentile F.T, Flavin K.S, Ansara M.F, Lacy P.E. Protection of encapsulated human islets implanted without immunosuppression in patients with type I or type II diabetes and in nondiabetic control subjects. Diabetes 1994;43:1167-1170.

Schmitt J.M. Optical coherence tomography (OCT): A review. IEEE Journal of selected topics in quantum electronics 1999;5(4):1205-1215.

Schonfeld W.H, Villa K.F, Fastenau J.M, Mazonson P.D, Falanga V. An economic assessment of Apligraf (Graftskin) for the treatment of hard-to-heal venous leg ulcers. Wound Repair &

Regeneration 2000;8(4):251-257.

Scott N.A, Cipolla G.D, Ross C.E, Dunn B, Martin F.H, Simonet L, Wilcox J.N. Identification of a potential role for the advenitita in vascular lesion formation after balloon overstretch injury of porcine cornonary arteries. Circulation 1996;93:2178-2187.

Sedivy J.M. Can ends justify the means?: Telomeres and the mechanisms of replicative senescence and immortalization in mammalian cells. Proceedings of the National Academy of Sciences of the United States of America 1998;95(16):9078-9081.

Seldon C, Roberts E, Stamp G, Parker K, Winlove P, Ryder T, Platt H, Hodgson H. Comparison of three solid phase supports for promoting three-dimensional growth and function of human liver cell lines. Artificial Organs 1998;22:308-319.

Seldon C, Sharial A, McCloskey P, Ryder T, Roberts E, Hodgson H. Three-dimensional in vitro cell culture leads to a marked upregulation of cell function in human hepatocyte cell lines - an important tool for the development of bioartificail liver machine. Annals of New York Academy of Sciences 1999;875:353-363.

Seldon C. Personal Communication 2000. Department of Medicine, Royal Free Hospital, Hampstead, Middlesex, UK.

Seldon C, Khalil M, Hodgson H. Three-dimensional culture upregulates extracellular matrix protein expression in human liver cell lines - a step towards mimicking the liver in vivo? International Journal of Artificial Organs 2000;23:774-781.

Shapiro L, Cohen S. Novel alginate sponges for cell culture and transplantation. Biomaterials 1997;18:583-590.

Shattill S.J. Function and regulation of the beta-3 integrins in the hemostatsis of and vascular biology. Thromobsis and Haemostasis 1995;74:149-155.

Shi Y, O'Brien J, Fard A, Mannion J.D, Wang D, Zalewshki A. Adventitial myofibroblasts contribute to neointimal formation in injured porcine coronary arteries. Circulation 1996;94:1655-1664.

Shin H, Jo S, Mikos AG. Modulation of marrow stromal osteoblast adhesion on biomimetic oligo[poly(ethylene glycol) fumarate] hydrogels modified with Arg-Gly-Asp peptides and a poly(ethylene glycol) spacer. Journal of Miomedical Materials Research 2002;61:169-179.

Short M, Nemenoff R.A, Zawada W.M, Stenmark K.R, Das M. Hypoxia induces differentiation of pulmonary artery adventitial fibroblasts into myofibroblasts. American Journal of Physiology - Cell Physiology 2004;286:C416-425.

Sibbald R.G, Torrance G.W, Walker V, Attard C, MacNeil P. Cost-effectiveness of Apligraf in the treatment of venous leg ulcers. Ostomy Wound Management 2001;47(8):36-46.

Skaugrud O, Hagen A, Borgersen B, Dornish M. Biomedical and pharmaceutical applications of alginate and chitosan. Biotechnology & Genetic Engineering Reviews 1999;16:23-40.

Skjåk-Bræk G, Grasdalen H, Smidsrød O. Inhomogeneous polysaccharide ionic gels. Carbohydrate Polymers 1988;10:31-54.

Skjåk-Braek G, Espevik T. Application of alginate gels in biotechnology and biomedicine. Carbohydrates in Europe 1996;14:19-25.

Slepian M.J, Massia S.P, Dehdashti B, Fritz A, Whitesell L. β3-integrins rather than β1-integrins dominate integrin-matrix interaction involved in postinjury smooth muscle cell migration. Circulation 1998;97:1818-1827.

Smentana K. Cell biology of hydrogels. Biomaterials 1993;14:1046-1050.

Smisrod O, Skjåk-Braek G. Alginate as immobilisation matrix for cells. Tibtech 1990;8:71-78.

Smith N. Personal communication 2002. Project Manager, Hoerbiger-Origa Ltd, Tewkesbury, Gloucestershire, UK.

Sofia S, McCarthy M.B, Gronowicz G, Kaplan D.L. Functionalised silk based biomaterials for bone formation. Journal of Biomedical Materials Research 2001;54:139-148.

Solan A, Mitchell S, Moses M, Niklason L. Effect of pulse rate on collagen deposition in the tissue-engineered blood vessel. Tissue Engineering 2003;9(4):579-586.

Soon Shiong P, Feldman E, Netson R, Heintz R, Yao Q, Yao Z, Zheng T, Merideth N, Skjåk-Braek G, Espevik T, Smidsrod O, Sandford P. Long-term reversal of diabetes by the injection of immunoprotective islets. Proceedings of the National Academy of Science USA 1993;90:5843-5847.

Soon Shiong P, Heintz P, Merideth N, Yao Q.X, Yao Z, Zeng T, Murphy M, Malony M.K, Schmehl M, Harris M, Mendez R, Sandford P. Insulin independence in a type I diabetic patient after encapsulated islet cell transplantation. Lancet 1994;343:950-951.

Soranzo C, Abatangelo G, Callegaro L. Artificial skin containing as support biocompatible materials based on hyaluronic acid derivatives 2000. US Patent No: 6110208.

Souw P, Rehm H.J. Mikroorganismen. In: Verdickungsmitteln IV. Mikrobieller Abbau von drei Pflanzenexudaten und zwei Meeresalgenextrakten [Microorganisms in gums IV. Microbial degradation of plant exudates and seaweed extracts]. Zeitschrift fur Lebensmittel-Untersuchung und-Forschung 1975;159(5):297-304.

Srivatas S.S, Fitzpatrick L.S, Tsao P.W, Reilly T.M, Holmes D.R Jr, Schwartz R.S, Mousa S.A. Selective αVβ3 integrin blockade potentially limits neointimal hyperplasia and lumen stenosis following deep coronary arterial stent injury: evidence for the functional importance of integrin αVβ3 and osteopontin expression during neointima formation. Cardiovascular Research 1997;36:408-128.

Stacey C. Practical Pneumatics. Published by Arnold 1998.

Stanford E.C.C. Manufacture of useful products from seaweeds. Office of the Commissioner of Patents 1881 No: 142.

Stanford E.C.C. New substance obtained from some of the commoner species of marine Algae. Abstracts of the Journal of the Chemical Society 1883a, Abstract 943.

Stanford E.C.C. On algin, a new substance obtained from some commoner species of marine algae. American Journal of Pharmacy December 1883b;55(12).

Stanford E.C.C. On algin: a new substance obtained from some commoner species of marine algae. Chemical News 1883c June 1st 254-257 and 267-269.

Stark T. Knife to the heart. The story of transplant surgery 1996(a):79-105. Publisher: MacMillan, London, UK.

Stark T. Knife to the heart. The story of transplant surgery 1996(b);135-153. Publisher: MacMillan, London, UK.

Strauch B. Use of nerve conduits in peripheral nerve repair. Hand Clinics 2000;16:123-130.

Strawich E, Hancock W.D, Nimni M.E. Chemical composition and biophysical properties

of porcine cardiovascular tissue. Biomaterials, Medical Devices and Artificial Organs 1975;3:309-318.

Steed D.L, Ricotta J.J, Prendergast J.J, Kaplan R.J, Webster M.W, McGill J.B, Schwartz S.L. Promotion and acceleration of diabetic ulcer healing by arginine-glycine-aspartic acid (RGD) peptide matrix. Diabetes Care 1995;18(1):39-46.

Stenmark K.R, Gerasimovskaya E, Nemenoff R.A, Das M. Hypoxic activation of adventitial fibroblasts: role in vascular remodeling. Chest 2002;122(Suppl):326S-334S.

Stouffer G.A, Hu Z, Sajid M, Li H, Jin G, Nakada M.T, Hanson S.R, Runge M.S. β3 integrins are upregulated after vascular injury and modulate thrombospondin- and thrombin-induced proliferation of cultured smooth muscle cells. Circulation 1998;97:907-915.

Stryer L. Connective-tissue proteins. In: Stryer L. Biochemistry 3rd Edition. W H Freeman, New York, USA 1988;261-281.

Sundararajan M.V, Matthew H.W.T. Porous chitosan scaffolds for tissue engineering. Bio materials 1999;20;1133-1142.

Sutherland I.W. Biotechnology of microbial exopolysaccharides. Cambridge Studies in Biotechnology 9, 1990; Chapter 8:107-111.

Swanson E.A, Izatt J.A, Hee M.R, Huang D, Lin C.P, Schuman J.S, Puliafito C.A, Fujimoto J.G. In vitro retinal imaging by optical coherence tomography. Optics Letter 1993;18:1864-1866.

Tadrous P.J. Methods for imaging the structure and function of living tissues and cells: 1. Optical coherence tomography. Journal of Pathology 2000:191:115-119.

Takada Y, Huang C, Hemler M,E. Fibronectin receptor structures in the VLA family of heterodimers. Nature 1987;326:607-609.

Taylor P.M. Personal communication 2000. National Heart and Lung Institute, Harefield Hospital, Harefield, Middlesex, UK.

Temenoff J.S, Mikos A.G. Review: tissue engineering for regeneration of articular cartilage. Biomaterials 2000;21:431-440.

Thomas S. Alginate dressing in surgery and wound management - part 1. Journal of Wound Care 2000;9(2):56-60.

Thompson J.A, Itskovitz-Eldor J, Shapiro S.S, Waknitz M.A, Swiergiel J.J, Marshall V.S, Jones J.M. Embryonic stem cell lines derived from human blastocysts. Science 1998;282:1145-1147.

Thomson R.C, Shung A.K, Yaszemski M.J, Mikos A.G. Polymer scaffold processing. In: Lanza R.P, Langer R, Vacanti J. Principles of Tissue Engineering, Academic Press, San Diego, USA 2000:Chapter 21.

Thu B, Smidsrød O, Skjåk-Bræk G. Alginate gels - Some structure-function correlations relevant to their use as immobilization matrix for cells. In: Wijffels R.H, Buitelaar R.M, Bucke C, Tramper J (Eds.). Immobilized cells: Basics and Applications. Elsevier Science B.V. 1996a;19-30.

Thu B, Espevik P, Soon Shiong P, Smidsrod O, Skjåk Braek G. Alginate polylysine capsules: Functional properties. Biomaterials 1996b;17:1069-79.

Tombs M.P, Harding S.E. An introduction to polysaccharide biotechnology. Taylor and Francis 1998;Chapter 4:123-153.

Tonnesen H.J, Karlsen J. Alginate in drug delivery systems. Drug Development and Industrial Pharmacy 2002;28(6):621-630.

Tranquillo R.T. The tissue-engineered small-diameter artery. Annals of the New York Academy of Sciences 2002:961:251-254.

Uludag H, De Vos P, Tresco P.A. Technology of mammalian cell encapsulation. Advanced Drug Delivery Reviews 2000;42(1-2):29-64.

Underwood S, Afoke A, Brown R.A, MacLeod A.J, Shamlou P.A, Dunnill P. Wet extrusion of fibronectin-fibrinogen cables for application in tissue engineering. Biotechnology and Bioengineering 2001;73(4):295-305.

Vacanti C.A, Langer R, Schloo B, Vacanti J.P. Synthetic polymers seeded with chondrocytes provide a template for new cartilage formation. Plastic and Reconstructive Surgery 1991;88(5):753-759.

Vacanti J.P, Langer R. Tissue engineering: the design and fabrication of living replacement devices for surgical reconstruction and transplantation. Lancet 1999;354 (Suppl 1):32-34.

Vacanti C.A, Vacanti J.P. Guided development and support of hydrogel cell composition, USA 2000. US Patent Number: 6027744.

Vacanti C.A, Bonassar L.J, Vacanti M.P, Shufegarger J . Replacement of an avulsed phalanx with tissue engineering. New England Journal of Medicine 2001;344:1511-1514.

Vandenbossche G.M, Remon J.P. Influence of the sterilization process on alginate dispersions. Journal of Pharmacy and Pharmacology 1993;45:484-486.

van der Rest M, Dublet B, Champliaud M.F. Fibril-associated collagens. Biomaterials 1990;11:28-31.

van der Rest M, Garrone R. Collagen family of proteins. FASEB Journal 1991;5:2814-2823.

Vernino A.R, Wang H.L, Papley J, Nechamkin S.J, Ringeisen T.A, Derhalli M, Brekke J. The use of biodegradable PLA barrier materials in the treatment of grade II periodondal furcation defects in humans - Part 2: A multicenter investigator surgical study. International Journal of Periodontic and Restorative Dentistry 1999;19:56-65.

Voytik-Harbin S.L, Brightman A.O, Kraine M.R, Waisner B, Badylak S.F. Identification of extractable growth factors from small intestinal submucosa. Journal of Cellular Biochemistry 1997;67:478-491.

Wallace D.G, Rosenblatt J. Collagen gel systems for sustained delivery and tissue engineering. Advanced Drug Delivery Reviews 2003;55(12):1631-1649.

Walter J.B, Talbot I.C. Connective tissue: its normal structure and effects of disease. In: Walter J.B, Talbot I.C. Walter and Israel General Pathology. Churchill Livingston, New York 7th Edition, 1996;103-116.

Wang J.C, Hu S.H, Lin C.Y. Lethal effect of microwaves on spores of Bacillus spp. Journal of Food Protection 2003;66(4):604-609.

Wang R.K, Elder J.B. High resolution opticasl tomographic imaging of soft biological tissues. Laser. Physics 2002;12(4):611-616.

Wang X, Montini E, Al-Dhalimy M, Lagasse E, Finegold M, Grompe M. Kinetics of liver repopulation after bone marrow transplantation. American Journal of Pathology 2002;161:565–574.

Wang X.J, Milner T.E, Nelson J.S. Charachterisation of fluid flow velocity by optical Doppler tomography. Optics Letters 1995;20(11):1337-1339.

Weinberg C.B, Bell E. Regulation of proliferation of bovine aortic endothelial cells, smooth muscle cells, and adventitial fibroblasts in collagen lattices. Journal of Cellular Physiology 1985;122:410-414.

Weightman B, Swanson S.A, Isaac G.H, Wroblewski B.M. Polyethylene wear from retrieved acetabular cups. Journal of Bone & Joint Surgery - British Volume. 1991;73(5):806-810.

Welzel J. Optical coherence tomography in dermatology: a review. Skin Research Technology 2001;7:1-9

Wideroe H, Danielsen S. Evaluation of the use of Sr2+ in alginate immobilization of cells Naturwissenschaften 2001;88:224-228.

Williams D.F. The William's Dictionary of Biomaterials, Liverpool University Press 1999.

Wilson Jr. W.C, Boland T. Cell and organ printing 1: Protein and cell printers. Anatomical Record Part A. Discoveries in Molecular Cellular & Evolutionary Biology 2003;272:491-496.

Woerly S, Maghami G, Duncan R, Subr V, Ulbrick K. Synthetic polymer derivatives as substrata fro neuronal adhesion and growth. Brain Research Bulletin 1993;30:423-432.

Wong M, Siegrist M, Wang X, Hunziker E. Development of mechanically stable alginate/ chondrocyte constructs: effects of guluronic acid content and matrix synthesis. Journal of Orthopaedic Research 2001;19:493-499.

Wong R.C, Yazdanfar S, Izatt J.A, Kulkarni M.D, Barton J.K, Welch A.J, Willis J, Sivak Jr M.V. Visualization of subsurface blood vessels by color Doppler optical coherence tomography in rats: before and after haemostatic therapy. Gastrointestinal Endoscopy 2002;55(1):88-95.

Wolinsky H. Response of the rat aortic media to hypertension. Morphological and chemical studies. Circulation Research 1970;26:507-522.

World Technology Evaluation Centre (WTEC) Panel Report on Tissue Engineering Research. International Technology Research Institute, January 2002.

Wu C. Roles of integrins in fibronectin matrix assembly. Histology and Histopathology 1997;12:233-240.

Wu S.Y, Lee K.F, Kam K.M, Shaw P.C. Restriction enzyme BliHKI from a thermophilic Bacillus licheniformis strain. Bioscience, Biotechnology & Biochemistry 1993;57:1193-1194.

Wu X, Ding S, Ding Q, Gray N.S, Schultz P.G. Small molecules that induce cardiomyogenesis in embryonic stem cells. Journal of the American Chemical Society 2004;126:1590-1591.

Wyrick J.D, Stern P.J. Secondary nerve reconstruction. Microsurgery 1992;8:587-598.

Xu W, Liu L, Charles I.G. Microencapsulated iNOS-expressing cells cause tumor suppression in mice. FASEB Journal 2002;16:213-215.

Yacoub M.H, Taylor P.M Personal Communication 2001. Imperial College School of Medicine, National Heart & Lung Institute, Heart Science Centre, Harefield Hospital, UK.

Yaffe D. Retention of differentiation potentialities during prolonged cultivation of myogenic cells. Proceedings of the National Academy of Sciences of the United States of America 1968;61:477-483.

Yagi K, Tsuda K, Serada M, Yamada C, Kondoh A, Miura Y. Rapid formation of multicellular spheroids of adult rat hepatocytes by rotation culture and their immobilization within calcium alginate. Artificial Organs 1993;17:929-934.

Yamada Y, Kleinman H.K. Functional domains of cell adhesion molecules. Current Opinions in Cell Biology 1992;4:819-823.

Yang Y, Whiteman S, Pittius D,He Y, Spiteri M, Wang R.K. Use of OCT in delineating airwaymicrostructures:comparison of OCT images with histopathologies. Physics in Medicine and Biology 2004;49:1247-1255.

Yannas I.V, Burke J.F, Gordon P.L, Huang C, Rubenstein R.H. Design of an artificial skin II Control of chemical composition. Journal of Biomedical Materials Research 1980;14:107-132.

Yannas I.V, Burke J.F. Design of an artificial skin 1: Basic design principles. Journal of Biomedical Materials Research 1980;14: 65-81.

Yannas I.V. Synthesis of tissues and organs. ChemBioChem 2004;5:26-39.

Yazdanfar S, Rollins A.M, Izatt J.A. Imaging and velocimetry of the human retinal circulation with colour Doppler optical coherence tomography. Optical Letters 2000;25(19):1448-1450.

Yazdanfar S, Rollins A.M, Izatt J.A. In vivo imaging of human retinal flow dynamics by color Doppler optical coherence tomography. Archives of Ophthalmology 2003;121(2):235-239.

Ye Q, Zund G, Benedikt P, Jockenhoevel S, Hoerstrup S.P, Sakyama S, Hubbell J.A, Turina M. Fibrin gel as a three dimensional matrix in cardiovascular tissue engineering. European Journal of Cardio-Thoracic Surgery 2000;17(5):587-591.

Yee K.O, Rooney M.M, Giachelli C.M, Lord S.T, Schwartz S.M. Role of β1 and β3 integrins in human smooth muscle cell adhesion to and contraction of fibrin clots in vitro. Circulation Research 1998;83:241-251.

Yee K.O, Schwartz S.M. Why atherosclerotic vessels narrow: the fibrin hypothesis. Thrombosis and Haemostasis 1999;28:762-771.

Yoshikawa Y, Komuta Y, Nishihara T, Itoh Y, Yoshikawa H, Takada K. Preparation and evaluation of once-a-day injectable microspheres of interferon alpha in rats. Journal of Drug Targeting 1999;6:449-461.

Zhang W, Kim J.H, Franco C.M.M, Middleberg A.P.J. Characterisation of the shrinkage of calcium alginate gel membrane with immobilised Lactobacillus rhamnosus. Applied Microbiology and Biotechnology. 2000;54:28-32.

Zhang W.J, Laue Ch, Hyder A, Schrezenmeir. Purity of alginate affects the viability and fibrotic overgrowth of encapsulated porcine islet xenografts. Transplantation Proceedings. 2001;33:3517-3519.

Zhao Y, Chen Z.P, Saxer C, Xiang S, de Boer J.F, Nelson J.S. Phase-resolved optical coherence tomography and opticl Doppler tomography for imaging blood flow in human skin with fast scanning speed and high velocity sensitivity. Optics Letters 2000;25(2):114-116.

Zimmermann U, Klöck G, Federlin K, Hannig K, Kowalski M, Bretzel R.G, Horcher A, Entenmann H, Siebers U, Zekorn T. Production of mitogen-free alginates with variable ratios of mannuronic acid to guluronic acid by free flow electrophoresis. Electrophoresis 1992;13:269-274.

Zimmermann U, Mimietz S, Zimmermann H, Hillgartner M, Schneider H, Ludwig J,

Haase A, Rothmund M, Fuhr G. Hydrogel-based non-autologous cell and tissue therapy. BioTechniques. 2000;29:564-581.

Zimmermann S, Voss M, Kaiser S, Kapp U, Waller C.F, Martens U.M. Lack of telomerase activity in human mesenchymal stem cells. Leukemia 2003;17(6):1146-1149.

COLOPHON

This thesis was most enjoyably written and finally produced using the following hardware and software:

Hardware:

- Apple 12-inch PowerBook G4 (1.5 GHz with 1.25 Gb RAM) - Computer
- Apple 23-inch Cinema Display - Screen
- Canon iR3100CN - Printer
- Hewlett Packard HP Business Inkjet 1200d - Printer
- Epson Stylus Photo R800 - Printer

Software:

- Apple OS X 10.3 (Panther) - Operating system
- Adobe Creative Suite 2 (Photoshop CS2, Illustrator CS2 and InDesign CS2) - Integrated publishing package
- OmniDictionary 2 - On-line dictionary
- Nisus Thesaurus 1 - On-line thesaurus
- OmniGraffle 3 Professional - Diagram drawing application
- Chartsmith 1 - Graph drawing application
- Adobe OpenType: Futura Standard (11 point heavy/heavy oblique and 11 point medium/medium oblique) - Typeface